

AD-A283 228



NAVAL POSTGRADUATE SCHOOL
Monterey, California



94-25214



152

DTIC
ELECTE
AUG 11 1994
S B D

THESIS

**EVALUATION OF ENERGY-SINK
STABILITY CRITERIA FOR
DUAL-SPIN SPACECRAFT**

by

Vincent Michael Ortiz

June 1994

Thesis Advisor:

I. Michael Ross

Approved for public release; distribution is unlimited

DTIC QUALITY INSPECTED 1

94 8 10 007

Unclassified

Security Classification of this page

REPORT DOCUMENTATION PAGE

1a Report Security Classification UNCLASSIFIED		1b Restrictive Markings	
2a Security Classification Authority		3 Distribution Availability of Report Approved for public release; distribution is unlimited	
2b Declassification/Downgrading Schedule		5 Monitoring Organization Report Number(s)	
4 Performing Organization Report Number(s)		7a Name of Monitoring Organization Naval Postgraduate School	
6a Name of Performing Organization Naval Postgraduate School	6b Office Symbol (If Applicable) AA-RO	7b Address (city, state, and ZIP code) Monterey, CA 93943-5000	
6c Address (city, state, and ZIP code) Monterey, CA 93943-5000	8a Name of Funding/Sponsoring Organization	8b Office Symbol (If Applicable)	9 Procurement Instrument Identification Number
8c Address (city, state, and ZIP code)		10 Source of Funding Numbers	
		Program Element Number	Project No.
		Task No.	Work Unit Accounting No.
11 Title (Include Security Classification) EVALUATION OF ENERGY-SINK STABILITY CRITERIA FOR DUAL-SPIN SPACECRAFT (U)			
12 Personal Author(s) Ortiz, Vincent Michael			
13a Type of Report Master's Thesis	13b Time Covered From To	14 Date of Report (year, month, day) June 1994	15 Page Count 152
16 Supplementary Notation [all unclassified theses] The views expressed in this thesis are those of the author and do not reflect the official policy or position of the Department of Defense or the U. S. Government			
17 Cosati Codes		18 Subject Terms (continue on reverse if necessary and identify by block number)	
Field	Group	Energy-Sink, Dual-Spin, Gyrostat	
		Energy-Sink Stability Criteria	
19 Abstract (continue on reverse if necessary and identify by block number)			
<p>The nutational stability of a dual-spin, quasi-rigid, axisymmetric spacecraft containing a driven rotor is analyzed. The purpose is to examine a revised energy-sink stability theory that properly accounts for the energy contribution of the motor. An inconsistency in the development disproves the existing energy-sink theory's assumption that the motor of the system contributes exactly enough energy to offset the frictional losses between the rotor and the platform. Using the concept of core energy, the revised stability criteria for a dual-spin, quasi-rigid, axisymmetric spacecraft containing a driven rotor is derived. An expression for nutation angle as a function of core energy over time is then determined. Numerical simulations are used to verify the revised energy-sink stability theory. The dual-spin, quasi-rigid, axisymmetric system presented by D. L. Mingori was chosen for the simulation. Equations for angular momentum and total energy were necessary to validate the numerical simulation and confirm aspects of the revised energy-sink stability theory. These equations are derived from the first principles of dynamics and are included in the analysis. An explicit relationship for core energy as a function of time does not exist. Various models postulating core energy are presented and analyzed. The numerical simulations of the computed nutation angles as a function of the postulated core energy compare well with the actual nutation angles of the system to confirm the revised energy-sink stability criteria.</p>			
20 Distribution/Availability of Abstract		21 Abstract Security Classification	
<input checked="" type="checkbox"/> unclassified/unlimited <input type="checkbox"/> same as report <input type="checkbox"/> DTIC only		Unclassified	
22a Name of Responsible Individual I. Michael Ross		22b Telephone (Include Area code) (408) 656-2312	22c Office Symbol AA-RO

DD FORM 1473, 84 MAR

83 APR edition may be used until exhausted
All other editions are obsoleteSecurity Classification of this page
Unclassified

Approved for public release; distribution is unlimited

**Evaluation of Energy-Sink Stability Criteria
For Dual-Spin Spacecraft**

by

**Vincent Michael Ortiz
Lieutenant Commander, United States Navy
B.M.E., Georgia Institute of Technology, 1983**

**Submitted in partial fulfillment of the
requirements for the degree of**

MASTER OF SCIENCE IN PHYSICS

from the


**NAVAL POSTGRADUATE SCHOOL
June 1994**

Author:




Vincent Michael Ortiz

Approved By:



I. M. Ross, Thesis Advisor



H. A. Dall, Second Reader



William Colson, Chairman, Department of Physics

ABSTRACT

The nutational stability of a dual-spin, quasi-rigid, axisymmetric spacecraft containing a driven rotor is analyzed. The purpose is to examine a revised energy-sink stability theory that properly accounts for the energy contribution of the motor. An inconsistency in the development disproves the existing energy-sink theory's assumption that the motor of the system contributes exactly enough energy to offset the frictional losses between the rotor and the platform. Using the concept of core energy, the revised stability criteria for a dual-spin, quasi-rigid, axisymmetric spacecraft containing a driven rotor is derived. An expression for nutation angle as a function of core energy over time is then determined. Numerical simulations are used to verify the revised energy-sink stability theory. The dual-spin, quasi-rigid, axisymmetric system presented by D. L. Mingori was chosen for the simulation. Equations for angular momentum and total energy were necessary to validate the numerical simulation and confirm aspects of the revised energy-sink stability theory. These equations are derived from the first principles of dynamics and are included in the analysis. An explicit relationship for core energy as a function of time does not exist. Various models postulating core energy are presented and analyzed. The numerical simulations of the computed nutation angles as a function of the postulated core energy compare well with the actual nutation angles of the system to confirm the revised energy-sink stability criteria.

Accession For	
NTIS GRA&I	<input checked="checked" type="checkbox"/>
DTIC TAB	<input type="checkbox"/>
Unannounced	<input type="checkbox"/>
Justification _____	
By _____	
Distribution/_____	
Availability Codes	
Dist	Avail and/or Special
A-1	

TABLE OF CONTENTS

I. INTRODUCTION	1
A. SINGLE SPIN SATELLITES	1
1. Equations of motion	1
2. Single Spin Satellite Stability	4
B. DUAL SPIN SATELLITES	7
II. PROBLEM DEFINITION	13
A. OVERVIEW	13
B. INCONSISTENCY OF THE ENERGY SINK THEORY	14
C. CORE ENERGY AND ENERGY DISSIPATION	15
D. NUTATIONAL MOTION	26
III. DYNAMICAL EQUATIONS	29
A. MINGORI'S DUAL-SPIN SYSTEM	29
B. ANGULAR MOMENTUM	32
C. ENERGY	38
D. MINGORI'S EQUATIONS OF MOTION	41
E. NUTATION ANGLE	42
F. CORE ENERGY	43
1. Exponential Core Energy Model	43
2. Verhulst Logistic Core Energy Model	43
IV. NUMERICAL SIMULATION	46
A. NUMERICAL SIMULATION EQUATIONS OF MOTION	46
1. Mingori's Equations of Motion	46

2. Angular Momentum	48
3. Nutation Angle	48
4. Energy	48
5. Core Energy and Postulated Core Energy	49
B. COMPUTER PROGRAM	50
1. Initialization	50
a. Variables	51
b. Input File	51
2. Preliminary Calculations	51
3. Numerical Integration	52
4. Calculation of System Parameters	52
5. Graphics Output	53
6. Computer Program Validation	53
V. ANALYSIS	55
A. INTRODUCTION	55
1. Objective	55
2. Numerical Simulation Cases	55
B. DISCUSSION	57
1. Angular Momentum	57
2. Total Energy, Platform and Rotor Core Energy	58
3. Stability Criteria	59
4. Postulated Core Energy and Nutation Angle	60
a. Exponential Core Energy Model	60
b. Verhulst Logistic Core Energy Model	62
C. FURTHER RESEARCH	63
VI. CONCLUSION	66

REFERENCES	67
APPENDIX A - NUMERICAL SIMULATION DATA	68
Case 1 - Inertia Ratio > 1 , Stable, Exponential Model	
Case 2 - Inertia Ratio < 1 , Stable, Exponential Model	
Case 3 - Inertia Ratio < 1 , Unstable, Exponential Model	
Case 4 - Inertia Ratio > 1 , Unstable, Exponential Model	
Case 5 - Inertia Ratio < 1 , Stable, Verhulst Model	
Case 6 - Inertia Ratio < 1 , Unstable, Verhulst Model	
Case 7 - Inertia Ratio > 1 , Unstable, Verhulst Model	
APPENDIX B - COMPUTER PROGRAM CODE	117
INITIAL DISTRIBUTION LIST	133

TABLE OF SYMBOLS

A	quantity as defined in Equation (138)
a	radial distance of rotor particle masses from the b_3 axis
a'	radial distance of platform particle masses from the b_3' axis
B	axisymmetric rigid body and reference frame, and entire dual-spin system body and reference frame
B^*	reference frame, coordinate axis origin, and center of mass of rotor coordinates b_i
B^{\sim}	reference frame, coordinate axis origin, and center of mass of platform coordinates b_i'
b_i	coordinate axes of the rigid body, coordinate axes of the rotor of the dual-spin system; which coincide with the principle axes of the body
b_i'	coordinate axes of the platform of the dual-spin system, which coincide with the principle axes of the platform
b_i^{\sim}	coordinate axes b_i moved to the center of mass of the dual-spin system
C	quantity as defined in Equation (138)
c	damping coefficient of the rotor damper of the dual-spin system
c'	damping coefficient of the platform damper of the dual-spin system
dm	differential mass element
dM	differential mass element of the rotor
$\frac{d}{dt}^B$	derivative with respect to time in the reference frame B
$\frac{d}{dt}^N$	derivative with respect to time in the inertial reference frame N
E	kinetic energy of the system
\dot{E}	time rate of change of kinetic energy

E_{total}	total energy of the system, is the sum of the kinetic and the potential energies of the system
\dot{E}_{total}	time rate of change of total energy of the quasi-rigid system, due to dissipative elements and to the addition or subtraction of energy from the motor
E_{dm}	kinetic energy of the differential mass dm
E_C	rotor core energy
\dot{E}_C	time rate of change of rotor core energy
E_C'	platform core energy
\dot{E}_C'	time rate of change of platform core energy
$E_C \text{ postulated}$	postulated rotor core energy as a function of time
$E_C \text{ postulated}'$	postulated platform core energy as a function of time
E_{C_0}	initial rotor core energy
E_{C_0}'	initial platform core energy
$E_C \text{ final}$	final postulated rotor core energy
$E_C \text{ final}'$	final postulated platform core energy
\dot{E}_D	time rate of change of energy in the rotor due to all dissipative elements
\dot{E}_D'	time rate of change of energy in the platform due to all dissipative elements
$\dot{E}_D \text{ total}$	time rate of change of energy of the quasi-rigid system due to all dissipative elements
h	angular momentum vector of the body with respect to the system center of mass
h_i	angular momentum of the i th particle with respect to the system center of mass
h_M	angular momentum of the rotor with respect to the system center of mass
$h_{M + 4 m}$	angular momentum of the rotor and the four rotor particle masses with respect to the system center of mass
$h_{M'}$	angular momentum of the platform with respect to the system center of mass
$h_{M' + 4 m'}$	angular momentum of the platform and the four platform particle masses with respect to the system center of mass

$ h , h$	magnitude (Euclidean norm) of the angular momentum vector
h_i	angular momentum of the rigid body along the b_i th coordinate axis, angular momentum of the rotor along the b_i th coordinate axis
h_i'	angular momentum of the platform along the b_i' th coordinate axis
\dot{h}_i	time rate of change of the angular momentum along the b_i th coordinate axis
I_i	principle moment of inertia of the rigid body about the b_i th coordinate axis, principle moment of inertia of the rotor about the b_i th coordinate axis
I_i'	principle moment of inertia of the platform about the b_i' th coordinate axis
$I_{i \text{ total}}$	total moment of inertia about the principal coordinate axis b_i
I_{\max}	maximum moment of inertia
I_{\min}	minimum moment of inertia
I_s	spin moment of inertia of rigid body, spin moment of inertia of rotor of the dual-spin system
I_s'	spin moment of inertia of platform of the dual-spin system
$I_{s \text{ total}}$	total moment of inertia of dual spin system about the spin axis
I_t	transverse moment of inertia of the rigid body, transverse moment of inertia of the rotor of the dual-spin system
I_t'	transverse moment of inertia of the platform of the dual-spin system
$I_{t \text{ total}}$	total moment of inertia of the dual-spin system about a transverse axis
I_j/I_i	inertia ratio of a single body
$I_{s \text{ total}}/I_{t \text{ total}}$	inertia ratio of the dual-spin system
i	$i = 1, 2, 3$ when referencing coordinate axes, $i = 1, 2, 3, 4$ when referencing particle masses, i = imaginary number in Equations (20), (21)

j	index that references a specific location of a variable's vector or matrix
J_3'	quantity as defined in Equation (138)
k	spring constant of the rotor damper of the dual-spin system
k'	spring constant of the platform damper of the dual-spin system
K_i	mathematical constant, $i = 1, 2, 3, 4$
l	distance between the rotor center of mass and the platform center of mass
l_1	quantity defined in Equation (138)
l_2	quantity defined in Equation (138)
L	distance between B^* and B^{**}
M	moment vector of all forces acting on the system
M_i	moment about the b_i th coordinate axis
M	mass of the rotor of the dual-spin system
M'	mass of the platform of the dual-spin system
M_T	total mass of the dual-spin system
m_b	mass of the mass-spring-dashpot-system of the rotor. In this paper it has the same value as the particle masses m_b
m_b'	mass of the mass-spring-dashpot-system of the platform. In this paper it has the same value as the platform particle masses m_b'
m_i	mass of the i th particle located on the rotor, $i = 1, 2, 3, 4$
m_i'	mass of i th particle located on the platform, $i = 1, 2, 3, 4$
N	inertial reference frame
o	coordinate axes origin and center of mass of the rigid body system, and coordinate axes origin and center of mass of the dual-spin system B with coordinates b_i^{**}
Q	quantity defined in Equation (107)
Q'	quantity defined in Equation (100)
\tilde{Q}	quantity defined in Equation (44)
r	exponential factor for postulated rotor core energy model
r'	exponential factor for postulated platform core energy model

\mathbf{R}_i	location of the i th particle with respect to the inertial reference frame N
\mathbf{r}_i	location of the i th particle with respect to the reference frame B
$\dot{\mathbf{r}}_i$	velocity of the i th particle with respect to the reference frame B
$\mathbf{r}_{\Delta M}$	definition of a differential mass element of the rotor with respect to the reference frame B
\mathbf{r}_{dm}	definition of a differential mass element with respect to the reference frame B
$\dot{\mathbf{r}}_{dm}$	velocity of the differential mass element with respect to the reference frame B
T_M	motor torque
T_P	net torque applied to the platform due to all forces
T_{PIM}	torque applied to the platform due to the motor
T_R	net torque applied to the rotor due to all forces
T_{RIM}	torque applied to the rotor due to the motor
T_{PIM}^*	torque applied to the platform due to the motor when both the platform and the rotor are quasi-rigid
T_{RIM}^*	torque applied to the rotor due to the motor when both the platform and the rotor are quasi-rigid
t	time
U	potential energy of the system
u	location of the differential mass element of the rotor with respect to the reference frame B along the b_1 axis
${}^N\vec{\mathbf{v}}^i$	velocity of the i th particle with respect to the inertial reference frame N
${}^N\vec{\mathbf{v}}^{dm}$	velocity of the differential mass element with respect to the inertial reference frame N
${}^N\vec{\mathbf{v}}^{cm}$	velocity of the system center of mass with respect to the inertial reference frame N

$V_{cm\ i}$	velocity of the system center of mass along the i th coordinate axis with respect to the inertial reference frame N , where $i = x, y, z$
v	location of the differential mass element of the rotor with respect to the reference frame B along the b_2 axis
\dot{W}	rate of work done by the motor torque
w	location of the differential mass element of the rotor with respect to the reference frame B along the b_3 axis
z	displacement of the rotor particle mass m_1 from the b_1 axis and parallel to b_3
\dot{z}	velocity of the rotor particle mass m_1 from the b_1 axis and parallel to b_3
\ddot{z}	acceleration of the rotor particle mass m_1 from the b_1 axis and parallel to b_3
z'	displacement of the platform particle mass m_1' from the b_1' axis and parallel to b_3'
\dot{z}'	velocity of the platform particle mass m_1' from the b_1' axis and parallel to b_3'
\ddot{z}'	acceleration of the platform particle mass m_1' from the b_1' axis and parallel to b_3'
z_{cm}	distance the system center of mass is located along the b_3 axis from the rotor coordinate axes (b_i) reference frame origin B^*
γ	mathematical variable as defined in Equation (22)
ϵ	small perturbation value
$\dot{\epsilon}$	time rate of change of perturbation
ζ	quantity defined in Equation (138)
$\dot{\zeta}$	time rate of change of ζ
η	postulated nutation angle as a function of rotor core energy
η'	postulated nutation angle as a function of platform core energy
$\dot{\eta}'$	time rate of change of postulated nutation angle as a function of platform core energy

θ	nutation angle
$\dot{\theta}$	time rate of change of nutation angle
λ	rotor nutation frequency
λ'	platform nutation frequency
λ_0	inertial nutation frequency
ν	quantity defined in Equation (138)
ρ	quantity defined in Equation (138)
ρ'	quantity defined in Equation (138)
σ	relative rotation rate of the rotor with respect to the platform
$\dot{\sigma}$	time rate of change of the relative rotation rate of the rotor with respect to the platform
ψ	angular position of the platform with respect to the rotor, is equal to $-\alpha$
$\overset{N \rightarrow B}{\omega}$	angular velocity vector of body and reference frame B with respect to inertial reference frame N
ω_0	initial angular velocity value along the b_3 th coordinate axis before the perturbation
$\dot{\omega}_0$	time rate of change of initial angular velocity value along the b_3 th coordinate axis
ω_i	angular velocity of body B along the b_i th coordinate axis
$\dot{\omega}_i$	time rate of change of the angular velocity of body B along the b_i th coordinate axis
$\ddot{\omega}_i$	second derivative with respect to time of the angular velocity of body B along the b_i th coordinate axis
ω_s	spin angular velocity of body B , spin angular velocity of rotor of the dual-spin system
$\dot{\omega}_s$	time rate of change of spin angular velocity of body B , time rate of change of spin angular velocity of rotor of the dual-spin system
ω_s'	spin angular velocity of platform of the dual-spin system
$\dot{\omega}_s'$	time rate of change of spin angular velocity of platform of the dual-spin system
$\bar{\omega}_t$	transverse angular velocity vector
ω_t	transverse angular velocity vector magnitude

$\dot{\omega}_t$ time rate of change of transverse angular velocity vector
magnitude**MINGORI'S EQUATIONS OF MOTION NOTATION**

$$M_T = M + M' + 4m_b + 4m_b'$$

$$V = \frac{(M' + 4m_b')}{M_T}$$

$$\rho = \frac{m}{M_T}$$

$$\rho' = \frac{m'}{M_T}$$

$$L_1 = L \frac{(M + 4m_b)}{M_T}$$

$$L_2 = L \frac{(M' + 4m_b')}{M_T}$$

$$\zeta = (\rho z + \rho' z')$$

$$A = I_1 + I_1' + 2m_b a^2 + 2m_b' a'^2 + (M' + 4m_b')(1 - V)L^2$$

$$C = I_3 + I_3' + 4m_b a^2 + 4m_b' a'^2$$

$$J_3' = I_3' + 4m_b' a'^2$$

$$A_1 = -(A - C)\omega_2\omega_3$$

$$A_2 = J_3'\sigma\omega_2$$

$$A_3 = 2M_T\dot{\zeta}\dot{\zeta}\omega_1$$

$$A_4 = M_T\dot{\zeta}^2$$

$$A_5 = -M_T\dot{\zeta}^2\omega_2\omega_3$$

$$A_6 = -2m(\zeta + L_2)z$$

$$A_7 = 2m(\zeta + L_2)z\omega_2\omega_3$$

$$A_8 = -2m(\zeta + L_2)\dot{z}\omega_1$$

$$A_9 = -2mz\dot{\zeta}\omega_1$$

$$A_{10} = 2mz\dot{z}\omega_1$$

$$A_{11} = mz^2$$

$$A_{12} = -mz^2\omega_2\omega_3$$

$$A_{13} = -mza$$

$$A_{14} = -mza\omega_1\omega_2$$

$$A_{15} = -2m'(\zeta - L_1)z'$$

$$A_{16} = 2m'(\zeta - L_1)z'\omega_2\omega_3$$

$$A_{17} = -2m'(\zeta - L_1)\dot{z}'\omega_1$$

$$A_{18} = -2m'z'\dot{\zeta}\omega_1$$

$$A_{19} = 2m'z'\dot{z}'\omega_1$$

$$A_{20} = m'z'^2$$

$$A_{21} = -m'z'^2\omega_2\omega_3$$

$$A_{22} = -m'z'd'\cos(\sigma t)$$

$$A_{23} = -m'z'd'\cos(\sigma t)\omega_1\omega_2$$

$$A_{24} = m'd'\sin(\sigma t)$$

$$A_{25} = m'd'\sin(\sigma t)z'((\omega_3 + \sigma)^2 - \omega_2^2)$$

$$A_{26} = A + A_4 + A_6 + A_{11} + A_{15} + A_{20}$$

$$A_{27} = A_{13} + A_{22}$$

$$A_{28} = A_1 + A_2 + A_3 + A_5 + A_7 + A_8 + A_9 + A_{10} + A_{12} + A_{14} + A_{16} + A_{17} + A_{18} + A_{19} + A_{21} + A_{23} + A_{25}$$

$$B_1 = -(A)\omega_1\omega_3$$

$$B_2 = -J_3'\sigma\omega_1$$

$$B_3 = 2M_T\dot{\zeta}\dot{\zeta}\omega_2$$

$$B_4 = M_T\dot{\zeta}^2$$

$$B_5 = M_T\dot{\zeta}^2\omega_1\omega_3$$

$$B_6 = -2m(\zeta + L_2)z$$

$$B_7 = -2m(\zeta + L_2)z\omega_1\omega_3$$

$$B_8 = -2m(\zeta + L_2)\dot{z}\omega_2$$

$$B_9 = -2mz\dot{\zeta}\omega_2$$

$$B_{10} = 2mz\dot{z}\omega_2$$

$$B_{11} = mz^2$$

$$B_{12} = mz^2\omega_1\omega_3$$

$$B_{13} = -ma$$

$$B_{14} = -maz(\omega_3^2 - \omega_1^2)$$

$$B_{15} = -2m'(\zeta - L_1)z'$$

$$B_{16} = -2m'(\zeta - L_1)z'\omega_1\omega_3$$

$$B_{17} = -2m'(\zeta - L_1)z'\omega_2$$

$$B_{18} = 2m'z'\omega_2(-\dot{\zeta} + \dot{z}')$$

$$B_{19} = m'z'^2$$

$$B_{20} = m'z'^2\omega_1\omega_3$$

$$B_{21} = -m'd\cos(\sigma t)$$

$$B_{22} = -m'd\cos(\sigma t)(\omega_3 + \sigma)^2 - \omega_1^2)z'$$

$$B_{23} = -m'd\sin(\sigma t)z'$$

$$B_{24} = m'd\sin(\sigma t)z'\omega_1\omega_2$$

$$B_{25} = A + B_4 + B_6 + B_{11} + B_{15} + B_{19}$$

$$B_{26} = B_1 + B_2 + B_3 + B_5 + B_7 + B_8 + B_9 + B_{10} + B_{12} + B_{14} + B_{16} + B_{17} + B_{18} + B_{20} + B_{22} + B_{24}$$

$$C_1 = -2maz\omega_1$$

$$C_2 = -maz$$

$$C_3 = maz\omega_2\omega_3$$

$$C_4 = -2m'd\sin(\alpha)\dot{z}'\omega_2$$

$$C_5 = -m'd\sin(\alpha)z'$$

$$C_6 = m'd\sin(\alpha)z'\omega_1\omega_3$$

$$C_7 = -2m'd\cos(\alpha)\dot{z}'\omega_1$$

$$C_8 = -m'd\cos(\alpha)z'$$

$$C_9 = m'd\cos(\alpha)z'\omega_2\omega_3$$

$$C_{10} = C_2 + C_8$$

$$C_{11} = C_1 + C_3 + C_4 + C_6 + C_7 + C_9$$

$$D_1 = m(1 - \rho)$$

$$D_2 = -m'\rho$$

$$D_3 = -ma$$

$$D_4 = ma\omega_1\omega_3$$

$$D_5 = -m(\omega_1^2 + \omega_2^2)(z + (1 - \rho) - L_2 - \rho'z')$$

$$D_6 = c\dot{z}$$

$$D_7 = kz$$

$$D_8 = D_4 + D_5 + D_6 + D_7$$

$$E_1 = -m\rho'$$

$$E_2 = m'(1 - \rho')$$

$$E_3 = m'd' \sin(\sigma t)$$

$$E_4 = m'd' \sin(\sigma t) \omega_2 (\omega_3 + 2\sigma)$$

$$E_5 = -m'd' \cos(\sigma t)$$

$$E_6 = m'd' \cos(\sigma t) \omega_1 (\omega_3 + 2\sigma)$$

$$E_7 = -m'(\omega_1^2 + \omega_2^2)(z'(1 - \rho') + L_1 - \rho z)$$

$$E_8 = c'z'$$

$$E_9 = k'z'$$

$$E_{10} = E_4 + E_6 + E_7 + E_8 + E_9$$

$$F_1 = \frac{\frac{A_{27}B_{26} + A_{28}}{A_{26}B_{23}} - \frac{E_{10}}{E_3}}{\frac{A_{27}B_{25} + E_5}{A_{26}B_{23}} + \frac{E_5}{E_3}}$$

$$F_2 = \frac{\frac{CB_{26}}{C_{10}B_{23}} - \frac{C_{11}}{C_{10}} - \frac{A_{27}B_{26} + A_{28}}{A_{26}B_{23}}}{\frac{A_{27}B_{25} + E_5}{A_{26}B_{23}} - \frac{CB_{25}}{C_{10}B_{23}} + \frac{C_5}{C_{10}}}$$

$$Z_1 = \frac{\frac{A_{27}B_{13}}{A_{26}B_{23}} - \frac{E_1}{E_3}}{\frac{A_{27}B_{25} + E_5}{A_{26}B_{23}} + \frac{E_5}{E_3}}$$

$$Z_2 = \frac{\frac{A_{27}B_{21} + A_{24}}{A_{26}B_{23}} - \frac{E_2}{E_3}}{\frac{A_{27}B_{25} + E_5}{A_{26}B_{23}} + \frac{E_5}{E_3}}$$

$$Z_3 = \frac{\frac{CB_{13}}{C_{10}B_{23}} - \frac{A_{27}B_{13}}{A_{26}B_{23}}}{\frac{A_{27}B_{25} + E_5}{A_{26}B_{23}} - \frac{CB_{25}}{C_{10}B_{23}} + \frac{C_5}{C_{10}}}$$

$$Z_4 = \frac{\frac{CB_{21}}{C_{10}B_{23}} - \frac{A_{27}B_{21}}{A_{26}B_{23}} + \frac{A_{24}}{A_{26}}}{\frac{A_{27}B_{25}}{A_{26}B_{23}} - \frac{CB_{25}}{C_{10}B_{23}} + \frac{C_5}{C_{10}}}$$

$$\bar{z} = \frac{\frac{-F_2 - \frac{D_1}{D_3}}{Z_4 + \frac{D_2}{D_3}} + \frac{F_1 + \frac{D_1}{D_3}}{Z_2 + \frac{D_2}{D_3}}}{\frac{-Z_1 - \frac{D_1}{D_3}}{Z_2 + \frac{D_2}{D_3}} + \frac{Z_3 + \frac{D_1}{D_3}}{Z_4 + \frac{D_2}{D_3}}}$$

$$\bar{z}' = \frac{\frac{-F_2 - \frac{D_1}{D_3}}{Z_3 + \frac{D_1}{D_3}} + \frac{F_1 + \frac{D_1}{D_3}}{Z_1 + \frac{D_1}{D_3}}}{\frac{-Z_2 - \frac{D_2}{D_3}}{Z_1 + \frac{D_1}{D_3}} + \frac{Z_4 + \frac{D_2}{D_3}}{Z_3 + \frac{D_1}{D_3}}}$$

$$\dot{\omega}_3 = \frac{\frac{C_5B_{13}\bar{z}}{CB_{25}} + \left(\frac{C_{10}A_{24}}{CA_{26}} + \frac{C_5B_{21}}{CB_{25}}\right)\bar{z}'}{1 - \frac{C_{10}A_{27}}{CA_{26}} - \frac{C_5B_{23}}{CB_{25}}}$$

$$\dot{\omega}_1 = -\frac{A_{27}}{A_{26}}\dot{\omega}_3 - \frac{A_{24}}{A_{26}}\bar{z}' - \frac{A_{28}}{A_{26}}$$

$$\dot{\omega}_2 = -\frac{B_{23}}{B_{25}}\dot{\omega}_3 - \frac{B_{13}}{B_{25}}\bar{z} - \frac{B_{21}}{B_{25}}\bar{z}' - \frac{B_{26}}{B_{25}}$$

I. INTRODUCTION

A chronological review of early spacecraft types, and the stability criteria developed for them, provides a sufficient background for the fundamental concepts of this thesis. The revised energy-sink stability criterion is then presented, and an equation for nutation angle as a function of energy dissipation over time is developed.

A. SINGLE SPIN SATELLITES

1. Equations of Motion

The earliest satellites took advantage of the fact that stability could be achieved via the 'gyroscopic stiffness' of a spinning body. A preliminary dynamic model for the satellite could be achieved with Euler's equations of motion for a rigid body. Eu' moment equation can be written as

$$\mathbf{M} = \frac{N d \mathbf{h}}{dt} = \frac{B d \mathbf{h}}{dt} + N \vec{\omega}^B \times \mathbf{h} \quad (1)$$

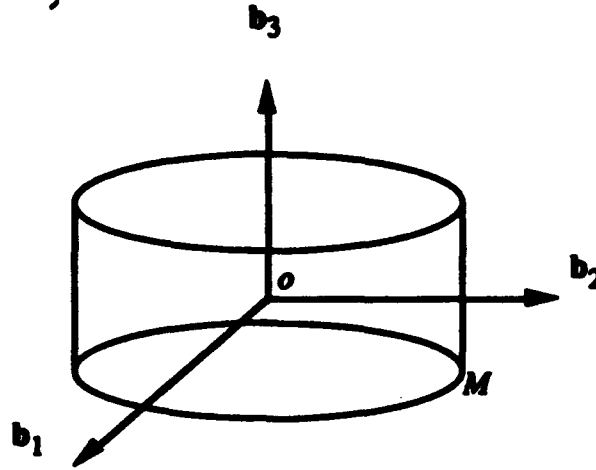
In component form this becomes

$$\begin{aligned} M_1 &= \dot{h}_1 + \omega_2 h_3 - \omega_3 h_2 \\ M_2 &= \dot{h}_2 + \omega_3 h_1 - \omega_1 h_3 \\ M_3 &= \dot{h}_3 + \omega_1 h_2 - \omega_2 h_1 \end{aligned} \quad (2)$$

Simplification of the model is accomplished by assuming that it is axisymmetric, that the body-fixed axes coincide with the principal axes (correct for simple spacecraft with $I_1 = I_2$), and that the body is in a torque-free environment (a valid approximation used throughout this thesis). The spacecraft is then represented by Figure (1) and the equations

of motion are

$$\begin{aligned} 0 &= I_1 \dot{\omega}_1 + (I_3 - I_1) \omega_2 \omega_3 \\ 0 &= I_2 \dot{\omega}_2 + (I_1 - I_2) \omega_3 \omega_1 \\ 0 &= I_3 \dot{\omega}_3 \end{aligned} \quad (3)$$



Axisymmetric Rigid Body

Figure (1)

The angular velocity vector, angular momentum vector, and the kinetic energy may be expressed respectively as

$$\vec{\omega} = \omega_1 \mathbf{b}_1 + \omega_2 \mathbf{b}_2 + \omega_3 \mathbf{b}_3 \quad (4)$$

$$\mathbf{h} = I_1 \omega_1 \mathbf{b}_1 + I_2 \omega_2 \mathbf{b}_2 + I_3 \omega_3 \mathbf{b}_3 \quad (5)$$

$$E = \frac{1}{2} (I_1 \omega_1^2 + I_2 \omega_2^2 + I_3 \omega_3^2) \quad (6)$$

A simplification of the notation can be made. Let $I_1 = I_2 = I_t$ and $I_3 = I_s$. From the third line of Equation (3) it can be seen that the angular velocity about the spin axis \mathbf{b}_3 is constant, therefore $\omega_3 = \omega_s$. The transverse angular velocity components interchange between the \mathbf{b}_1 and the \mathbf{b}_2 axes but the magnitude is constant, so one can let

$\vec{\omega} = \omega_1 \mathbf{b}_1 + \omega_2 \mathbf{b}_2$. Therefore,

$$N \vec{\omega} = \vec{\omega} + \omega_3 \mathbf{b}_3 \quad (7)$$

$$\mathbf{h} = I_1 \vec{\omega} + I_3 \omega_3 \mathbf{b}_3 \quad (8)$$

$$h^2 = I_1^2 \omega_1^2 + I_3^2 \omega_3^2 \quad (9)$$

$$E = \frac{1}{2} (I_1 \omega_1^2 + I_3 \omega_3^2) \quad (10)$$

Because the motion is torque-free, $|\mathbf{h}|$ is constant and \mathbf{h} is fixed in space. Because there are no energy sources or sinks, E is also constant. Finally, the above conditions result in $N \vec{\omega}$ being a constant.

An expression for the nutation angle may now be developed. The orientation of the body axes with respect to an inertial reference frame is desired to provide a measure of the body's dynamic behavior. Because the angular momentum vector is fixed in space, the nutation angle is defined as the angle between the body-fixed axis about which spin is desired and the angular momentum vector, and can be expressed in one of the following forms

$$\theta = \cos^{-1} \left(\frac{\mathbf{h} \cdot \mathbf{b}_3}{|\mathbf{h}|} \right) = \cos^{-1} \left(\frac{h_3}{|\mathbf{h}|} \right) = \cos^{-1} \left(\frac{I_3 \omega_3}{|\mathbf{h}|} \right) = \cos^{-1} \left(\frac{I_3 \omega_s}{|\mathbf{h}|} \right) \quad (11)$$

$$\theta = \sin^{-1} \left(\frac{h_1 \mathbf{b}_1 + h_2 \mathbf{b}_2}{|\mathbf{h}|} \right) = \sin^{-1} \left(\frac{I_1 \omega_1 \mathbf{b}_1 + I_2 \omega_2 \mathbf{b}_2}{|\mathbf{h}|} \right) = \sin^{-1} \left(\frac{I_1 \omega_d}{|\mathbf{h}|} \right) \quad (12)$$

$$\theta = \tan^{-1} \left(\frac{h_1 \mathbf{b}_1 + h_2 \mathbf{b}_2}{h_3 \mathbf{b}_3} \right) = \tan^{-1} \left(\frac{I_1 \omega_1 \mathbf{b}_1 + I_2 \omega_2 \mathbf{b}_2}{I_3 \omega_3 \mathbf{b}_3} \right) = \tan^{-1} \left(\frac{I_1 \omega_d}{I_3 \omega_s} \right) \quad (13)$$

In these equations the first and second terms correspond to the general case with spin about the \mathbf{b}_3 axis, and the third term uses the simplified notation to describe an axisymmetric body. In the special case of spin about only one principal axis of an axisymmetric body, the angular momentum vector and the angular velocity vector will lie on the spin axis. With spin components on two or more principal axes, the three vectors will not be coincident, although they still will lie on the same plane.

2. Single Spin Satellite Stability

A torque-free, axisymmetric rigid body with the body axes coinciding with the principle moments of inertia will be stable about the axis of either the maximum moment of inertia or the minimum moment of inertia. To prove this, one begins with an arbitrary rigid body. The body is given the initial condition of steady angular velocity, ω_0 , about a principal axis, and is then perturbed slightly. It is assumed that the angular velocities about the other axes are small, and are approximately the same order of magnitude as the perturbation ($\omega_1 = \omega_2 = \epsilon$). The system will be considered stable if the perturbation does not increase over time. Given an initial angular velocity with a perturbation, ${}^N\vec{\omega} = \omega_1 \mathbf{b}_1 + \omega_2 \mathbf{b}_2 + (\omega_0 + \epsilon) \mathbf{b}_3$, and given arbitrary inertias I_1, I_2, I_3 , Euler's equations of motion can be written as

$$\begin{aligned} 0 &= I_1 \dot{\omega}_1 + (I_3 - I_2) \omega_2 (\omega_0 + \epsilon) \\ 0 &= I_2 \dot{\omega}_2 + (I_1 - I_3) \omega_1 (\omega_0 + \epsilon) \\ 0 &= I_3 \dot{\omega}_3 + (I_2 - I_1) \omega_1 \omega_2 \end{aligned} \tag{14}$$

The equations are linearized by neglecting terms of magnitude ϵ^2 . Rewriting the equations by eliminating the terms $\epsilon \omega_1$, $\epsilon \omega_2$, and $\omega_1 \omega_2$ results in

$$\dot{\omega}_1 = \frac{(I_2 - I_3)}{I_1} \omega_2 \omega_0 \tag{15}$$

$$\dot{\omega}_2 = \frac{(I_3 - I_1)}{I_2} \omega_1 \omega_0 \tag{16}$$

$$\dot{\omega}_3 = \dot{\omega}_0 + \dot{\epsilon} = \dot{\epsilon} = 0 \tag{17}$$

From Equation (17), one can conclude that $\epsilon \equiv \text{constant}$. By differentiating Equation (15), and using Equation (16) to eliminate $\dot{\omega}_2$, one gets

$$\ddot{\omega}_1 + \left(\frac{(I_3 - I_2)(I_3 - I_1)}{I_1 I_2} \omega_0^2 \right) \omega_1 = 0 \tag{18}$$

Similarly, from differentiating Equation (16), and using Equation (15) to eliminate $\dot{\omega}_1$, one

arrives at

$$\ddot{\omega}_2 + \left(\frac{(I_3 - I_2)(I_3 - I_1)}{I_1 I_2} \omega_0^2 \right) \omega_2 = 0 \quad (19)$$

These equations are identified as second order, linear, ordinary differential equations with constant coefficients. The general solution for these differential equations are

$$\omega_1 = K_1 e^{i\gamma t} + K_2 e^{-i\gamma t} \quad (20)$$

$$\omega_2 = K_3 e^{i\gamma t} + K_4 e^{-i\gamma t} \quad (21)$$

where

$$\gamma = \sqrt{\frac{(I_3 - I_2)(I_3 - I_1)}{I_1 I_2} \omega_0^2} \quad (22)$$

If γ is imaginary, ω_1 and ω_2 will increase without bound over time, and the motion will be unstable. Stability is achieved if γ is real. The first case occurs when the maximum moment of inertia is about the spin (b_3) axis; then $I_3 > I_1$, $I_3 > I_2$, and $(I_3 - I_2)(I_3 - I_1) > 0$. In this case the inertia ratio I_s / I_t , defined as the inertia about the spin axis over the inertia about a transverse axis, is greater than one. The second case occurs when the minimum moment of inertia is about the spin (b_3) axis; then $I_3 < I_1$, $I_3 < I_2$, and $(I_3 - I_2)(I_3 - I_1) > 0$ as well. Here the inertia ratio is less than one. In both of the above cases γ is real and the motion is stable. However, if I_3 is the intermediate moment of inertia about the spin (b_3) axis, then $(I_3 - I_2)(I_3 - I_1) < 0$, γ is imaginary, and the motion is unstable.

The previous model cannot be applied to a satellite since the assumption of a rigid body cannot be extended to the spacecraft. Structural elasticity, liquid propellant slosh, etc., cause energy dissipation in an actual spacecraft. This spacecraft can be generalized by a quasi-rigid body with an unspecified energy damper mechanism. A priori, one can conclude that energy in the above system will dissipate until the minimum energy state is reached. The kinetic energy of the system with spin about the principal axis with maximum moment of inertia and spin about the principal axis with minimum moment of inertia can be

written respectively as

$$\begin{aligned} E &= \frac{1}{2} \frac{h^2}{I_{max}} & I_{max} \text{ about } b_3 \\ E &= \frac{1}{2} \frac{h^2}{I_{min}} & I_{min} \text{ about } b_3 \end{aligned} \quad (23)$$

The angular momentum is constant in the torque-free case. Thus the minimum kinetic energy state occurs when the rotation is about the axis of the maximum moment of inertia. Therefore, a quasi-rigid body is stable only when it is spinning about its major axis, with a corresponding inertia ratio that is greater than one.

A relationship can be established between the time rate of change of the nutation angle and the energy dissipation of a quasi-rigid, axisymmetric body. One must assume that the angular momentum and moments of inertia of the quasi-rigid body do not change appreciably from a comparable rigid body. For the generalized model, with arbitrary inertias $I_1 = I_2$, and I_3 , Equations (5) and (6) are substituted into Equation (12) to obtain

$$\sin^2 \theta = \left(\frac{I_1}{I_3 - I_1} \right) \frac{(2 I_3 E - h^2)}{h^2} \quad (24)$$

The time rate of change of the nutation angle is determined by taking the derivative of the above equation

$$\dot{\theta} = \frac{1}{\sin(2\theta)} \frac{2 I_1 I_3}{(I_3 - I_1) h^2} \dot{E}_{D \text{ total}} \quad (25)$$

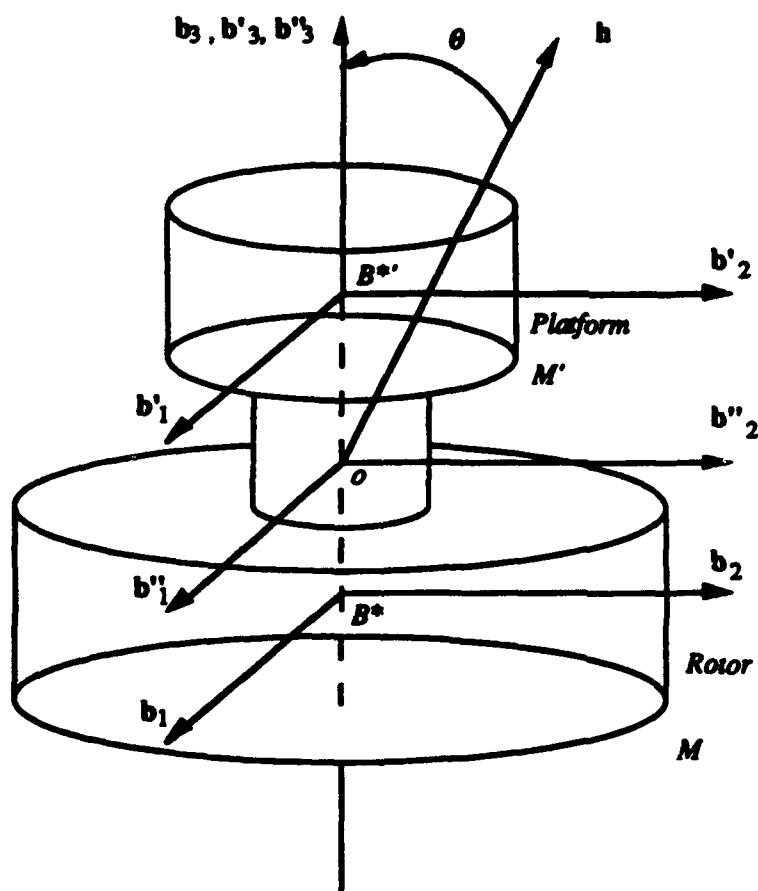
where the only rate of change of energy \dot{E} is attributed to the damping mechanism and is written as $\dot{E}_{D \text{ total}}$ to emphasize this point. Because $\dot{E}_{D \text{ total}}$ is negative, the nutation angle will decrease only if I_3 is greater than I_1 . This reaffirms the previous conclusion that a quasi-rigid body is spin stabilized only about the axis of maximum moment of inertia. The foregoing development is referred to as the energy-sink method.

B. DUAL SPIN SATELLITES

The logical progression from the single spin satellite was to incorporate a de-spun platform. This permitted the replacement of the low gain omnidirectional antenna with directional antennas for communication satellites, and a more capable spacecraft for scientific observation. A simple control system about the b_3 axis would maintain the platform rotating at a constant relative rate with respect to the rotor (and would usually have the platform rotate at the earth's rotational rate). Initially, the platforms were sufficiently small, and the overall dimensions of the satellite were such that the inertia ratio would be greater than one. For this type of satellite, the previously developed theory proved adequate. However, as satellites continued to grow in size, the launch vehicle shroud diameter became a constraint. In order to provide the size spacecraft needed to satisfy mission requirements and still fit within the shroud, a spacecraft with an inertia ratio of less than one ($I_{s \text{ total}} / I_{t \text{ total}} < 1$) would need to be built. From the previously developed theory, a spacecraft with an inertia ratio of less than one was believed to be inherently unstable. It was not until the development of the energy-sink theory for dual-spin, quasi-rigid, axisymmetric spacecraft containing a driven rotor, developed simultaneously by V. D. Landon (unpublished work) and A. J. Iorillo [Ref. 1], that a spacecraft with an inertia ratio less than one was considered feasible. Several rigorous stability analyses using the equations of motion for specific dual spinners have been performed by P. W. Likins [Ref. 2], D. L. Mingori [Ref. 3], and others, to validate the energy-sink theory. The difficulty of a rigorous analysis is in accurately modeling all the forms of energy dissipation. A more general and practical approach was required to determine stability, and the energy-sink theory proved suitable. The development of this theory is as follows.

The spacecraft, shown in Figure (2), is assumed to fulfill the following conditions:

- Both the rotor and the platform are axisymmetric
- Both the rotor and the platform are quasi-rigid
- The damping mechanisms do not significantly alter the energy value, although the mechanisms will contribute to the energy rate
- No external torques are applied
- The only relative motion is spin about the b_3 axis
- The motor, driven by the control system, inputs just enough energy to exactly offset the shaft frictional losses, maintaining a constant relative angular velocity between the rotor and the platform



Dual-Spin Quasi-Rigid Axisymmetric Spacecraft

Figure (2)

The magnitude of the angular momentum and the kinetic energy of the dual-spin system can be expressed respectively by the following equations

$$h^2 = I_{i, total}^2 \omega_i^2 + (I_s \omega_s + I_s' \omega_s')^2 = I_{i, total}^2 \omega_i^2 + (I_s \sigma + I_{s, total} \omega_s')^2 \quad (26)$$

$$E = \frac{1}{2} I_{i, total} \omega_i^2 + \frac{1}{2} I_s \omega_s^2 + \frac{1}{2} I_s' \omega_s'^2 = \frac{1}{2} I_{i, total} \omega_i^2 + \frac{1}{2} I_{s, total} \omega_s'^2 + \frac{1}{2} I_s \sigma^2 + I_s \omega_s' \sigma \quad (27)$$

where σ is the relative rotation rate of the rotor with respect to the platform. Although the equations actually represent a rigid body system, they are also applicable to the quasi-rigid system because of the above assumptions. If the damping mechanisms do make significant contributions to the energy of the system, then Equations (26) and (27) do not hold, and the energy-sink criterion will not apply. Additionally, the potential energy of the system (for example the energy stored in the spring of a mass-spring-dashpot damper) will not make a significant contribution to the total energy of the system. Therefore, for the remainder of the thesis, it is assumed that the kinetic energy of the system is effectively the total energy of the system ($E \equiv E_{total}$). Because the system experiences no external torques, angular momentum is conserved. Because the motor contributes no energy to the system, the time rate of change of the kinetic energy \dot{E} is represented by only the quasi-rigid energy dissipation $\dot{E}_{D, total}$, and is negative. Differentiating the above two equations with respect to time, one obtains

$$0 = I_{i, total}^2 \omega_i \dot{\omega}_i + (I_s \omega_s + I_s' \omega_s') (I_s \dot{\omega}_s + I_s' \dot{\omega}_s') \quad (28)$$

$$\dot{E} = \dot{E}_{D, total} = I_{i, total} \omega_i \dot{\omega}_i + I_s \omega_s \dot{\omega}_s + I_s' \omega_s' \dot{\omega}_s' \quad (29)$$

Eliminating the common term $\omega_i \dot{\omega}_i$ by combining the above equations

$$\dot{E} = \dot{E}_{D, total} = \frac{-(I_s \omega_s + I_s' \omega_s') (I_s \dot{\omega}_s + I_s' \dot{\omega}_s')}{I_{i, total}} + I_s \omega_s \dot{\omega}_s + I_s' \omega_s' \dot{\omega}_s' \quad (30)$$

One may now define the inertial nutation frequency, λ_0 , the rotor nutation frequency,

λ , and the platform nutation frequency, λ' , as follows

$$\lambda_0 = \frac{I_s \omega_s + I_s' \omega_s'}{I_{t \text{ total}}} \quad (31)$$

$$\lambda = \lambda_0 - \omega_s = \frac{(I_s - I_{t \text{ total}}) \omega_s + I_s' \omega_s'}{I_{t \text{ total}}} \quad (32)$$

$$\lambda' = \lambda_0 - \omega_s' = \frac{I_s \omega_s + (I_s' - I_{t \text{ total}}) \omega_s'}{I_{t \text{ total}}} \quad (33)$$

The nutation angle for a dual-spin system is defined as

$$\theta = \cos^{-1} \left(\frac{\mathbf{h} \cdot \mathbf{b}_3}{|\mathbf{h}|} \right) = \cos^{-1} \left(\frac{h_3 + h_3'}{|\mathbf{h}|} \right) = \cos^{-1} \left(\frac{I_s \omega_s + I_s' \omega_s'}{|\mathbf{h}|} \right) \quad (34)$$

By imposing the condition

$$\lambda_0 > 0 \quad (35)$$

the analysis of nutational motion is restricted to the following region without any loss of generality

$$0 \leq \theta \leq \frac{\pi}{2} \quad (36)$$

Incorporating the nutation frequency terms, the equation for energy dissipation is written as

$$\dot{E} = \dot{E}_{D \text{ total}} = \dot{E}_D + \dot{E}_{D'} = -I_s \lambda \dot{\omega}_s - I_s' \lambda' \dot{\omega}_s' \quad (37)$$

Recalling the assumption that the rotor and platform are uncoupled about the \mathbf{b}_3 axis, we may incorporate Equation (37) into the reaction torques which tend to change the angular rates

$$\begin{aligned} I_s \dot{\omega}_s &= -\frac{\dot{E}_D}{\lambda} \\ I_s' \dot{\omega}_s' &= -\frac{\dot{E}_{D'}}{\lambda'} \end{aligned} \quad (38)$$

Combining Equation (30), (37), and (38), one arrives at the transverse rate equation

$$I_{t \text{ total}} \omega_t \dot{\omega}_t = \lambda_0 \left(\frac{\dot{E}_D}{\lambda} + \frac{\dot{E}_{D'}}{\lambda'} \right) \quad (39)$$

Differentiating Equation (12) and substituting Equation (39) into it, the time rate of change of nutation angle as a function of energy dissipation rates is

$$\dot{\theta} = \frac{2 I_{t \text{ total}} \lambda_0}{\sin(2\theta) h^2} \left(\frac{\dot{E}_D}{\lambda} + \frac{\dot{E}_{D'}}{\lambda'} \right) \quad (40)$$

The energy-sink equation for a single spin-stabilized body is obtained by letting λ and λ' become λ_0 and $\dot{E}_D + \dot{E}_{D'}$ become $\dot{E}_{D \text{ total}}$ for a single body. The definition of stability requires the nutation angle θ to remain constant or decrease as a function of time, so that $\dot{\theta}$ is zero or negative. Because the factors outside the parenthesis on the right hand side of Equation (40) are positive, the stability criterion for a dual-spin, quasi-rigid, axisymmetric system becomes

$$\boxed{\frac{\dot{E}_D}{\lambda} + \frac{\dot{E}_{D'}}{\lambda'} \leq 0} \quad (41)$$

One of the following cases will guarantee stability

- 1) $\lambda > 0$ and $\lambda' > 0$
- 2) $\lambda > 0$, $\lambda' < 0$, and $\left| \frac{\dot{E}_{D'}}{\lambda'} \right| < \left| \frac{\dot{E}_D}{\lambda} \right|$
- 3) $\lambda < 0$, $\lambda' > 0$, and $\left| \frac{\dot{E}_{D'}}{\lambda'} \right| > \left| \frac{\dot{E}_D}{\lambda} \right|$

A specific example would be the model of a typical communications satellite, a prolate dual-spinner possessing an inertia ratio of less than one. In general, the rotor nutation

frequency, expressed as

$$\lambda = \frac{I_s \omega_s + I_s' \omega_s'}{I_{t \text{ total}}} - \omega_s = \frac{(I_s - I_{t \text{ total}}) \omega_s + I_s' \omega_s'}{I_{t \text{ total}}} \quad (42)$$

would be negative because $(I_s - I_{t \text{ total}})$ is negative and $\omega_s \gg \omega_s'$ if ω_s' is rotating at the earth's rotation rate. Thus, energy damping in the rotor, \dot{E}_D , would be destabilizing while energy damping in the platform, \dot{E}_D' , would be stabilizing. It is from this result that satellites will have a damping mechanism placed on the platform to improve nutational stability. Such a damper is called a nutation damper.

II. PROBLEM DEFINITION

A. OVERVIEW

The existing energy-sink theory relies on several assumptions, perhaps the most important relating to the driven rotor. As previously stated, it has been assumed that the motor, driven by the control system, inputs just enough energy to exactly offset the shaft frictional losses, maintaining a constant relative angular velocity between the rotor and the platform. In actual systems, contrary to this assumption, the motor may add or remove energy from the system, depending on the dynamics of the spacecraft. Consequently, a revised energy sink stability theory, properly accounting for the energy contribution of the motor, is derived. The revised theory, based on the concept of core energy, will remain consistent with the existing energy-sink stability criterion. Continuing, an equation for nutation angle over time, as a function of core energy, is developed. Given a postulated energy dissipation function modeling the nutation dampers, structural elasticity, fuel slosh, etc., one can accurately predict the nutation angle behavior. Numerical simulation of D. L. Mingori's dual-spin, quasi-rigid, axisymmetric system containing a driven rotor [Ref. 3] is used to validate the revised energy-sink stability theory. The predicted nutation angle, based on this revised energy-sink theory, and the postulated energy dissipation function, is compared to the exact nutation angle of the Mingori system. By using a suitable postulated energy dissipation function, one can achieve excellent agreement between the predicted and the exact nutation angle. I. Michael Ross [Ref. 4] performed this analysis on a dual spin system with a damper on the platform only. The remainder of this thesis will use the same analysis, but on the Mingori system with dampers on both the rotor and the platform.

B. INCONSISTENCY OF THE ENERGY SINK THEORY

There exists a contradiction between the existing energy-sink theory and the nutation angle derived from it. This will provide the motivation for developing a revised energy-sink theory and an alternative equation for nutation angle over time. From before, the existing energy-sink stability criterion can be expressed as

$$\boxed{\frac{\dot{E}_D}{\lambda} + \frac{\dot{E}_D'}{\lambda'} \leq 0} \quad (41)$$

and the nutation angle for the dual-spin system was defined as

$$\theta = \cos^{-1} \left(\frac{\mathbf{h} \cdot \mathbf{b}_3}{|\mathbf{h}|} \right) = \cos^{-1} \left(\frac{h_3 + h_3'}{|\mathbf{h}|} \right) = \cos^{-1} \left(\frac{I_s \omega_s + I_s' \omega_s'}{|\mathbf{h}|} \right) \quad (34)$$

As previously stated, for a prolate dual-spinner ($I_{s \text{ total}} / I_{t \text{ total}} < 1$), energy dissipation in the platform is stabilizing and energy dissipation in the rotor is destabilizing. The angular velocity of the platform about the spin axis, ω_s' , can be expressed in terms of the angular momentum and the kinetic energy of the system. Combining Equation (26) and Equation (27), one arrives at

$$\omega_s' = -\frac{I_s \sigma}{I_{s \text{ total}}} \pm \sqrt{\left(\frac{I_s \sigma}{I_{s \text{ total}}} \right)^2 - \frac{h^2 - 2 I_{t \text{ total}} E + I_s \sigma^2 (I_{t \text{ total}} - I_s)}{I_{s \text{ total}} (I_{t \text{ total}} - I_s)}} \quad (42)$$

Substituting this expression into Equation (34) results in

$$\theta = \cos^{-1} (\pm \sqrt{\tilde{Q}}) \quad (43)$$

where \tilde{Q} is represented as

$$\tilde{Q} = \frac{(2 E - I_s \sigma^2) I_{s \text{ total}} + I_s^2 \sigma^2}{h^2 \left(1 - \frac{I_{s \text{ total}}}{I_{t \text{ total}}} \right)} - \frac{I_{s \text{ total}}}{I_{t \text{ total}} - I_{s \text{ total}}} \quad (44)$$

Initial conditions at $t = 0$ will determine the correct sign, with continuity considerations maintaining the sign for all of $t > 0$. Additionally, no external torques are applied to this

system, resulting in $|\mathbf{h}|$ being constant. Differentiation of Equation (43) results in

$$\dot{\theta} = -\frac{1}{\sqrt{1-(\pm\sqrt{Q})^2}} \frac{d}{dt}(\pm\sqrt{Q}) = \pm \frac{1}{\sin\theta} \frac{1}{\sqrt{Q}} \frac{(-\dot{E}_{D \text{ total}}) I_{S \text{ total}}}{h^2 \left(1 - \frac{I_{S \text{ total}}}{I_{I \text{ total}}}\right)} \quad (45)$$

From the definition of nutation angle, Equation (34), and the condition imposed on it, Equation (36), the positive sign must be chosen in Equations (43) and (45). An important observation is made at this time. Choosing the positive sign will result in a positive rate of change in the nutation angle, indicating an unstable condition. The relative rotor spin rate is an independent variable, and is arbitrarily selected here as a constant value over time. Therefore, energy dissipation in a prolate dual-spin spacecraft will make the nutation angle increase, regardless of whether the dissipation is in the platform or in the rotor. This is not consistent with the stability criterion of Equation (41). Thus, the existing energy-sink stability criterion contradicts itself.

C. CORE ENERGY AND ENERGY DISSIPATION

The existing energy-sink stability criterion does not properly account for any energy that may be provided by, or absorbed by, the motor. To accurately represent the system, the total rate of change of energy must be written as

$$\dot{E} = \dot{E}_{D \text{ total}} + \dot{W} \quad (46)$$

where \dot{W} is the rate of work due to the motor, and may be either positive or negative and the rate of change of energy due to dissipative elements can occur in either the platform or the rotor. Recall that the kinetic energy of the dual-spin system was expressed in Equation (27). If the work due to the motor torque as a function of time is written in analytical form, then the time rate of change of the energy of the system due to all dissipative elements, $\dot{E}_{D \text{ total}}$, can then be expressed solely in terms of the quasi-rigid parameters of the dual-spin system. With this expression, the condition that $\dot{E}_{D \text{ total}} \leq 0$ will result in the required

stability criterion. The difficulty arises in that to get the work due to the motor torque W (or \dot{W}), one needs to know the exact dynamics of the dissipative mechanism. In the development of the modified energy-sink stability, Equation (46) will be used to determine the expression for \dot{E}_D and ultimately derive the revised stability criterion and nutation angle equation.

Additionally, the existing energy-sink theory can be shown to be incorrect for both the case of total energy decreasing and for the case of total energy increasing. For example, if the rotor is rigid and total energy decreases, Equation (41) predicts that the system will be stable, but Equation (45) predicts that it will be unstable. Allowing the total energy to increase would reverse the conditions, but still show a contradiction between Equation (41) and Equation (45).

A modification of the energy-sink stability theory and the associated expression for nutation angle is now presented. The development of the theory is from I. Michael Ross' unpublished notes. The basis of the new theory is centered on the core energy of the system. As defined by Hubert [Ref. 5]

Core energy is the total energy of the spacecraft minus the portion of the rotor energy that is due to the relative rotation between the rotor and the platform. It is assumed that the mass, inertia, and motion of the damping device are sufficiently small that its energy is negligible relative to the spacecraft core energy. The damper will be treated as an undefined 'energy sink' for the purposes of the energy sink analysis.

From the above statement one can define the core body as that body whose inertial dynamics are selected for analysis. Hubert defines the platform as the core body. The core energy is simply the rotational kinetic energy of a fictitious rigid body that possesses the inertia properties of the entire dual-spinner but moves in inertial space exactly like the core

body. For a dual-spin spacecraft the platform core energy is defined as

$$E_C' = \frac{1}{2} I_{1 \text{ total}} \omega_1'^2 + \frac{1}{2} I_{2 \text{ total}} \omega_2'^2 + \frac{1}{2} I_{3 \text{ total}} \omega_3'^2 = \frac{1}{2} I_{1 \text{ total}} \omega_i'^2 + \frac{1}{2} I_{s \text{ total}} \omega_s'^2 \quad (47)$$

The center expression is for an arbitrary dual-spin spacecraft with the spin axis about the b_3 axis, and the right expression is for a dual-spin, axisymmetric spacecraft with the simplified notation. Extending this concept to the rotor, the rotor core energy is defined as

$$E_C = \frac{1}{2} I_{1 \text{ total}} \omega_1^2 + \frac{1}{2} I_{2 \text{ total}} \omega_2^2 + \frac{1}{2} I_{3 \text{ total}} \omega_3^2 = \frac{1}{2} I_{1 \text{ total}} \omega_i^2 + \frac{1}{2} I_{s \text{ total}} \omega_s^2 \quad (48)$$

Necessary to the development of the modified theory is what will be termed the Separation Axiom. This is when analysis is first performed with the rotor considered rigid and the platform quasi-rigid. Euler's equations are written for the rotor, and through manipulation, an equation is derived relating the torque on the quasi-rigid platform solely in terms of platform variables. Then the platform is considered rigid and the rotor quasi-rigid. An equation is derived relating the torque on the quasi-rigid rotor solely in terms of rotor variables. These two separate equations are then combined and applied to a system in which the rotor and the platform may both be quasi-rigid.

The case of a rigid rotor with a quasi-rigid platform is first analyzed. Because the rotor is rigid, the torque applied by the motor to the rotor is the net torque on the rotor and is determined from Euler's moment equations. For the case of the axisymmetric rotor,

$$T_R = T_{R/M} = I_s \dot{\omega}_s \quad (49)$$

One can observe that $T_{P/M} = -T_{R/M}$, but $T_P \neq T_R$ since the damping mechanism contributes additional torques to the quasi-rigid platform. The rate of work needed by the motor torque to maintain constant relative motion between the rotor and the platform is

$$\dot{W} = T_R \sigma = I_s \sigma \dot{\omega}_s = I_s \sigma (\dot{\omega}_s' + \dot{\sigma}) \quad (50)$$

By substituting the platform core energy, Equation (47), into the kinetic energy expression,

Equation (27), kinetic energy may be expressed as

$$E = E_C' + \frac{1}{2} I_s \sigma^2 + I_s \omega_s' \sigma \quad (51)$$

The above equation is differentiated to arrive at the time rate of change of the kinetic energy of the dual-spin system

$$\dot{E} = \dot{E}_C' + I_s \sigma \dot{\sigma} + I_s (\sigma \dot{\omega}_s' + \omega_s' \dot{\sigma}) = \dot{E}_C' + I_s \sigma (\dot{\omega}_s' + \dot{\sigma}) + I_s \omega_s' \dot{\sigma} \quad (52)$$

Substituting into this equation the rate of work done by the motor torque, Equation (50), one gets

$$\dot{E} = \dot{E}_C' + \dot{W} + I_s \omega_s' \dot{\sigma} \quad (53)$$

Comparing this to Equation (46), it can be seen that

$$\dot{E}_{D \text{ total}} = \dot{E}_C' + I_s \omega_s' \dot{\sigma} \quad (54)$$

Taking the derivative of Equation (47) to get the time rate of change of the platform core energy

$$\dot{E}_C' = I_{t \text{ total}} \omega_t \dot{\omega}_t + I_{s \text{ total}} \omega_s' \dot{\omega}_s' \quad (55)$$

and then substituting this into Equation (54), one arrives at the total energy dissipation of a rigid rotor, quasi-rigid platform system

$$\begin{aligned} \dot{E}_{D \text{ total}} &= I_{t \text{ total}} \omega_t \dot{\omega}_t + I_{s \text{ total}} \omega_s' \dot{\omega}_s' + I_s \omega_s' \dot{\sigma} \\ &= I_{t \text{ total}} \omega_t \dot{\omega}_t + I_s \omega_s' \dot{\omega}_s' + I_s' \omega_s' \dot{\omega}_s' + I_s \omega_s' \dot{\sigma} \end{aligned} \quad (56)$$

Because the system has no external forces applied, it remains torque-free. Thus, Equation (28) can be used to eliminate the $\omega_t \dot{\omega}_t$ term and arrive at

$$\dot{E}_{D \text{ total}} = (I_s \dot{\omega}_s + I_s' \dot{\omega}_s') \left[\frac{(I_{t \text{ total}} - I_{s \text{ total}}) \omega_s' - I_s \sigma}{I_{t \text{ total}}} \right] \quad (57)$$

Noting that the platform nutational frequency, Equation (33), can be written as

$$\lambda' = \lambda_0 - \omega_s' = \left(\frac{I_s \omega_s + I_s' \omega_s'}{I_{t \text{ total}}} \right) - \omega_s' = \frac{(I_{s \text{ total}} - I_{t \text{ total}}) \omega_s' + I_s \sigma}{I_{t \text{ total}}} \quad (58)$$

then Equation (57) can be written as

$$\dot{E}_{D \text{ total}} = (I_s \dot{\omega}_s + I_s' \dot{\omega}_s')(-\lambda') = \dot{\lambda}_0 I_t (-\lambda') \quad (59)$$

Referring to Equation (34), the nutation angle can be written as

$$\cos \theta = \left(\frac{I_s \omega_s + I_s' \omega_s'}{|\mathbf{h}|} \right) \quad (60)$$

Taking the derivative and comparing it to the rate of total energy dissipation, Equation (59), the following relationship can be established

$$-\dot{\theta} \sin \theta = \left(\frac{I_s \dot{\omega}_s + I_s' \dot{\omega}_s'}{|\mathbf{h}|} \right) = \frac{-\dot{E}_{D \text{ total}}}{\lambda' |\mathbf{h}|} \quad (61)$$

Because the rotor is rigid, all energy dissipation will occur in the platform, such that

$$\frac{\dot{E}_{D'}}{\lambda'} = |\mathbf{h}| \dot{\theta} \sin \theta \quad (62)$$

Equations (61) and (62) can be rewritten by including the motor torque, Equation (49), as

$$-|\mathbf{h}| \dot{\theta} \sin \theta = T_R + I_s' \dot{\omega}_s' = \frac{-\dot{E}_{D'}}{\lambda'} \quad (63)$$

Because $T_{P/M} = -T_{R/M}$ (action - reaction pair), the final relationship is written as

$$T_{P/M} = \frac{\dot{E}_{D'}}{\lambda'} + I_s' \dot{\omega}_s' \quad (64)$$

This equation describes the motor torque on the quasi-rigid platform as a function of platform variables only. It can be seen at this point that the classical analysis can be

achieved by assuming no torque is applied by the motor, resulting in $T_{P/M} = 0$ and

$$\frac{\dot{E}_D'}{\lambda'} = -I_s' \dot{\omega}_s' \quad (65)$$

This analysis can now be performed on the system containing a quasi-rigid rotor and a rigid platform. It is observed that the selection of the body to be the rotor and the body to be the platform is completely arbitrary, and no physical distinction exists between the two bodies. Therefore, by analogy, the equation describing the torque on the quasi-rigid rotor as a function of rotor variables must be

$$T_{R/M} = \frac{\dot{E}_D}{\lambda'} + I_s \dot{\omega}_s \quad (66)$$

Now let $T_{P/M}^*$ and $T_{R/M}^*$ represent the motor torques on the platform and on the rotor respectively for the system containing both a quasi-rigid rotor and a quasi-rigid platform. Then the separation axiom would require the following two conditions

$$T_{P/M}^* = T_{P/M} = \frac{\dot{E}_D'}{\lambda'} + I_s' \dot{\omega}_s' \quad (67)$$

$$T_{R/M}^* = T_{R/M} = \frac{\dot{E}_D}{\lambda} + I_s \dot{\omega}_s \quad (68)$$

Once again, since the system is an action - reaction pair

$$T_{P/M}^* + T_{R/M}^* = 0 \quad (69)$$

and then

$$\frac{\dot{E}_D}{\lambda} + \frac{\dot{E}_D'}{\lambda'} = -(I_s \dot{\omega}_s + I_s' \dot{\omega}_s') = |\mathbf{h}| \dot{\theta} \sin \theta \quad (70)$$

The stability criterion dictates that $\dot{\theta}$ remain zero or be negative, thus

$$\frac{\dot{E}_D}{\lambda} + \frac{\dot{E}_{D'}}{\lambda'} \leq 0 \quad (1)$$

This is seen to be the existing energy sink criterion. Therefore, despite the presence of motor torque, the existing stability criterion still applies. Referring to Equations (67) and (68), the second term in the equations would represent the torque applied by the damping mechanism to the platform and the rotor respectively. Equations (67) and (68) state that the motor torque minus the damper torque will equal the net torque of the platform and the rotor respectively.

In determining the revised energy-sink stability theory, the energy dissipation equation for the system with no energy contribution from the motor, Equation (37), must be rewritten to account for the motor torque. Thus

$$\dot{E} = \dot{E}_{D \text{ total}} + \dot{W} = -I_s \lambda \dot{\omega}_s - I_s' \lambda' \dot{\omega}_s' \quad (71)$$

Substituting in Equations (67) and (68), one arrives at

$$\begin{aligned} \dot{E} = \dot{E}_{D \text{ total}} + \dot{W} &= \lambda \left(\frac{\dot{E}_D}{\lambda} - T_{R/M}^* \right) + \lambda' \left(\frac{\dot{E}_{D'}}{\lambda'} - T_{P/M}^* \right) \\ &= \dot{E}_D + \dot{E}_{D'} - (\lambda T_{R/M}^* + \lambda' T_{P/M}^*) \end{aligned} \quad (72)$$

By assigning the motor torque values as

$$T_M = T_{R/M}^* = -T_{P/M}^* \quad (73)$$

then the above equation can be rewritten as

$$\dot{E} = \dot{E}_{D \text{ total}} + \dot{W} = \dot{E}_D + \dot{E}_{D'} + T_M (\lambda' - \lambda) \quad (74)$$

Because the total time rate of change of energy dissipation equals the rate of change of energy dissipation in the rotor plus that in the platform, the rate of work due to the motor

torque must be

$$\dot{W} = T_M (\lambda' - \lambda) = T_M \sigma \quad (75)$$

Referring to the example from Chapter 1, the prolate dual-spin communications satellite, typically the rotor nutation frequency would be negative and the platform nutation frequency would be positive. For rotor spin-up $T_M > 0$ and the motor torque would add energy to the system, and for rotor spin-down $T_M < 0$ and the motor torque would remove energy from the system. For the arbitrary system, the motor torque, T_M , and the sign of the term $\lambda' - \lambda$ ($= \sigma$), would determine whether the motor adds or removes energy from the system.

The rates of change of the energies of the system may now be represented. Rewriting Equation (46) to determine the total energy dissipation of the system

$$\dot{E}_{D \text{ total}} = \dot{E} - \dot{W} \quad (76)$$

The rate of work due to the motor torque can be expressed by combining Equations (75) and (68) (or Equation (67)) to arrive at

$$\dot{W} = \frac{\dot{E}_D}{\lambda} \sigma + I_s \dot{\omega}_s \sigma \left(= -\frac{\dot{E}_D'}{\lambda'} \sigma - I_s' \dot{\omega}_s' \sigma \right) \quad (77)$$

The rate of change of the kinetic energy of the system as a function of platform core energy and system parameters was determined previously as

$$\dot{E} = \dot{E}_C' + I_s \sigma (\dot{\omega}_s' + \dot{\sigma}) + I_s \omega_s' \dot{\sigma} \quad (52)$$

Substituting the above two equations into Equation (76), the expression for total energy dissipation of the system may now be written as

$$\dot{E}_{D \text{ total}} = \dot{E}_C' + I_s \sigma (\dot{\omega}_s' + \dot{\sigma}) + I_s \omega_s' \dot{\sigma} - \frac{\dot{E}_D}{\lambda} \sigma - I_s \dot{\omega}_s \sigma \quad (78)$$

Because $\dot{\omega}_s' + \dot{\sigma} = \dot{\omega}_p$, this equation can be further simplified

$$\dot{E}_{D \text{ total}} = \dot{E}_C' + I_s \omega_s' \dot{\sigma} - \frac{\dot{E}_D}{\lambda} \sigma \quad (79)$$

Comparing this equation, representing the system with a quasi-rigid rotor and a quasi-rigid platform, with Equation (54), representing the system with a rigid rotor and a quasi-rigid platform, reveals an additional term, $-\frac{\dot{E}_D}{\lambda} \sigma$. The first term of Equation (79) represents the rate of change of core energy, with the platform as the core body. The second term will account for the change in energy associated with a change in the relative rotation rate of the rotor with respect to the platform. The final term accounts for the energy loss due to the quasi-rigidity of the rotor that is not represented in the platform core body expression.

The case that will be analyzed is that which occurs when there is a constant relative rotation rate between the platform and the rotor. For the remainder of the analysis, let

$$\dot{\sigma} = 0 \quad (80)$$

and the total rate of energy dissipation becomes

$$\dot{E}_{D \text{ total}} = \dot{E}_C' - \frac{\dot{E}_D}{\lambda} \sigma \quad (81)$$

Further simplification can be achieved by noting that $\sigma = \lambda' - \lambda$ and from Equation (37) that $\dot{E}_{D \text{ total}} = \dot{E}_D + \dot{E}_D'$. Therefore

$$\dot{E}_D + \dot{E}_D' = \dot{E}_C' - \dot{E}_D \left(\frac{\lambda' - \lambda}{\lambda} \right) \quad (82)$$

which reduces to

$$\frac{\dot{E}_D}{\lambda} + \frac{\dot{E}_D'}{\lambda'} = \frac{\dot{E}_C'}{\lambda'} \quad (83)$$

A similar development can be performed using rotor core energy vice platform core energy.

The result is

$$\frac{\dot{E}_D}{\lambda} + \frac{\dot{E}_D'}{\lambda'} = \frac{\dot{E}_C}{\lambda} \quad (84)$$

There is an expected symmetry between Equations (83) and (84), due to the arbitrary assignment of one body of the system as the rotor, and the other body as the platform. To confirm the results of Equations (83) and (84), one must prove that when σ is constant

$$\frac{\dot{E}_C}{\lambda} = \frac{\dot{E}_C'}{\lambda'} \quad (85)$$

Taking the derivative of the rotor core energy, Equation (48)

$$\begin{aligned} \dot{E}_C &= I_{t \text{ total}} \omega_t \dot{\omega}_t + I_{s \text{ total}} \omega_s \dot{\omega}_s \\ &= I_{t \text{ total}} \omega_t \dot{\omega}_t + I_{s \text{ total}} (\omega_s' + \sigma) (\dot{\omega}_s' + \dot{\sigma}) \end{aligned} \quad (86)$$

and similarly, for the platform core energy

$$\dot{E}_C' = I_{t \text{ total}} \omega_t \dot{\omega}_t + I_{s \text{ total}} \omega_s' \dot{\omega}_s' \quad (87)$$

Substituting Equation (87) into Equation (86) and noting that $\dot{\sigma} = 0$,

$$\dot{E}_C = \dot{E}_C' + I_{s \text{ total}} \sigma \dot{\omega}_s' \quad (88)$$

Multiplying through by the platform nutation frequency

$$\dot{E}_C \lambda' = \dot{E}_C' \lambda' + I_{s \text{ total}} \lambda' \sigma \dot{\omega}_s' \quad (89)$$

and recalling that $\lambda' = \lambda + \sigma$,

$$\dot{E}_C \lambda' = \dot{E}_C' \lambda + \dot{E}_C' \sigma + I_{s \text{ total}} \lambda' \sigma \dot{\omega}_s' \quad (90)$$

which is the same expression as Equation (85) if it can be proven that

$$\dot{E}_C' + I_{s \text{ total}} \lambda' \dot{\omega}_s' = 0 \quad (91)$$

Eliminating the transverse angular velocity of Equation (47) by substituting in Equation

(26), one arrives at

$$E_C' = \frac{1}{2} \left(\frac{h^2 - (I_s \omega_s + I_s' \omega_s')^2}{I_{s \text{ total}}} \right) + \frac{1}{2} I_{s \text{ total}} \omega_s'^2 \quad (92)$$

Taking the derivative

$$\dot{E}_C' = - \frac{(I_s \omega_s + I_s' \omega_s')(I_s \dot{\omega}_s + I_s' \dot{\omega}_s')}{I_{s \text{ total}}} + I_{s \text{ total}} \omega_s' \dot{\omega}_s' \frac{I_{s \text{ total}}}{I_{s \text{ total}}} \quad (93)$$

and simplifying

$$\dot{E}_C' = - \frac{(I_s^2 \omega_s \dot{\omega}_s + I_s I_s' \omega_s \dot{\omega}_s' + I_s I_s' \omega_s' \dot{\omega}_s - I_s'^2 \omega_s' \dot{\omega}_s')}{I_{s \text{ total}}} + I_{s \text{ total}} I_{s \text{ total}} \omega_s' \dot{\omega}_s' \quad (94)$$

Noting that $I_{s \text{ total}} = I_s + I_s'$ and recalling that $\dot{\omega}_s = \dot{\omega}_s'$ because $\dot{\sigma} = 0$, the above equation can be reduced to

$$\dot{E}_C' = -I_{s \text{ total}} \frac{(I_s \omega_s + I_s' \omega_s' - I_{s \text{ total}} \omega_s') \dot{\omega}_s}{I_{s \text{ total}}} \quad (95)$$

finally, invoking the definition of the platform nutation frequency, one arrives at

$$\dot{E}_C' = -I_{s \text{ total}} \lambda' \dot{\omega}_s \quad (96)$$

Therefore, Equation (91) holds and the revised stability criterion can be expressed as

$$\boxed{\frac{\dot{E}_C}{\lambda} = \frac{\dot{E}_C'}{\lambda'} = \frac{\dot{E}_D}{\lambda} + \frac{\dot{E}_D'}{\lambda'} \leq 0} \quad (97)$$

A few remarks can be made concerning this stability criterion. The third expression is the existing energy sink stability criterion. This criterion must equal the stability criterion as a function of the rotor core energy which must equal the stability criterion as a function of the platform core energy. It can be seen that one no longer needs to know the energy dissipation rates in the platform and in the rotor to determine stability. By knowing or postulating the core energy over time, the stability of the system can be determined.

Continuing with the prolate dual-spinner example of Chapter 1, any one of the above expressions apply. For a stable system, the rotor core energy will be positive, and increase over time. Additionally, the rotor nutation frequency will be negative, resulting in a negative expression for the rotor core energy stability criterion. The platform core energy will be positive, but will decrease over time. The platform nutation frequency will be positive, resulting in a negative expression for the platform stability criterion. According to Equation (97), the platform and rotor stability criteria must equal one another. From the numerical simulation of a dual-spin quasi-rigid axisymmetric system, the rotor and platform core energies as a function of time will be determined and graphed.

D. NUTATIONAL MOTION

The development of a modified expression for the nutation angle as a function of time may now be presented. The actual nutation angle of the system is defined as θ . The nutation angle as a function of platform core energy will be represented by η' , and the nutation angle as a function of rotor core energy will be represented by η . The derivation is similar to the one previously given in this chapter, except that the total energy of the system has been replaced by the core energy of the system to eliminate the transverse angular velocity, ω_t . The derivation for the platform core energy will be shown. From before, the angular momentum of the dual-spin, quasi-rigid, axisymmetric system is

$$h^2 = I_{t \text{ total}}^2 \omega_t^2 + (I_s \omega_s + I_s' \omega_s')^2 = I_{t \text{ total}}^2 \omega_t^2 + (I_s \sigma + I_{s \text{ total}} \omega_s')^2 \quad (26)$$

Combining this with the platform core energy, and solving for the platform angular velocity about the spin axis

$$I_{s \text{ total}} (I_{s \text{ total}} - I_{t \text{ total}}) \omega_s'^2 - 2 I_{s \text{ total}} I_s \sigma \omega_s' + I_s^2 \sigma^2 + 2 E_C' I_{t \text{ total}} - h^2 = 0 \quad (98)$$

and

$$\omega_3' = \frac{I_s \sigma}{(I_{t \text{ total}} - I_{s \text{ total}})} \pm \sqrt{Q'} \left(\frac{I_{t \text{ total}}}{I_{t \text{ total}} - I_{s \text{ total}}} \right) \frac{1}{I_{s \text{ total}}} \quad (99)$$

where

$$Q' = 2 E_c' I_{s \text{ total}} \left(1 - \frac{I_{s \text{ total}}}{I_{t \text{ total}}} \right) - h^2 \left(\frac{I_{s \text{ total}}}{I_{t \text{ total}}} \right) \left(1 - \frac{I_{s \text{ total}}}{I_{t \text{ total}}} \right) + \left(\frac{I_{s \text{ total}}}{I_{t \text{ total}}} \right) I_s^2 \sigma^2 \quad (100)$$

The initial conditions at $t = 0$ will determine the proper sign of Equation (99). As before, continuity will ensure this sign for all $t > 0$. Substituting Equation (99) into Equation (11)

$$\eta' = \cos^{-1} \left(\frac{I_{s \text{ total}} \omega_3' + I_s \sigma}{h} \right) = \cos^{-1} \left(\left[\frac{I_{t \text{ total}}}{I_{t \text{ total}} - I_{s \text{ total}}} \right] \frac{1}{h} [I_s \sigma \pm \sqrt{Q'}] \right) \quad (101)$$

The time rate of change of the nutation angle will determine the stability. Differentiating the above equation results in

$$\dot{\eta}' = \frac{-E_c'}{\sin \eta} \frac{1}{h} \left(\frac{I_{s \text{ total}}}{\pm \sqrt{Q'}} \right) \quad (102)$$

A stable system would require that the lower sign be chosen for the radical, thus

$$\eta' = \cos^{-1} \left(\left[\frac{I_{t \text{ total}}}{I_{t \text{ total}} - I_{s \text{ total}}} \right] \frac{1}{h} [I_s \sigma - \sqrt{Q'}] \right) \quad (103)$$

When this sign selection is applied to Equation (52), one gets

$$\omega_3' (I_{t \text{ total}} - I_{s \text{ total}}) + I_s \sigma = -\sqrt{Q'} \left(\frac{I_{t \text{ total}}}{I_{s \text{ total}}} \right) \quad (104)$$

This can be rewritten as the well established dual-spin stability condition, as written by P. C. Hughes [Ref 6],

$$(I_{t \text{ total}} - I_{s \text{ total}}) \omega_3' + I_s \sigma \leq 0 \quad (105)$$

It is important to note that this analysis does not produce a contradiction to Equation (41).

In a similar manner, the modified nutation angle can be derived with respect to the rotor as

$$\eta = \cos^{-1} \left(\left[\frac{I_{s \text{ total}}}{I_{t \text{ total}} - I_{s \text{ total}}} \right] \frac{1}{h} [I_s' \sigma - \sqrt{Q}] \right) \quad (106)$$

where

$$Q = 2 E_c I_{s \text{ total}} \left(1 - \frac{I_{s \text{ total}}}{I_{t \text{ total}}} \right) - h^2 \left(\frac{I_{s \text{ total}}}{I_{t \text{ total}}} \right) \left(1 - \frac{I_{s \text{ total}}}{I_{t \text{ total}}} \right) + \left(\frac{I_{s \text{ total}}}{I_{t \text{ total}}} \right) I_s'^2 \sigma^2 \quad (107)$$

Therefore, if one is given the core energy or the postulated core energy as a function of time, the nutational motion can then be determined. This leads to an extremely important conclusion. By determining a sufficiently accurate postulation of the core energy of a dual-spin, quasi-rigid, axisymmetric spacecraft over time, one can predict the nutational behavior and the stability of that spacecraft. Numerical simulation of such a system will confirm this conclusion.

III. DYNAMICAL EQUATIONS

A. MINGORI DUAL-SPIN SYSTEM

A specific model is required to validate the modified energy-sink stability theory. The development of the previous chapters was completely general in nature and applies to any dual-spin spacecraft with an arbitrary damping mechanism. D. L. Mingori's dual-spin system [Ref. 3] provided the needed model required to validate the proposed stability theory, Figure (3). Additionally, the complete non-linear equations of motion were presented by Mingori; however, the expressions for the important parameters in attitude dynamics, angular momentum and kinetic and total energy, were not presented in his paper and had to be derived before any analysis could be performed.

The Mingori system is comprised of two symmetric rigid bodies, the lower which shall be defined as the rotor, and the upper body shall be defined as the platform. By convention, all terms referring to the platform will be the same notation as that of the rotor, except that they will carry the prime mark. Both the rotor and the platform have coordinate axes fixed to the body and located at the respective centers of mass. The distance between the centers of mass is specified by L . The entire spacecraft has coordinate axes fixed to the spacecraft center of mass, denoted by the double prime coordinate axes, and rotating in the same manner as the rotor coordinate axes. The coordinate axes b_3 , b_3' , and b_3'' are all collinear. The spacecraft center of mass will vary along the b_3 axis as the point masses in the rotor and the platform oscillate. The only relative motion of the platform with respect to the rotor is angular rotation about the b_3 axis. A motor driven by a control system maintains a constant relative rotation rate σ . The angle between a line parallel to b_1 and passing through the platform center of mass, and b_1' is represented by $\psi = \sigma t$.

30

Each body contains a mass-spring-dashpot mechanism. An actual spacecraft undergoes damping from various mechanisms. Undesired damping can occur due to structural elasticity and liquid propellant slosh. Nutation dampers are incorporated into spacecraft to improve the nutational motion. The dual-spin axisymmetric system with mass-spring-dashpot dampers cannot accurately model an actual spacecraft, but is used to illustrate and validate the theory. A description of the rotor is as follows. The mass-spring-dashpot mechanism can be modelled by a particle mass m_1 attached to a spring with constant k inside a tube filled with viscous fluid with damping coefficient c . The motion of the particle is constrained parallel to the b_3 axis only. At rest, the particle mass lies along the rotor's b_1 coordinate axis, at a distance a from the rotor's center of mass. Three balancing masses, m_2 , m_3 , and m_4 , each equal to the mass of the mass-spring-dashpot mechanism, are rigidly fixed a distance a on the b_2 , $-b_1$, and $-b_2$ axes. These masses maintain the axisymmetry of the system about the b_3 axis. Displacement of the particle mass m_1 is denoted by the variable z . A simplification in this paper of the Mingori dual-spinner system is the assumption of a massless spring-dashpot system. Thus the particle of the mass-spring-dashpot system, m_1 , is the same mass as the corresponding three other balancing masses, m_2 , m_3 , and m_4 . The platform can be described in a similar manner, with all notation modified with the prime mark.

The dual-spin system center of mass coordinate axes rotates at the same rate as the rotor coordinate axes, but is located along the b_3 axis at a distance z_{cm} from the rotor center of mass. This distance will vary as the particle masses are displaced. Relating the dual-spin system's coordinate axes to the rotor coordinate axes was arbitrary. Equivalent results would be achieved by selecting the platform coordinate axes instead.

B. ANGULAR MOMENTUM

The angular momentum of the Mingori dual-spin, quasi-rigid, axisymmetric system is now derived from first principles.

The angular momentum (moment of momentum) of a particle of mass m_i located in body B is defined as

$$\mathbf{h}_i = \mathbf{r}_i \times m_i \mathbf{\overset{N}{V}}^i \quad (108)$$

where \mathbf{h}_i is the angular momentum of the i th particle with respect to the system center of mass, \mathbf{r}_i specifies the location of the i th particle with respect to the system center of mass, and $\mathbf{\overset{N}{V}}^i = \left. \frac{d \mathbf{R}_i}{dt} \right|_N$ is the absolute velocity of the i th particle with respect to the inertial reference frame N . Expressing the absolute velocity in the system reference frame

$$\mathbf{\overset{N}{V}}^i = \mathbf{\overset{N}{V}}^{cm} + \dot{\mathbf{r}}_i + \mathbf{\overset{N \rightarrow B}{\omega}} \times \mathbf{r}_i \quad (109)$$

where B represents the reference coordinate axes of the system. For the following derivation, all displacements and velocities are referenced with respect to the rotor (\mathbf{b}_i) coordinate axes. The angular momentum vector is rewritten as

$$\mathbf{h}_i = \mathbf{r}_i \times m_i \left(\mathbf{\overset{N}{V}}^{cm} + \dot{\mathbf{r}}_i + \mathbf{\overset{N \rightarrow B}{\omega}} \times \mathbf{r}_i \right) \quad (110)$$

Applying this equation to particle 1 with mass m_1 and position

$$\mathbf{r}_1 = a \mathbf{b}_1 + 0 \mathbf{b}_2 + (z - z_{cm}) \mathbf{b}_3 \quad (111)$$

one arrives at

$$h_1 = m_1 \left(\begin{bmatrix} (z - z_{cm})^2 & 0 & -a(z - z_{cm}) \\ 0 & a^2 + (z - z_{cm})^2 & 0 \\ -a(z - z_{cm}) & 0 & a^2 \end{bmatrix} \begin{Bmatrix} \omega_1 \\ \omega_2 \\ \omega_3 \end{Bmatrix} + \begin{bmatrix} 0 & -(z - z_{cm}) & 0 \\ (z - z_{cm}) & 0 & -a \\ 0 & a & 0 \end{bmatrix} \begin{Bmatrix} V_{cm x} \\ V_{cm y} \\ V_{cm z} \end{Bmatrix} + \begin{bmatrix} 0 \\ -a(\dot{z} - \dot{z}_{cm}) \\ 0 \end{bmatrix} \right) \begin{Bmatrix} b_1 \\ b_2 \\ b_3 \end{Bmatrix} \quad (112)$$

For the rigid body, Equation (110) is applied to a differential volume at location

$$r_{\Delta M} = u b_1 + v b_2 + (w - z_{cm}) b_3 \quad (113)$$

Integrating, one arrives at

$$h_M = \left(\begin{bmatrix} I_1 + M z_{cm}^2 & 0 & 0 \\ 0 & I_2 + M z_{cm}^2 & 0 \\ 0 & 0 & I_3 \end{bmatrix} \begin{Bmatrix} \omega_1 \\ \omega_2 \\ \omega_3 \end{Bmatrix} + \begin{bmatrix} 0 & M z_{cm} & 0 \\ -M z_{cm} & 0 & 0 \\ 0 & 0 & 0 \end{bmatrix} \begin{Bmatrix} V_{cm x} \\ V_{cm y} \\ V_{cm z} \end{Bmatrix} + \begin{bmatrix} 0 \\ -a(\dot{z} - \dot{z}_{cm}) \\ 0 \end{bmatrix} \right) \begin{Bmatrix} b_1 \\ b_2 \\ b_3 \end{Bmatrix} \quad (114)$$

Similar calculations are performed for the remaining seven point masses and the platform.

For the rotor, one arrives at

$$\begin{aligned}
 & \mathbf{h}_M + 4m = \\
 & \left(\begin{aligned} & \begin{bmatrix} I_1 + M z_{cm}^2 + m(2a^2 + 4z_{cm}^2 + z^2 - 2z z_{cm}) & 0 & -m a z \\ 0 & I_2 + M z_{cm}^2 + m(2a^2 + 4z_{cm}^2 + z^2 - 2z z_{cm}) & 0 \\ -m a z & 0 & I_3 + 4 m a^2 \end{bmatrix} \begin{pmatrix} \omega_1 \\ \omega_2 \\ \omega_3 \end{pmatrix} \\ & + \begin{bmatrix} 0 \\ -m a z \\ 0 \end{bmatrix} \\ & + \begin{bmatrix} 0 & (M + 4 m) z_{cm} & 0 \\ (M + 4 m) z_{cm} & 0 & 0 \\ 0 & 0 & 0 \end{bmatrix} \begin{pmatrix} V_{cmx} \\ V_{cmy} \\ V_{cms} \end{pmatrix} \end{aligned} \right) \begin{pmatrix} b_1 \\ b_2 \\ b_3 \end{pmatrix} \quad (115)
 \end{aligned}$$

Similarly, for the platform

(116)

$$\begin{aligned}
 & \text{bar} + 4m' = \\
 & \left(\begin{bmatrix} I_1' + M'(l - z_{cm})^2 + m' \left(2a'^2 + 4(l - z_{cm})^2 + z'^2 + 2z'(l - z_{cm}) \right) & 0 & -m' a' z' \cos(\sigma t) \\ 0 & I_2' + M'(l - z_{cm})^2 + m' \left(2a'^2 + 4(l - z_{cm})^2 + z'^2 + 2z'(l - z_{cm}) \right) & -m' a' z' \sin(\sigma t) \\ -m' a' z' \cos(\sigma t) & -m' a' z' \sin(\sigma t) & I_3' + 4m' a'^2 \end{bmatrix} \begin{Bmatrix} \omega_1 \\ \omega_2 \\ \omega_3 \end{Bmatrix} \right. \\
 & \quad + \begin{bmatrix} -m' a' \sigma \cos(\sigma t) z' + m' a' \sin(\sigma t) \dot{z}' \\ -m' a' \sigma \sin(\sigma t) z' - m' a' \cos(\sigma t) \dot{z}' \\ (I_3' + 4m' a'^2) \sigma \end{bmatrix} \begin{Bmatrix} b_1 \\ b_2 \\ b_3 \end{Bmatrix} \\
 & \quad \left. + \begin{bmatrix} 0 & -(M' + 4m')(l - z_{cm}) & 0 \\ (M' + 4m')(l - z_{cm}) + m' z' & 0 & 0 \\ 0 & 0 & 0 \end{bmatrix} \begin{Bmatrix} V_{cmx} \\ V_{cmy} \\ V_{cmz} \end{Bmatrix} \right)
 \end{aligned}$$

The angular momentum equations have terms corresponding to the velocity of the center of mass. Angular momentum, when taken about the center of mass of a system, by definition must be independent of the translation of the system's center of mass (with respect to an inertial reference frame). To verify that this occurs in the above equations, the equation for the position of the center of mass is substituted into the center of mass velocity terms, and then these equations are equated. If they have the same magnitude but opposite sign, they will cancel each other out and it will be proven that the system angular momentum is independent of the translation of the system center of mass.

One must prove

$$-\left(h_{M' + 4 m'}\right)\left(N_{\vec{V}^{cm}}\right) \stackrel{?}{=} \left(h_{M + 4 m}\right)\left(N_{\vec{V}^{cm}}\right) \quad (117)$$

Looking at the b_1 components, one finds

$$-\left[\left(M' + 4 m'\right)\left(-l + z_{cm}\right) - m' z'\right] \stackrel{?}{=} \left[\left(M + 4 m\right) z_{cm} - m z\right] \quad (118)$$

Rewriting this, one obtains

$$\left(M' + 4 m'\right) l + m z + m' z' \stackrel{?}{=} \left(M + 4 m + M' + 4 m'\right) z_{cm} \quad (119)$$

The center of mass with reference to the b_1, b_2, b_3 coordinate axes is

$$z_{cm} = \frac{\sum_i M_i z_i + m_i z_i}{\sum_i M_i + m_i} = \frac{m z + \left(M' + 4 m'\right) l + m' z'}{M + 4 m + M' + 4 m'} \quad (120)$$

Substituting Equation (120) into Equation (119) results in

$$\left(M' + 4 m'\right) l + m z + m' z' \stackrel{?}{=} \left(M + 4 m + M' + 4 m'\right) \left(\frac{m z + \left(M' + 4 m'\right) l + m' z'}{M + 4 m + M' + 4 m'}\right) \quad (121)$$

This reduces to

$$\left(M' + 4 m'\right) l + m z + m' z' = \left(M' + 4 m'\right) l + m z + m' z' \quad (122)$$

Therefore, the angular momentum along the b_1 axis is independent of the velocity of the center of mass. Verifying this along the other axes can be done in a similar manner. This proves that the angular momentum of the entire system about the system center of mass is independent of the translation of the system center of mass. The angular momentum of the entire system can be written as

$$h = h_{M + 4 m} + h_{M' + 4 m'} \quad (123)$$

where

$$h_M + 4m = \left(\begin{bmatrix} \frac{I_1 + M z_{cm}^2 + m(2a^2 + 4z_{cm}^2 + z'^2 - 2z z_{cm})}{m} & 0 & -m a z \\ 0 & \frac{I_2 + M z_{cm}^2 + m(2a^2 + 4z_{cm}^2 + z'^2 - 2z z_{cm})}{m} & 0 \\ -m a z & 0 & I_3 + 4 m a^2 \end{bmatrix} \begin{pmatrix} \omega_1 \\ \omega_2 \\ \omega_3 \end{pmatrix} + \begin{bmatrix} 0 \\ -m a \dot{z} \\ 0 \end{bmatrix} \right) \begin{pmatrix} b_1 \\ b_2 \\ b_3 \end{pmatrix} \quad (124)$$

and

$$h_{M'} + 4m' = \left(\begin{bmatrix} \frac{I_1' + M'(l - z_{cm})^2 + m'(2a'^2 + 4(l - z_{cm})^2 + z'^2 + 2z'(l - z_{cm}))}{m'} & 0 & -m' a' z' \cos(\sigma t) \\ 0 & \frac{I_2' + M'(l - z_{cm})^2 + m'(2a'^2 + 4(l - z_{cm})^2 + z'^2 + 2z'(l - z_{cm}))}{m'} & -m' a' z' \sin(\sigma t) \\ -m' a' z' \cos(\sigma t) & -m' a' z' \sin(\sigma t) & I_3' + 4 m' a'^2 \end{bmatrix} \begin{pmatrix} \omega_1 \\ \omega_2 \\ \omega_3 \end{pmatrix} + \begin{bmatrix} -m' a' \sigma \cos(\sigma t) z' + m' a' \sin(\sigma t) \dot{z}' \\ -m' a' \sigma \sin(\sigma t) z' - m' a' \cos(\sigma t) \dot{z}' \\ (I_3' + 4 m' a'^2) \sigma \end{bmatrix} \right) \begin{pmatrix} b_1 \\ b_2 \\ b_3 \end{pmatrix} \quad (125)$$

C. ENERGY

The kinetic energy, E , and the total energy, E_{total} , are now derived. From first principles the kinetic energy of a differential particle is written as

$$E_{dm} = \frac{1}{2} |N\vec{v}^{dm}|^2 dm = \frac{1}{2} \{ (N\vec{v}^{dm}) \cdot (N\vec{v}^{dm}) \} dm \quad (126)$$

where the absolute velocity is defined from before

$$N\vec{v}^{dm} = N\vec{v}^{cm} + \dot{r}_{dm} + \frac{N\vec{\omega}}{\omega} \times r_{dm} \quad (109)$$

The kinetic energy of the Mingori system is determined by integrating the differential kinetic energy over the rotor and over the platform, and summing the differential kinetic energy equation over the eight point masses to arrive at

$$E = \frac{1}{2} \int_{R_{\text{rotor}}} \{ (N\vec{v}^{dm}) \cdot (N\vec{v}^{dm}) \} dm + \sum_{i=1}^4 \frac{1}{2} \{ (N\vec{v}^i) \cdot (N\vec{v}^i) \} m_i + \quad (127)$$

$$\frac{1}{2} \int_{R_{\text{platform}}} \{ (N\vec{v}^{dm'}) \cdot (N\vec{v}^{dm'}) \} dm' + \sum_{i'=1}^4 \frac{1}{2} \{ (N\vec{v}^{i'}) \cdot (N\vec{v}^{i'}) \} m_{i'}$$

Performing the steps on particle m_1 , the following is obtained

$$E_1 = \frac{1}{2} m_1 \sum_{i=1}^4 \left\{ \frac{1}{2} (N\vec{v}^{cm} \cdot N\vec{v}^{cm}) + (\dot{r}_1 \cdot \dot{r}_1) + \left(\left(\frac{N\vec{\omega}}{\omega} \times r_1 \right) \cdot \left(\frac{N\vec{\omega}}{\omega} \times r_1 \right) \right) + \right. \quad (128)$$

$$\left. \frac{1}{2} (N\vec{v}^{cm} \cdot r_1) + 2 (N\vec{v}^{cm} \cdot \left(\frac{N\vec{\omega}}{\omega} \times r_1 \right)) + 2 \left(\dot{r}_1 \cdot \left(\frac{N\vec{\omega}}{\omega} \times r_1 \right) \right) \right\}$$

Substituting in the values, one arrives at

$$E_1 = \frac{1}{2} m_1 \left\{ \begin{aligned} & V_{cmx}^2 + V_{cmy}^2 + V_{cmz}^2 + (\dot{z} - \dot{z}_{cm})^2 + (z - z_{cm})^2 \omega_2^2 + \\ & a^2 \omega_3^2 + (z - z_{cm})^2 \omega_1^2 - 2a(z - z_{cm})\omega_1\omega_3 + \\ & a^2 \omega_2^2 + 2(\dot{z} V_{cmz} - \dot{z}_{cm} V_{cmz}) + \\ & 2 \left(\begin{aligned} & z \omega_2 V_{cmx} - z_{cm} \omega_2 V_{cmx} + a \omega_3 V_{cmy} - \\ & z \omega_1 V_{cmy} + z_{cm} \omega_1 V_{cmy} - a \omega_2 V_{cmz} \end{aligned} \right) + \\ & 2(-a\dot{z}\omega_2 + a\dot{z}_{cm}\omega_2) \end{aligned} \right\} \quad (129)$$

This operation is then performed over the other three particles in the rotor. Performing these same steps on the body of the rotor,

(130)

$$E_M = \frac{1}{2} \int_{\text{Rotor}} \left\{ \begin{aligned} & (N_{\vec{V}^{cm}} \cdot N_{\vec{V}^{cm}}) + (\dot{r}_1 \cdot \dot{r}_1) + ((N_{\vec{\omega}^{cm}} \times r_1) \cdot (N_{\vec{\omega}^{cm}} \times r_1)) + \\ & 2(N_{\vec{V}^{cm}} \cdot r_1) + 2(N_{\vec{V}^{cm}} \cdot (N_{\vec{\omega}^{cm}} \times r_1)) + 2(\dot{r}_1 \cdot (N_{\vec{\omega}^{cm}} \times r_1)) \end{aligned} \right\} dM$$

Substituting in values, and specifying the position vector of the differential particle as

$$r_{dM} = u b_1 + v b_2 + (w - z_{cm}) b_3 \quad (131)$$

then

(132)

$$E_M = \frac{1}{2} \int_{\text{Rotor}} \left\{ \begin{aligned} & V_{cm x}^2 + V_{cm y}^2 + V_{cm z}^2 + \dot{z}_{cm}^2 + w^2 \omega_2^2 - 2 w z_{cm} \omega_2^2 + \\ & z_{cm}^2 \omega_2^2 + v^2 \omega_3^2 - 2 w v \omega_2 \omega_3 + 2 v z_{cm} \omega_2 \omega_3 + w^2 \omega_1^2 + \\ & z_{cm}^2 \omega_1^2 + u^2 \omega_3^2 - 2 w z_{cm} \omega_1^2 - 2 u w \omega_1 \omega_3 + 2 u z_{cm} \omega_1 \omega_3 + \\ & v^2 \omega_1^2 - 2 v u \omega_1 \omega_2 + u^2 \omega_2^2 + 2(-\dot{z}_{cm} V_{cm z}) + \\ & 2 \left(\begin{aligned} & w \omega_2 V_{cm x} - z_{cm} \omega_2 V_{cm x} - v \omega_3 V_{cm x} - w \omega_1 V_{cm y} + \\ & z_{cm} \omega_1 V_{cm y} + u \omega_3 V_{cm y} + v \omega_1 V_{cm z} - u \omega_2 V_{cm z} \end{aligned} \right) + \\ & 2(-v \dot{z}_{cm} \omega_1 + u \dot{z}_{cm} \omega_2) \end{aligned} \right\} dM$$

Integrating over the limits of the symmetrical body, the kinetic energy of the rotor becomes

$$E_M = \frac{1}{2} M \left(\begin{aligned} & V_{cm x}^2 + V_{cm y}^2 + V_{cm z}^2 + \dot{z}_{cm}^2 + z_{cm}^2 (\omega_1^2 + \omega_2^2) + \\ & I_1 \omega_1^2 + I_2 \omega_2^2 + I_3 \omega_3^2 - \\ & 2 z_{cm} \omega_2 V_{cm x} + 2 z_{cm} \omega_1 V_{cm y} - 2 \dot{z}_{cm} V_{cm z} \end{aligned} \right) \quad (133)$$

These same steps are performed on the platform and on the remaining seven particles.

These equations are then combined and simplified.

The total kinetic energy for the Mingori system is

(134)

$$E = \left(\begin{aligned} & \frac{1}{2} M_{total} (V_{cm}^2 x + V_{cm}^2 y + V_{cm}^2 z) + \\ & \frac{1}{2} (I_1 \omega_1^2 + I_2 \omega_2^2 + I_3 \omega_3^2) + \frac{1}{2} (I_1' \omega_1^2 + I_2' \omega_2^2 + I_3' (\omega_3 + \sigma)^2) + \\ & \frac{1}{2} (\dot{z}^2 + z^2 (\omega_1^2 + \omega_2^2) - 2 a z \omega_1 \omega_3) + \\ & \frac{1}{2} (\dot{z}'^2 + z'^2 (\omega_1^2 + \omega_2^2) - 2 a' z' \cos(\sigma t) \omega_1 \omega_3 + 2 a' z' \sin(\sigma t) \omega_2 \omega_3) + \\ & m (-a \dot{z} \omega_2) + \\ & m' (-a' \dot{z}' \cos(\sigma t) \omega_2 + a' \dot{z}' \sin(\sigma t) \omega_1 - a' z' \sigma \cos(\sigma t) \omega_1 - a' z' \sigma \sin(\sigma t) \omega_2) \\ & + \frac{1}{2} \frac{(\omega_1^2 + \omega_2^2) (m z + m' z')^2 - (m \dot{z} + m' \dot{z}')^2}{M_T} + \\ & \frac{1}{2} (\omega_1^2 + \omega_2^2) (M + 4 m) l^2 \left(\frac{M' + 4 m'}{M_T} \right)^2 + \\ & \frac{1}{2} (\omega_1^2 + \omega_2^2) (M' + 4 m') l^2 \left(\frac{M + 4 m}{M_T} \right)^2 - \\ & m z (\omega_1^2 + \omega_2^2) \left(\frac{m z + m' z' + (M' + 4 m') l}{M_T} \right) - \\ & m' z' (\omega_1^2 + \omega_2^2) \left(\frac{m z + m' z' - (M + 4 m) l}{M_T} \right) \end{aligned} \right)$$

The total energy of the Mingori system can be determined by adding the kinetic energy of the system to the potential energy of the system. The only potential energy of the system is the energy stored in the springs of the mass-spring-dashpot damper. From Hooke's law, the system potential energy is written as

$$U(z) = \frac{1}{2} k z^2 + \frac{1}{2} k' z'^2 \quad (135)$$

The total energy of the Mingori system is then

$$E_{total} = E + U = E + \frac{1}{2} k z^2 + \frac{1}{2} k' z'^2 \quad (136)$$

D. MINGORI'S EQUATIONS OF MOTION

Mingori's equations of motion [Ref 3] are written as follows

$$\begin{aligned}
 & A \dot{\omega}_1 - (A - C) \omega_2 \omega_3 - J_3' \sigma \omega_2 + 2 M_T \zeta \dot{\zeta} \omega_1 + M_T \zeta^2 (\dot{\omega}_1 + \omega_2 \omega_3) + \\
 & m \left\{ \begin{aligned} & -2(\zeta + l_2)[z(\dot{\omega}_1 - \omega_2 \omega_3) + \dot{z} \omega_1] + \\ & z[-2 \dot{\zeta} \omega_1 + 2 \dot{z} \omega_1 + z(\dot{\omega}_1 - \omega_2 \omega_3) - a(\dot{\omega}_3 + \omega_1 \omega_2)] \end{aligned} \right\} + \\
 & m' \left\{ \begin{aligned} & -2(\zeta - l_1)[z'(\dot{\omega}_1 - \omega_2 \omega_3) + \dot{z}' \omega_1] + \\ & z'[-2 \dot{\zeta} \omega_1 + 2 \dot{z}' \omega_1 + z'(\dot{\omega}_1 - \omega_2 \omega_3) - a' \cos \psi (\dot{\omega}_3 + \omega_1 \omega_2)] + \\ & a' \sin \psi \{ \ddot{z}' + z'[(\omega_3 + \sigma)^2 - \omega_2^2] \} \end{aligned} \right\} = 0 \\
 & A \dot{\omega}_2 - (C - A) \omega_1 \omega_3 - J_3' \sigma \omega_1 + 2 M_T \zeta \dot{\zeta} \omega_2 + M_T \zeta^2 (\dot{\omega}_2 + \omega_1 \omega_3) + \\
 & m \left\{ \begin{aligned} & -2(\zeta + l_2)[z(\dot{\omega}_2 + \omega_1 \omega_3) + \dot{z} \omega_2] + \\ & z[-2 \dot{\zeta} \omega_2 + 2 \dot{z} \omega_2 + z(\dot{\omega}_2 + \omega_1 \omega_3)] - a[\ddot{z} + z(\omega_3^2 - \omega_1^2)] \end{aligned} \right\} + \\
 & m' \left\{ \begin{aligned} & -2(\zeta - l_1)[z'(\dot{\omega}_2 + \omega_1 \omega_3) + \dot{z}' \omega_2] + \\ & z'[-2 \dot{\zeta} \omega_2 + 2 \dot{z}' \omega_2 + z'(\dot{\omega}_2 + \omega_1 \omega_3)] - \\ & a' \cos \psi \{ \ddot{z}' + z'[(\omega_3 + \sigma)^2 - \omega_1^2] \} - a' \sin \psi z'(\dot{\omega}_3 - \omega_1 \omega_2) \end{aligned} \right\} = 0 \quad (137) \\
 & C \dot{\omega}_3 - m a [2 \dot{z} \omega_1 + z(\dot{\omega}_1 - \omega_2 \omega_3)] - \\
 & m' a' \sin \psi [2 \dot{z}' \omega_2 + z'(\dot{\omega}_2 + \omega_1 \omega_3)] - \\
 & m' a' \cos \psi [2 \dot{z}' \omega_1 + z'(\dot{\omega}_1 - \omega_2 \omega_3)] = 0 \\
 & m(1 - \rho) \ddot{z} - m' \rho \ddot{z}' - m a (\dot{\omega}_2 - \omega_1 \omega_3) - \\
 & m(\omega_1^2 + \omega_2^2)[z(1 - \rho) - l_2 - \rho' z'] + c \dot{z} + k z = 0 \\
 & -m \rho' \ddot{z} + m'(1 - \rho') \ddot{z}' + \\
 & m' a' \{ \sin \psi [\dot{\omega}_1 + \omega_2(\omega_3 + 2 \sigma)] - \cos \psi [\dot{\omega}_2 - \omega_1(\omega_3 + 2 \sigma)] \} - \\
 & m'(\omega_1^2 + \omega_2^2)[z'(1 - \rho') + l_1 - \rho z] + c' \dot{z}' + k' z' = 0
 \end{aligned}$$

In the above equations, the following relationships are used

$$\begin{aligned}
 M_T &= M + M' + 4 m_b + 4 m_b' \\
 v &= \frac{M' + 4 m_b'}{M_T} \\
 \rho &= \frac{m}{M_T} & \rho' &= \frac{m'}{M_T} \\
 I_1 &= I \left(\frac{M + 4 m_b}{M_T} \right) & I_2 &= I \left(\frac{M' + 4 m_b'}{M_T} \right) \\
 \zeta &= (\rho z + \rho' z') & \psi &= \sigma t \\
 A &= I_1 + I_1' + 2 m_b a^2 + 2 m_b' a'^2 + (M' + 4 m_b') (1 - v) I^2 \\
 C &= I_3 + I_3' + 4 m_b a^2 + 4 m_b' a'^2 \\
 J_3' &= I_3' + 4 m_b' a'^2
 \end{aligned} \tag{138}$$

Chapter IV discusses how these equations are adapted for use in the numerical integration routine.

E. NUTATION ANGLE

The nutation angle of the dual-spin system can be determined by substituting Equations (124) and (125) into Equation (34) to arrive at

$$\theta = \cos^{-1} \left(\frac{\mathbf{h} \cdot \mathbf{b}_3}{|\mathbf{h}|} \right) = \cos^{-1} \left(\frac{h_3 + h_3'}{|\mathbf{h}|} \right) = \cos^{-1} \left(\frac{\begin{aligned} &(-m a z - m' a' z' \cos(\sigma t)) \omega_1 + \\ &(-m' a' z' \sin(\sigma t)) \omega_2 + \\ &(I_3 + 4 m a^2 + I_3' + 4 m' a'^2) \omega_3 \\ &+ (I_3' + 4 m' a'^2) \sigma \end{aligned}}{|\mathbf{h}|} \right) \tag{139}$$

F. CORE ENERGY

The platform core energy and the rotor core energy were defined in Equations (47) and (48). The nutation angle as a function of core energy was then developed and is stated in Equations (101) and (106). These equation can be used to predict the nutation angle of the system as a function of time. Because the core energy as a function of time is not available for the prediction, a postulated core energy must be developed. The initial value of the actual core energy and the postulated core energy must match and is dictated by the initial conditions. Parameters of the postulated core energy must be selected to accurately model the actual core energy, to include the final energy state and the rate at which the it approaches the final energy state. Two models were considered.

1. Exponential Core Energy Model

An exponential representation of rotor and platform core energy as a function of time are expressed as follows

$$E_{C \text{ postulated}}(t) = (E_{C_0} - E_{C \text{ final}}) e^{(-rt)} + E_{C \text{ final}} \quad (140)$$

$$E_{C \text{ postulated}}'(t) = (E_{C_0}' - E_{C \text{ final}}') e^{(-r't)} + E_{C \text{ final}}' \quad (141)$$

The initial core energies, E_{C_0} , E_{C_0}' , are determined by the initial conditions of the system. The final core energies, $E_{C \text{ final}}$, $E_{C \text{ final}}'$, as well as the exponential factors r , r' , must be selected. The methodology for selecting these values is explained in Chapter V, Computer Analysis.

2. Verhulst Logistic Core Energy Model

The exponential model, as will be explained in Chapter V, has excellent agreement for stable conditions, but performs poorly for the unstable conditions. As an alternative model, the following first order differential model is selected for the rotor and

platform respectively.

$$E_{C \text{ postulated}}(t) = \frac{(E_{C_0})(E_{C \text{ final}})}{E_{C_0} + (E_{C \text{ final}} - E_{C_0})e^{-rt}} \quad (142)$$

$$E_{C \text{ postulated}}'(t) = \frac{(E_{C_0}')(E_{C \text{ final}}')}{E_{C_0}' + (E_{C \text{ final}}' - E_{C_0}')e^{-r't}} \quad (143)$$

This type of equation was first introduced by P. F. Verhulst to model human and other populations [Ref 7]. It is often referred to as the Verhulst equation or the logistic equation. Although population dynamics appears to be unrelated to the stability of a dual-spin system, the behavior over time of this equation compared to the stable and unstable systems provides some insight. Figure (4) shows the Verhulst equation versus time for varying initial conditions.

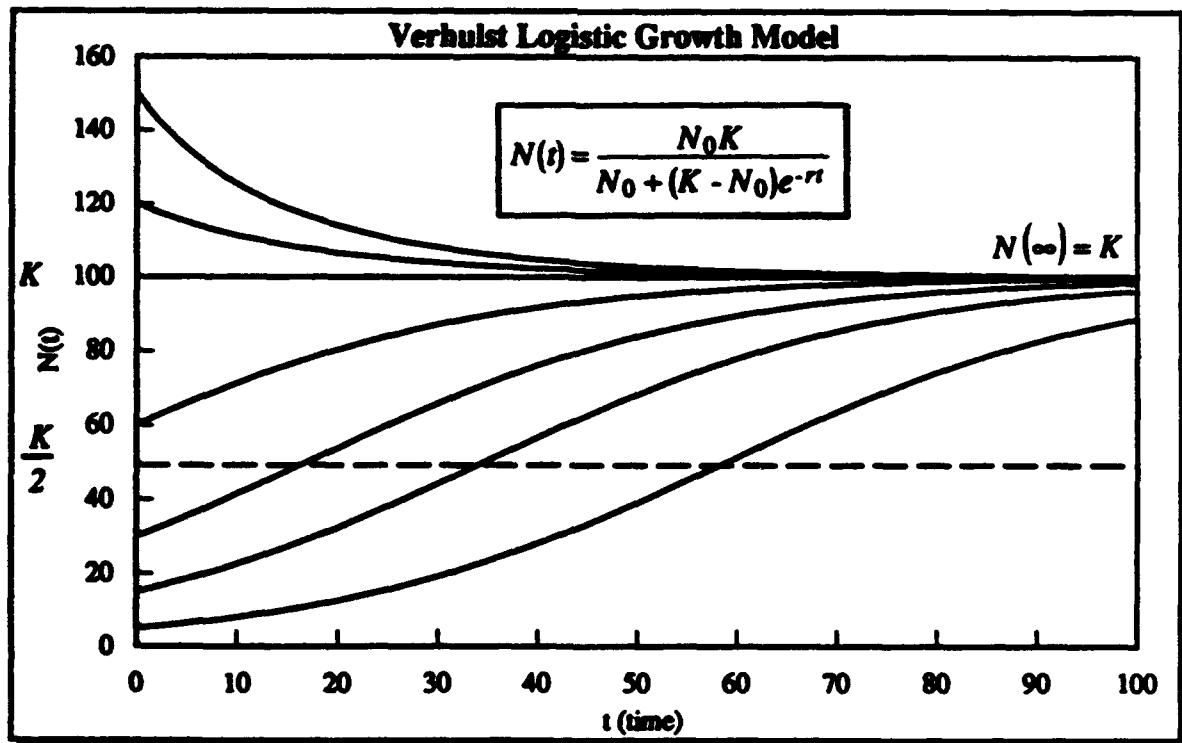


Figure (4) Verhulst Logistic Equation Versus Time

It can be noted that if the initial value of the variable (in our case core energy) is greater than the equilibrium value, it will approach the equilibrium value in a manner similar to that of an exponential decay. For initial values that are less than but within one half of the equilibrium value, the variable will asymptotically approach the equilibrium value. If the initial value is less than one half of the initial value, the variable over time has a somewhat different shape as it approaches equilibrium. Initially the slope is very small, but increases to a maximum at about the one-half of the equilibrium position. After this inflection point the variable approaches equilibrium asymptotically. The value of N_0 equals K is an asymptotically stable equilibrium. A value of N_0 equals zero is an unstable equilibrium. If the value of N_0 is slightly greater than zero, then $N(t)$ will, as $t \rightarrow \infty$, achieve the stable equilibrium of K . These types of curves will be utilized to describe both the stable and unstable dual-spin system. The initial core energies, E_{C_0} , E_{C_0}' , would be determined by the initial conditions of the system. The final core energies, $E_{C \text{ final}}$, $E_{C \text{ final}}'$, must be known or a best estimate used. The exponential factors, r , r' , must be determined experimentally, and are a function of the system parameters and initial conditions. Chapter V provides additional details on the selection process.

IV. NUMERICAL SIMULATION

A. NUMERICAL SIMULATION EQUATIONS OF MOTION

The equations for the dynamical quantities needed for analysis of the dual-spin system were previously developed. Manipulation was required to make these equations suitable for numerical analysis, and is described below. The computer code is included as Appendix B.

1. Mingori's Equations of Motion

The equations of motion for the dual-spin system are listed as Equation set (137) and (138). The Runge-Kutta numerical integration routine necessitated that the equations of motion be a set of first order differential equations. Mathematical manipulation was required to put them in this form. Variables representing groups of terms (A_i , B_i , C_i , etc) were introduced to simplify the manipulations of the equations and provide a suitable format for incorporating the equations into the computer program. Mingori's equations can be expressed in terms of these variables and the five time-dependent variables of motion

$$\begin{aligned}A_{26} \dot{\omega}_1 + A_{27} \dot{\omega}_3 + A_{24} \ddot{z} + A_{28} &= 0 \\B_{25} \dot{\omega}_2 + B_{23} \dot{\omega}_3 + B_{13} \ddot{z} + B_{21} \ddot{z}' + B_{26} &= 0 \\C_{10} \dot{\omega}_1 + C_5 \dot{\omega}_2 + C \dot{\omega}_3 + C_{11} &= 0 \\D_1 \ddot{z} + D_2 \ddot{z}' + D_3 \dot{\omega}_2 + D_8 &= 0 \\E_1 \ddot{z} + E_2 \ddot{z}' + E_3 \dot{\omega}_1 + E_5 \dot{\omega}_2 + E_{10} &= 0\end{aligned}\tag{144}$$

where the variables A_i , B_i , C_i , D_i , E_i , F_i , and Z_i are defined in the Notation section. Clearly, these equations are highly coupled. Through a series of manipulations, including substitution and combining sets of equations to eliminate common variables, one can arrive

at a series of first order differential equations suitable for numerical integration techniques

$$\begin{aligned}
 \frac{dz}{dt} &= \dot{z} \\
 \frac{dz'}{dt} &= \dot{z}' \\
 \frac{d\bar{z}}{dt} = \dot{\bar{z}} &= \frac{\frac{-F_2 - \frac{D_1}{D_3}}{Z_4 + \frac{D_2}{D_3}} + \frac{F_1 + \frac{D_1}{D_3}}{Z_2 + \frac{D_2}{D_3}}}{\frac{-Z_1 - \frac{D_1}{D_3}}{Z_2 + \frac{D_2}{D_3}} + \frac{Z_3 + \frac{D_1}{D_3}}{Z_4 + \frac{D_2}{D_3}}} \\
 \frac{d\bar{z}'}{dt} = \dot{\bar{z}}' &= \frac{\frac{-F_2 - \frac{D_1}{D_3}}{Z_3 + \frac{D_1}{D_3}} + \frac{F_1 + \frac{D_1}{D_3}}{Z_1 + \frac{D_1}{D_3}}}{\frac{-Z_2 - \frac{D_2}{D_3}}{Z_1 + \frac{D_1}{D_3}} + \frac{Z_4 + \frac{D_2}{D_3}}{Z_3 + \frac{D_1}{D_3}}} \\
 \frac{d\omega_3}{dt} = \dot{\omega}_3 &= \frac{\left(\frac{C_5 B_{13}}{C B_{25}}\right) \bar{z} + \left(\frac{C_{10} A_{24}}{C A_{26}} + \frac{C_5 B_{21}}{C B_{25}}\right) \bar{z}' + \frac{C_{10} A_{28}}{C A_{26}} + \frac{C_5 B_{26}}{C B_{25}} - \frac{C_{11}}{C}}{1 - \frac{C_{10} A_{27}}{C A_{26}} - \frac{C_5 B_{23}}{C B_{25}}} \\
 \frac{d\omega_1}{dt} = \dot{\omega}_1 &= -\frac{A_{27}}{A_{26}} \dot{\omega}_3 - \frac{A_{24}}{A_{26}} \bar{z}' - \frac{A_{28}}{A_{26}} \\
 \frac{d\omega_2}{dt} = \dot{\omega}_2 &= -\frac{B_{23}}{B_{25}} \dot{\omega}_3 - \frac{B_{13}}{B_{25}} \bar{z} - \frac{B_{21}}{B_{25}} \bar{z}' - \frac{B_{26}}{B_{25}}
 \end{aligned} \tag{145}$$

The equations remain coupled, so the sequence in which the equations are numerically integrated is important. Because the equations for \bar{z} and the equation for \bar{z}' are functions of z and z' , z and z' must be integrated first. Similarly, \bar{z} and \bar{z}' must be integrated before $\dot{\omega}_3$, $\dot{\omega}_3$ before $\dot{\omega}_1$, and $\dot{\omega}_1$ before $\dot{\omega}_2$. In the computer program, the seven variables that describe the motion are stored in a seven column matrix where $\omega_1 = y[1][j]$, $\omega_2 = y[2][j]$, $\omega_3 = y[3][j]$, $z = y[4][j]$, $\dot{z} = y[5][j]$, $z' = y[6][j]$, and $\dot{z}' = y[7][j]$. The index j identifies the

matrix location for each set of saved variables over time. All other needed quantities can be calculated by using the seven time dependent variables describing the motion, and the parameters of the dual-spin system. These additional dynamical quantities are stored as one dimensional vectors in the computer.

2. Angular Momentum

Angular momentum was derived in Equations (123), (124), and (125). The angular momentum is a vector, but for verification of the conservation of angular momentum, only the magnitude is required. Therefore, the three vectorial components for both the rotor and the platform are computed individually as H1, H2, H3, H1p, H2p, H3p, and then the magnitude of the angular momentum, h , is determined and stored.

3. Nutation Angle

The nutation angle is determined using the previously determined relation

$$\theta = \cos^{-1} \left(\frac{\mathbf{h} \cdot \mathbf{b}_3}{|\mathbf{h}|} \right) = \cos^{-1} \left(\frac{h_3 + h_3'}{|\mathbf{h}|} \right) = \cos^{-1} \left(\frac{I_s \omega_s + I_s' \omega_s'}{|\mathbf{h}|} \right) \quad (34)$$

Since it is a function of angular momentum, it can now be calculated and stored as theta [i].

4. Energy

The total energy of the system, Equation (136), is determined by the sum of the kinetic energy, as derived in Equation (134), and the potential energy of the particle masses of the mass-spring-dashpot damper system, Equation (135). It is written as

$$E_{total} = E + U = E + \frac{1}{2} k z^2 + \frac{1}{2} k' z'^2 \quad (136)$$

In the computer program the kinetic energy, ke [i], is the sum of the constituents of Equation (134), identified as T1 through T13. The potential energy is not explicitly stated in the program, but instead is included in the calculation of the total energy, etotal [i].

5. Core Energy and Postulated Core Energy

The platform and rotor core energy of the dual-spin system is defined in Equations (47) and (48) respectively. All of the variables are available, such that in the computer program the energies are readily calculated as $E_{cp} [J]$ and $E_c [J]$. The postulated nutation angle may now be computed. Equation (101) indicates a sign must be selected depending on whether the system is stable or unstable. The calculation of nutation angle over time in Equation (34) will indicate stability. The computer program incorporates conditional statements to assign the correct sign in the postulated nutation angle expression, Equations (101) and (106). In the derivation leading up to the postulated nutation angle, σ has been defined as the relative rotation rate of the rotor with respect to the platform, and is a positive value. This provides a positive contribution to the angular momentum vector, thus providing stability to the system. In Mingori's equations of motion, the reference coordinate axes are fixed to the rotor, resulting in the relative rotation of the platform in the counter-clockwise, or negative, direction. The postulated nutation angle equations were developed using the former reference frame. To compensate for the difference in the reference frames, the postulated nutation angle equations in the computer program have σ replaced by $-\sigma$.

The postulated core energy as a function of time is computed for the platform and the rotor, using Equations (140) and (141) for the exponential model and Equations (142) and (143) for the Verhulst model. A postulated core energy model that accurately models the actual core energy required several iterations to find the proper values of the exponential factor.

Once the postulated core energy models are computed, the Q' and Q values, as defined in Equations (100) and (107), are determined. The postulated nutation angles,

ϵ_{tah} [], and ϵ_{ta} [], are computed using Equation (101) and (106) with the proper sign previously determined.

The revised stability criterion, Equation (97), requires the time rate of change of the core energy and the nutation frequency. Since both of these parameters may vary with time, an estimate is made to determine if the modified stability criteria correctly predicts stability or instability. The time rate of change of the core energy is approximated by taking the difference of the final and the initial core energy values, and dividing by the time of the simulation. This quantity is then divided by the initial nutation frequency. This stability quantity is computed for both the rotor and the core, but is indicated in Table (1), Summary of Analyzed Cases, simply as a negative or positive value.

B. COMPUTER PROGRAM

Essential to the verification of the stability criteria is the computer program that integrates the dual-spin system equations of motion, calculates other dynamical quantities of motion, and graphs the results. The system used was a Sun SPARC 2 workstation with the computer code written in C. Intermediate graphics results were created using an in-house computer graphics program. Final graphics output was performed by sending output data to the Deltagraph graphics package. The sequence of steps of the computer code are explained below. The computer code is included as Appendix B.

1. Initialization

The main computer program is compiled, along with the header file 'rkk.h' and the function 'derivs' immediately preceding it. The function 'derivs' contains Mingori's equations of motion rewritten into Equation (145), suitable for numerical integration. Included in the header file 'rkk.h' is the numerical integration routine 'rk4,' the adaptive step size function 'rkqc,' and the driver for the numerical integration routine 'odeint.' Also included are functions for creating and freeing the vectors and matrices used by the

computer to store the data, and a function for error messages.

a. Variables

The variables required for both the numerical integration routine and subsequent calculations are defined as global variables before the main program. Variables used only within a specific function or only in the main program are defined in their respective functions. Symbolic constants are also defined before the main program using the `#define` statement.

The time dependent variables of motion of the Mingori system, $\omega_1, \omega_2, \omega_3, z, \dot{z}, z', \dot{z}'$, are stored in a seven column matrix. All other parameters to be graphed are stored in one dimensional vectors. Storage in the vectors and the matrix permits retrieval by the graphics subroutine for plotting the variable over time.

b. Input File

The main computer program scans the input file for the necessary parameters. All parameters of the Mingori system, $I_1, I_2, I_3, M, m, a, k, c, I_1', I_2', I_3', M', m', a', k', c'$, and L , are controlled with the input file. Also, the initial conditions for the time dependent variables of the system, $\omega_1, \omega_2, \omega_3, z, \dot{z}, z', \dot{z}'$, are specified. The length of time of the simulation and a variable determining the desired accuracy are specified. Finally, the exponential factor and the final energy for the postulated core energy functions are read.

2. Preliminary Calculations

After the input values are read in, initial calculations are performed prior to the numerical integration routine. All of the defined terms used by D. L. Mingori [Ref 3] in his non-linear equations of motion are computed, as well as definitions required for the core energy calculations, $I_s, I_s', I_{s \text{ total}}, I_t, I_t', I_{t \text{ total}}$, and h_{rigid} .

An option is available to specify critical damping in either the platform or the

rotor. By using the number 1000.0 in the input file for the damping coefficient, the main program will automatically compute the coefficient required for critical damping of the mass-spring-dashpot system and then use this value in all subsequent calculations.

Also computed is the factor 'dxsav', used in determining when to save data. The steps between evaluating the equations of motion can become small, particularly when high accuracy is desired. The interval required for graphics resolution is not as restrictive. Accordingly, the variables are saved only if the step is greater than the previously saved step by the factor 'dxsav.'

3. Numerical Integration

Mingori's nonlinear equations of motion are numerically integrated by the fourth order Runge-Kutta method, with adaptive step size control. The computer code used is based on the Runge-Kutta method listed in Numerical Recipes in C, [Ref 8]. The adaptive step size control permits larger integration steps during smooth, well behaved portions of the functions, and smaller steps during the more irregular sections of the functions. The integration routine accuracy can be controlled by a variable in the input file.

Mingori's non-linear equations of motion are contained in the function 'derivs.' As described previously, the equations have been rewritten as a series of first order coupled differential equations suitable for numerical integration.

The output of the time dependent variables of the system, ω_1 , ω_2 , ω_3 , z , \dot{z} , z' , \dot{z}' , is stored in an array of seven columns, with the number of rows required a function of the specified time interval and accuracy. A one dimensional vector is also created, with the time stored for each step saved. This permits plotting the time dependent variables and other quantities versus the time.

4. Calculation of System Parameters

With the array of the time dependent variables of motion as a function of time, the other system quantities listed in Section A may now be calculated, with the values stored in

vectors suitable for graphing.

5. Graphics Output

The remainder of the program is the necessary code for the in-house graphics program. The graphics program is initialized, and the graphics window is opened. The following parameters are then plotted over time: ω_1 , ω_2 , $\omega_3 - \omega_3 \text{ initial}$, z , \dot{z} , z' , \dot{z}' , $h - h_{\text{initial}}$, $E - E_{\text{initial}}$, $E_{\text{total}} - E_{\text{total initial}}$, $E_c - E_c \text{ initial}$, $E_c \text{ postulated} - E_c \text{ postulated initial}$, $E_c' - E_c \text{ initial}'$, $E_c \text{ postulated}' - E_c \text{ postulated initial}'$, θ , η , and η' . The window is then closed and the initial conditions and pertinent time dependent variables and other quantities of the simulation are then printed. This displays the graphical representation of the behavior of the dual-spin system, and provides the actual initial and final values of the variables and associated quantities.

For final graphics output, the Deltagraph graphics program is utilized. Computer simulation data is sent as an output file. The data is then manipulated into a suitable graphic with proper scaling and axes limits to best represent the dynamics of the computer simulation. The graphs are contained in Appendix A.

6. Computer Program Validation

The two aspects of the computer code requiring validation were the numerical integration routine and Mingori's equations of motion with its associated dynamical quantities for the dual-spin system.

The validation of the numerical integration routine was performed by using the equations of motion for a simple torque-free axisymmetric body. Various initial conditions were read in, and the dynamical quantities were then plotted versus time. The plotted behavior was then compared to the actual response of the system.

The validation of Mingori's equations of motion and the associated dynamical quantities required a more comprehensive approach. The equations of motion required

validation for proper behavior of each time-dependent variable of motion. Then the kinetic energy, total energy, and angular momentum must be verified. Several cases were run where the platform mass and inertia would become infinitesimally small. Then cases were run where the rotor mass and inertia would become infinitesimally small. In each of these cases, subcases were run where the mass-spring-dashpot system would be large, dominating the dynamics, to the subcase where it became very small, so the system approximates a rigid body. These different scenarios would uncouple and isolate the various parts of the equations of motion to verify proper derivation of the equations. In general, the platform and the rotor were tested under conditions varying from those in a rigid body scenario to those in a lightly damped body. The system was then tested as a rigid dual-spin system, as a dual-spin system with rotor damping only, and as a dual spin system with platform damping only. The dual-spin system was then tested with both the rotor and the platform containing dampers. For each case, the time dependent variables of motion were plotted and analyzed. In all cases, the angular momentum was compared with the initial angular momentum. Since all cases were torque free, the angular momentum must remain constant. In all cases explored, the angular momentum verified the correctness of the equations of motion. The code validation cases were not included in this thesis due to the large number of graphs and data that were required to establish validation.

V. ANALYSIS

A. INTRODUCTION

1. Objective

The development of the revised energy-sink stability theory has been presented in Chapter II, and the equations of motion for a dual-spin system are contained in Chapter III. With the numerical integration code of Chapter IV, the revised energy sink stability theory can now be verified. The core energy of the system is plotted as a function of time and compared to the total energy for agreement with theory. The stability criterion computed from the numerical simulation must then agree with Equation (97). Conservation of angular momentum is used in each case to verify the correctness of the equations, and to ensure the accuracy of the numerical integration routine. To approximate the core energies over time, an exponential model and a model based on logistic growth are then explored. The logistic growth model uses an equation presented by Verhulst [Ref 7], and is referred to as the Verhulst model. Postulated models of core energy and the associated nutation angles are then compared with the actual core energies and nutation angle for agreement.

2. Numerical Simulation Cases

Four distinct cases needed to be addressed. With the inertia ratio of the dual-spin system greater than one, a stable case and an unstable case are analyzed (Cases (1) and (4)). With the inertia ratio less than one, a stable case and an unstable case are also analyzed (Cases (2) and (3)). For these four cases, an exponential model is used to postulate the core energy and the corresponding nutation angle. For the case of the inertia ratio greater than one and unstable, and the two cases of the inertia ratio less than one, stable and unstable, the Verhulst model is postulated (Cases (5), (6), and (7)). The case of

the inertia ratio greater than one and stable was not included; from the excellent agreement of Cases (5), (6), and (7), one can see that excellent agreement would also occur for this trivial case, making it unnecessary to include. All seven cases are summarized in Table (1). For each case, the dynamical quantities are plotted versus time until the system reaches a stable state. Each quantity is then plotted for the first one hundred seconds to show detail.

<u>CASE</u>	<u>$\frac{I_{s \text{ total}}}{I_{t \text{ total}}}$</u>	<u>STABILITY</u>	<u>$\frac{\dot{E}_C}{\lambda}$</u>	<u>$\frac{\dot{E}_C'}{\lambda'}$</u>	<u>MODEL</u>	<u>COMMENTS</u>
1	1.039	stable	negative	negative	exponential	large damping in platform
2	0.907	stable	negative	negative	exponential	large damping in platform
3	0.897	unstable	positive	positive	exponential	insufficient damping in platform
4	1.025	unstable	positive	positive	exponential	insufficient damping in platform
5	0.907	stable	negative	negative	Verhulst	same conditions as Case 2
6	0.897	unstable	positive	positive	Verhulst	same conditions as Case 3
7	1.025	unstable	positive	positive	Verhulst	same conditions as Case 4

Table (1) Summary of Analyzed Cases

In Appendix A, tables (2) through (8) list the system parameters, core energy parameters, and initial conditions. Immediately following these tables are the graphs of the important dynamical quantities. A typical geosynchronous dual-spin satellite was selected for the numerical simulation. The platform and rotor masses and inertias are listed as part of the initial conditions, and are the same for all cases. The inertia ratio is made greater than or less than one by selecting L , the distance between the rotor and platform centers of mass, to be 0.3 or 1.0 meter respectively. As a default set of values, all of the mass-

spring-dashpot systems have m and m' equal to 1.0 kg, k and k' equal to 1.0 N/m, and c and c' equal to 1.0 kg/sec. To establish the stable cases, additional energy dissipation is required in the platform. To achieve this, cases (1), (2), and (5) have m' increased to 20.0 kg and c' increased to 10.0 kg/sec. In all seven cases, the initial conditions are the same. The platform rotates at a geosynchronous angular velocity, the rotor spins at the higher rate of 1.5 rad/sec, and a perturbation is introduced by an initial transverse angular velocity of 0.1 rad/sec. The mass-spring-dashpot systems have no initial displacement or initial velocity. The core energy parameters are also listed in the tables. The initial core energies are determined by the system's initial conditions. The final core energies were taken from the numerical simulation data. The exponential factors, r and r' , were then determined through an iterative process to best fit the modeled core energy to the actual core energy.

B. DISCUSSION

The individual cases can now be analyzed. The graphs of the dynamical quantities are explored, and the data will affirm the revised stability theory.

1. Angular Momentum

For each case, the angular momentum is plotted versus time, Figures (5), (6), (16), (17), (27), (28), (38), (39), (49), (50), (60), (61), (71), and (72). Because the dual-spin system has no external forces, angular momentum must be conserved. For the stable cases, there is excellent agreement, with angular momentum varying by less than one one-hundredth of a percent over the length of the data run. This confirms the equations of motion and validates the accuracy of the numerical integration routine. For the unstable cases, the angular momentum percent difference increases to approximately four one-hundredths of a percent. This is attributed to the increased dynamics of the system as it establishes the spin about the transverse axis, introducing very small errors in the numerical

integration routine. The errors remain very small, and the equations of motion and the numerical integration routine remain accurate.

2. Total Energy, Platform and Rotor Core Energy

The graphs of energy are in Figures (7) through (10), (18) through (21), (29) through (32), (40) through (43), (51) through (54), (62) through (65), and (73) through (76). Several observations can be made.

The total energy curve reaches equilibrium before both the platform and the rotor core energies do. For Case 2 and 5, the total energy appears to reach a maximum and then drop down to a final equilibrium value. Careful comparison of Figures (18) and (49), shows the same system with the same initial conditions, but with a slightly different curve. It can be deduced that the energy is not steady, but is still oscillating. The sampling frequency coincidentally saved values near the same magnitude of energy in the region from about 3000 seconds to 10000 seconds.

The total energy for Cases (1), (3), (5), and (6) decreased. For Cases (2), (4), and (7), representing both stable and unstable systems, it increased. This can be explained easiest with the use of equations (26) and (27). For Cases (2), (4), and (7), the system is settling out about the axis with the minimum moment of inertia. Because there are no external forces, the angular momentum is constant. In the equation for angular momentum, Equation (26), the inertia terms are squared. But in the equation for energy, Equation (27), the inertia terms are not squared. Therefore, as the angular velocity transfers to the axis with the minimum moment of inertia, Equations (26) and (27) show that the energy will increase. These equations apply to a simple dual-spin system. Equations (123) and (136) for the Mingori dual-spin system would show the same result, provided the energy absorbed by the mass-spring-dashpot system and the energy associated with the motor is less than the energy increase associated with transferring the spin to the axis of minimum moment of inertia. This is the situation for Cases (2), (4), and (7).

The total energy value will always be between that of the platform core energy and the rotor core energy. The platform core energy will have smaller values as its equation assumes that the rotor is rotating at the same rate as the platform, thereby not accounting for the large amount of kinetic energy associated with the rotor. The rotor core energy will be higher than the total energy as it assumes that the slowly spinning platform is rotating at the same rate as the rotor, providing the system with additional kinetic energy.

The hundred-seconds graphs of total energy versus time shows curves with several different behaviors. The time rate of change of total energy includes the energy dissipation rate of the rotor and platform mass-spring-dashpot systems, and the rate of work due to the motor torque maintaining the relative rotation rate. In the hundred-seconds graphs, aside from the general slope of the curve, there is no apparent correlation between the specific behavior of the total energy to that of the core energies. Any relationship that exists is masked by the motor and mass-spring-dashpot system's influences on total energy.

3. Stability Criterion

The revised stability criterion of equation (97) states that the time rate of change of the core energy over the respective nutation frequency must be less than or equal to zero. The sign of the stability criterion for each case must be determined. The time rate of change of the core energy was determined by dividing the final less the initial value of the core energy by the length of time of the case. The nutation frequencies were computed using initial conditions. The sign of the stability criterion is listed in Tables (1) through (8). The numerical value was not listed because the above assumptions used during the computation give it no merit. Cases with inertia ratios very close to one were intentionally selected to test the inertia ratio in this transition region. In all cases analyzed, the sign of the revised stability criterion was consistent with the stability of the system.

4. Postulated Core Energy and Nutation Angle

An explicit relationship for core energy as a function of time does not exist. If an equation describing core energy did exist, then by using Equations (101) and (106) the nutation angle as a function of core energy and time could be predicted for a dual-spin system. This could then be extended to an actual dual-spin satellite. Given a sufficient model of the satellite, the stability and the nutation angle as a function of time could be predicted. An objective of this thesis is to see if an equation for the core energy can be developed that would adequately describe the nutation angle as a function of time for both the stable and unstable conditions. The exponential model and the Verhulst logistic model were explored.

a. Exponential Core Energy Model

Observation of the core energy as a function of time for a stable system would lead one to conclude that it behaves in an exponential manner. Equations (140) and (141) are exponential representations of rotor and platform energy as a function of time. The initial core energy was determined by the initial conditions of the dual-spin system. The final core energy was determined by running the numerical simulation and calculating it at the end of the simulation. If this was not available, a value could be estimated. Applying the principle of conservation of angular momentum and noting that the system will eventually spin about one of the primary axes, then the equations for angular momentum and total energy can be used to solve for the angular velocity about that axis. Substituting this into Equation (47) or (48), one would arrive at an estimated final core energy. Although it would not be the actual final core energy, as motor torque contribution and the mass-spring-dashpot system's energy dissipation was not accounted for, it would be sufficiently close to satisfy the computational requirements. The exponential factor is dependent upon the system parameters and initial conditions. For the cases presented, different values were tried until good agreement was established with the core energy

curve. Additional research would be required to determine a suitable exponential factor for an actual satellite, taking into account the parameters and the initial conditions. Cases 1 through 4 contain the numerical simulation data for the exponential model. The actual and postulated curves for core energy are contained in Figures (11) through (15), (22) through (24), (33) through (37), and (44) through (48). For cases 1 and 2, both stable, there is excellent agreement between the core energy and the postulated core energy. This in turn, results in excellent agreement between the actual nutation angle and the modeled nutation angle. The actual nutation angle is determined using the angular momentum quantities, as shown in Equation (34). The time dependent variable required to compute the nutation angle is the angular velocity about the spin axis. The modeled nutation angle is determined in Equations (101) and (106), and is a function of only one time-dependent variable, core energy. Herein lies the potential of the core energy theory. A sufficient model of core energy over time, as in Cases 1 and 2, will provide an excellent prediction of nutation angle, without requiring any knowledge of the specific angular velocities of the system as a function of time.

Cases 3 and 4 illustrate the exponential model for an unstable dual-spin system. The exponential model for core energy, and its associated nutation angle, rapidly approach their final values. The actual core energy and nutation angle, however, behave quite differently. The initial conditions have the system near an unstable equilibrium. The system moves from the unstable to the stable equilibrium slowly at first. It then increases the rate at which it approaches stable equilibrium, passes through an inflection point, and then approaches equilibrium asymptotically. It is clear that the exponential model represents this behavior poorly. Verhulst's logistic equation was then addressed to determine its adequacy in modeling the dual spin system.

b. Verhulst Logistic Core Energy Model

The Verhulst logistic equation was introduced in Chapter III. Figure (4) and the associated description explains the characteristics of the equation. The general shape of the curves in Figure (4) is very similar to the stable and unstable cases of the dual-spin system. Case 5 is the Verhulst model of the Case 2 stable system. Figures (55) through (59) show that the Verhulst logistic equation can achieve excellent agreement with core energy and nutation angle, just as the exponential model did.

Cases 6 and 7 are the same as Cases 3 and 4, except the Verhulst logistic equation is used to model the core energies. Figures (66) through (70) and (77) through (81) illustrate the modeled and actual core energies. Although the Verhulst model for rotor core energy had excellent agreement, it performs poorly when modeling the unstable system. The rotor core energy begins at an initial value and then decreases to an equilibrium value. Referencing Figure (4), the Verhulst logistic equation will model the rotor core energy exponentially.

To take advantage of the Verhulst logistic equation's curve beginning near the the unstable equilibrium and its progression to the asymptotically stable equilibrium, the core energy must increase over time. The platform core energy behaves in this manner as the nutation angle goes from a small angle to ninety degrees. Figures (68) through (70) and (79) through (81) show the Verhulst modeled and the actual platform core energies, and the modeled and the actual nutation angles. The agreement between the actual and modeled energies and nutation angles was very good. The general shape of curve was consistent, with only a slight deviation in the center of the curve, and then a small deviation as the nutation angle approaches the equilibrium value of ninety degrees. With this agreement, it is established that a core energy model exists that can represent both stable and unstable cases. For each of the cases, core energy is plotted versus nutation the angle,

Figures (15), (26), (37), (48), (59), (70), and (81). The graphics package permitted only a semi-log plot of rotor core energy. The plot did not provide any insight on relationships for the dynamics of the dual-spin system. For both the stable and unstable cases, the log-log plot between platform core energy and the nutation angle is linear from ninety degrees until about two degrees. For nutation angles less than two degrees, the platform core energy asymptotically approaches the equilibrium value. Case 5 and 6 is the same system with the same initial conditions, with the exception of the increased damping system in the platform for Case 5. The initial platform core energies and nutation angles are very nearly the same for each case, as shown in Figures (57), (58), (59), (68), (69), and (70). One can conclude by this observation and the definition of nutation angle as a function of core energy, Equation (101), that there exists a continuous platform core energy versus nutation angle curve. The appearance would look similar to the curve created by splicing Figures (59) and (70) together. By varying one parameter, for example platform energy dissipation rate, the system would progress along this curve and achieve equilibrium with a zero degree nutation angle or achieve equilibrium with a ninety degree nutation angle. This is what was done with cases 5 and 6. Adding as the third dimension to the curve the time rate of change of core energy would then reveal the stability, the initial direction, and the rate at which the system will arrive at the equilibrium condition.

C. FURTHER RESEARCH

The revised stability criterion for a dual-spin, quasi-rigid, axisymmetric system was established. Numerical simulation was then used to verify the revised stability theory. Further research could be conducted in several areas. The specific contributions to the total energy could provide some insight. How much energy and in what manner does the motor torque contribute to the total energy for both the stable and the unstable cases? Also, by plotting the energy dissipation system's contributions over time, one could determine its

effect on total energy, as well as comparing it to the core energy theory in Equation (97).

Relationships for core energy as a function of time were explored. It was established that the Verhulst logistic equation could be applied to a stable dual-spin system. By changing its parameters, this equation also applied to the unstable dual-spin system with very good agreement. Further research could be directed to find one equation that would address both the stable and unstable cases of the dual-spin system without changing its parameters. The equation for logistic growth with a threshold [Ref. 7] as applied to the platform core energy shows promise in this regard.

$$\dot{E}_C' = -r' \left(1 - \frac{E_C'}{E_{C \text{ unstable}}'} \right) \left(1 - \frac{E_C'}{E_{C \text{ final}}'} \right) E_C' \quad (146)$$

Given the initial conditions, the platform core energy will typically start at some intermediate value and will either increase or decrease as the dual-spin system reaches equilibrium with a nutation angle of either zero degrees or ninety degrees. Equation (146) would be well suited to model the platform core energy. There exists a platform core energy value, $E_{C \text{ unstable}}'$, where the system is at an unstable equilibrium. Equation (146) shows that at exactly this value, the rate of change of the platform core energy will be zero. For any value below the unstable equilibrium value, the core energy will approach the value of zero. For Case 5, the final core energy for the stable condition was 0.122 J. Although this final condition cannot be represented in Equation (146), it is sufficiently close that the equation may still be used to represent the platform core energy. For any value above the unstable equilibrium value, the core energy will approach the equilibrium value of $E_{C \text{ final}}'$, associated with the nutation angle at ninety degrees. Initial conditions would determine the initial core energy. The final core energy can be estimated as described earlier in this chapter. Finally, the exponential factor r' may then be determined based on the system parameters and initial conditions.

Additional analysis can be performed on the revised stability criterion. The time rate

of change of core energy over nutational frequency may be calculated and plotted versus time or versus other parameters. The behavior of this stability criterion and the magnitude of it for various conditions could provide some insight on postulating a relationship for core energy as a function of time.

VI. CONCLUSION

The existing energy-sink stability criterion was introduced as

$$\boxed{\frac{\dot{E}_D}{\lambda} + \frac{\dot{E}_D'}{\lambda'} \leq 0} \quad (41)$$

It was shown that an inconsistency in the development disproves the existing assumption that the motor energy input exactly balances shaft frictional losses. A revised energy-sink stability criterion was then developed based on Hubert's definition of core energy and was presented as

$$\boxed{\frac{\dot{E}_C}{\lambda} = \frac{\dot{E}_C'}{\lambda'} = \frac{\dot{E}_D}{\lambda} + \frac{\dot{E}_D'}{\lambda'} \leq 0} \quad (97)$$

This criterion compliments the existing theory. Numerical simulation was required to validate the theory. The Mingori dual-spin, quasi-rigid, axisymmetric system was selected for the numerical simulation. Several cases were analyzed to verify the revised energy-sink stability criterion. By correctly postulating the platform or the rotor core energy, the stability of the system could be determined. Specific knowledge of the energy dissipation rates for both the platform and the rotor are no longer required.

An exponential model and the Verhulst logistic model for core energy, and their relationship to the nutation angle, were explored. The exponential model had excellent agreement with the stable cases, but was inadequate in representing the unstable cases. The Verhulst logistic model established that an explicit relationship for core energy could be developed. Nutation angle as a function of core energy for the dual-spin system could then be predicted. The excellent agreement of the postulated core energy and nutation angle with the actual core energy and nutation angle confirms the revised energy-sink stability criterion. Additional research is required to find an optimum equation for core energy as a function of time to represent both the stable and unstable cases.

REFERENCES

¹Iorillo, A. J., "Nutation Damping Dynamics of Axisymmetric Rotor Stabilized Satellites," Paper presented at ASME Winter Meeting, Chicago, IL, 1965; see also "Analyses Related to the Hughes Gyrostat System," Hughes Aircraft Co., El Segundo, CA, Dec. 1967.

²Likins, P. W., "Attitude Stability Criteria of Dual-Spin Spacecraft," *Journal of Spacecraft and Rockets*, Vol. 4, No. 12, Dec. 1967, pp. 1638-1643.

³Mingori, D. L., "Effects of Energy Dissipation on the Attitude Stability of Dual-Spin Satellites," *AIAA Journal*, Vol. 7, 1969, pp. 20-27.

⁴Ross, I. M., "Nutational Stability and Core Energy of a Quasi-Rigid Gyrostat," Paper presented at AAS/AIAA Spaceflight Mechanics Meeting, Houston, TX, Feb. 1991.

⁵Hubert, C., "Spacecraft Attitude Acquisition from an Arbitrary Spinning or Tumbling State," *Journal of Guidance and Control*, Vol. 4, No. 2, Mar.-Apr. 1981, pp. 164-170.

⁶Hughes, P. C., *Spacecraft Attitude Dynamics*, p 203, John Wiley and Sons, Inc, 1986

⁷Boyce, W. E., and DiPrima, R. C., *Elementary Differential Equations and Boundary Value Problems*, pp 64-65, John Wiley and Sons, 1986.

⁸Press, W. H., and others, *Numerical Recipes in C*, pp. 566-580, Cambridge University Press, 1988.

APPENDIX A NUMERICAL SIMULATION DATA

CASE 1: $\frac{I_z}{I_t} > 1$, Stable, Exponential Model

System Parameters		Initial Conditions	
Platform	Rotor	Platform	Rotor
$I_1' = 1600 \text{ kgm}^2$	$I_1 = 1000 \text{ kgm}^2$	$z' = 0.0 \text{ m}$	$z = 0.0 \text{ m}$
$I_3' = 1500 \text{ kgm}^2$	$I_3 = 1200 \text{ kgm}^2$	$\dot{z}' = 0.0 \frac{\text{m}}{\text{s}}$	$\dot{z} = 0.0 \frac{\text{m}}{\text{s}}$
$M' = 1000.0 \text{ kg}$	$M = 700.0 \text{ kg}$	$\omega_3' = 7.27 \times 10^{-5} \frac{\text{rad}}{\text{sec}}$	$\omega_3 = 1.5 \frac{\text{rad}}{\text{sec}}$
$m' = 20.0 \text{ kg}$	$m = 1.0 \text{ kg}$	$\omega_1 = 0.10 \frac{\text{rad}}{\text{sec}}$	$\omega_2 = 0.0 \frac{\text{rad}}{\text{sec}}$
$a' = 1.0 \text{ m}$	$a = 1.0 \text{ m}$	Core Energy Parameters	
$k' = 1.0 \frac{\text{N}}{\text{m}}$	$k = 1.0 \frac{\text{N}}{\text{m}}$		
$c' = 10.0 \frac{\text{kg}}{\text{sec}}$	$c = 1.0 \frac{\text{kg}}{\text{sec}}$	Platform	Rotor
$L = 0.3 \text{ m}$	$\frac{I_z \text{ total}}{I_t \text{ total}} = 1.039$	$E_{c \text{ initial}}' = 13.402 \text{ J}$	$E_{c \text{ initial}} = 3145.4 \text{ J}$
		$E_{c \text{ final}}' = 0.072 \text{ J}$	$E_{c \text{ final}} = 3161.7 \text{ J}$
		$\frac{\dot{E}_C'}{\lambda'} = \text{negative}$	$\frac{\dot{E}_C}{\lambda} = \text{negative}$
		$r' = -.00134 \text{ s}^{-1}$	$r = -.00134 \text{ s}^{-1}$

Table (2) Case 1 Parameters

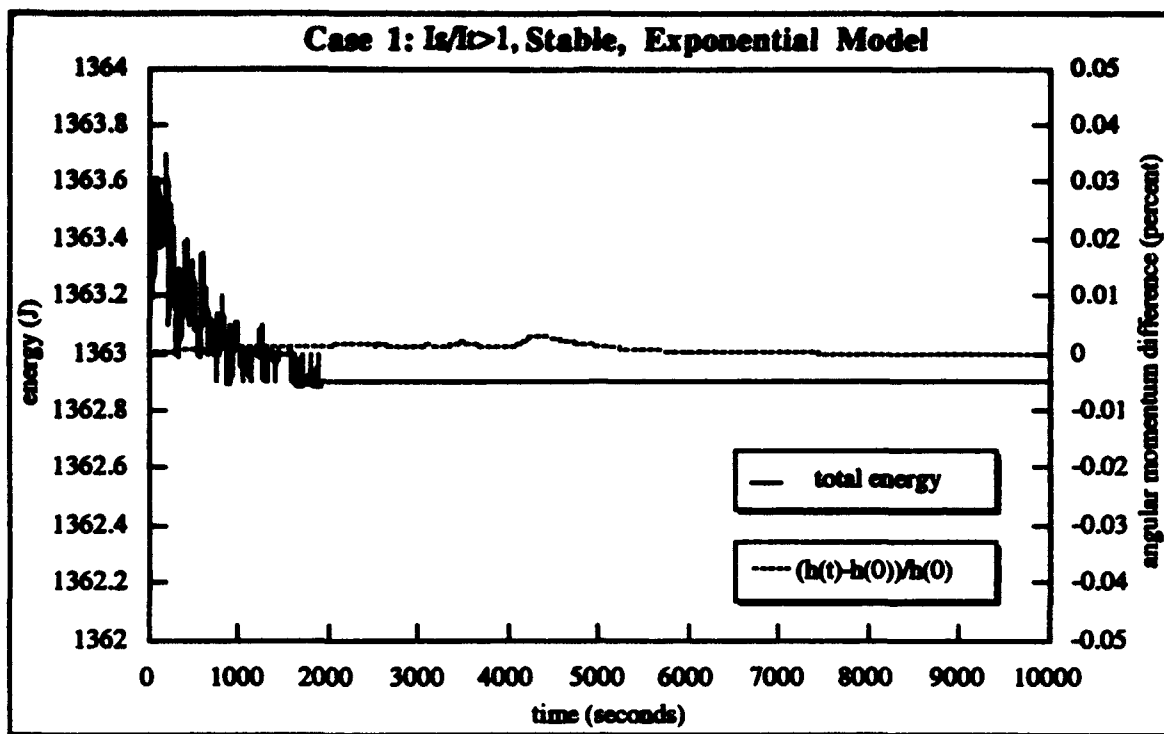


Figure (5) Total Energy and Percent Difference Angular Momentum Versus Time

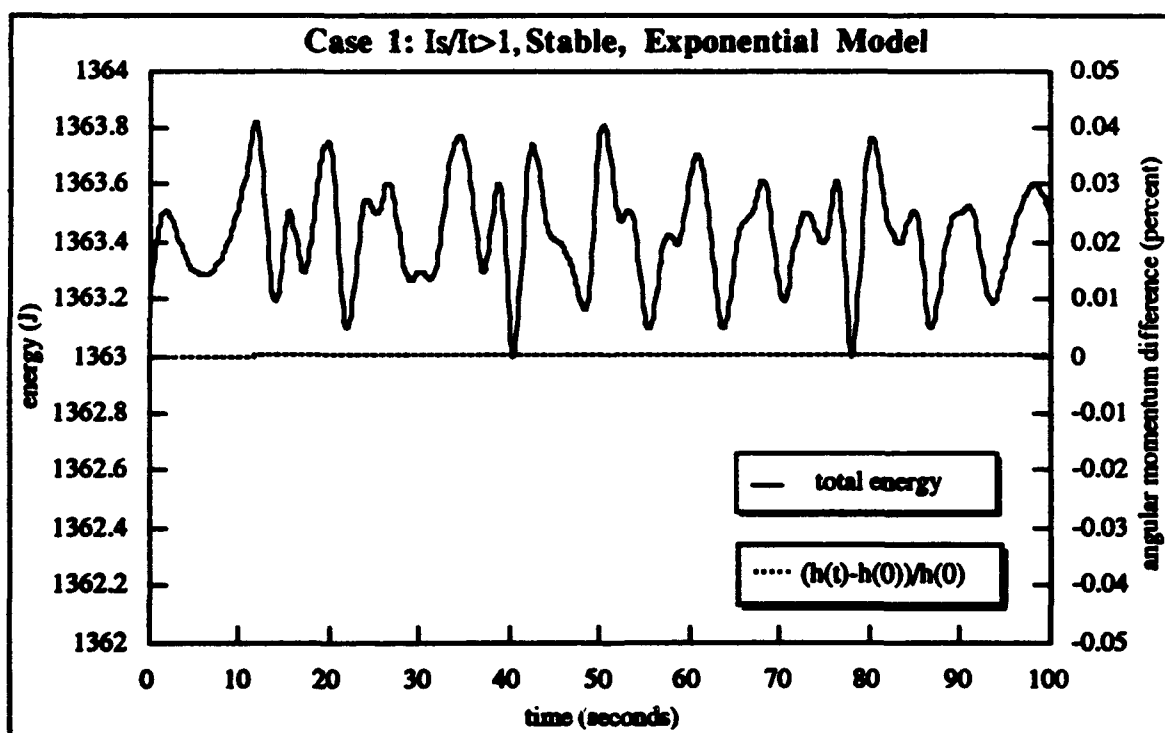


Figure (6) Total Energy and Percent Difference Angular Momentum - First 100 Seconds

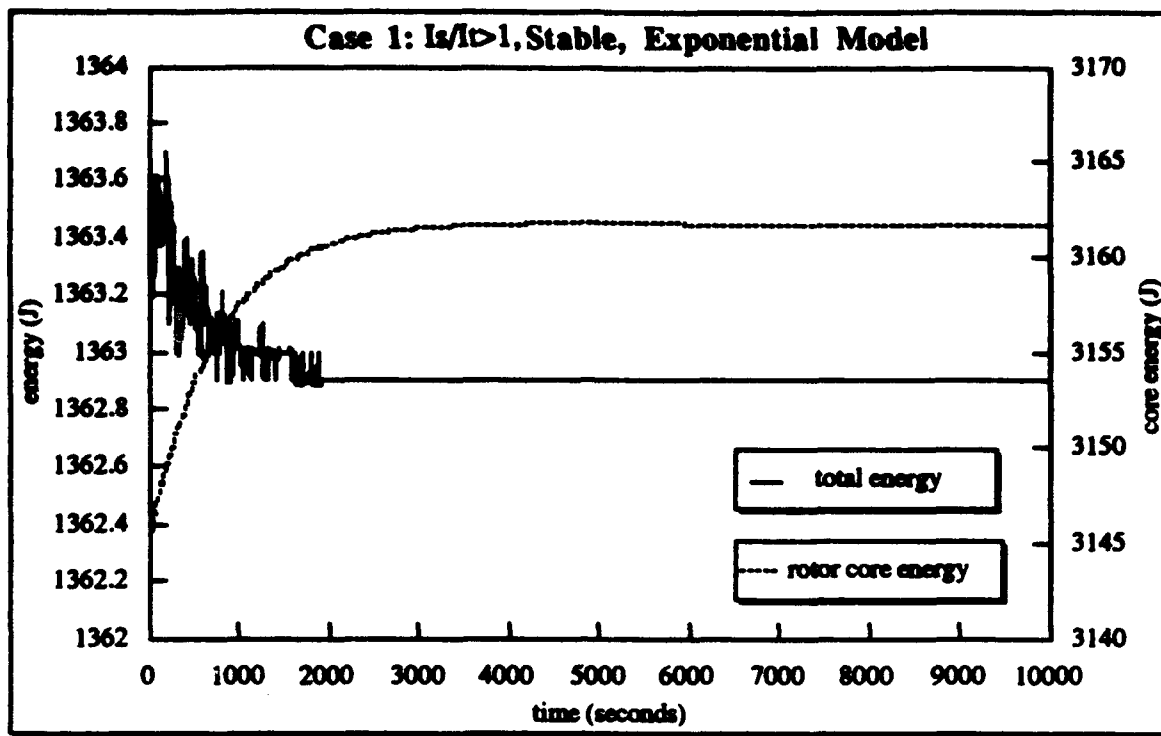


Figure (7) Total Energy and Rotor Core Energy Versus Time

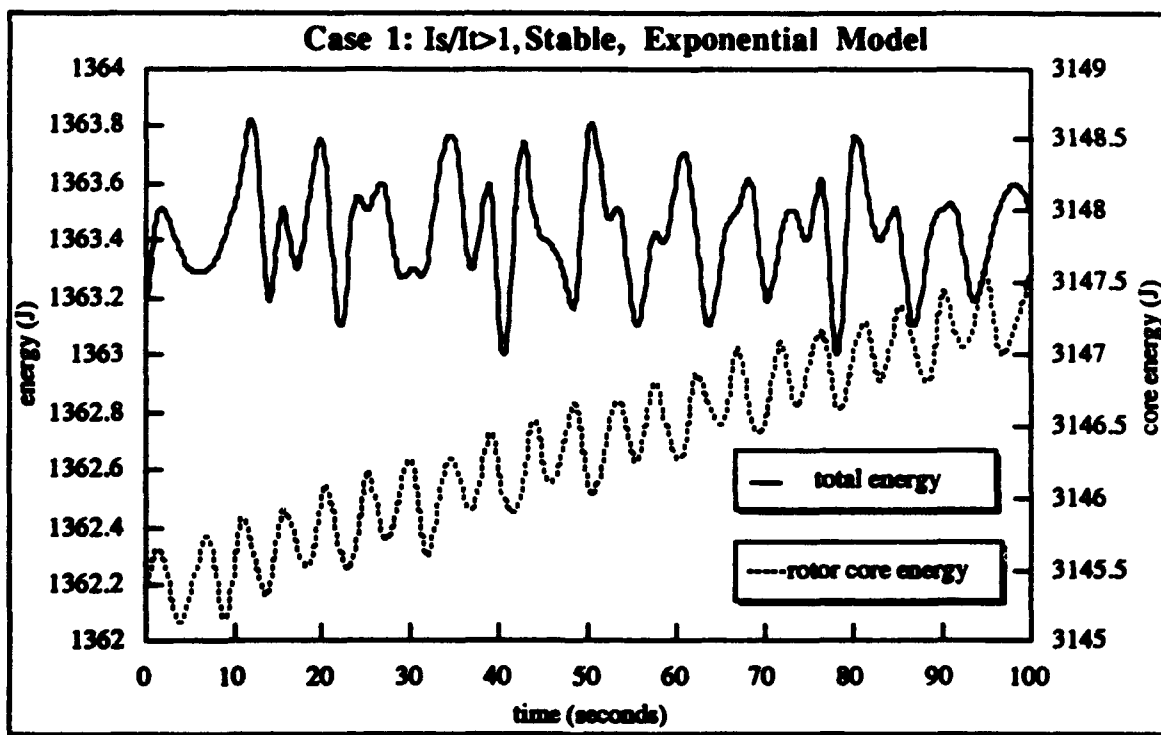


Figure (8) Total Energy and Rotor Core Energy First 100 Seconds

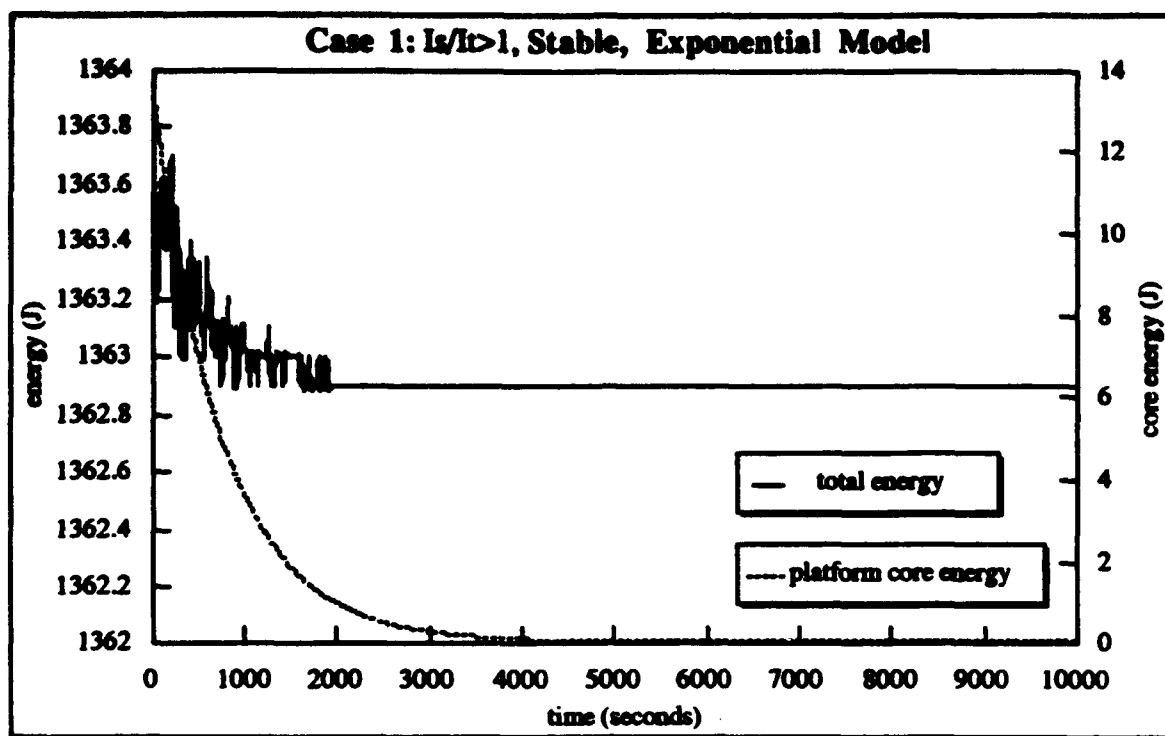


Figure (9) Total Energy and Platform Core Energy Versus Time

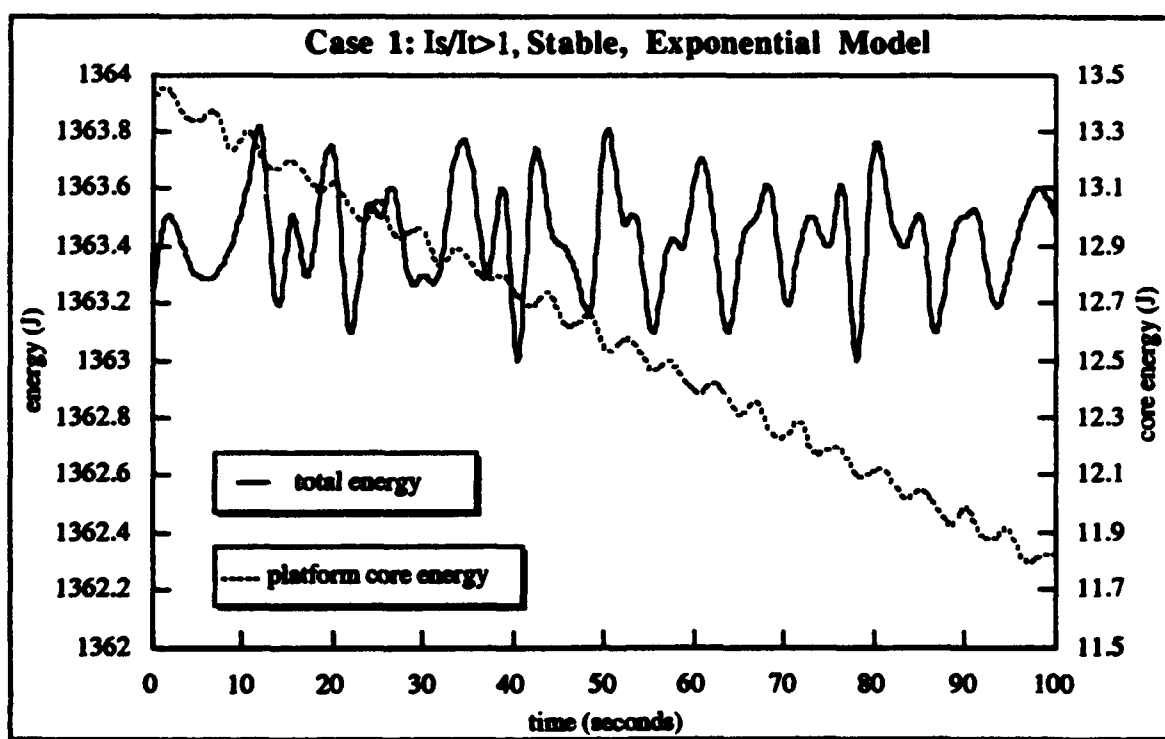


Figure (10) Total Energy and Platform Core Energy - First 100 Seconds

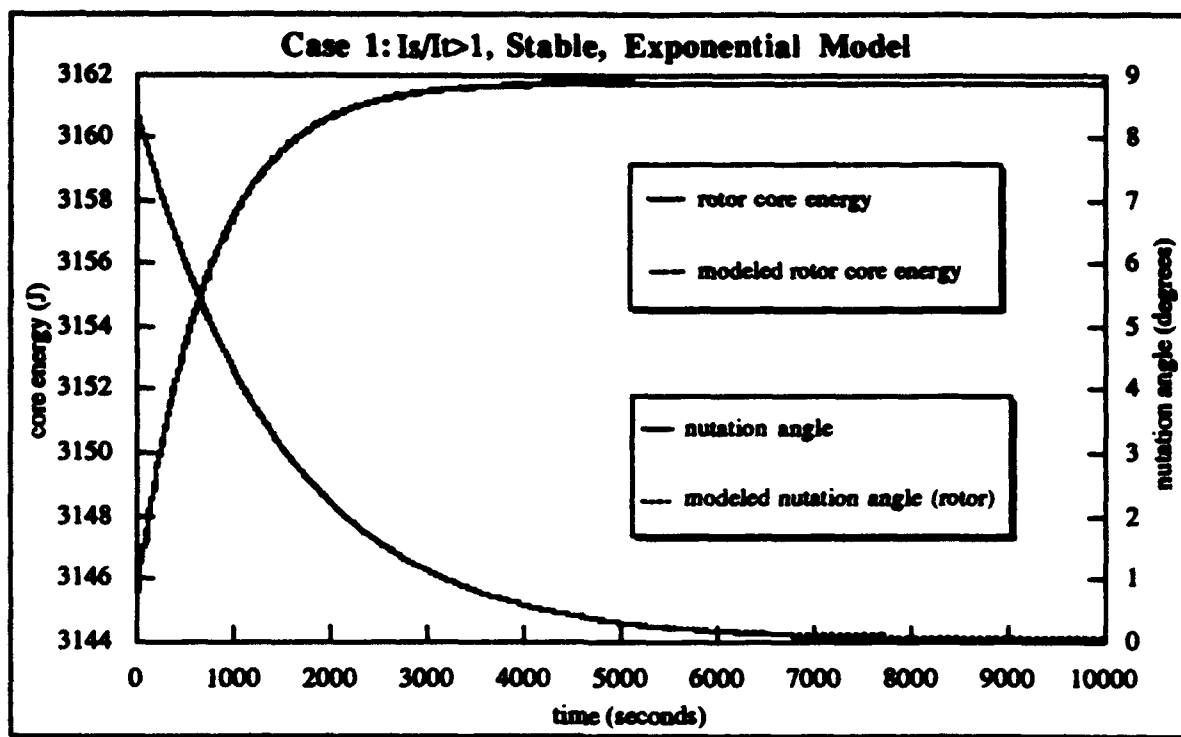


Figure (11) Modeled and Actual Rotor Core Energy and Nutation Angle Versus Time

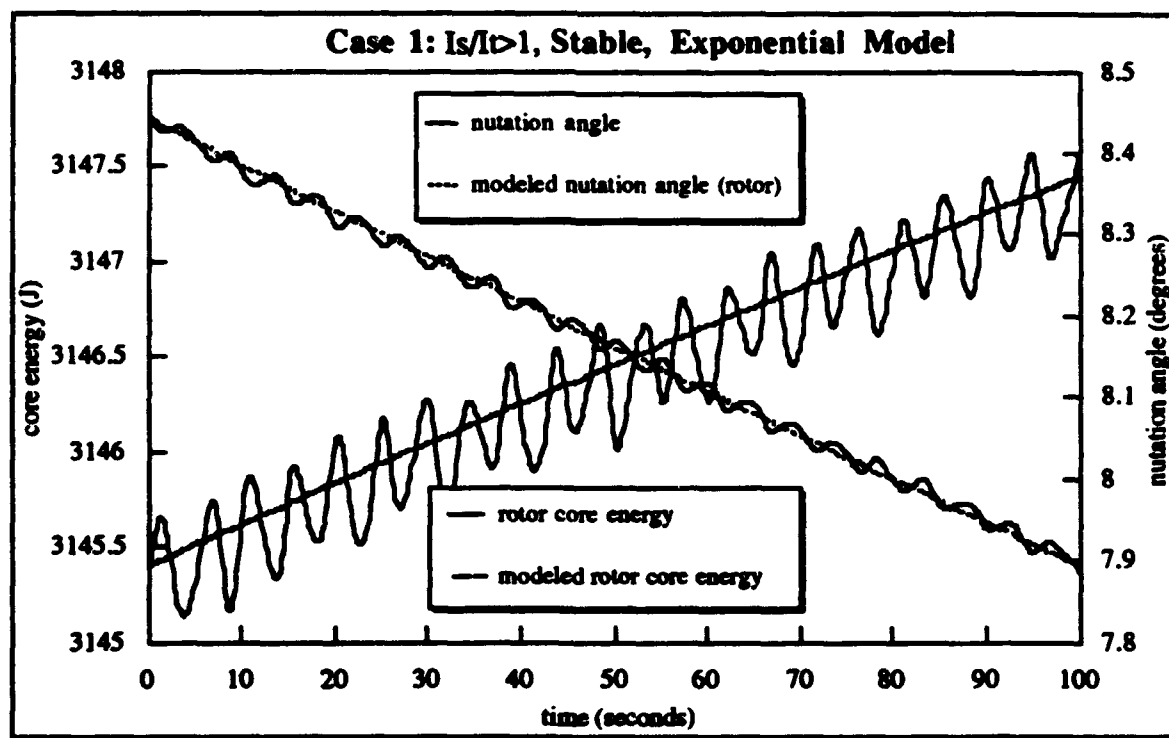


Figure (12) Modeled and Actual Rotor Core Energy and Nutation Angle- First 100 Seconds

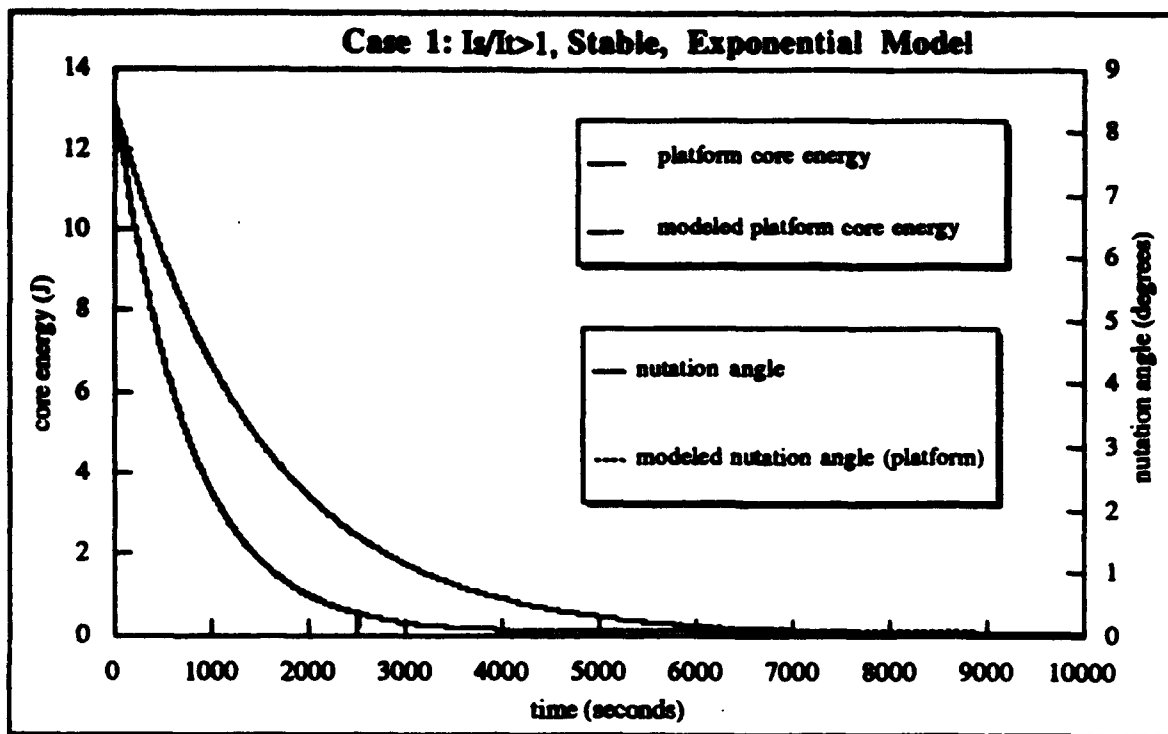


Figure (13) Modeled and Actual Platform Core Energy and Nutation Angle Versus Time

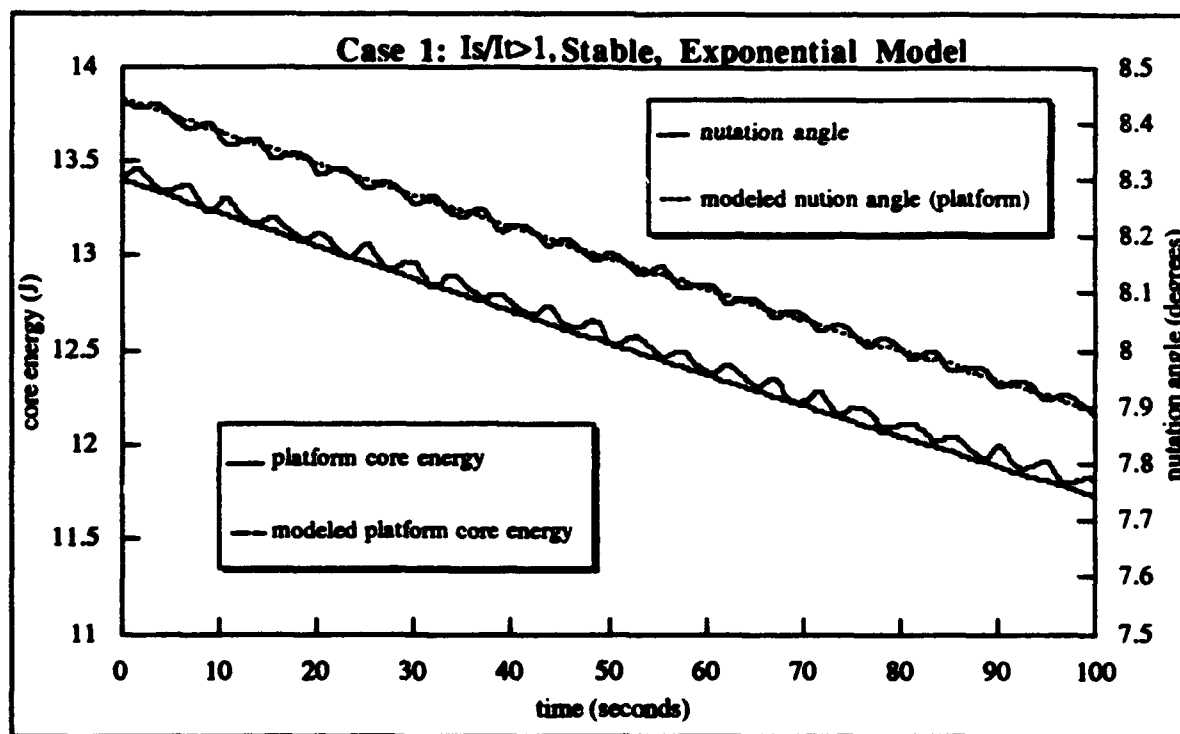


Figure (14) Modeled, Actual Platform Core Energy and Nutation Angle- First 100 Seconds

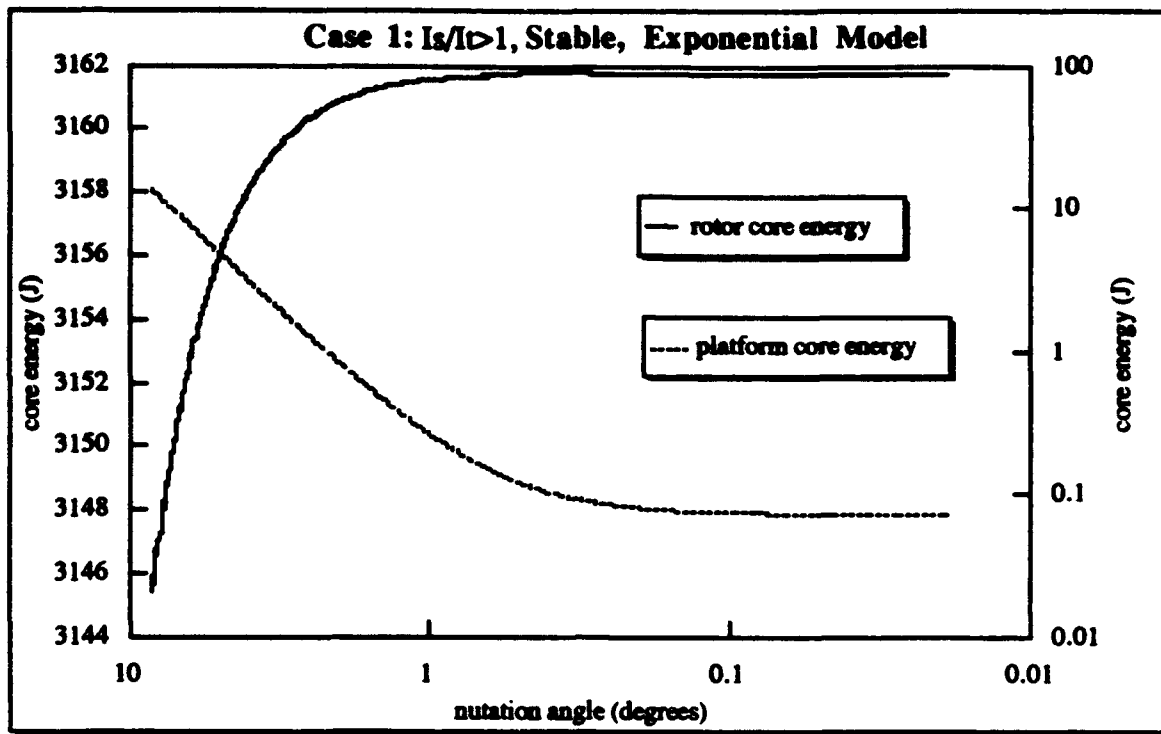


Figure (15) Core Energy Versus Nutation Angle

CASE 2: $\frac{I_2}{I_1} < 1$, Stable, Exponential Model

System Parameters		Initial Conditions	
Platform	Rotor	Platform	Rotor
$I_1' = 1600 \text{ kgm}^2$	$I_1 = 1000 \text{ kgm}^2$	$z' = 0.0 \text{ m}$	$z = 0.0 \text{ m}$
$I_3' = 1500 \text{ kgm}^2$	$I_3 = 1200 \text{ kgm}^2$	$\dot{z}' = 0.0 \frac{\text{m}}{\text{s}}$	$\dot{z} = 0.0 \frac{\text{m}}{\text{s}}$
$M' = 1000.0 \text{ kg}$	$M = 700.0 \text{ kg}$	$\omega_3' = 7.27 \times 10^{-5} \frac{\text{rad}}{\text{sec}}$	$\omega_3 = 1.5 \frac{\text{rad}}{\text{sec}}$
$m' = 20.0 \text{ kg}$	$m = 1.0 \text{ kg}$	$\omega_1 = 0.10 \frac{\text{rad}}{\text{sec}}$	$\omega_2 = 0.0 \frac{\text{rad}}{\text{sec}}$
$a' = 1.0 \text{ m}$	$a = 1.0 \text{ m}$	Core Energy Parameters	
$k' = 1.0 \frac{\text{N}}{\text{m}}$	$k = 1.0 \frac{\text{N}}{\text{m}}$		
$c' = 10.0 \frac{\text{kg}}{\text{sec}}$	$c = 1.0 \frac{\text{kg}}{\text{sec}}$	Platform	Rotor
$L = 1.0 \text{ m}$	$\frac{I_{s \text{ total}}}{I_{t \text{ total}}} = 0.907$	$E_{c \text{ initial}}' = 15.34 \text{ J}$	$E_{c \text{ initial}} = 3147.3 \text{ J}$
		$E_{c \text{ final}}' = 0.123 \text{ J}$	$E_{c \text{ final}} = 3170.9 \text{ J}$
		$\frac{\dot{E}_C'}{\lambda'} = \text{negative}$	$\frac{\dot{E}_C}{\lambda} = \text{negative}$
		$r' = -0.00102 \text{ s}^{-1}$	$r = -0.00102 \text{ s}^{-1}$

Table (3) Case 2 Parameters

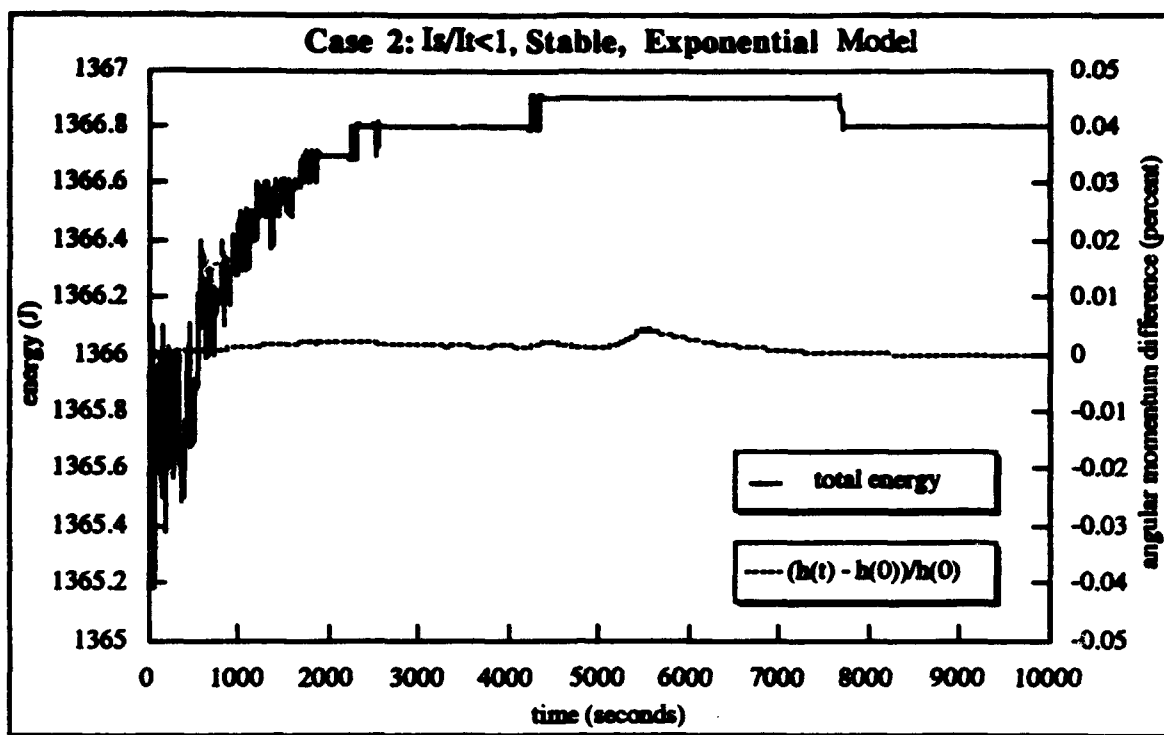


Figure (16) Total Energy and Percent Difference Angular Momentum Versus Time

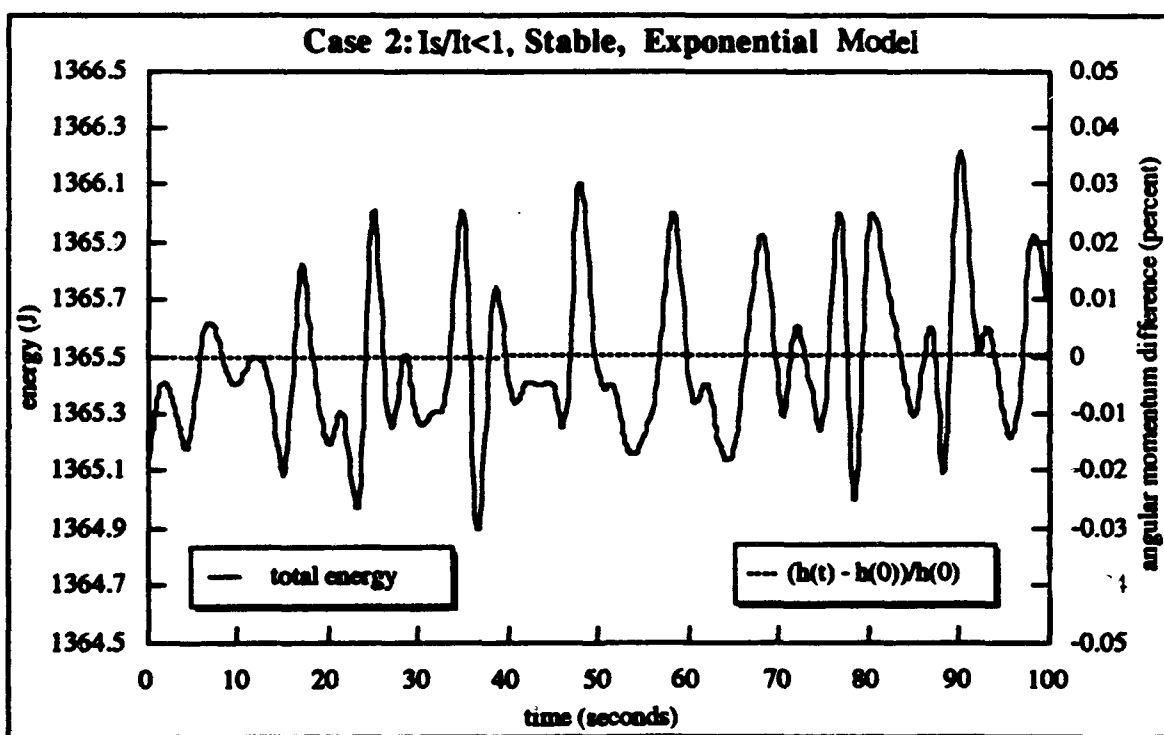


Figure (17) Total Energy and Percent Difference Angular Momentum - First 100 Seconds

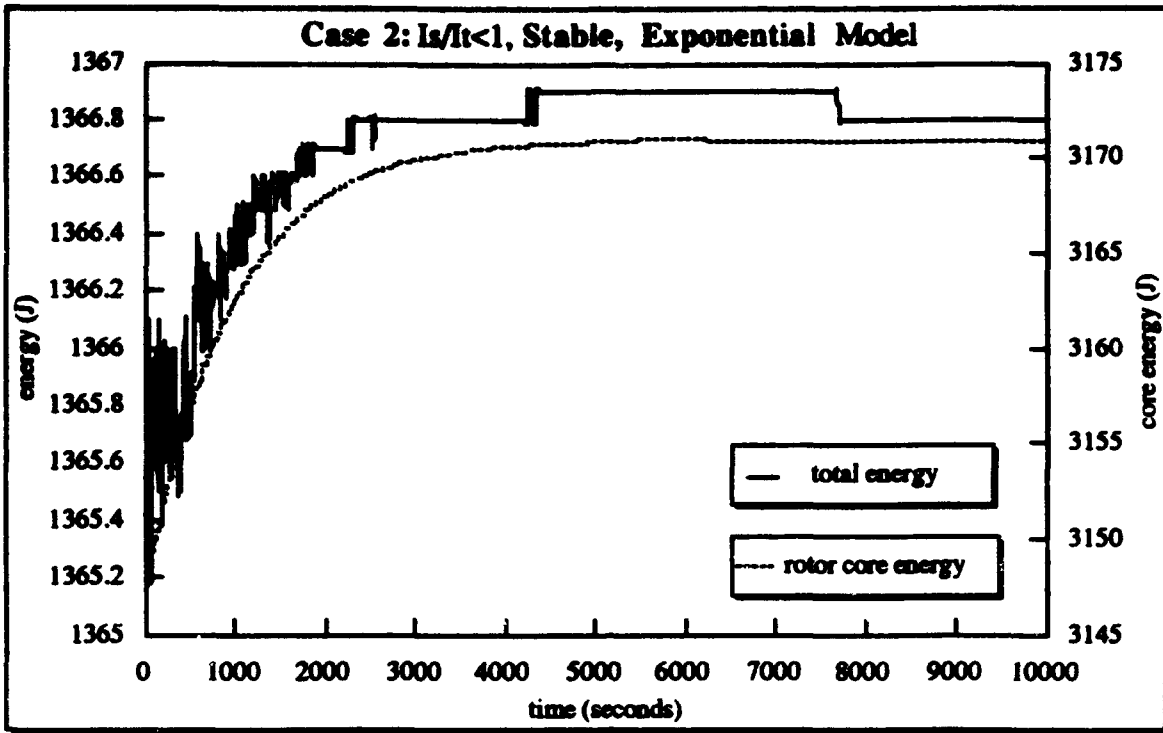


Figure (18) Total Energy and Rotor Core Energy Versus Time

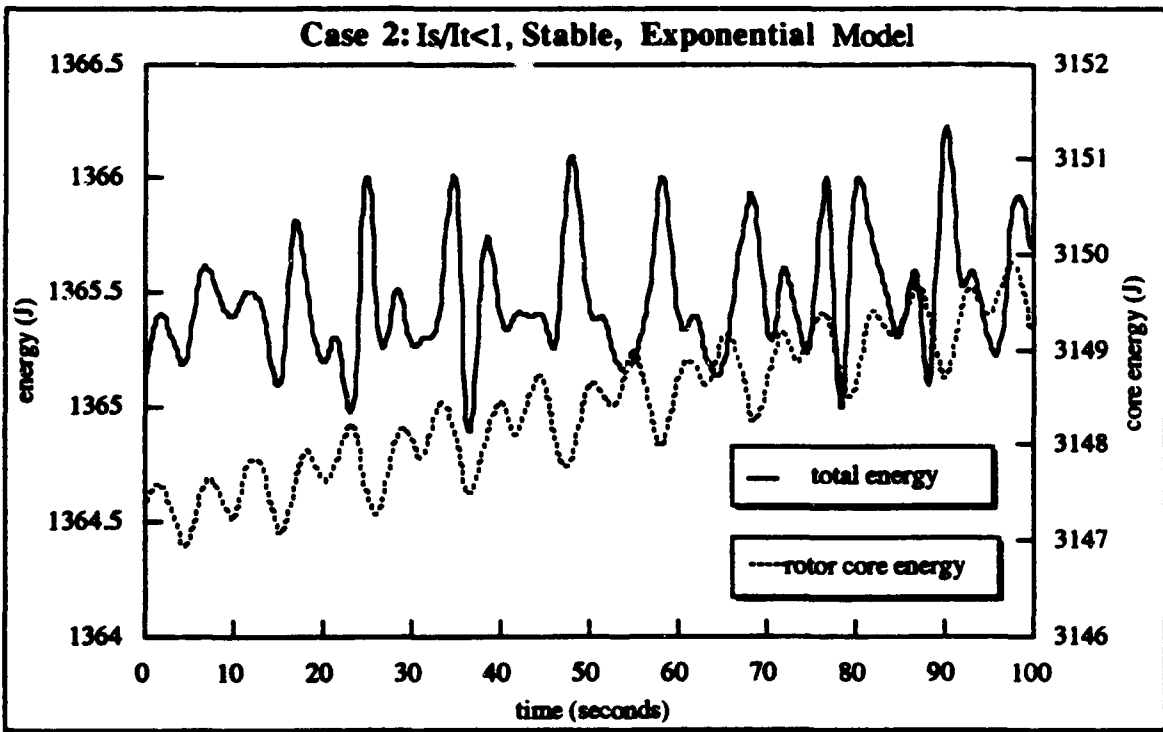


Figure (19) Total Energy and Rotor Core Energy - First 100 Seconds

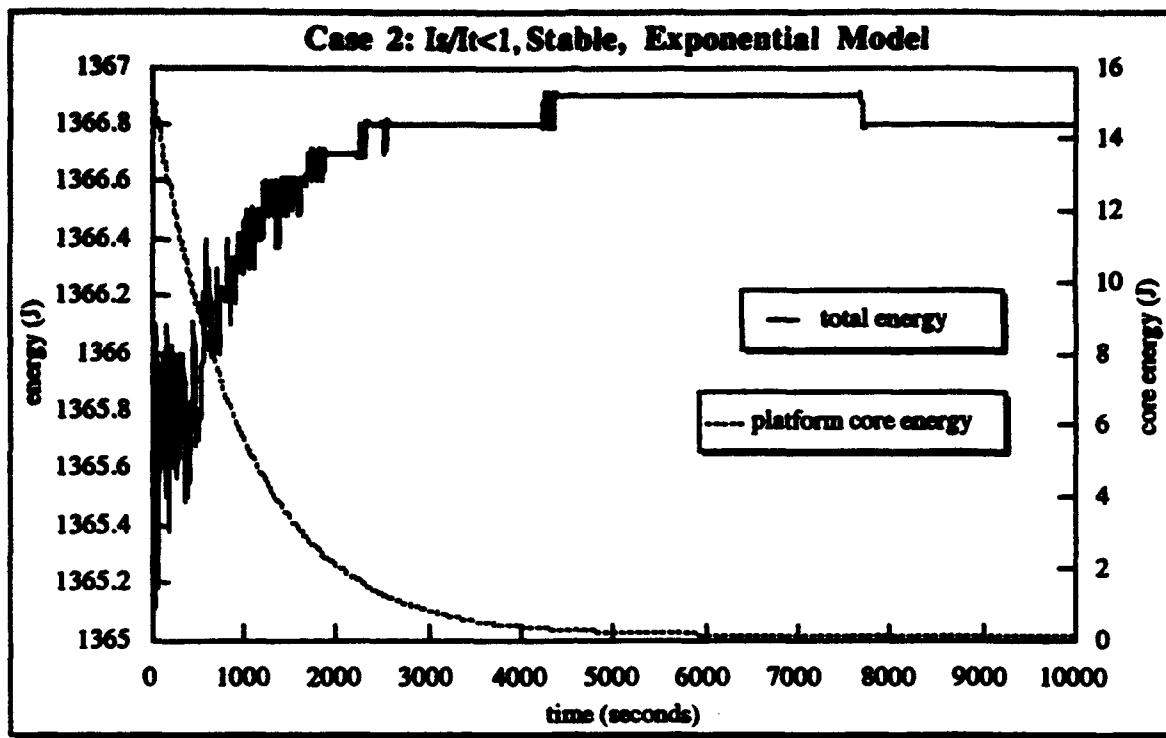


Figure (20) Total Energy and Platform Core Energy Versus Time

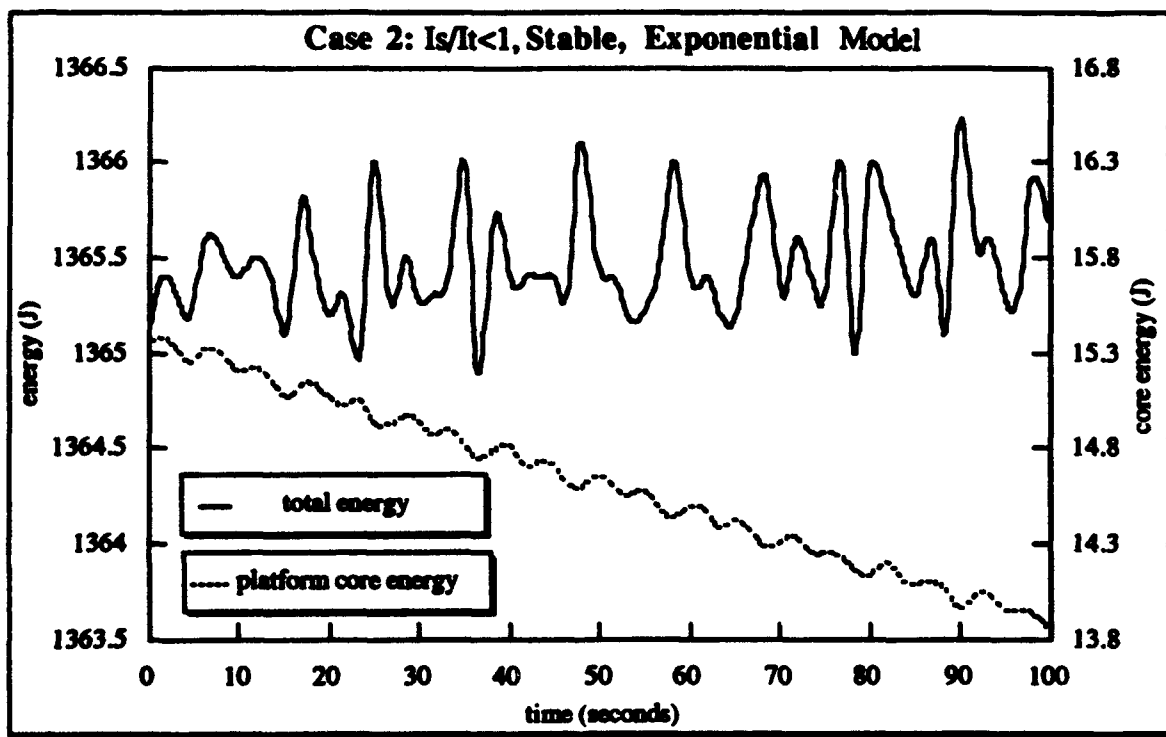


Figure (21) Total Energy and Platform Core Energy - First 100 Seconds

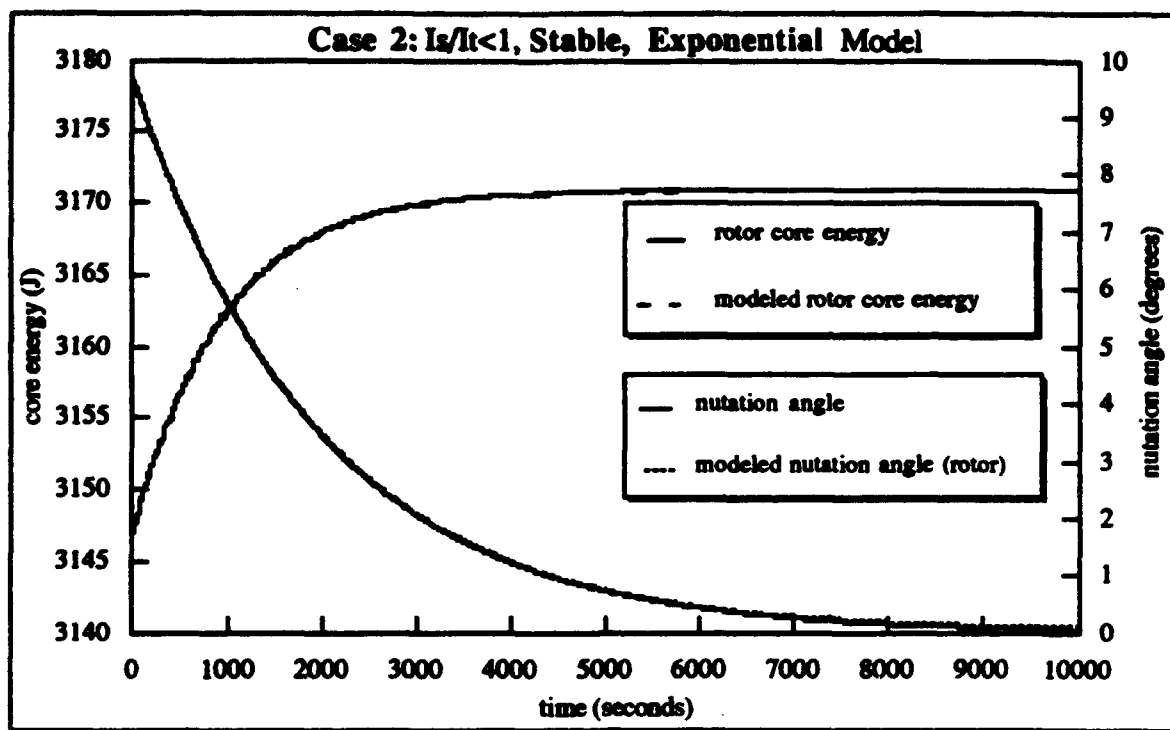


Figure (22) Modeled and Actual Rotor Core Energy and Nutation Angle Versus Time

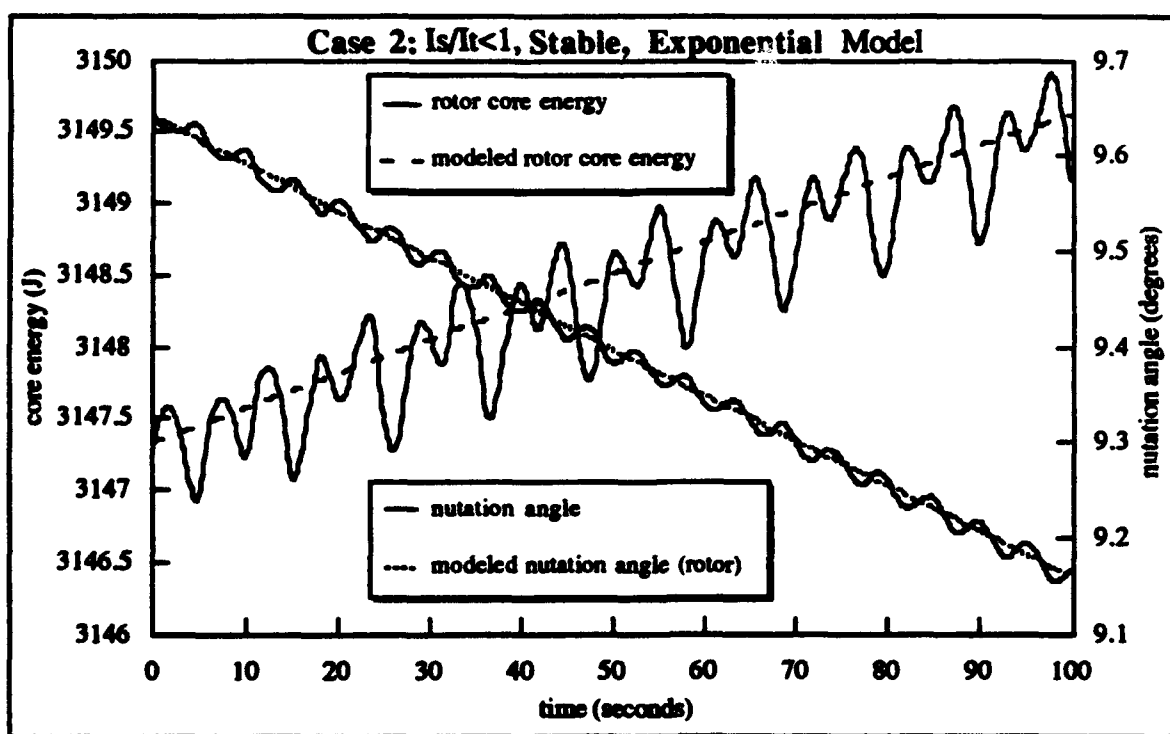


Figure (23) Modeled, Actual Rotor Core Energy and Nutation Angle - First 100 Seconds

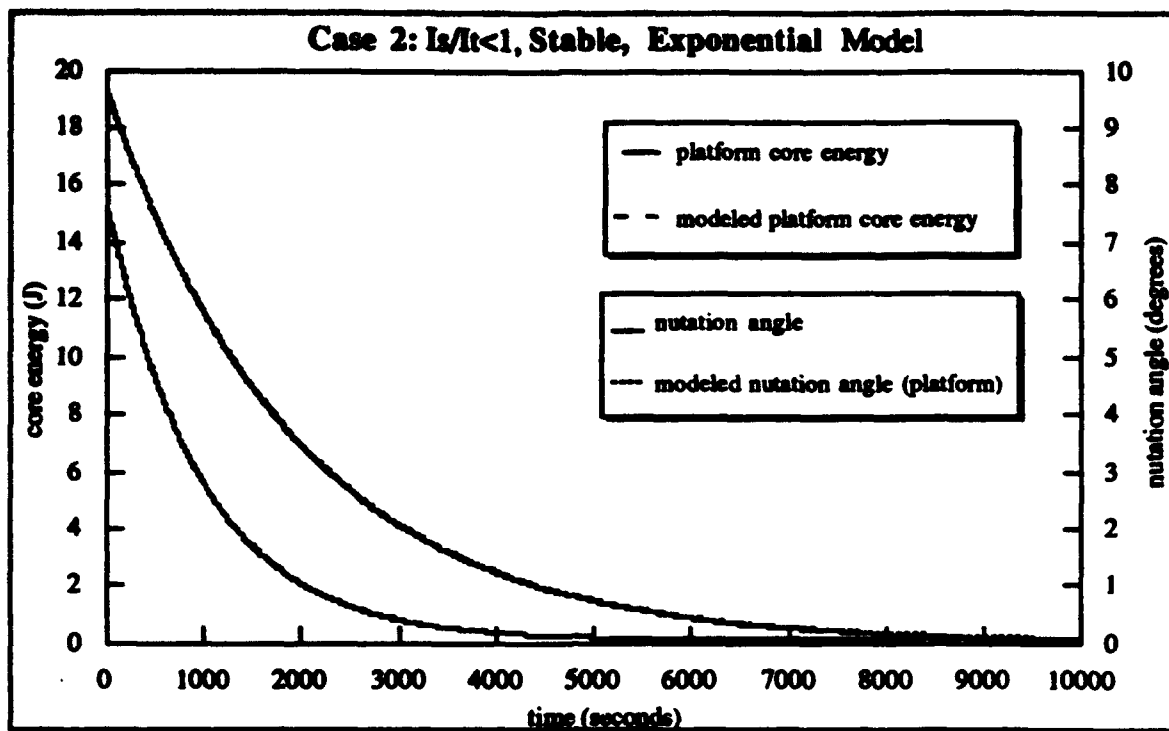


Figure (24) Modeled and Actual Platform Core Energy and Nutation Angle Versus Time

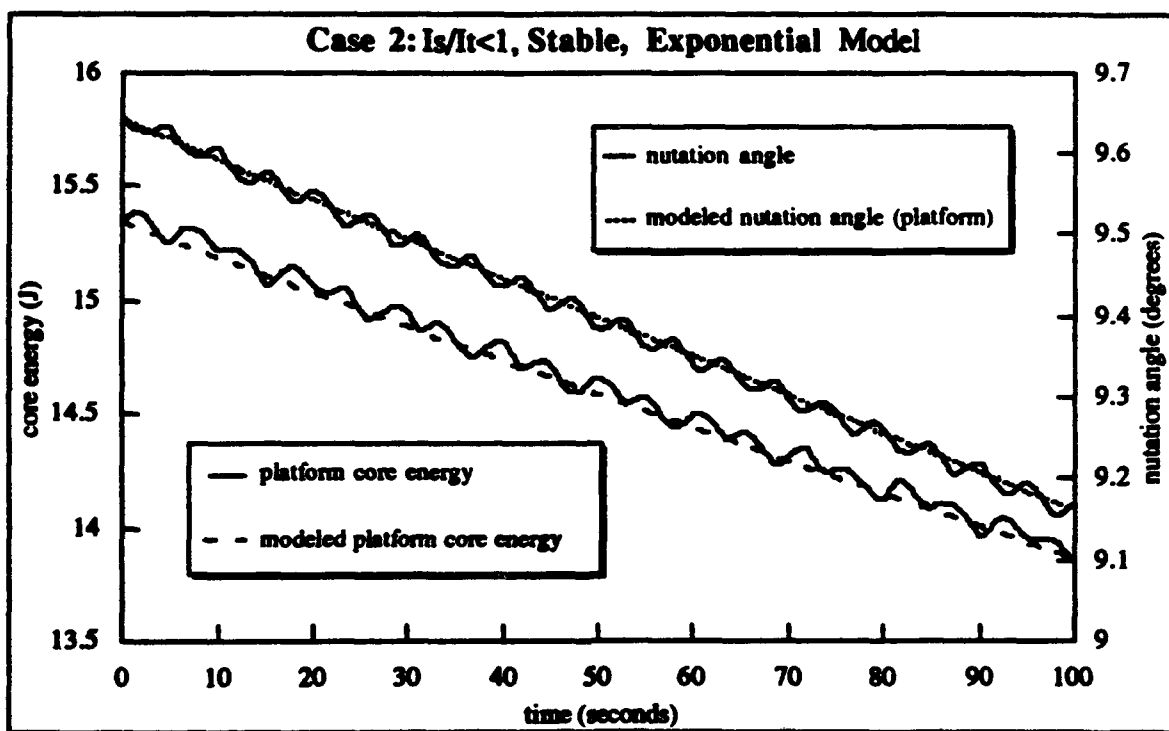


Figure (25) Modeled, Actual Platform Core Energy and Nutation Angle- First 100 Seconds

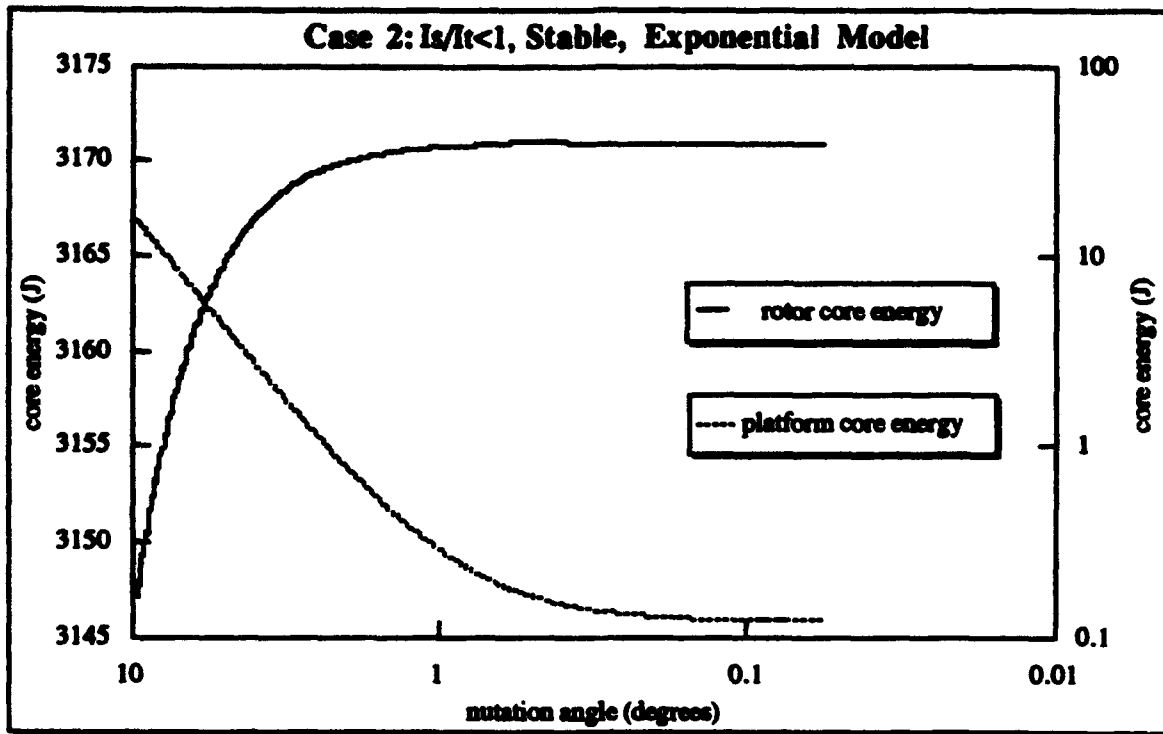


Figure (26) Core Energy Versus Nutation Angle

CASE 3: $\frac{I_a}{I_t} < 1$, Unstable, Exponential Model

System Parameters		Initial Conditions	
Platform	Rotor	Platform	Rotor
$I_1' = 1600 \text{ kgm}^2$	$I_1 = 1000 \text{ kgm}^2$	$z' = 0.0 \text{ m}$	$z = 0.0 \text{ m}$
$I_3' = 1500 \text{ kgm}^2$	$I_3 = 1200 \text{ kgm}^2$	$\dot{z}' = 0.0 \frac{\text{m}}{\text{s}}$	$\dot{z} = 0.0 \frac{\text{m}}{\text{s}}$
$M' = 1000.0 \text{ kg}$	$M = 700.0 \text{ kg}$	$\omega_3' = 7.27 \times 10^{-5} \frac{\text{rad}}{\text{sec}}$	$\omega_3 = 1.5 \frac{\text{rad}}{\text{sec}}$
$m' = 1.0 \text{ kg}$	$m = 1.0 \text{ kg}$	$\omega_1 = 0.10 \frac{\text{rad}}{\text{sec}}$	$\omega_2 = 0.0 \frac{\text{rad}}{\text{sec}}$
$a' = 1.0 \text{ m}$	$a = 1.0 \text{ m}$	Core Energy Parameters	
$k' = 1.0 \frac{\text{N}}{\text{m}}$	$k = 1.0 \frac{\text{N}}{\text{m}}$		
$c' = 1.0 \frac{\text{kg}}{\text{sec}}$	$c = 1.0 \frac{\text{kg}}{\text{sec}}$	Platform	Rotor
$L = 1.0 \text{ m}$	$\frac{I_{s \text{ total}}}{I_{t \text{ total}}} = 0.897$	$E_{c \text{ initial}}' = 15.1 \text{ J}$	$E_{c \text{ initial}} = 3061.6 \text{ J}$
		$E_{c \text{ final}}' = 1160.9 \text{ J}$	$E_{c \text{ final}} = 1489.9 \text{ J}$
		$\frac{\dot{E}_C'}{\lambda'} = \text{positive}$	$\frac{\dot{E}_C}{\lambda} = \text{positive}$
		$r' = -.0005 \text{ s}^{-1}$	$r = -.0005 \text{ s}^{-1}$

Table (4) Case 3 Parameters

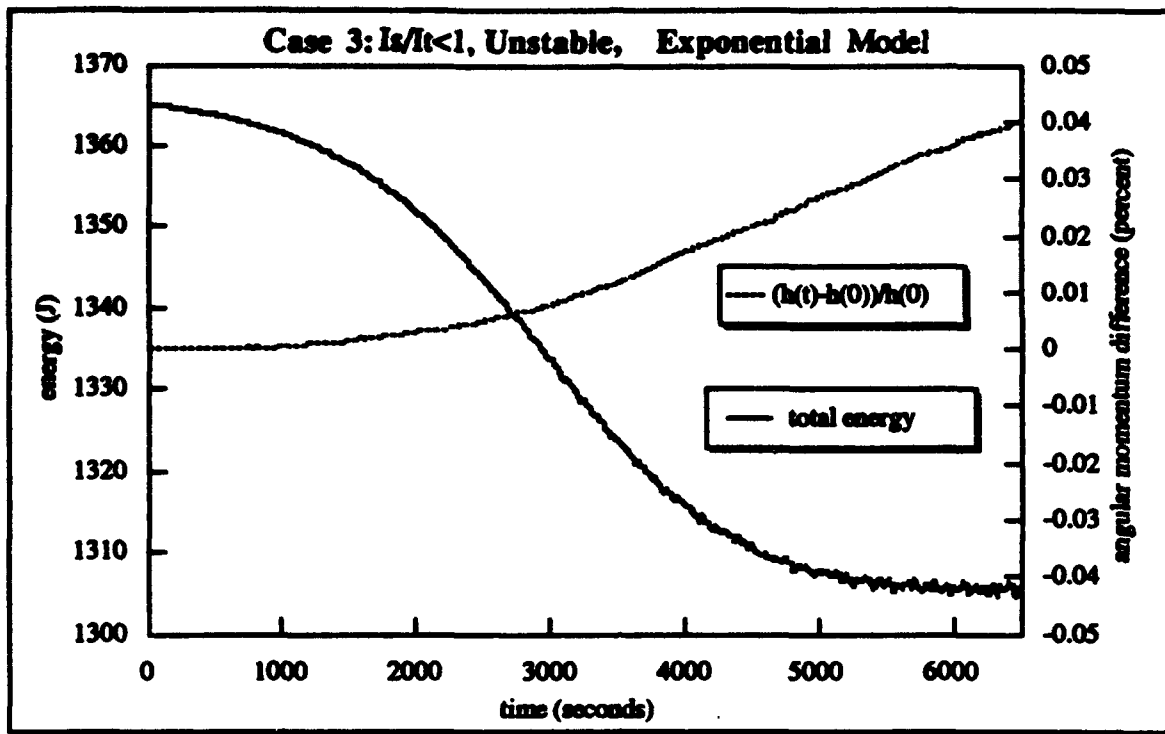


Figure (27) Total Energy and Percent Difference Angular Momentum Versus Time

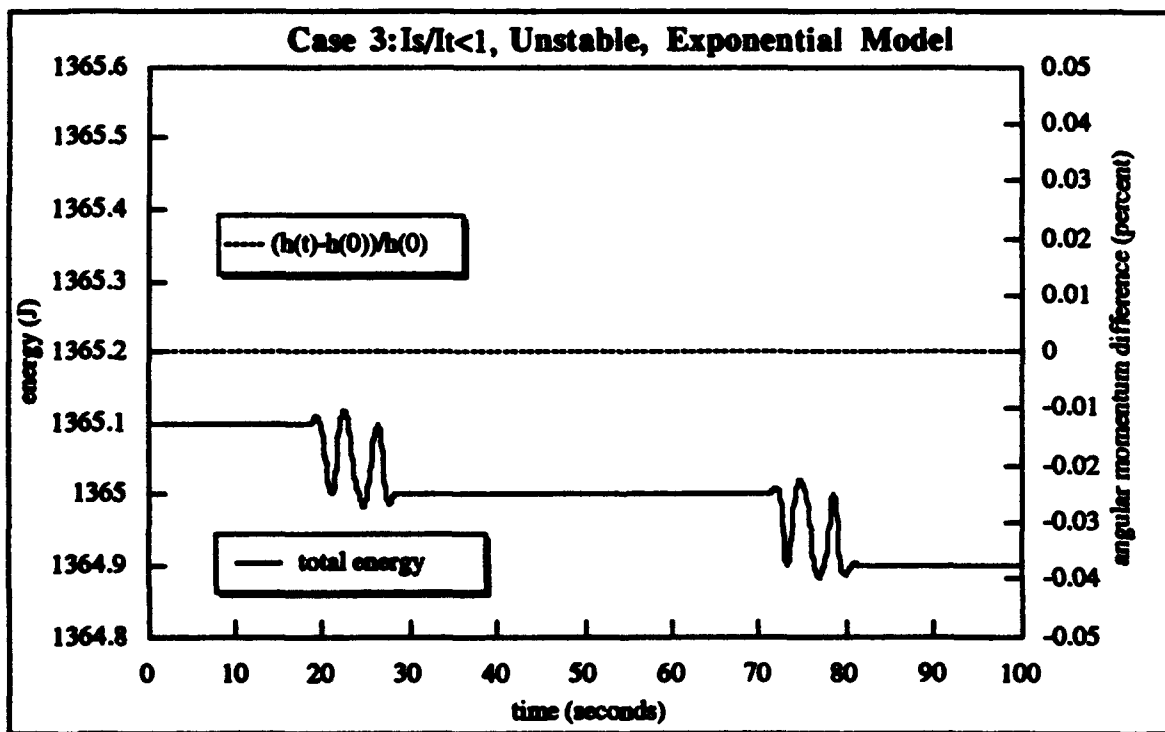


Figure (28) Total Energy and Percent Difference Angular Momentum - First 100 Seconds

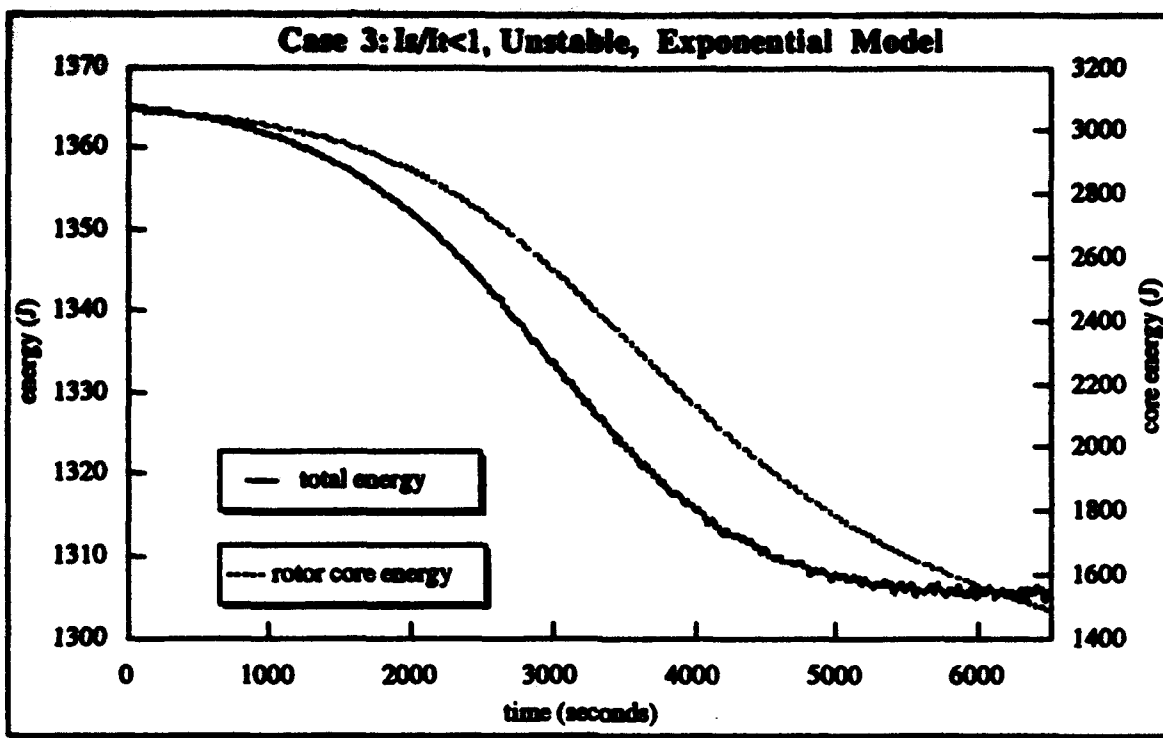


Figure (29) Total Energy and Rotor Core Energy Versus Time

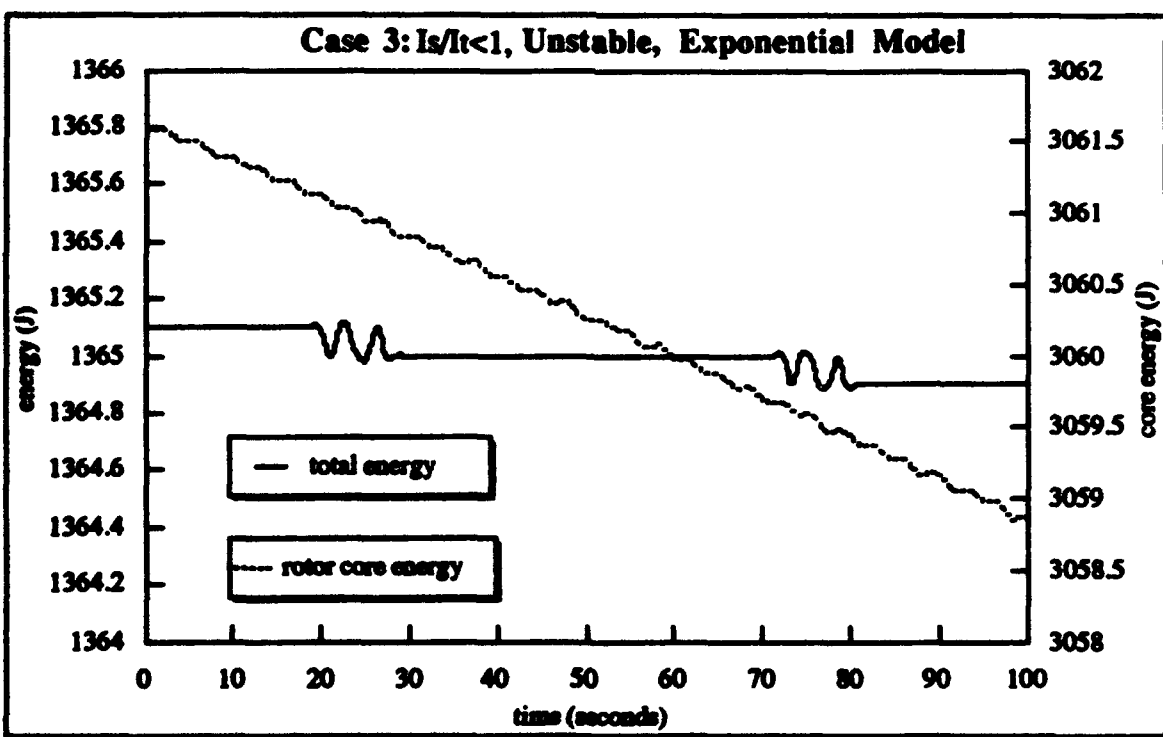


Figure (30) Total Energy and Rotor Core Energy - First 100 Seconds

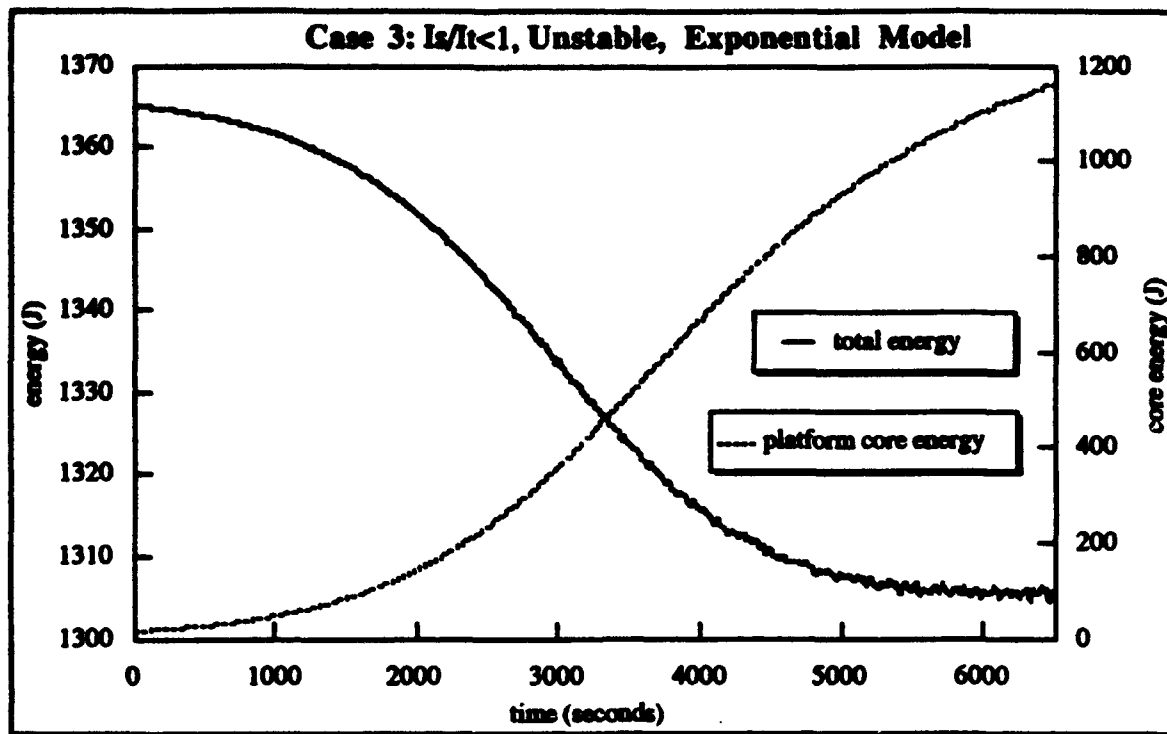


Figure (31) Total Energy and Platform Core Energy Versus Time

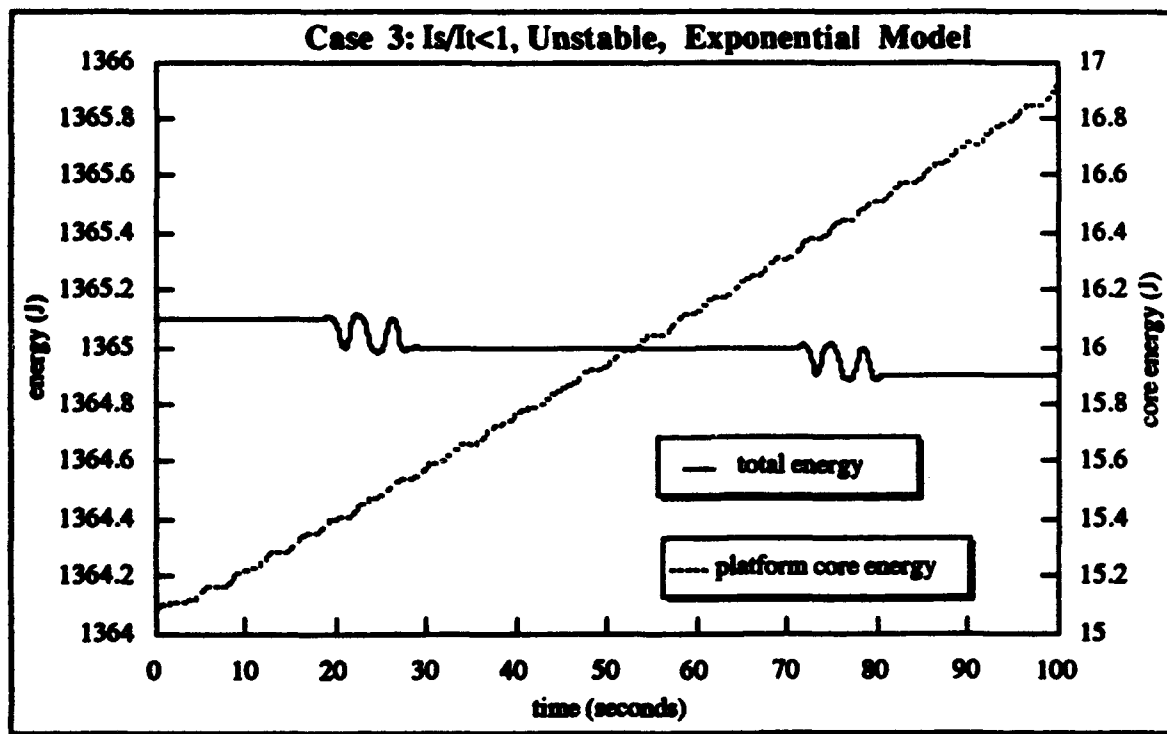


Figure (32) Total Energy and Platform Core Energy - First 100 Seconds

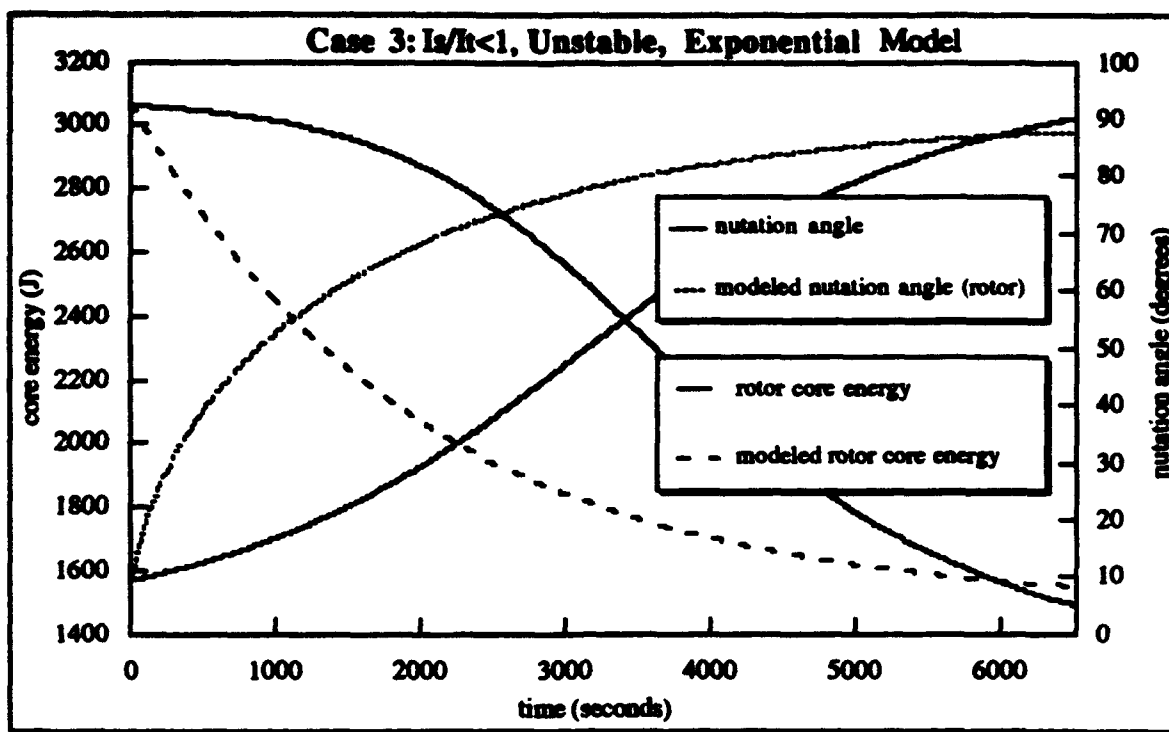


Figure (33) Modeled and Actual Rotor Core Energy and Nutation Angle Versus Time

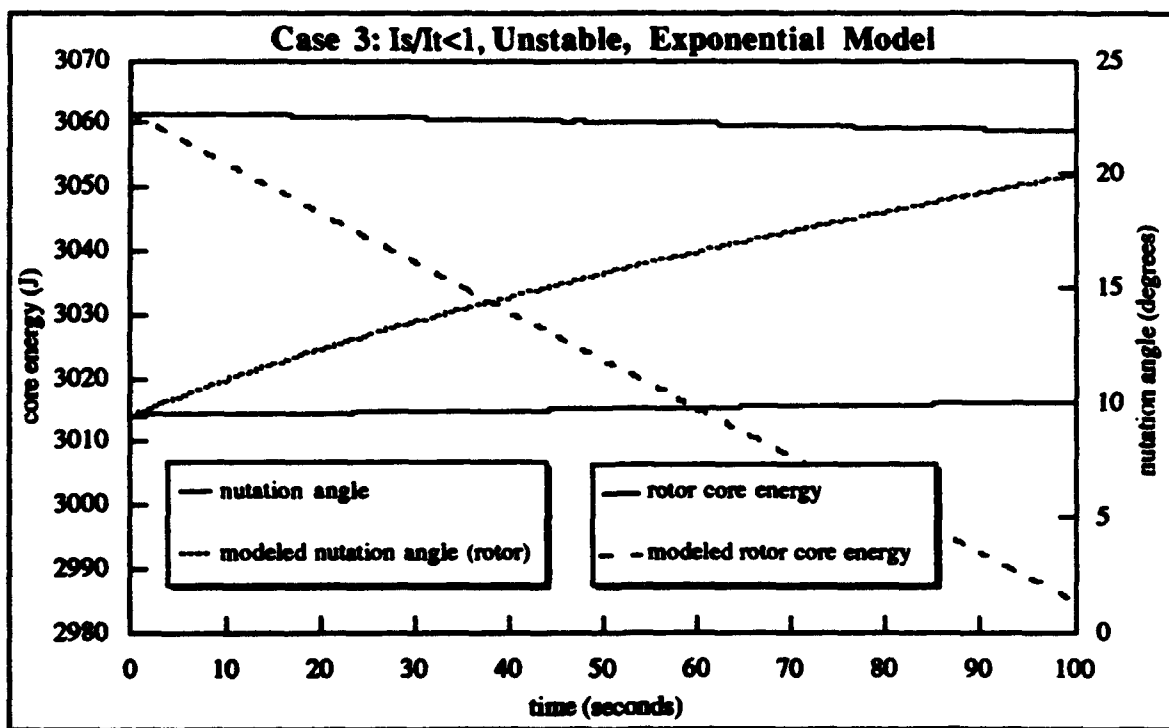


Figure (34) Modeled, Actual Rotor Core Energy and Nutation Angle - First 100 Seconds

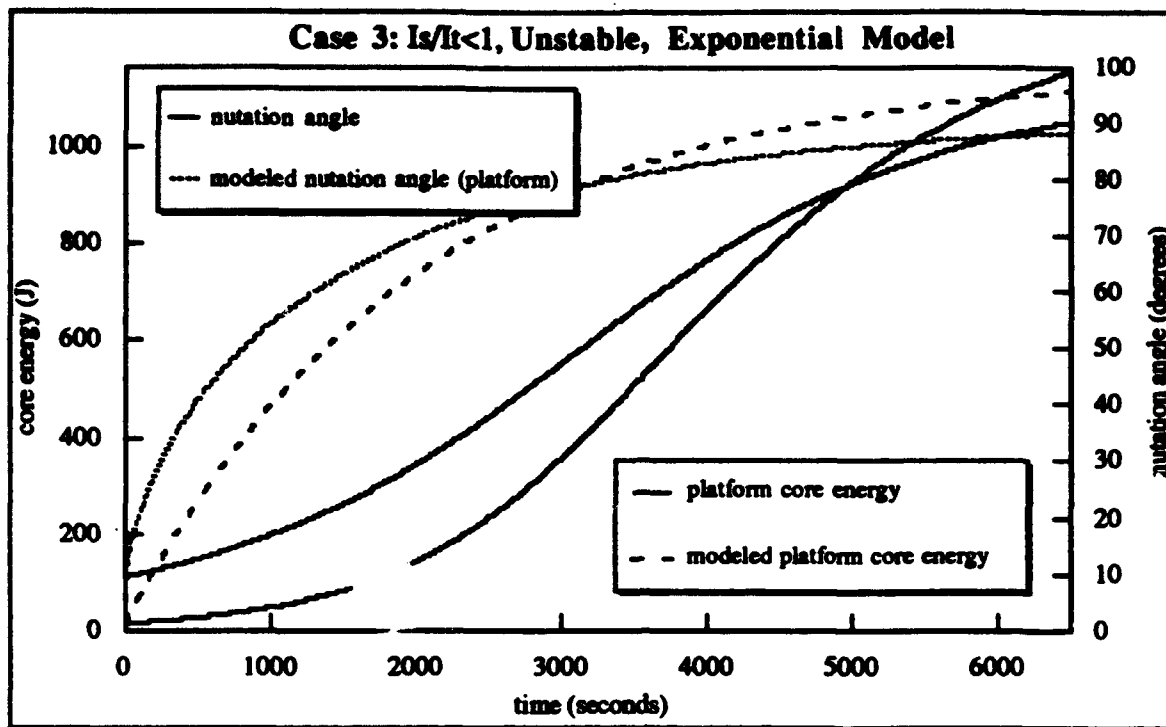


Figure (35) Modeled and Actual Platform Core Energy and Nutation Angle Versus Time

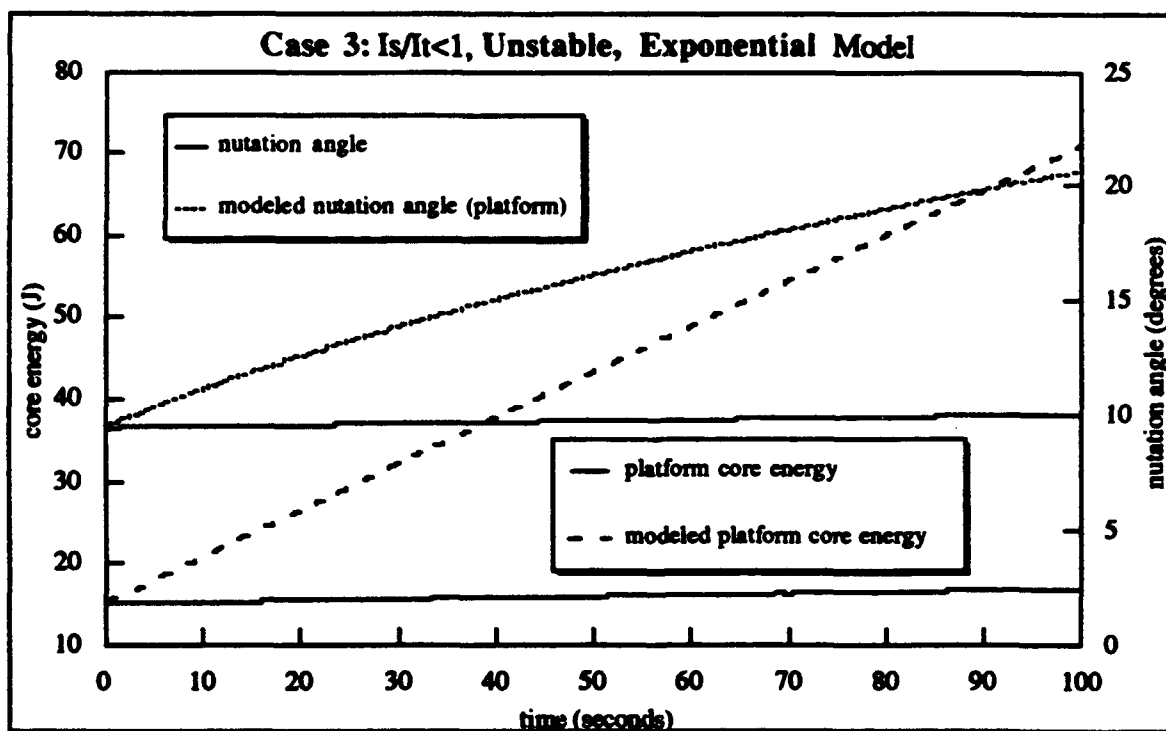


Figure (36) Modeled, Actual Platform Core Energy and Nutation Angle- First 100 Seconds

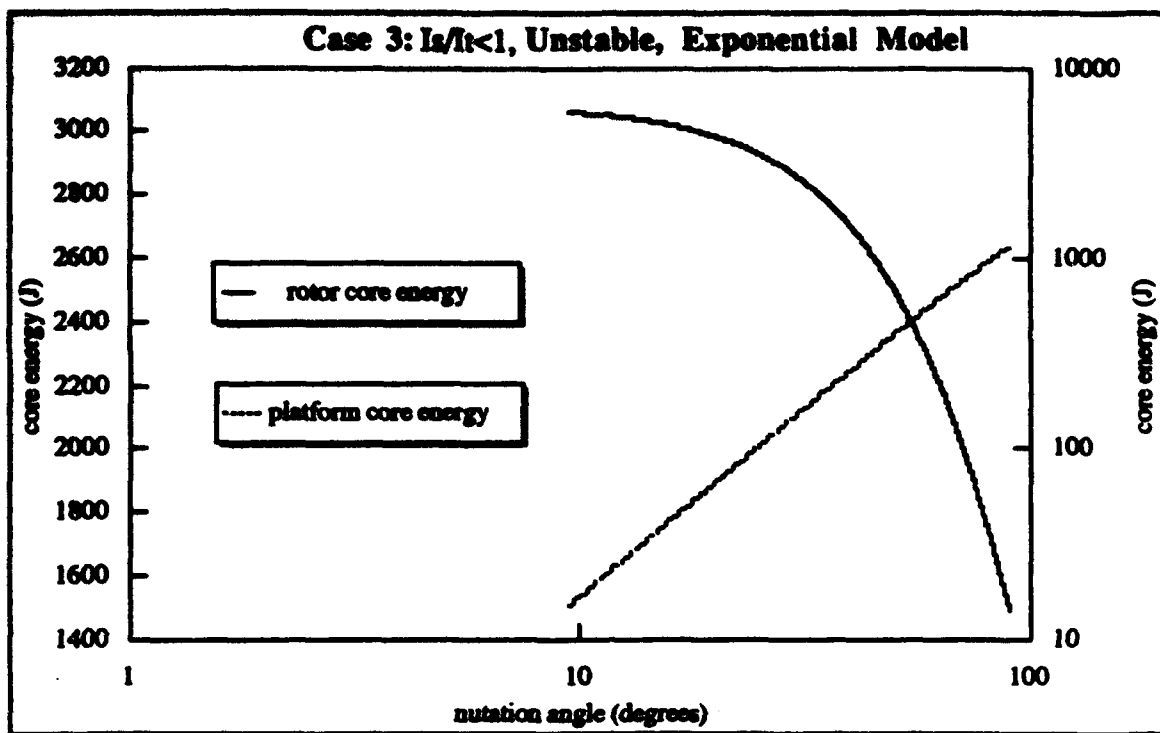


Figure (37) Core Energy Versus Nutation Angle

CASE 4: $\frac{I_x}{I_t} > 1$, Unstable, Exponential Model

System Parameters		Initial Conditions	
Platform	Rotor	Platform	Rotor
$I_1' = 1600 \text{ kgm}^2$	$I_1 = 1000 \text{ kgm}^2$	$z' = 0.0 \text{ m}$	$z = 0.0 \text{ m}$
$I_3' = 1500 \text{ kgm}^2$	$I_3 = 1200 \text{ kgm}^2$	$\dot{z}' = 0.0 \frac{\text{m}}{\text{s}}$	$\dot{z} = 0.0 \frac{\text{m}}{\text{s}}$
$M' = 1000.0 \text{ kg}$	$M = 700.0 \text{ kg}$	$\omega_3' = 7.27 \times 10^{-5} \frac{\text{rad}}{\text{sec}}$	$\omega_3 = 1.5 \frac{\text{rad}}{\text{sec}}$
$m' = 1.0 \text{ kg}$	$m = 1.0 \text{ kg}$	$\omega_1 = 0.10 \frac{\text{rad}}{\text{sec}}$	$\omega_2 = 0.0 \frac{\text{rad}}{\text{sec}}$
$a' = 1.0 \text{ m}$	$a = 1.0 \text{ m}$	Core Energy Parameters	
$k' = 1.0 \frac{\text{N}}{\text{m}}$	$k = 1.0 \frac{\text{N}}{\text{m}}$		
$c' = 1.0 \frac{\text{kg}}{\text{sec}}$	$c = 1.0 \frac{\text{kg}}{\text{sec}}$	Platform	Rotor
$L = 0.3 \text{ m}$	$\frac{I_{s \text{ total}}}{I_{t \text{ total}}} = 1.025$	$E_{c \text{ initial}}' = 13.2 \text{ J}$	$E_{c \text{ initial}} = 3059.7 \text{ J}$
		$E_{c \text{ final}}' = 1247.1 \text{ J}$	$E_{c \text{ final}} = 1552.5 \text{ J}$
		$\frac{\dot{E}_C'}{\lambda'} = \text{positive}$	$\frac{\dot{E}_C}{\lambda} = \text{positive}$
		$r' = -.0005 \text{ s}^{-1}$	$r = -.0005 \text{ s}^{-1}$

Table (5) Case 4 Parameters

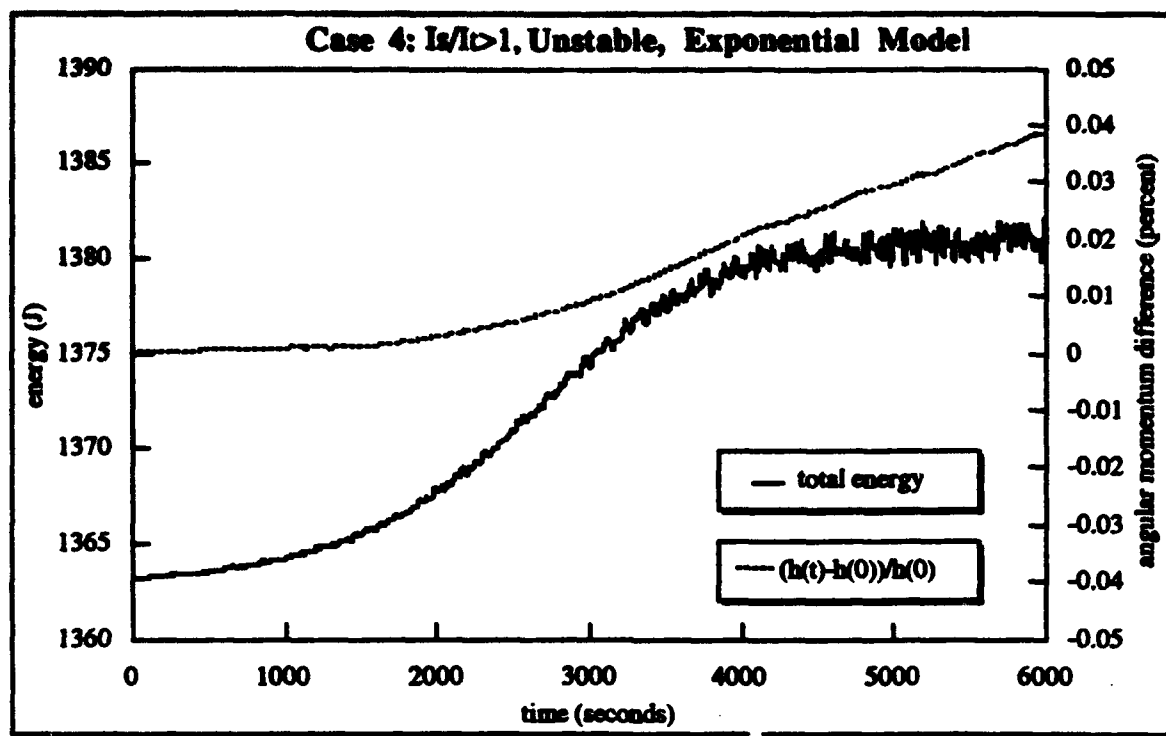


Figure (38) Total Energy and Percent Difference Angular Momentum Versus Time

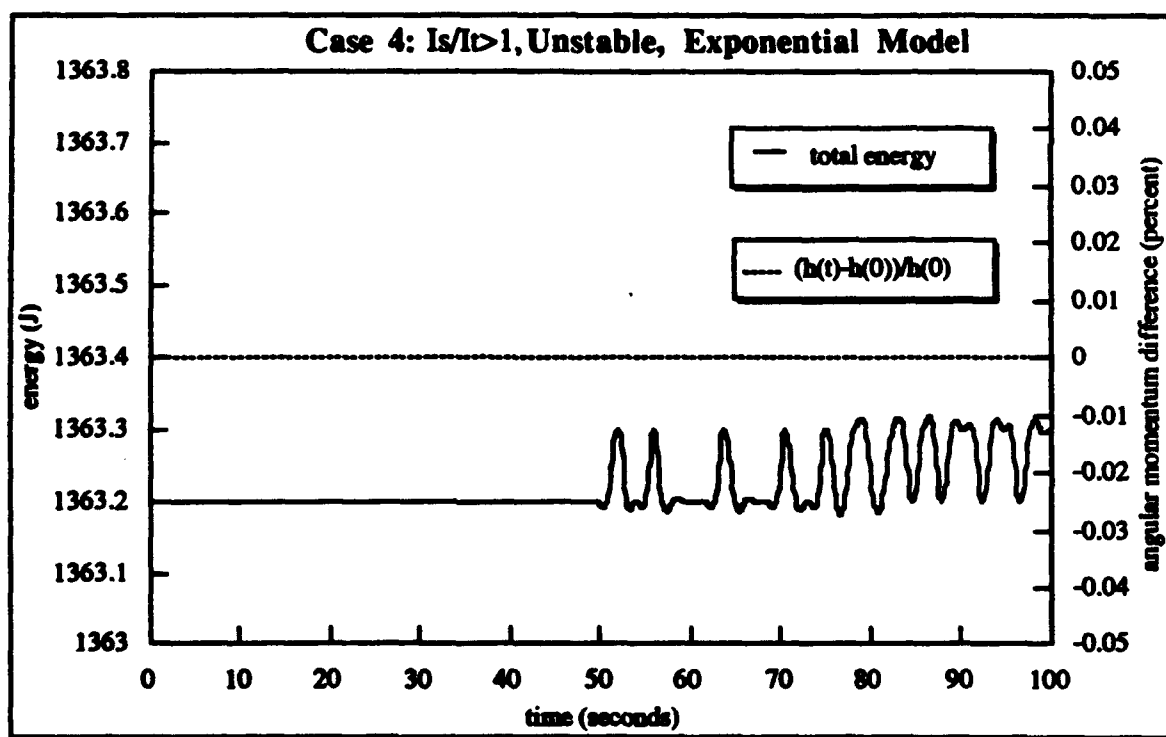


Figure (39) Total Energy and Percent Difference Angular Momentum - First 100 Seconds

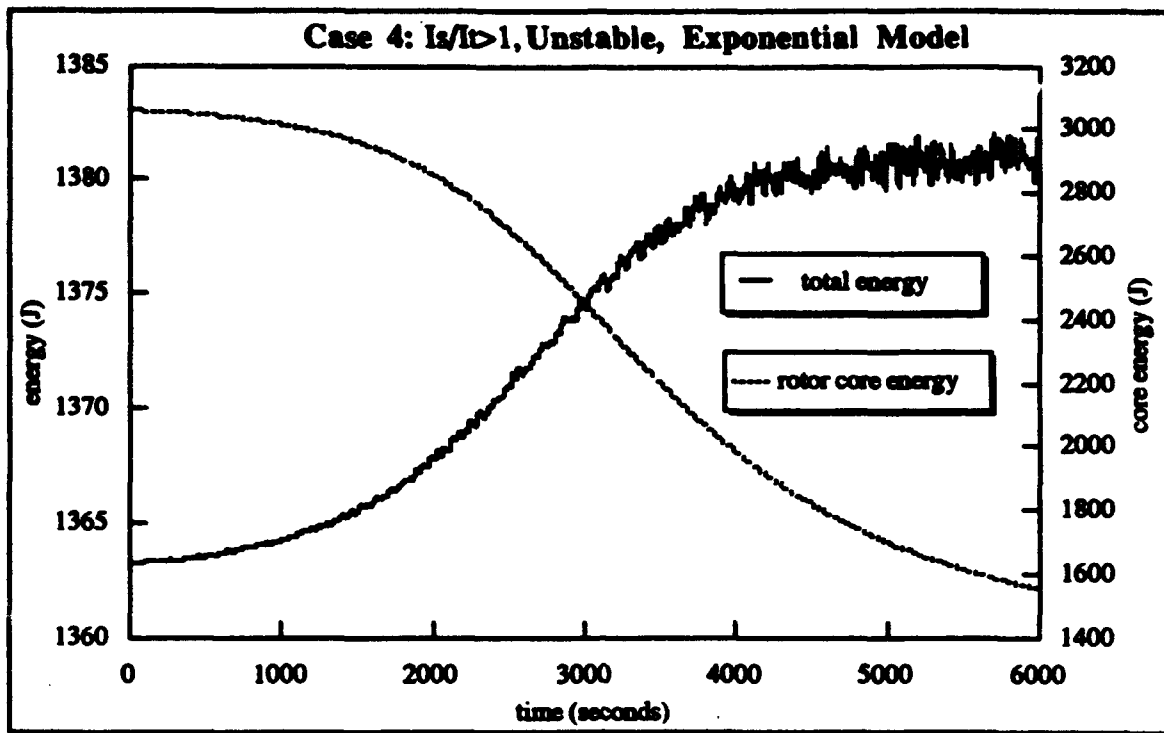


Figure (40) Total Energy and Rotor Core Energy Versus Time

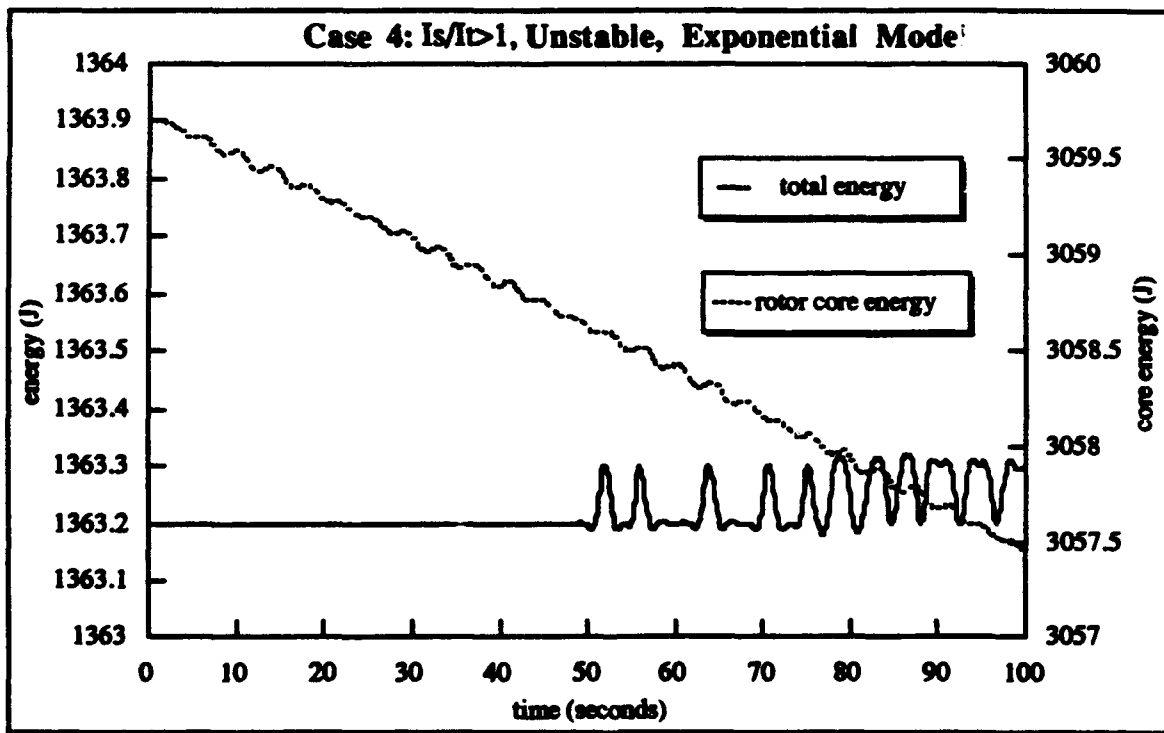


Figure (41) Total Energy and Rotor Core Energy - First 100 Seconds

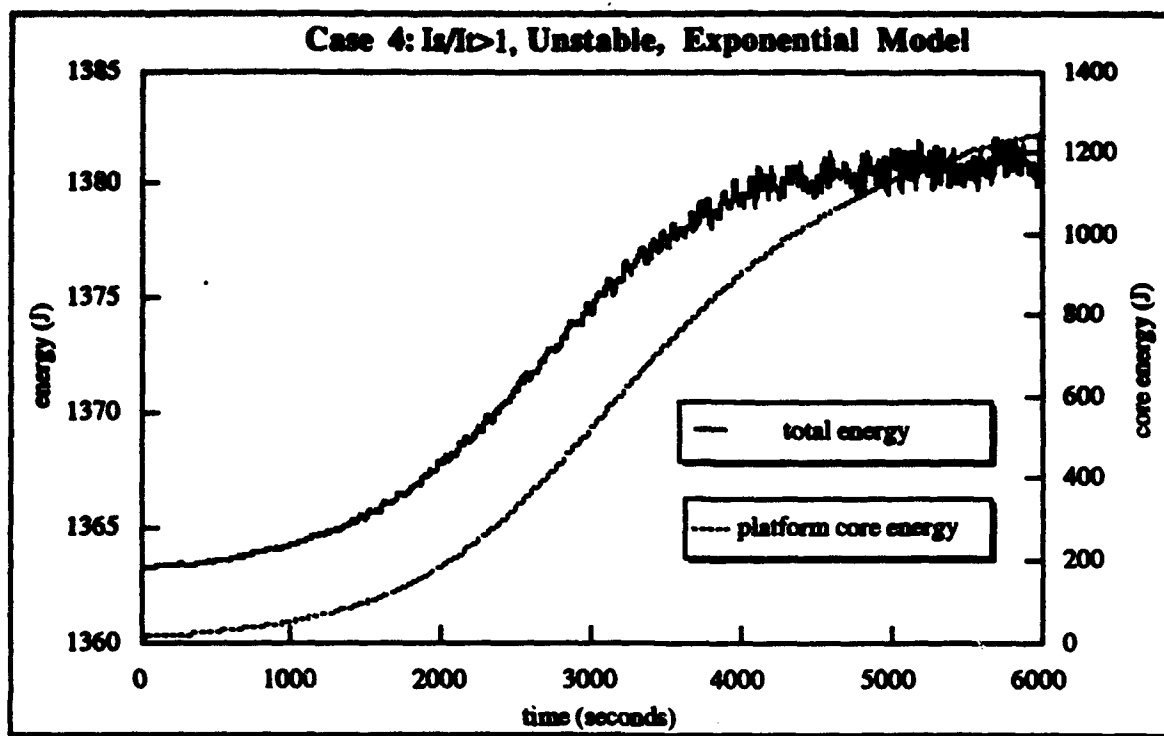


Figure (42) Total Energy and Platform Core Energy Versus Time

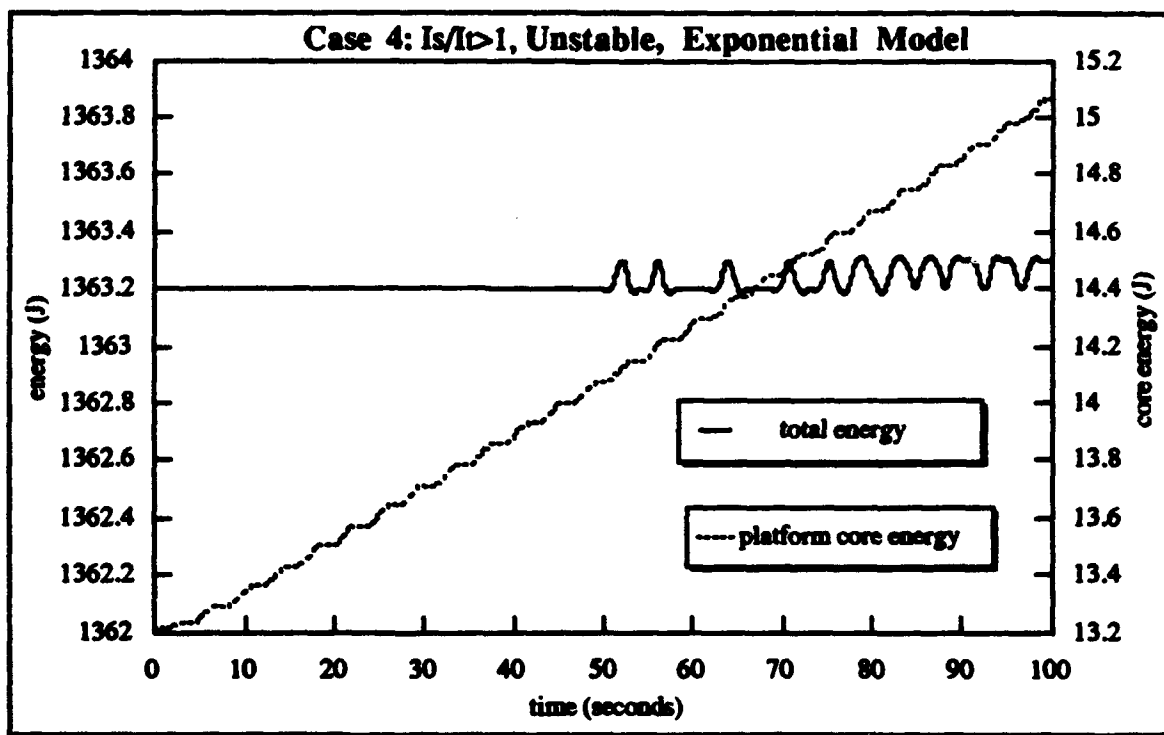


Figure (43) Total Energy and Platform Core Energy - First 100 Seconds

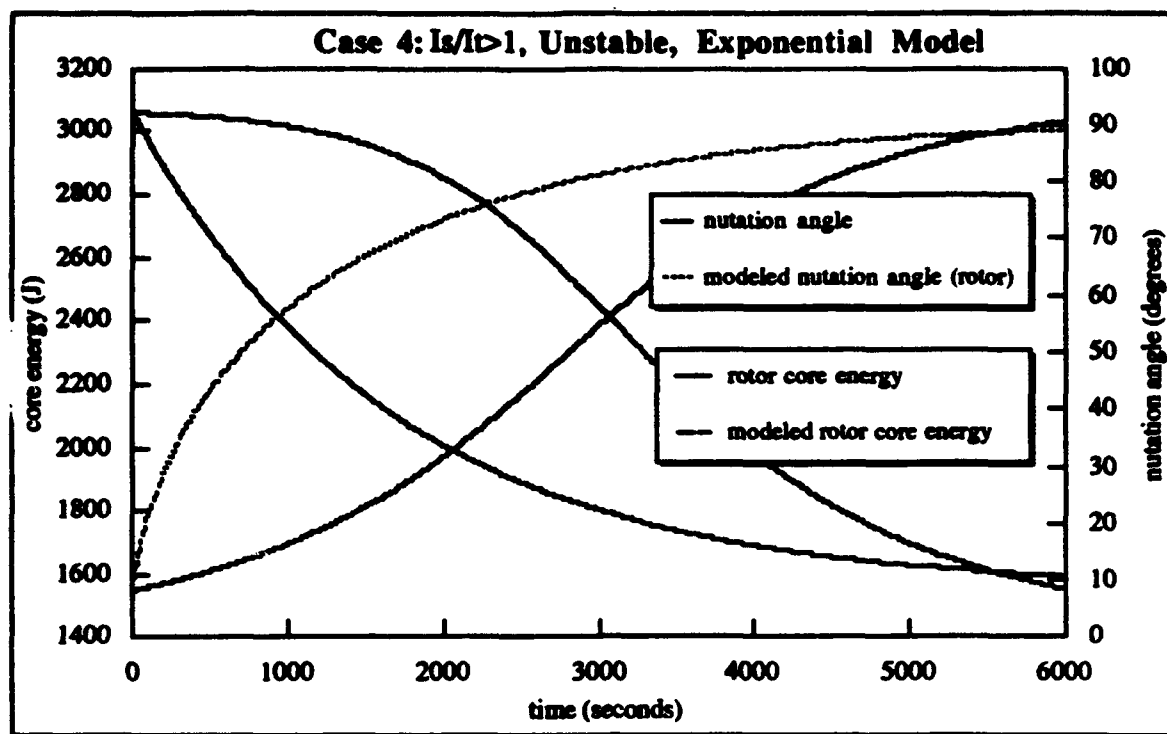


Figure (44) Modeled and Actual Rotor Core Energy and Nutation Angle Versus Time

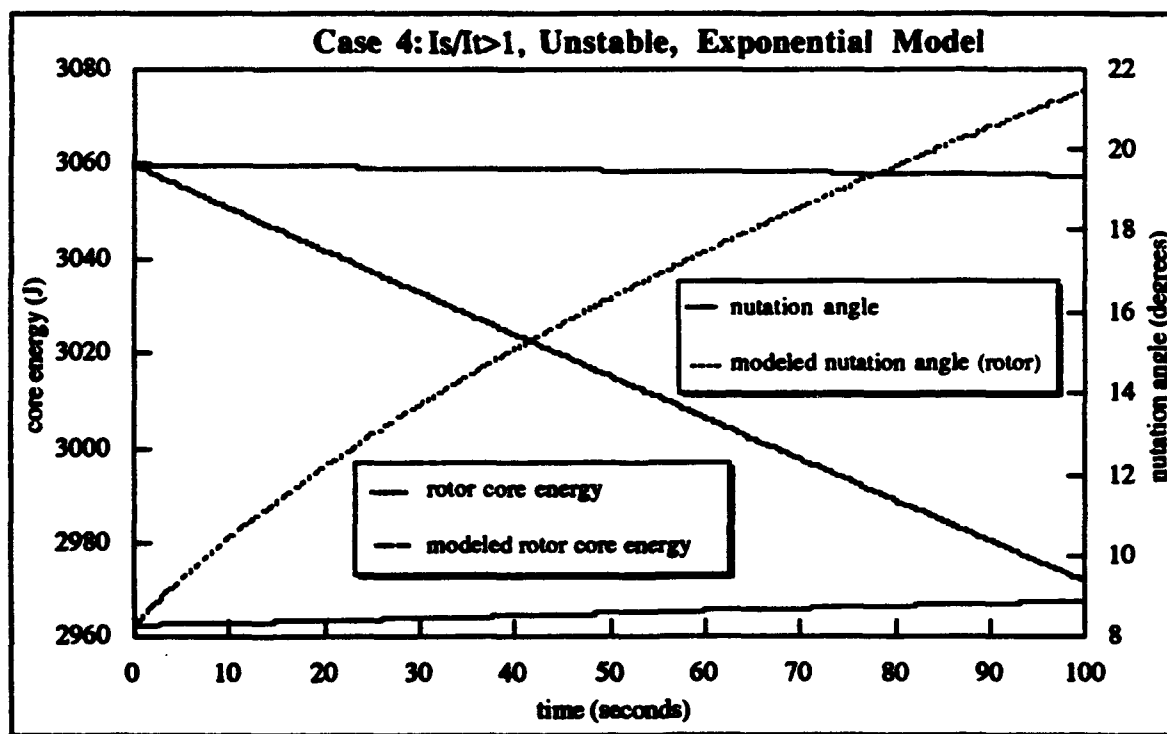


Figure (45) Modeled, Actual Rotor Core Energy and Nutation Angle - First 100 Seconds

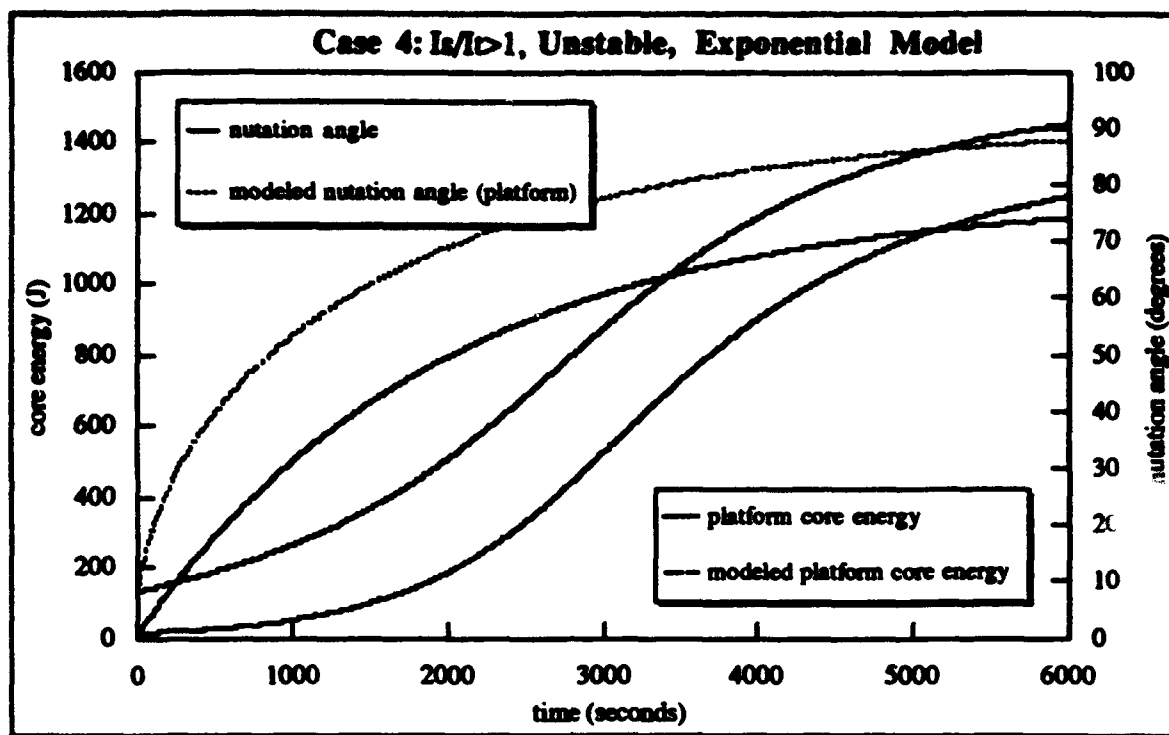


Figure (46) Modeled and Actual Platform Core Energy and Nutation Angle Versus Time

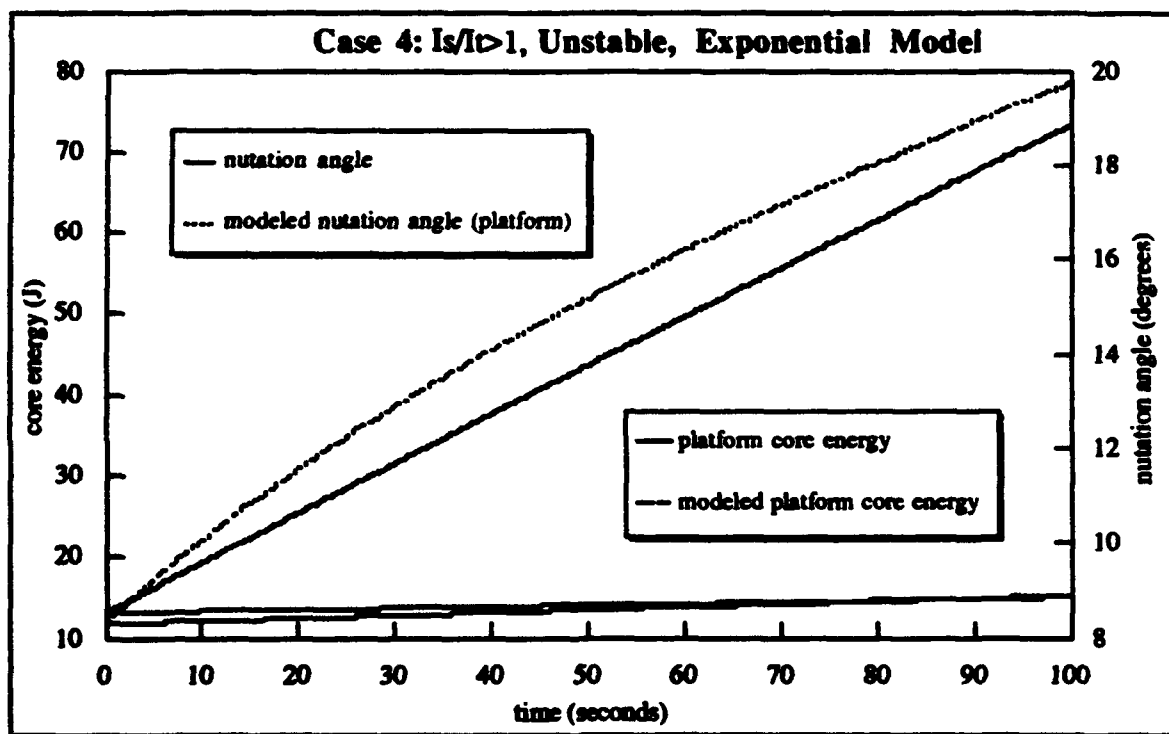


Figure (47) Modeled, Actual Platform Core Energy and Nutation Angle- First 100 Seconds

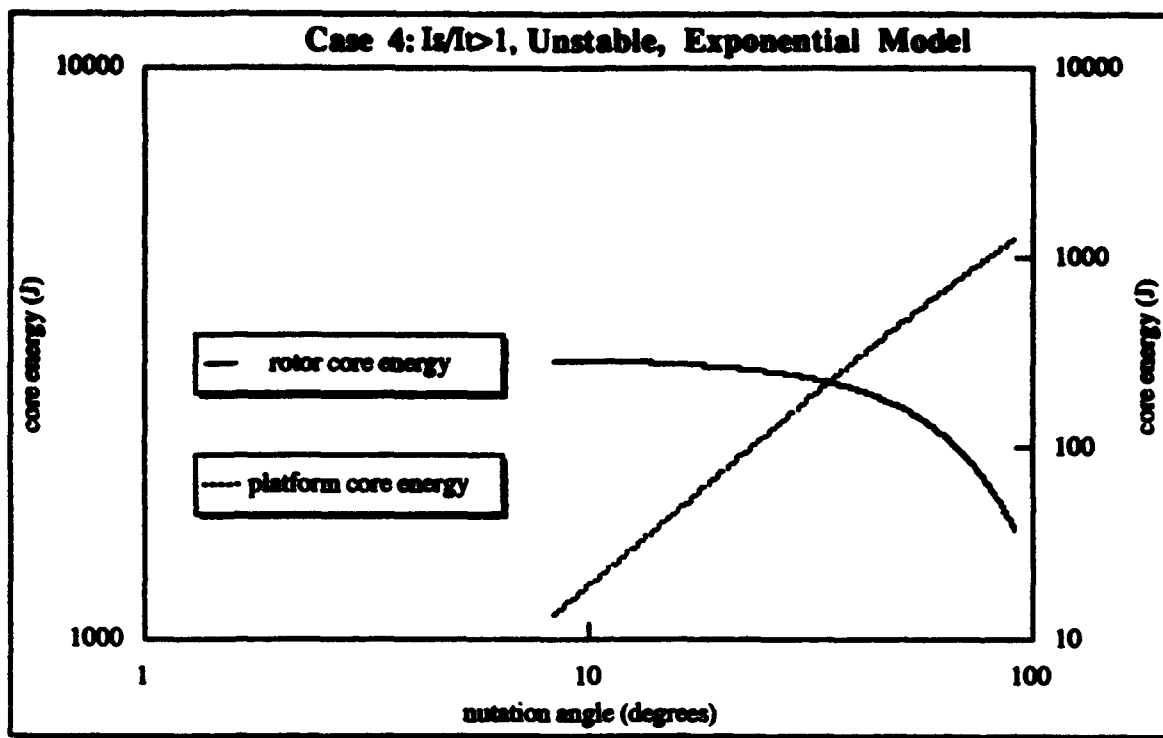


Figure (48) Core Energy Versus Nutation Angle

CASE 5: $\frac{I_1}{I_t} < 1$, Stable, Verhulst Model

System Parameters		Initial Conditions	
Platform	Rotor	Platform	Rotor
$I_1' = 1600 \text{ kgm}^2$	$I_1 = 1000 \text{ kgm}^2$	$z' = 0.0 \text{ m}$	$z = 0.0 \text{ m}$
$I_3' = 1500 \text{ kgm}^2$	$I_3 = 1200 \text{ kgm}^2$	$\dot{z}' = 0.0 \frac{\text{m}}{\text{s}}$	$\dot{z} = 0.0 \frac{\text{m}}{\text{s}}$
$M' = 1000.0 \text{ kg}$	$M = 700.0 \text{ kg}$	$\omega_3' = 7.27 \times 10^{-5} \frac{\text{rad}}{\text{sec}}$	$\omega_3 = 1.5 \frac{\text{rad}}{\text{sec}}$
$m' = 20.0 \text{ kg}$	$m = 1.0 \text{ kg}$	$\omega_1 = 0.10 \frac{\text{rad}}{\text{sec}}$	$\omega_2 = 0.0 \frac{\text{rad}}{\text{sec}}$
$a' = 1.0 \text{ m}$	$a = 1.0 \text{ m}$	Core Energy Parameters	
$k' = 1.0 \frac{\text{N}}{\text{m}}$	$k = 1.0 \frac{\text{N}}{\text{m}}$		
$c' = 10.0 \frac{\text{kg}}{\text{sec}}$	$c = 1.0 \frac{\text{kg}}{\text{sec}}$	Platform	Rotor
$L = 1.0 \text{ m}$	$\frac{I_{s \text{ total}}}{I_t \text{ total}} = 0.907$	$E_{c \text{ initial}}' = 15.341 \text{ J}$	$E_{c \text{ initial}} = 3147.3 \text{ J}$
		$E_{c \text{ final}}' = 0.122 \text{ J}$	$E_{c \text{ final}} = 3170.9 \text{ J}$
		$\frac{\dot{E}_C'}{\lambda'} = \text{negative}$	$\frac{\dot{E}_C}{\lambda} = \text{negative}$
		$r' = -.0002 \text{ s}^{-1}$	$r = -.0002 \text{ s}^{-1}$

Table (6) Case 5 Parameters

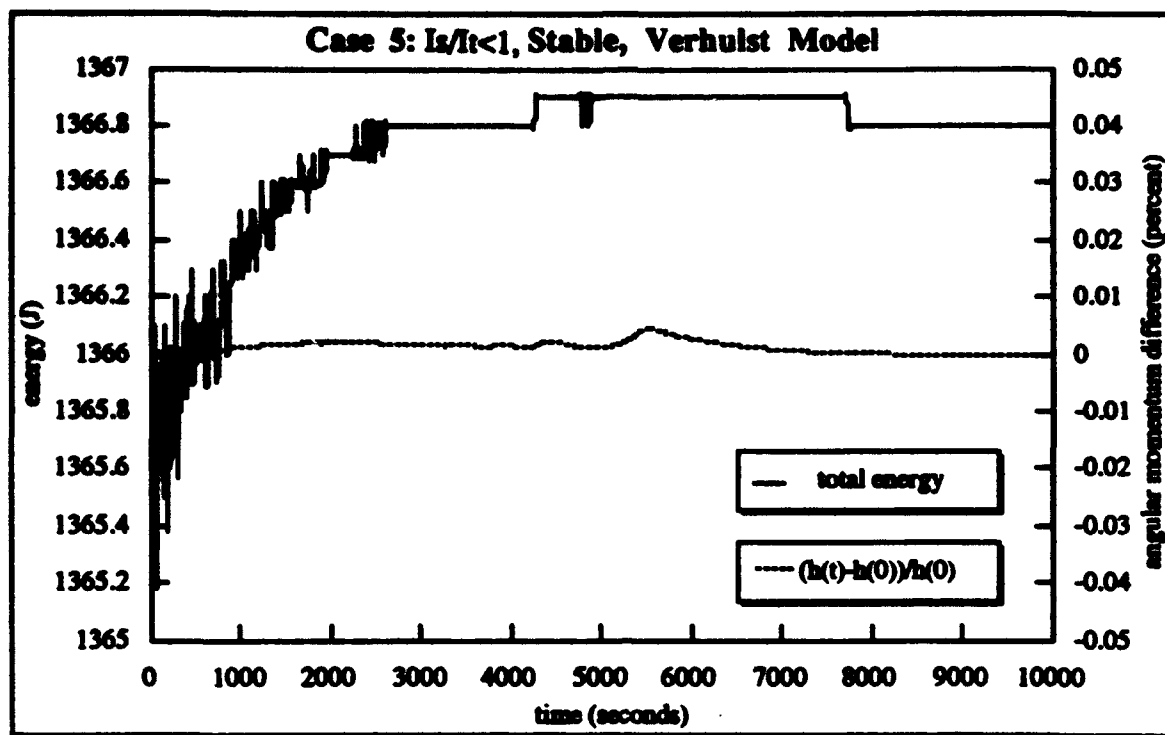


Figure (49) Total Energy and Percent Difference Angular Momentum Versus Time

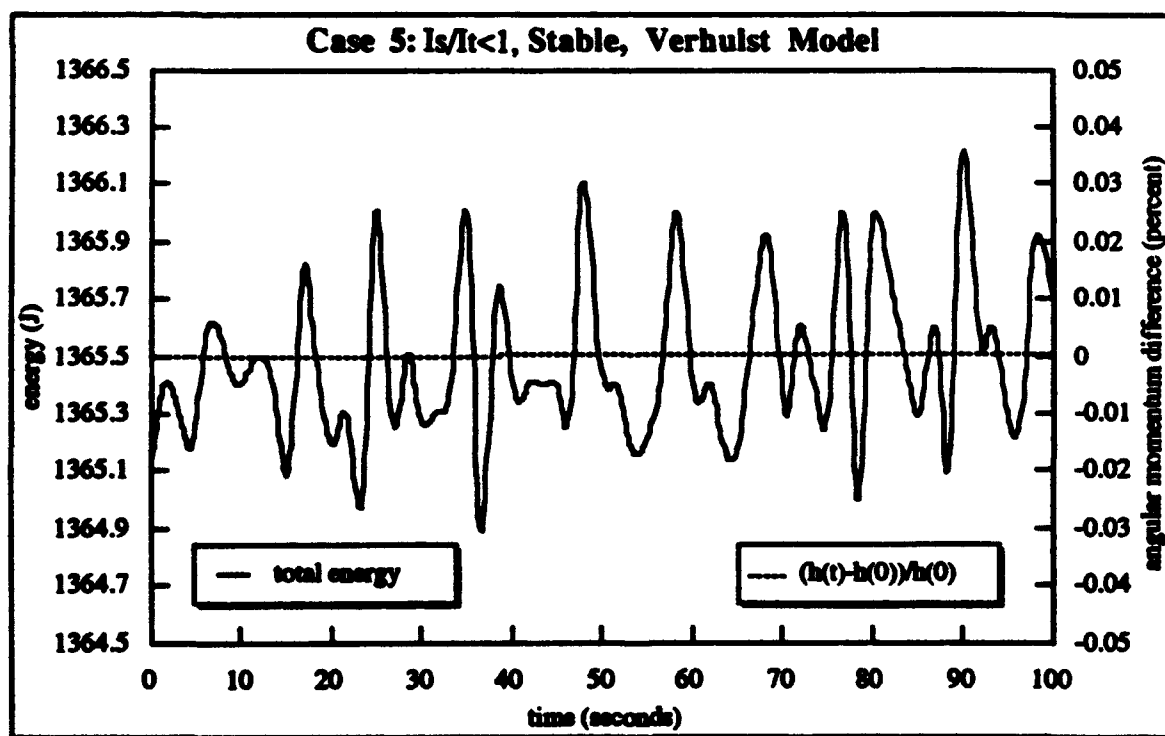


Figure (50) Total Energy and Percent Difference Angular Momentum - First 100 Seconds

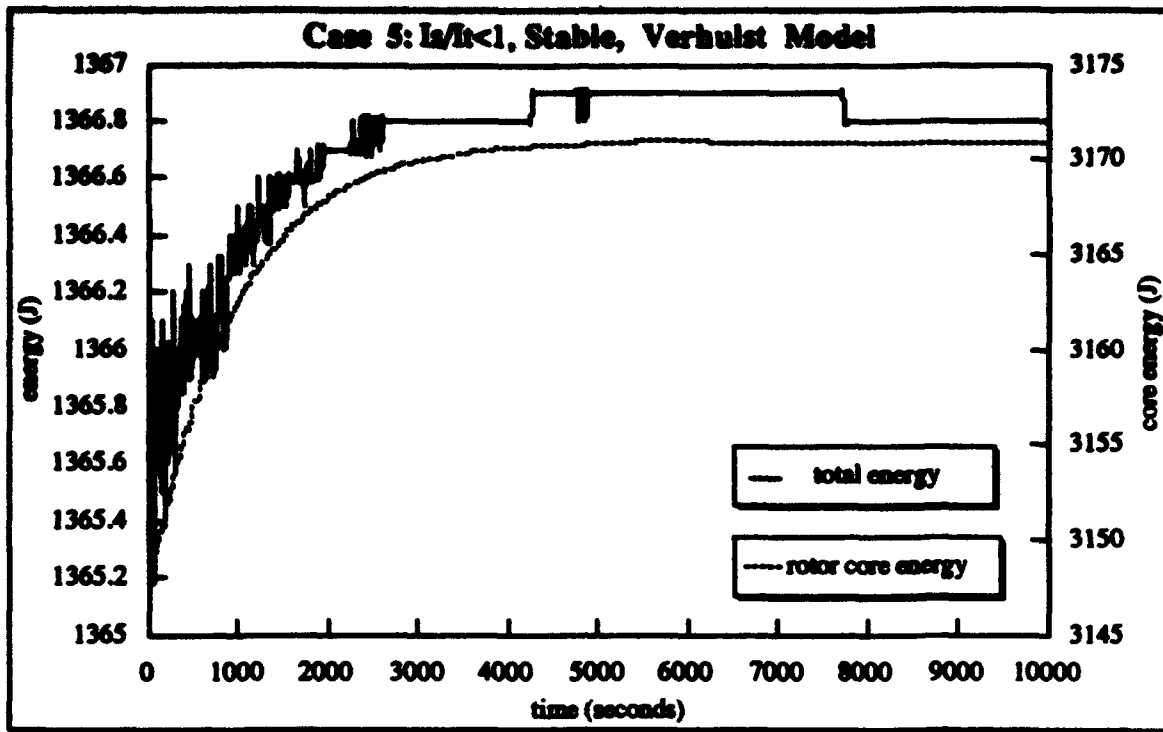


Figure (51) Total Energy and Rotor Core Energy Versus Time

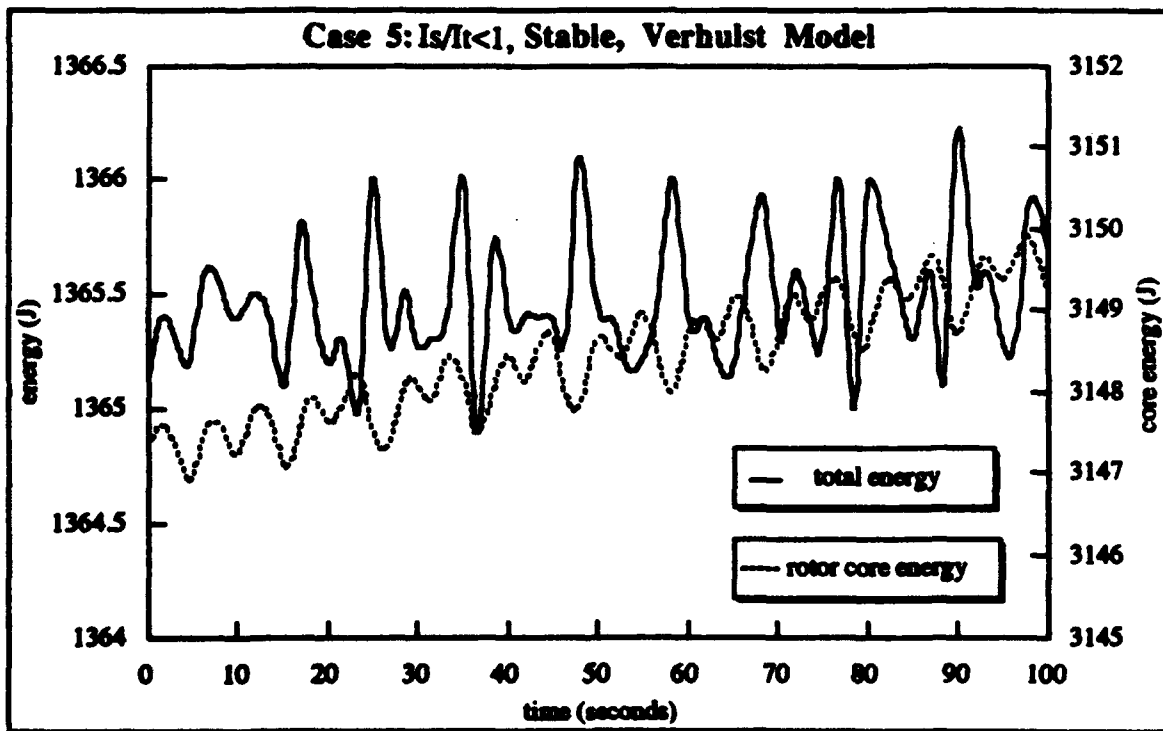


Figure (52) Total Energy and Rotor Core Energy - First 100 Seconds

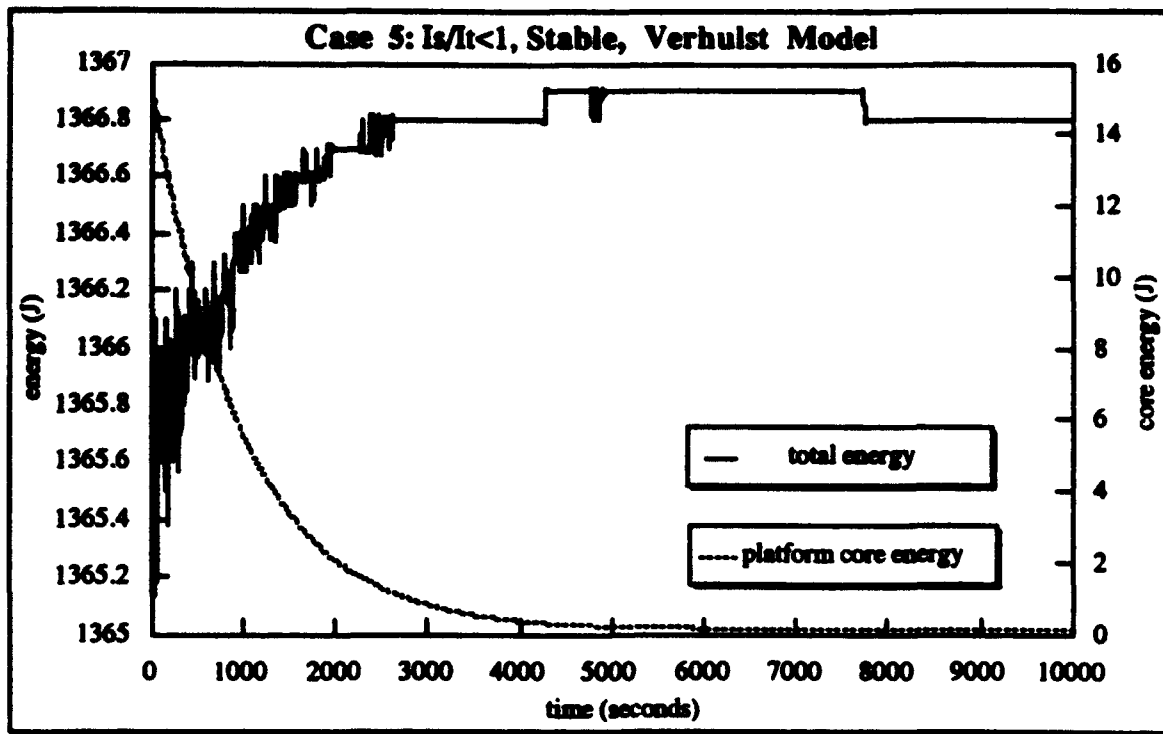


Figure (53) Total Energy and Platform Core Energy Versus Time

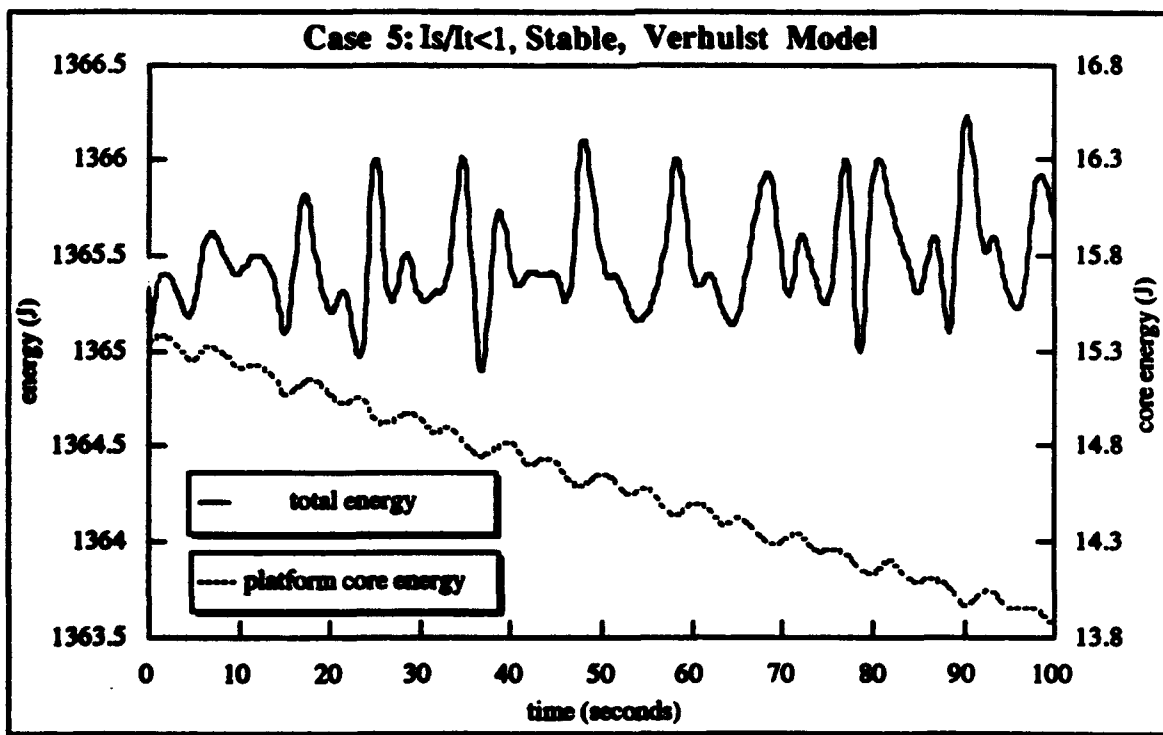


Figure (54) Total Energy and Platform Core Energy - First 100 Seconds

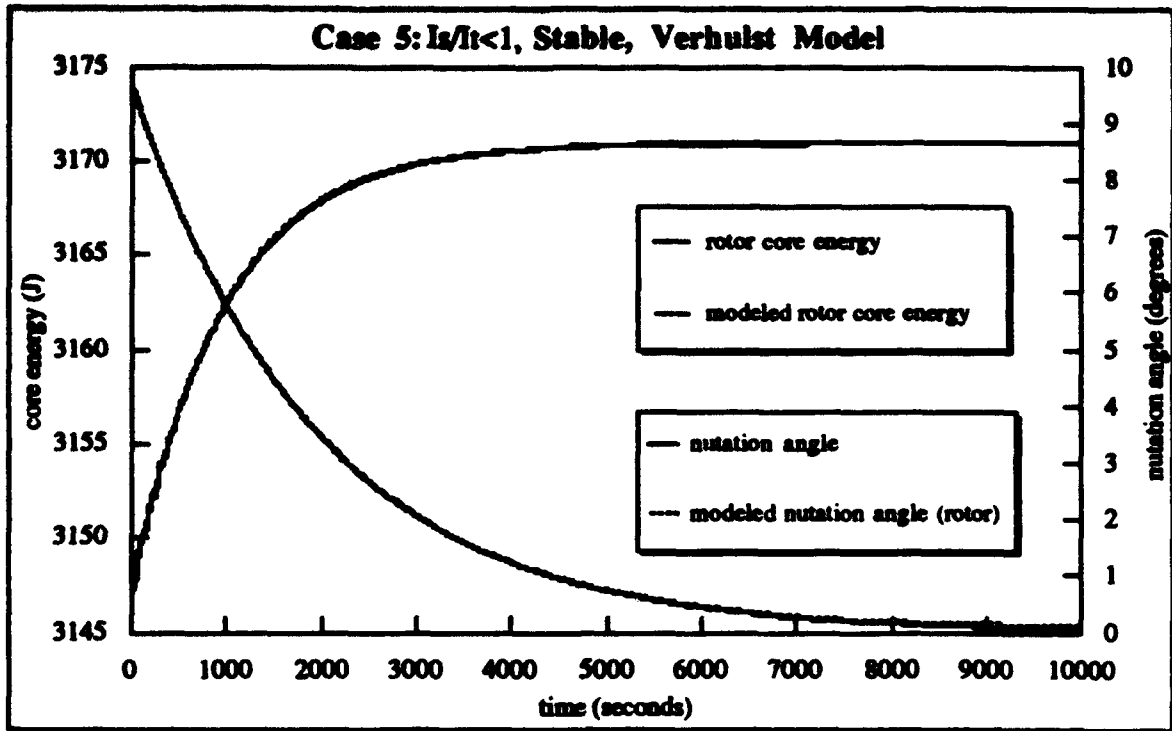


Figure (55) Modeled and Actual Rotor Core Energy and Nutation Angle Versus Time

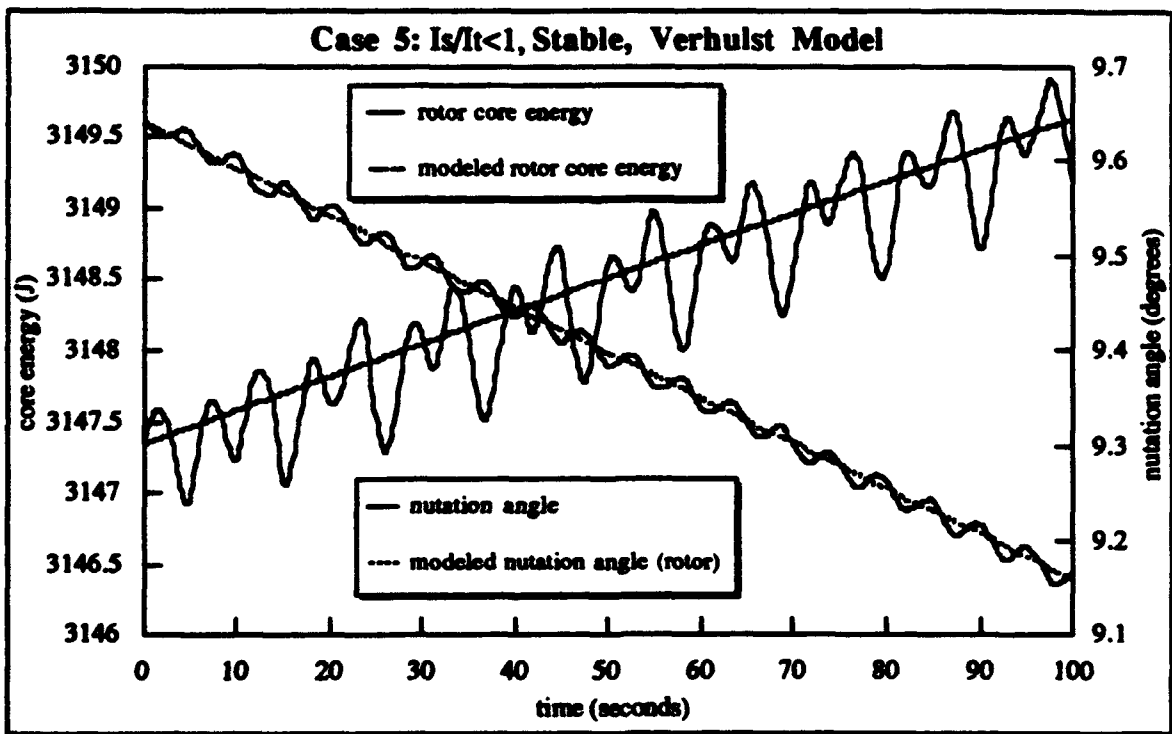


Figure (56) Modeled, Actual Rotor Core Energy and Nutation Angle - First 100 Seconds

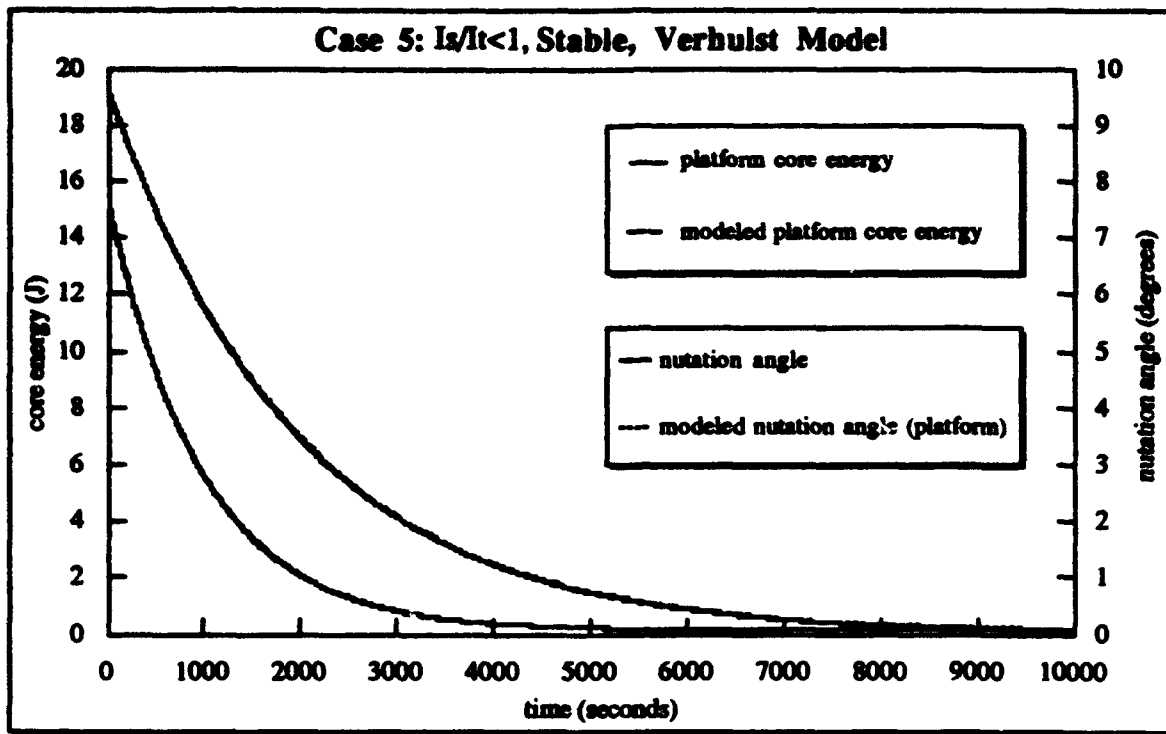


Figure (57) Modeled and Actual Platform Core Energy and Nutation Angle Versus Time

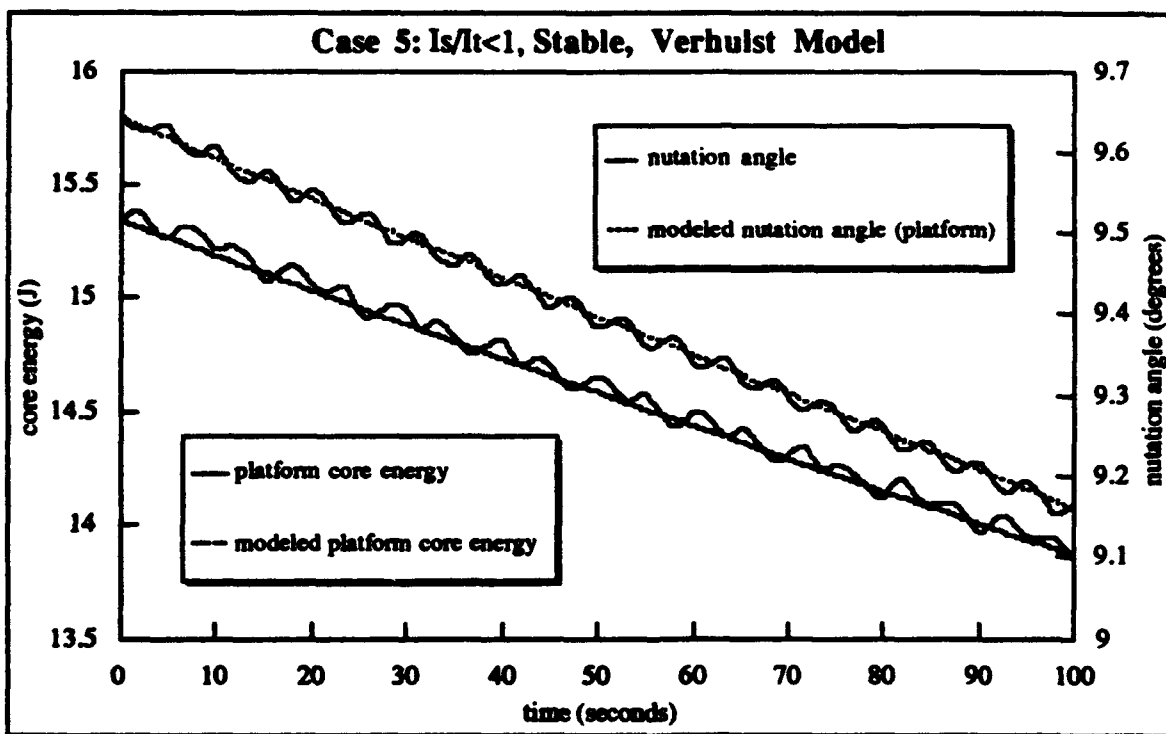


Figure (58) Modeled, Actual Platform Core Energy and Nutation Angle- First 100 Seconds

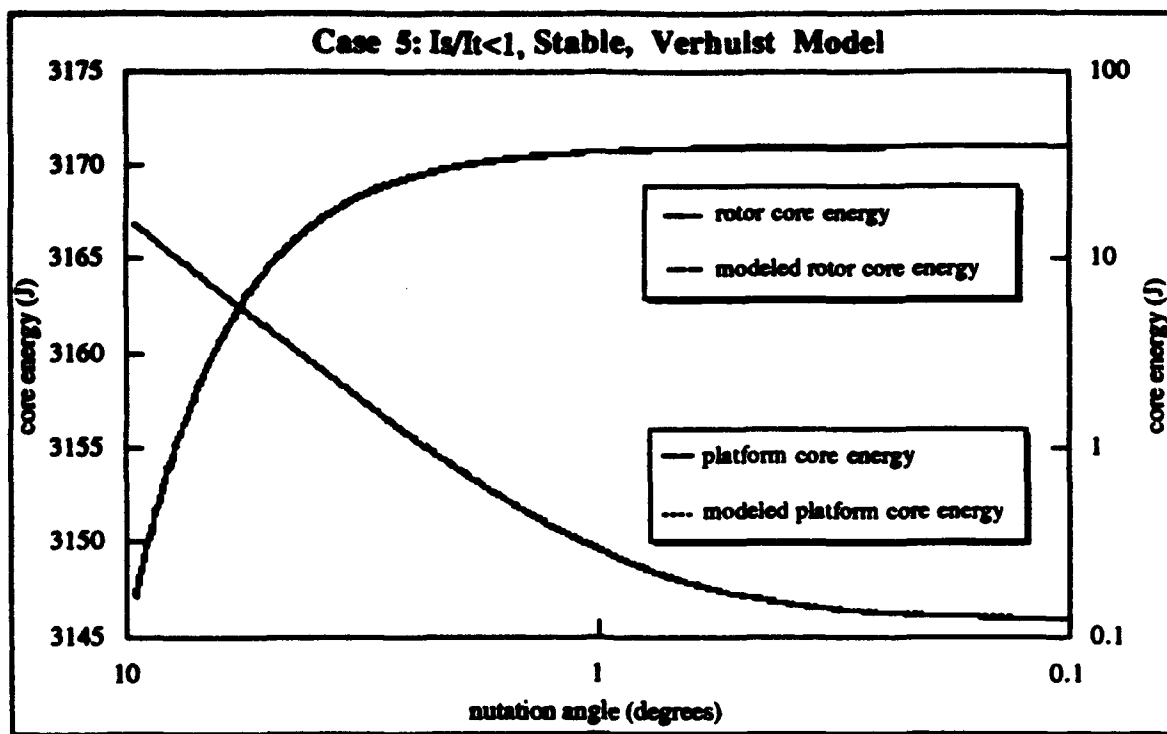


Figure (59) Core Energy Versus Nutation Angle

CASE 6: $\frac{I_z}{I_t} < 1$, Unstable, Verhulst Model

System Parameters		Initial Conditions	
Platform	Rotor	Platform	Rotor
$I_1' = 1600 \text{ kgm}^2$	$I_1 = 1000 \text{ kgm}^2$	$z' = 0.0 \text{ m}$	$z = 0.0 \text{ m}$
$I_3' = 1500 \text{ kgm}^2$	$I_3 = 1200 \text{ kgm}^2$	$\dot{z}' = 0.0 \frac{\text{m}}{\text{s}}$	$\dot{z} = 0.0 \frac{\text{m}}{\text{s}}$
$M' = 1000.0 \text{ kg}$	$M = 700.0 \text{ kg}$	$\omega_3' = 7.27 \times 10^{-5} \frac{\text{rad}}{\text{sec}}$	$\omega_3 = 1.5 \frac{\text{rad}}{\text{sec}}$
$m' = 1.0 \text{ kg}$	$m = 1.0 \text{ kg}$	$\omega_1 = 0.10 \frac{\text{rad}}{\text{sec}}$	$\omega_2 = 0.0 \frac{\text{rad}}{\text{sec}}$
$a' = 1.0 \text{ m}$	$a = 1.0 \text{ m}$	Core Energy Parameters	
$k' = 1.0 \frac{\text{N}}{\text{m}}$	$k = 1.0 \frac{\text{N}}{\text{m}}$		
$c' = 1.0 \frac{\text{kg}}{\text{sec}}$	$c = 1.0 \frac{\text{kg}}{\text{sec}}$	Platform	Rotor
$L = 1.0 \text{ m}$	$\frac{I_{z \text{ total}}}{I_{t \text{ total}}} = 0.897$	$E_{c \text{ initial}}' = 15.1 \text{ J}$	$E_{c \text{ initial}} = 3061.6 \text{ J}$
		$E_{c \text{ final}}' = 1161.0 \text{ J}$	$E_{c \text{ final}} = 1489.9 \text{ J}$
		$\frac{\dot{E}_C'}{\lambda'} = \text{positive}$	$\frac{\dot{E}_C}{\lambda} = \text{positive}$
		$r' = -1 \times 10^{-6} \text{ s}^{-1}$	$r = -1 \times 10^{-6} \text{ s}^{-1}$

Table (7) Case 6 Parameters

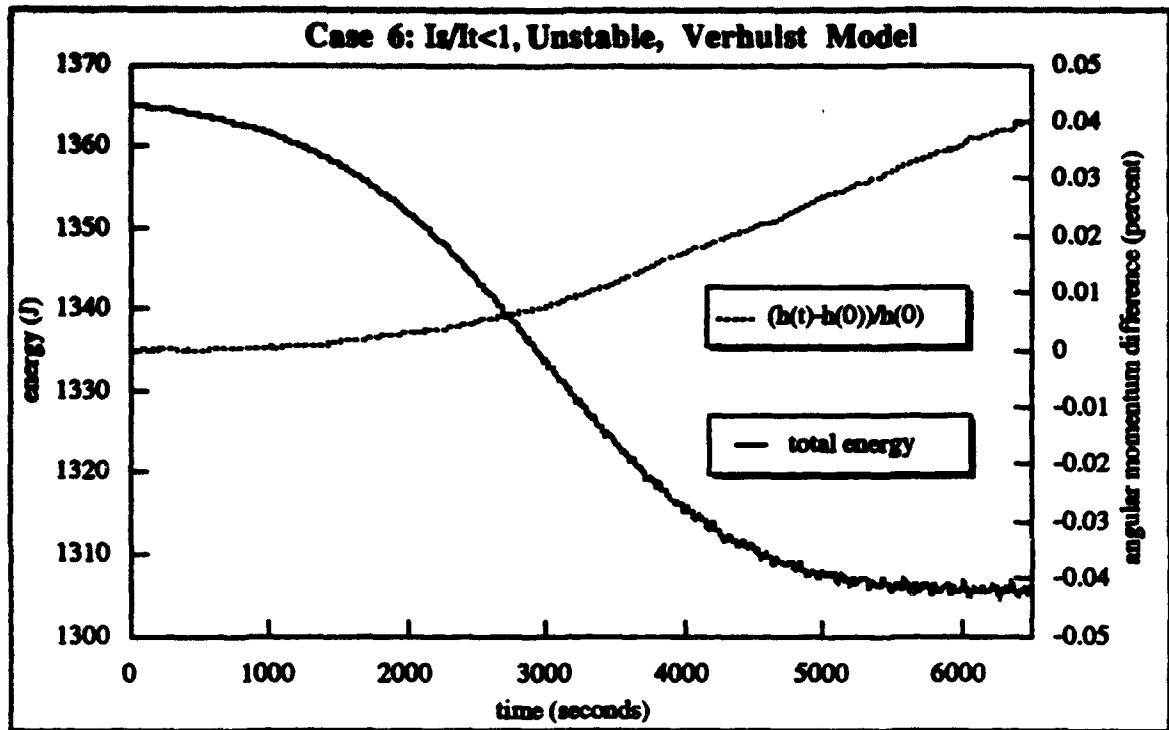


Figure (60) Total Energy and Percent Difference Angular Momentum Versus Time

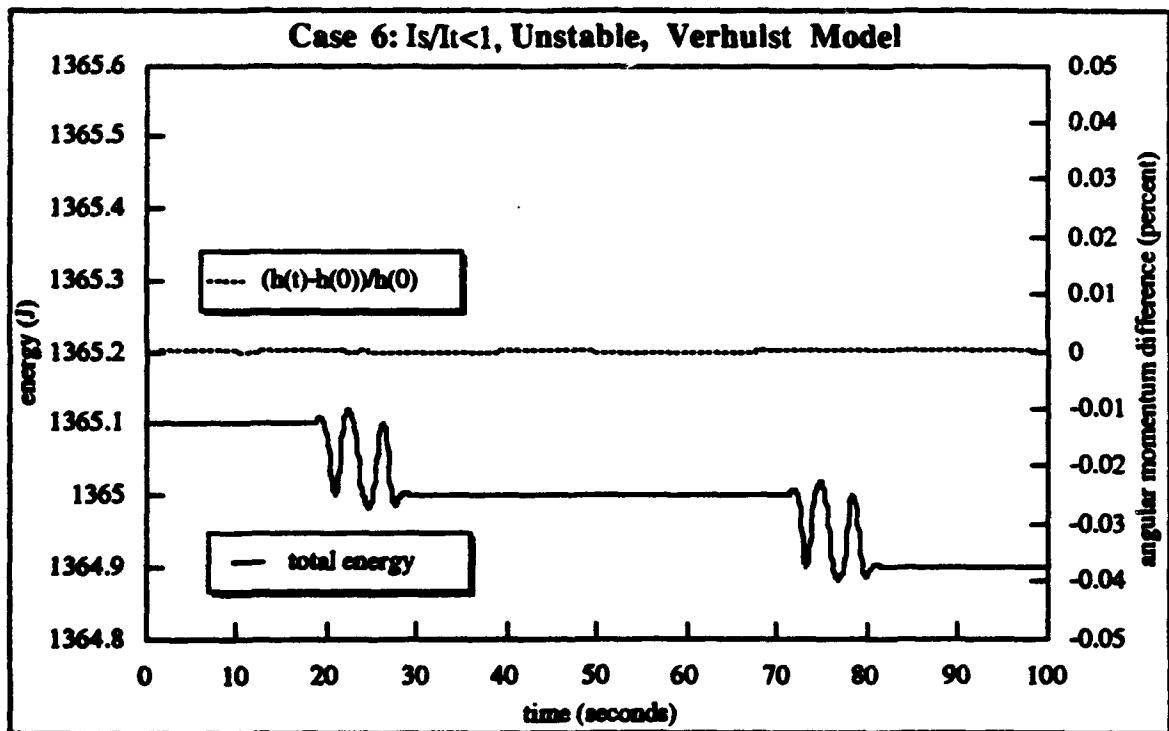


Figure (61) Total Energy and Percent Difference Angular Momentum - First 100 Seconds

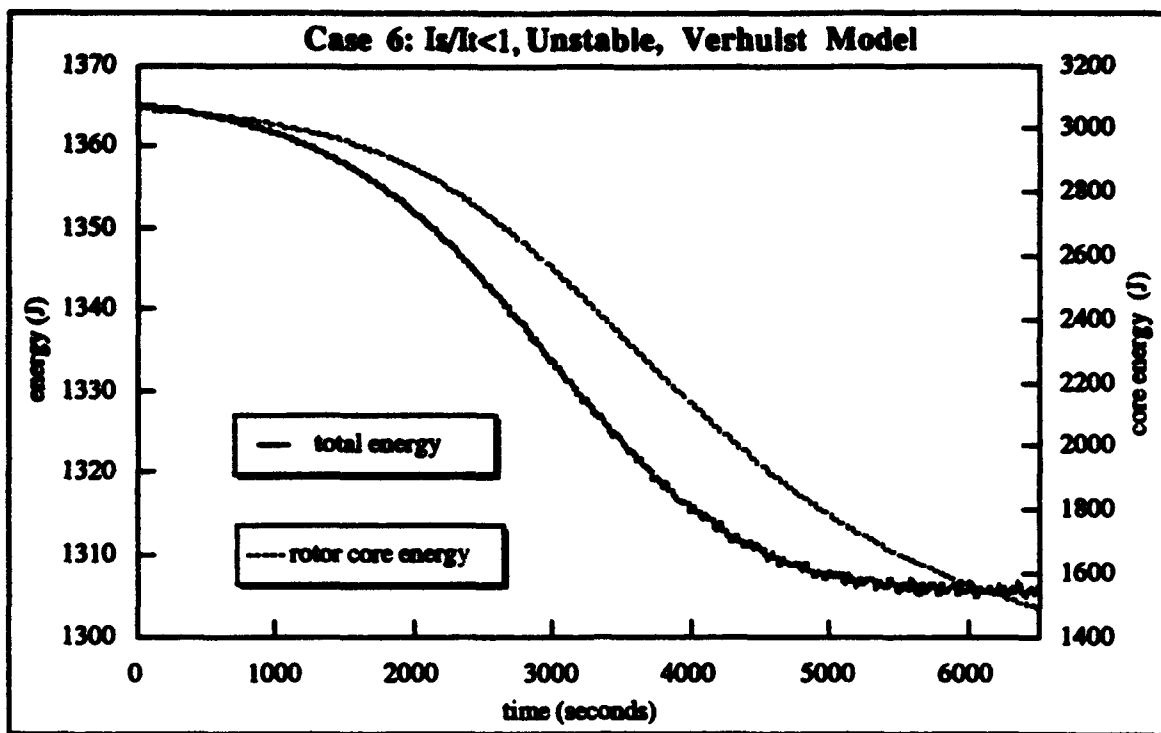


Figure (62) Total Energy and Rotor Core Energy Versus Time

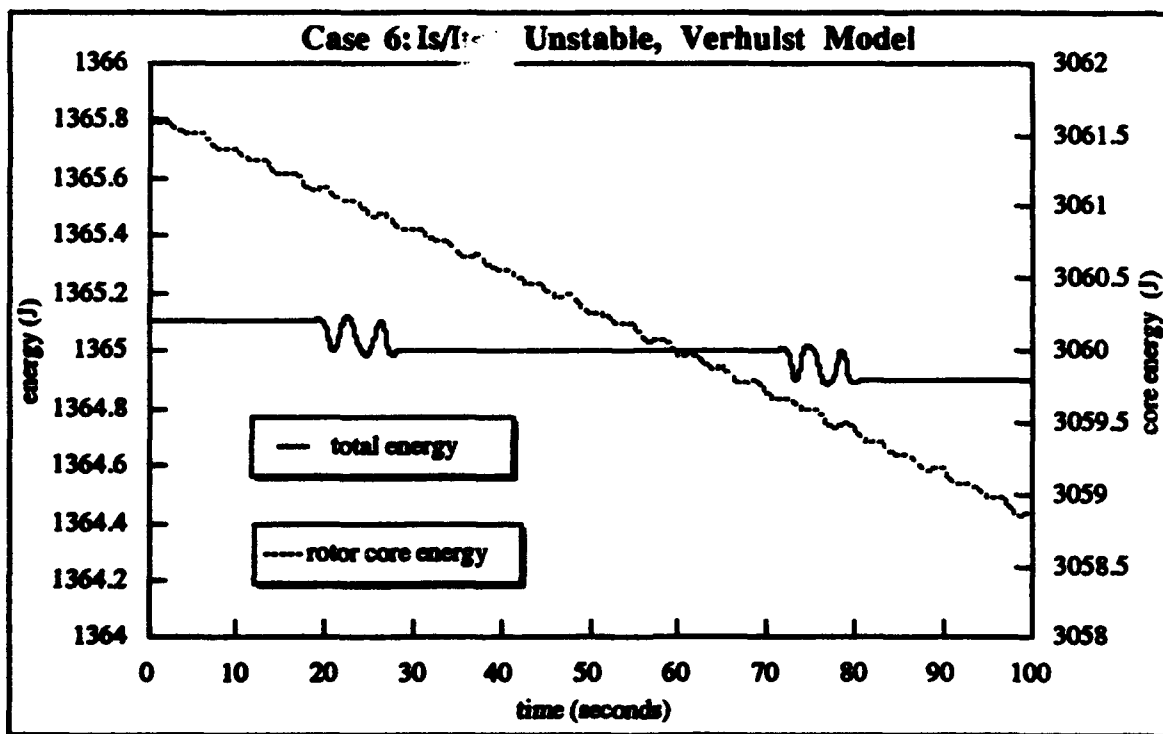


Figure (63) Total Energy and Rotor Core Energy - First 100 Seconds

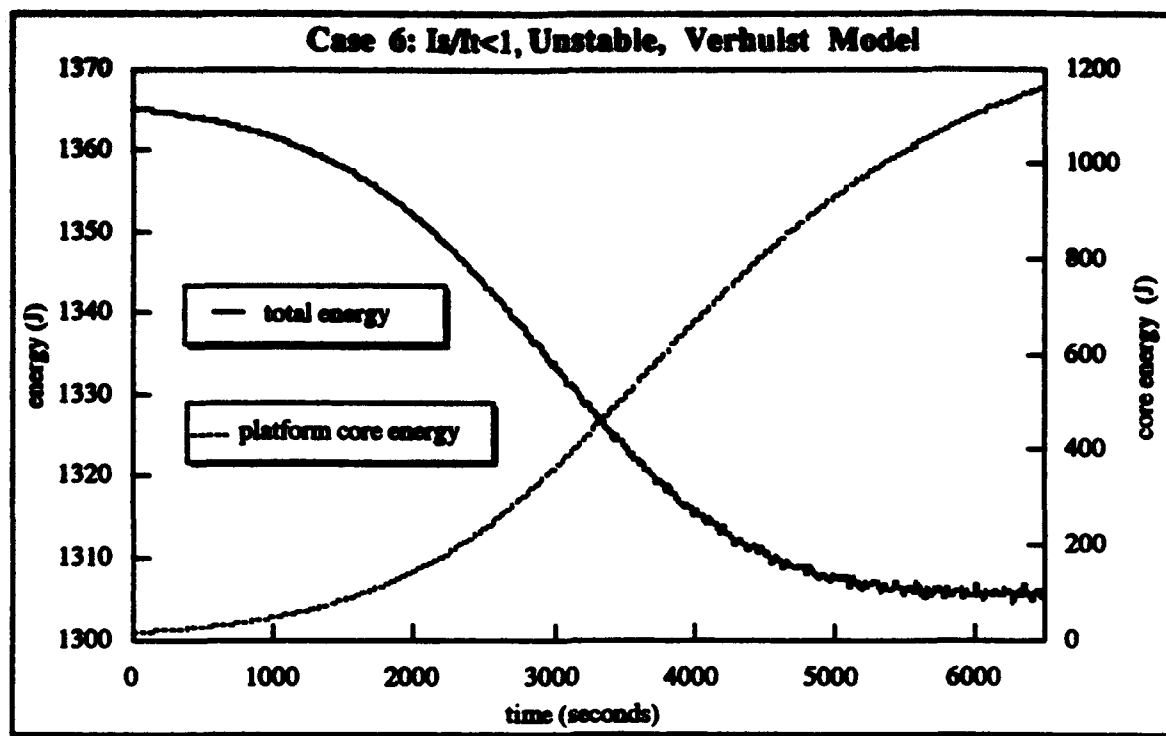


Figure (64) Total Energy and Platform Core Energy Versus Time

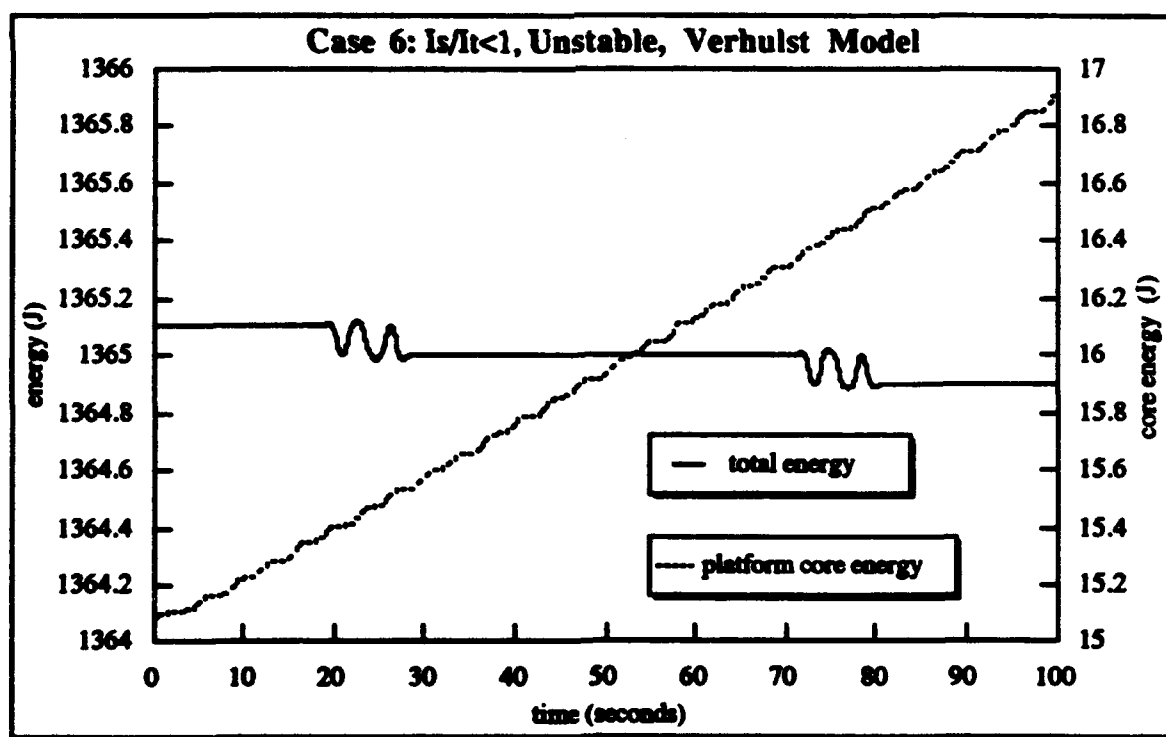


Figure (65) Total Energy and Platform Core Energy - First 100 Seconds

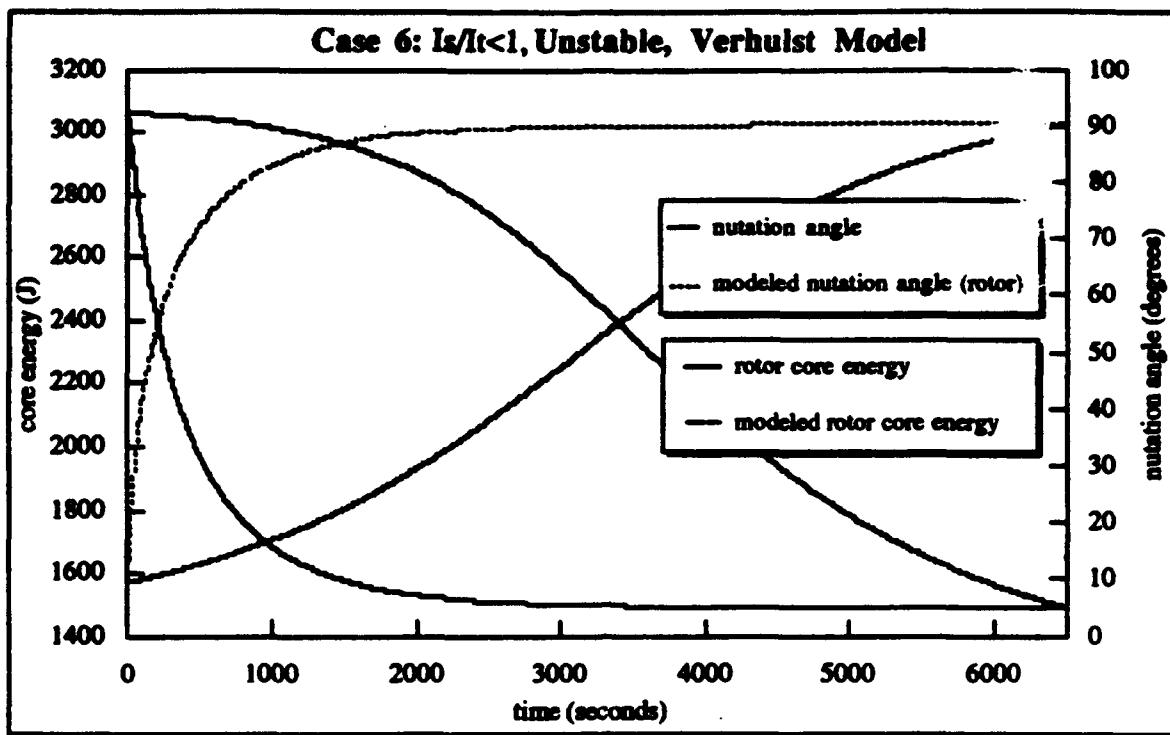


Figure (66) Modeled and Actual Rotor Core Energy and Nutation Angle Versus Time

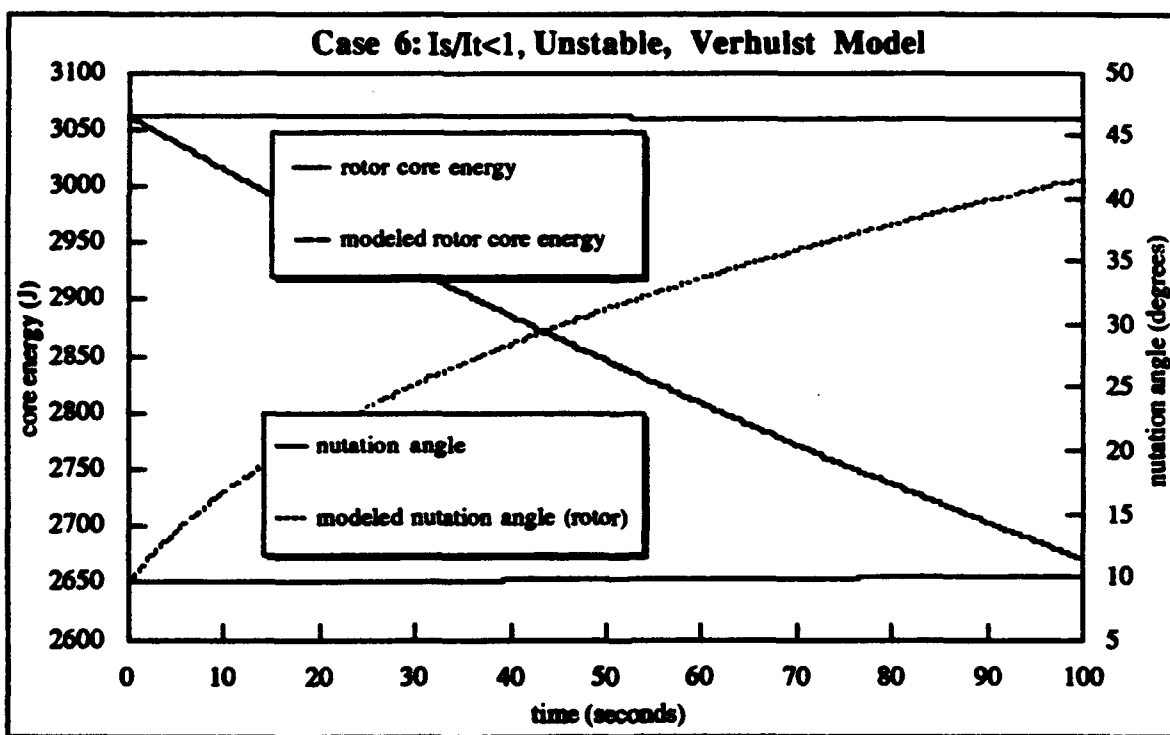


Figure (67) Modeled, Actual Rotor Core Energy and Nutation Angle - First 100 Seconds

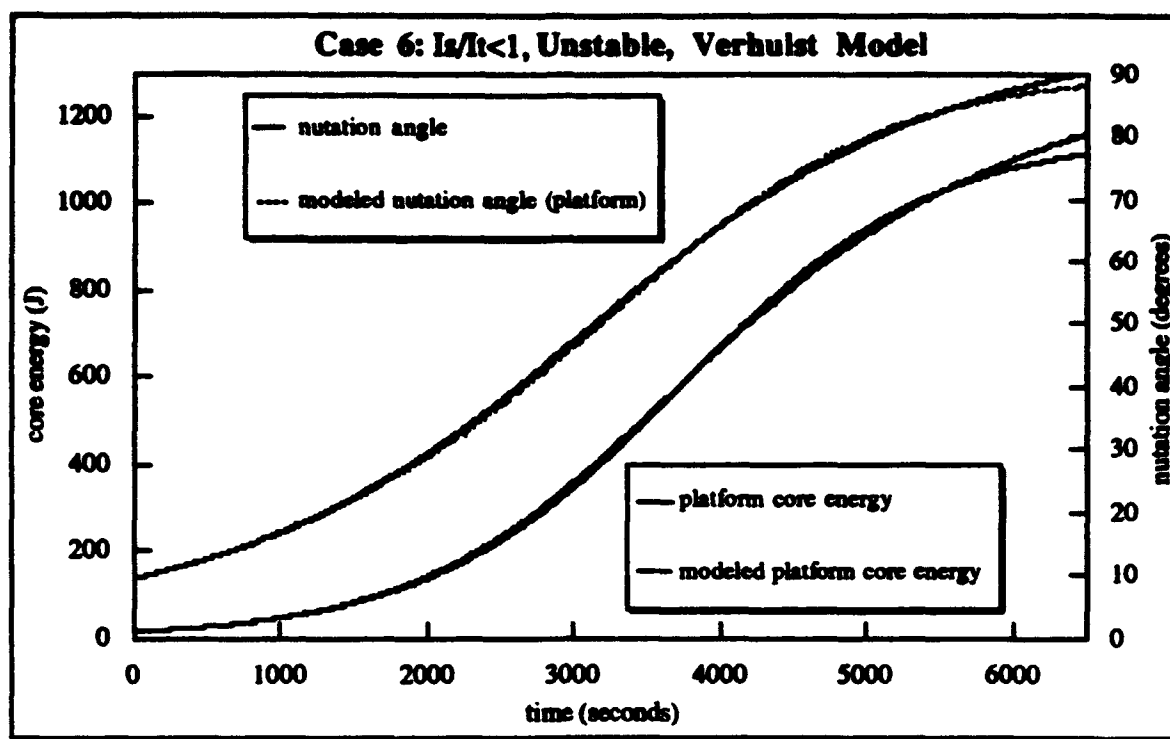


Figure (68) Modeled and Actual Platform Core Energy and Nutation Angle Versus Time

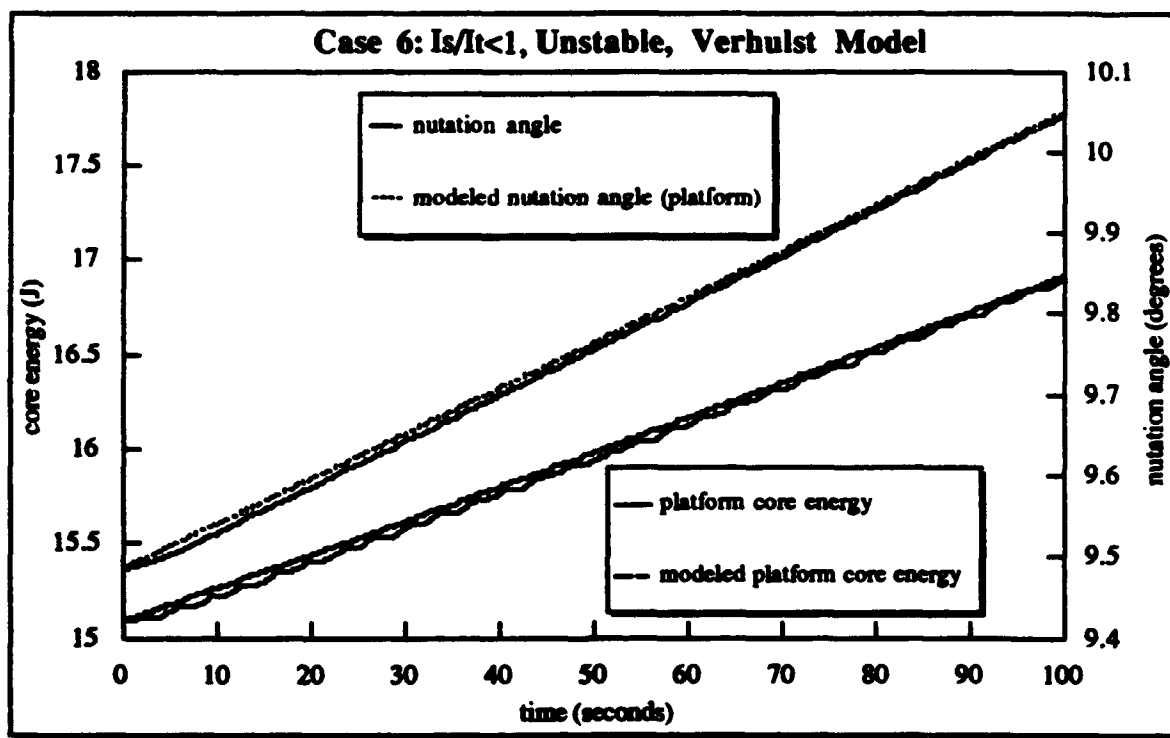


Figure (69) Modeled, Actual Platform Core Energy and Nutation Angle- First 100 Seconds

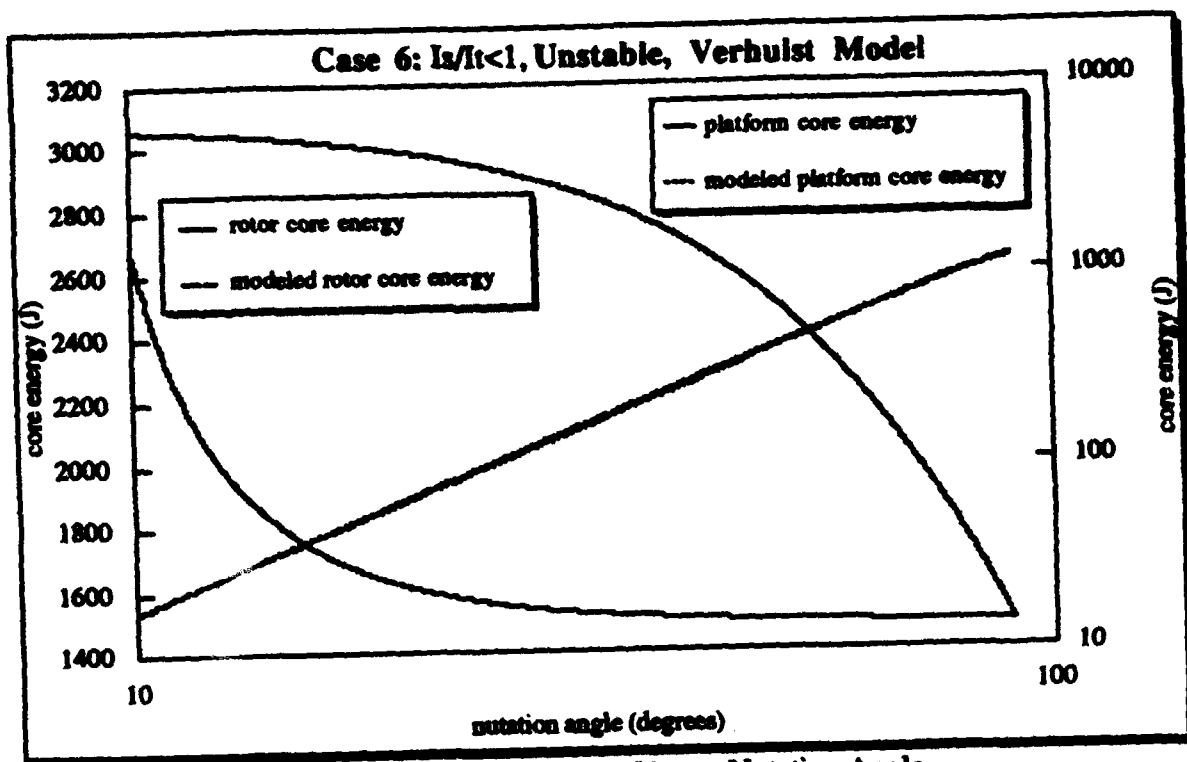


Figure (70) Core Energy Versus Nutation Angle

CASE 7: $\frac{I_z}{I_t} > 1$, Unstable, Verhulst Model

System Parameters		Initial Conditions	
Platform	Rotor	Platform	Rotor
$I_1' = 1600 \text{ kgm}^2$	$I_1 = 1000 \text{ kgm}^2$	$z' = 0.0 \text{ m}$	$z = 0.0 \text{ m}$
$I_3' = 1500 \text{ kgm}^2$	$I_3 = 1200 \text{ kgm}^2$	$\dot{z}' = 0.0 \frac{\text{m}}{\text{s}}$	$\dot{z} = 0.0 \frac{\text{m}}{\text{s}}$
$M' = 1000.0 \text{ kg}$	$M = 700.0 \text{ kg}$	$\omega_3' = 7.27 \times 10^{-5} \frac{\text{rad}}{\text{sec}}$	$\omega_3 = 1.5 \frac{\text{rad}}{\text{sec}}$
$m' = 1.0 \text{ kg}$	$m = 1.0 \text{ kg}$	$\omega_1 = 0.10 \frac{\text{rad}}{\text{sec}}$	$\omega_2 = 0.0 \frac{\text{rad}}{\text{sec}}$
$a' = 1.0 \text{ m}$	$a = 1.0 \text{ m}$	Core Energy Parameters	
$k' = 1.0 \frac{\text{N}}{\text{m}}$	$k = 1.0 \frac{\text{N}}{\text{m}}$		
$c' = 1.0 \frac{\text{kg}}{\text{sec}}$	$c = 1.0 \frac{\text{kg}}{\text{sec}}$	Platform	Rotor
$L = 0.3 \text{ m}$	$\frac{I_{z \text{ total}}}{I_{t \text{ total}}} = 1.025$	$E_{c \text{ initial}}' = 13.2 \text{ J}$	$E_{c \text{ initial}} = 3059.7 \text{ J}$
		$E_{c \text{ final}}' = 1247.1 \text{ J}$	$E_{c \text{ final}} = 1552.5 \text{ J}$
		$\frac{\dot{E}_C'}{\lambda'} = \text{positive}$	$\frac{\dot{E}_C}{\lambda} = \text{positive}$
		$r' = -1.1 \times 10^{-6} \text{ s}^{-1}$	$r = -1.1 \times 10^{-6} \text{ s}^{-1}$

Table (8) Case 7 Parameters

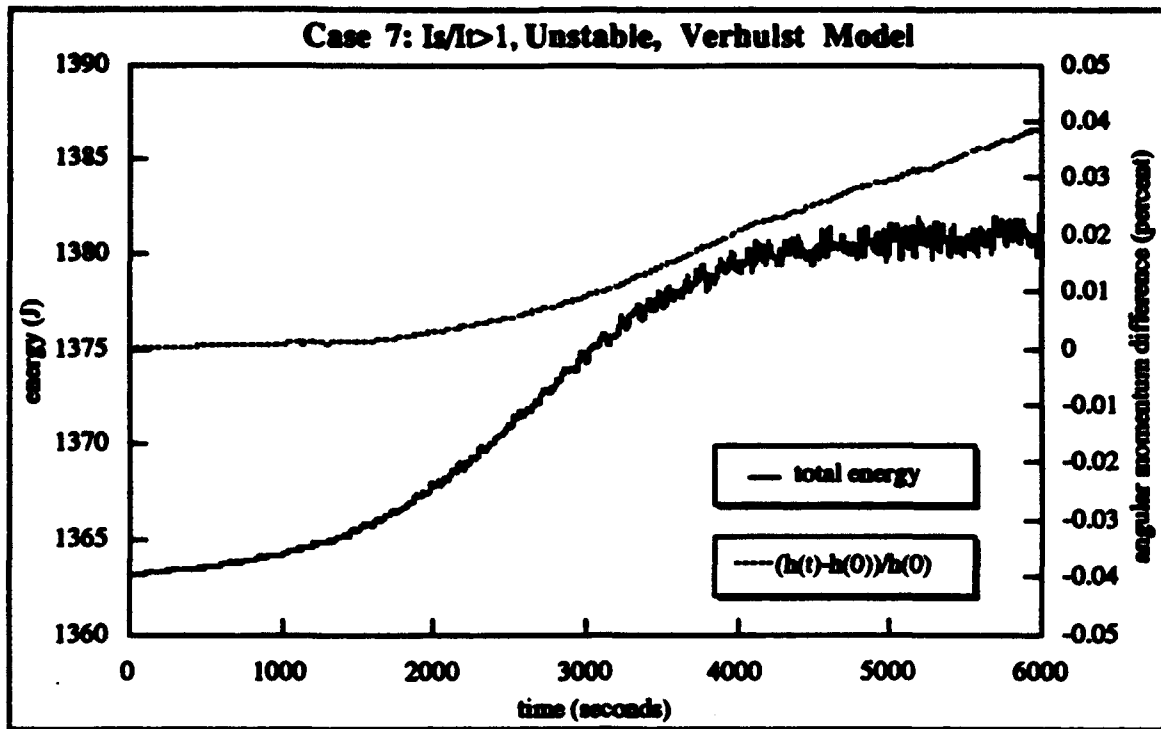


Figure (71) Total Energy and Percent Difference Angular Momentum Versus Time

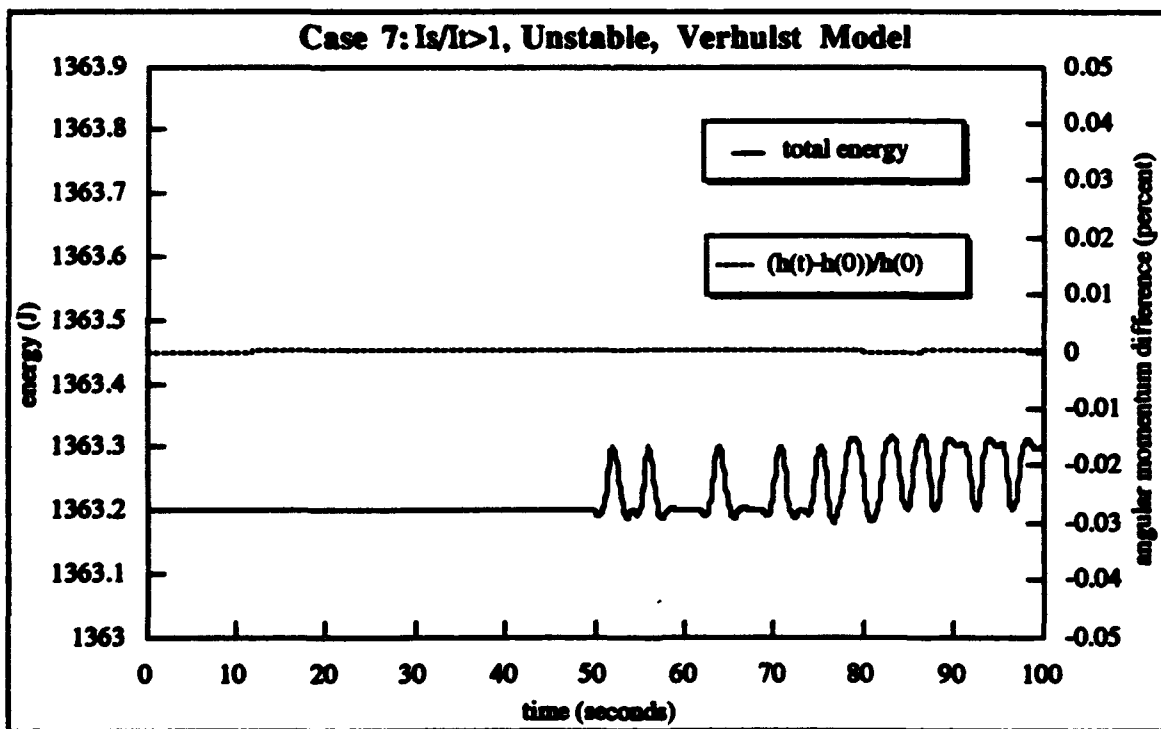


Figure (72) Total Energy and Percent Difference Angular Momentum - First 100 Seconds

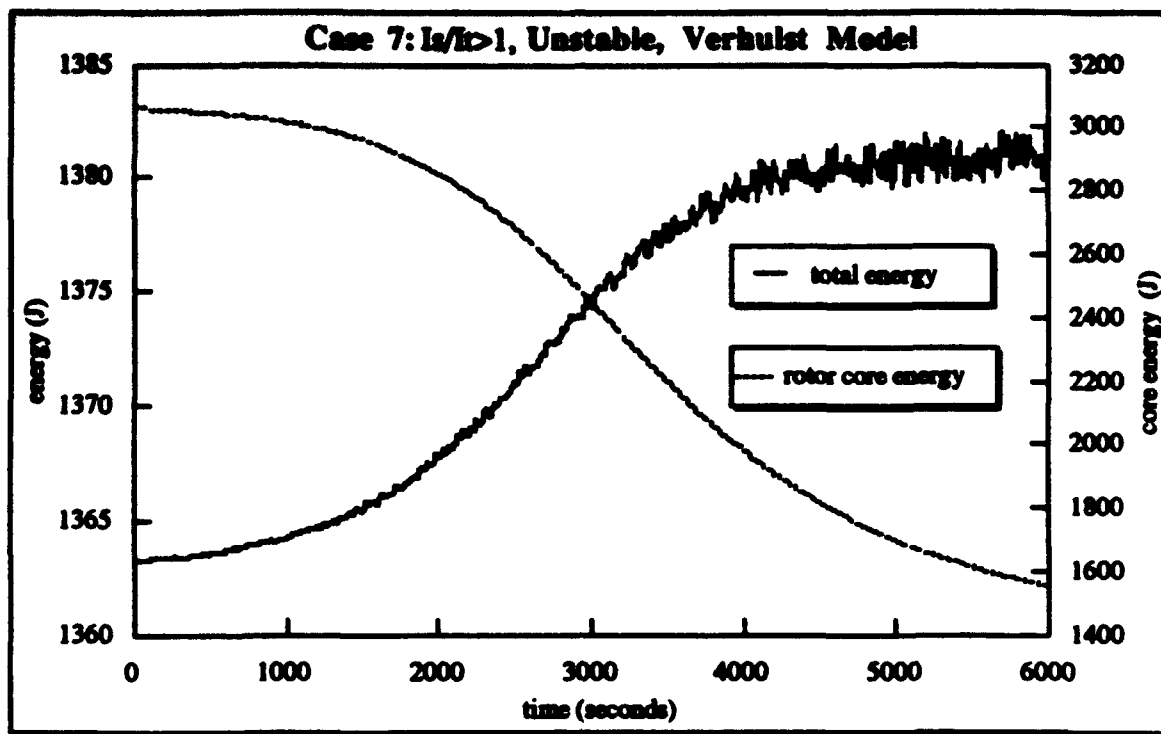


Figure (73) Total Energy and Rotor Core Energy Versus Time

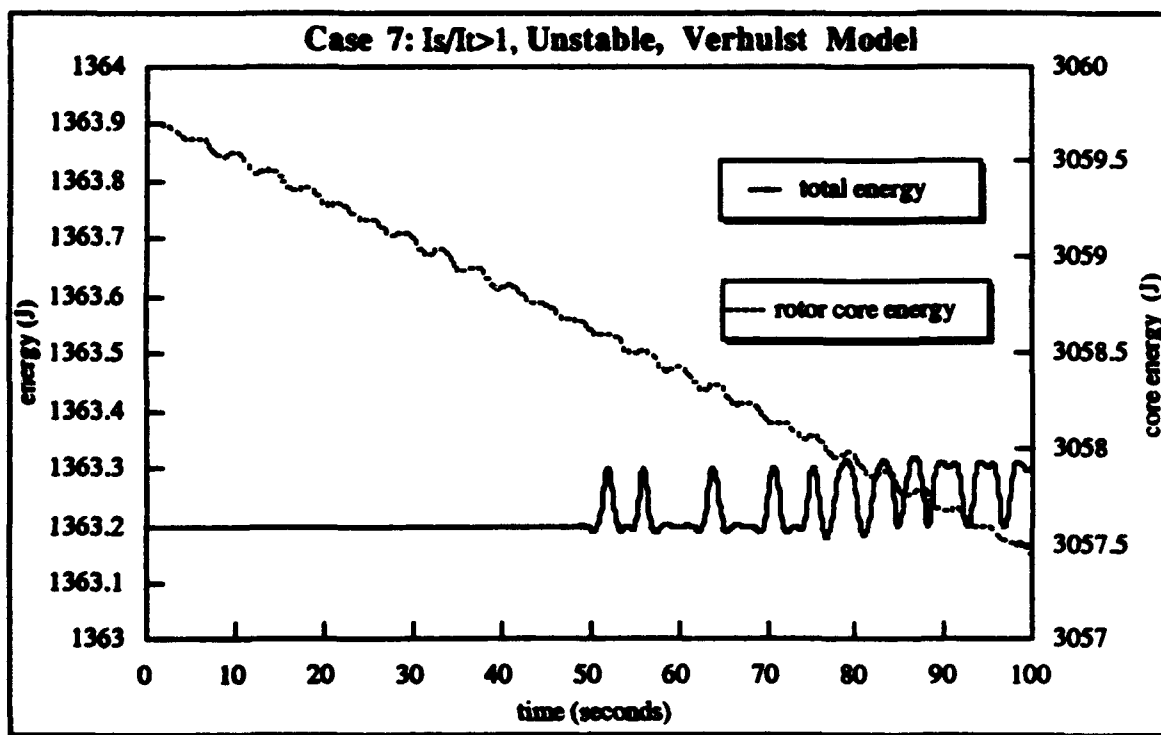


Figure (74) Total Energy and Rotor Core Energy - First 100 Seconds

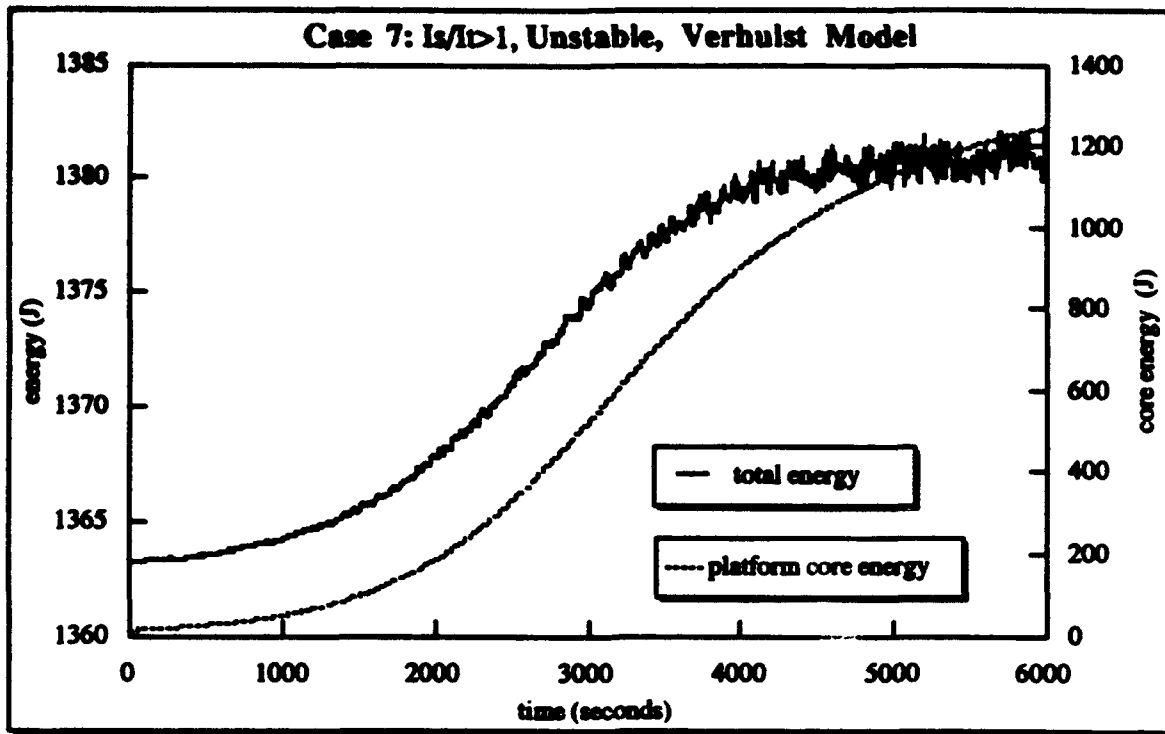


Figure (75) Total Energy and Platform Core Energy Versus Time

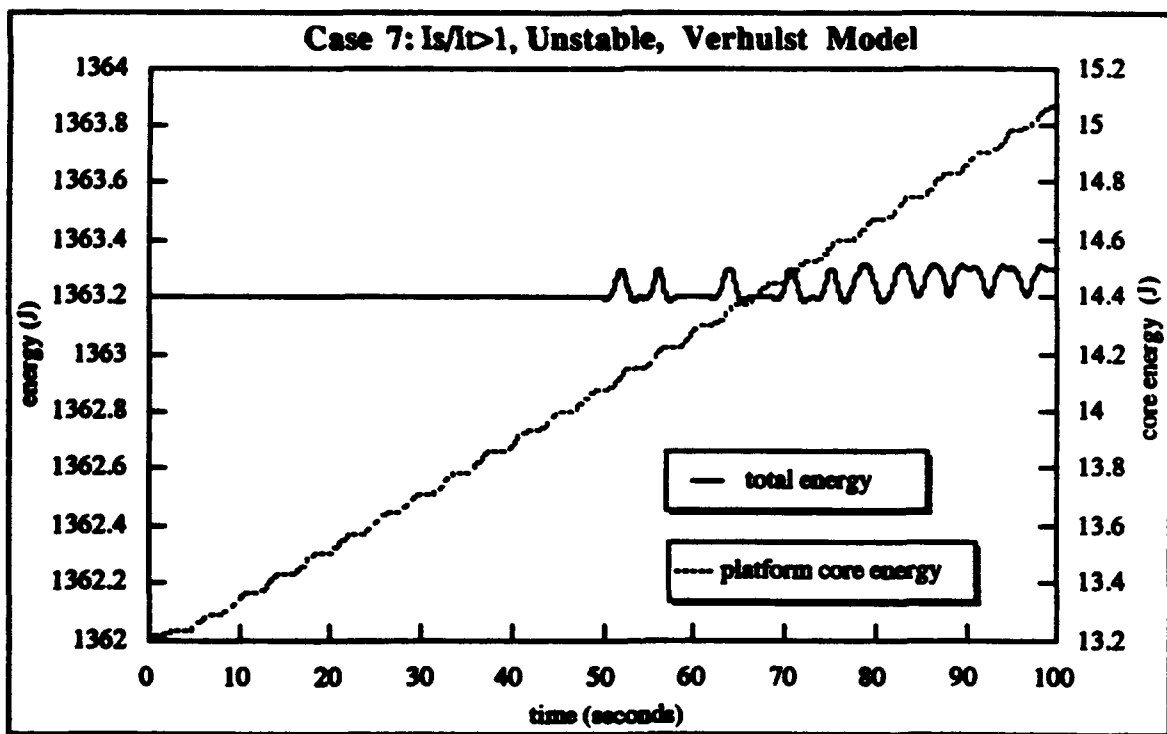


Figure (76) Total Energy and Platform Core Energy - First 100 Seconds

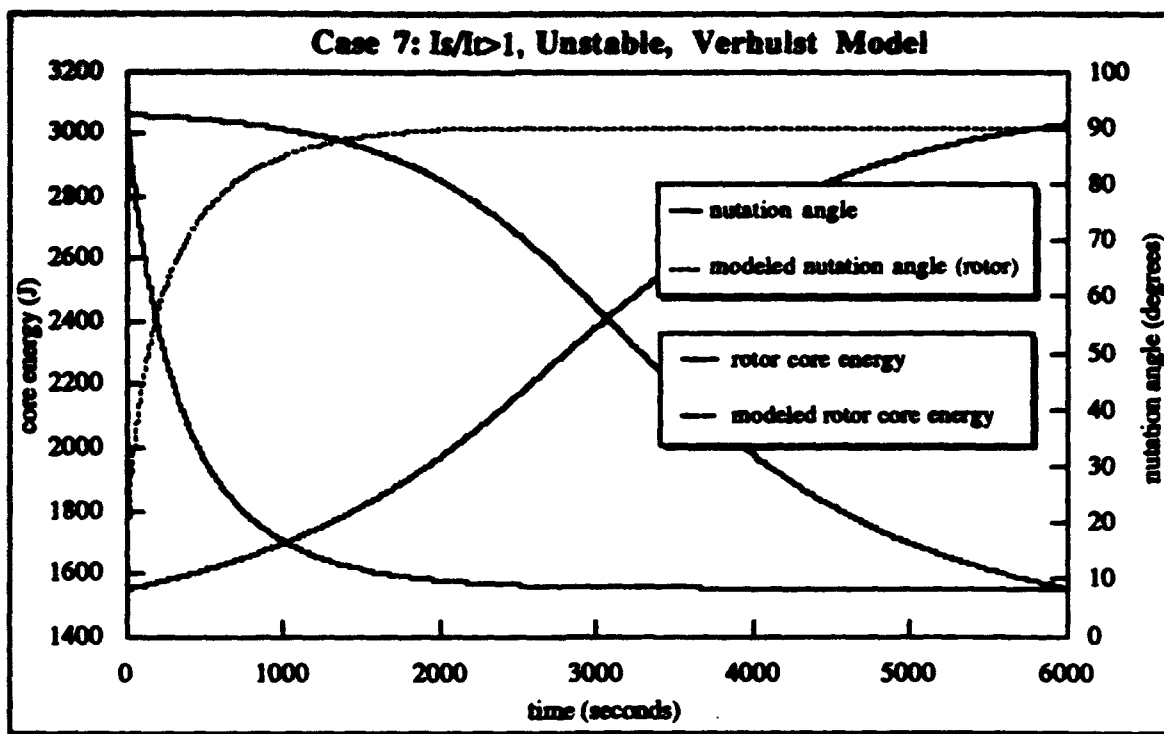


Figure (77) Modeled and Actual Rotor Core Energy and Nutation Angle Versus Time

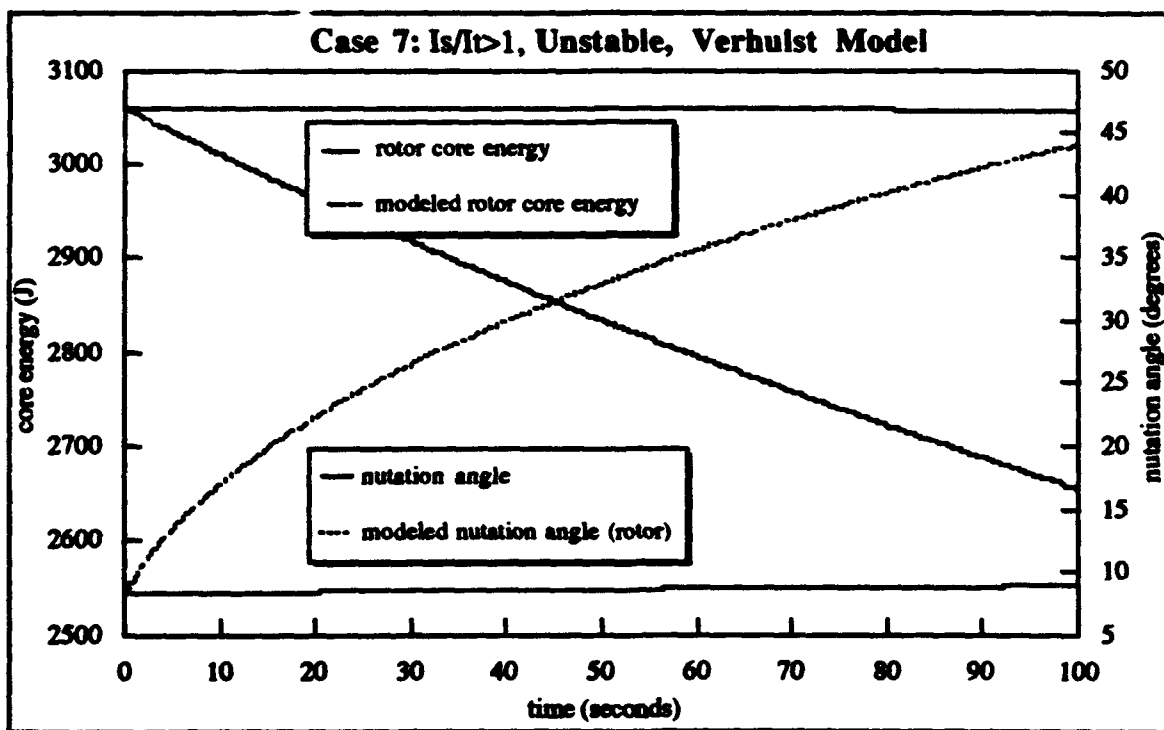


Figure (78) Modeled, Actual Rotor Core Energy and Nutation Angle - First 100 Seconds

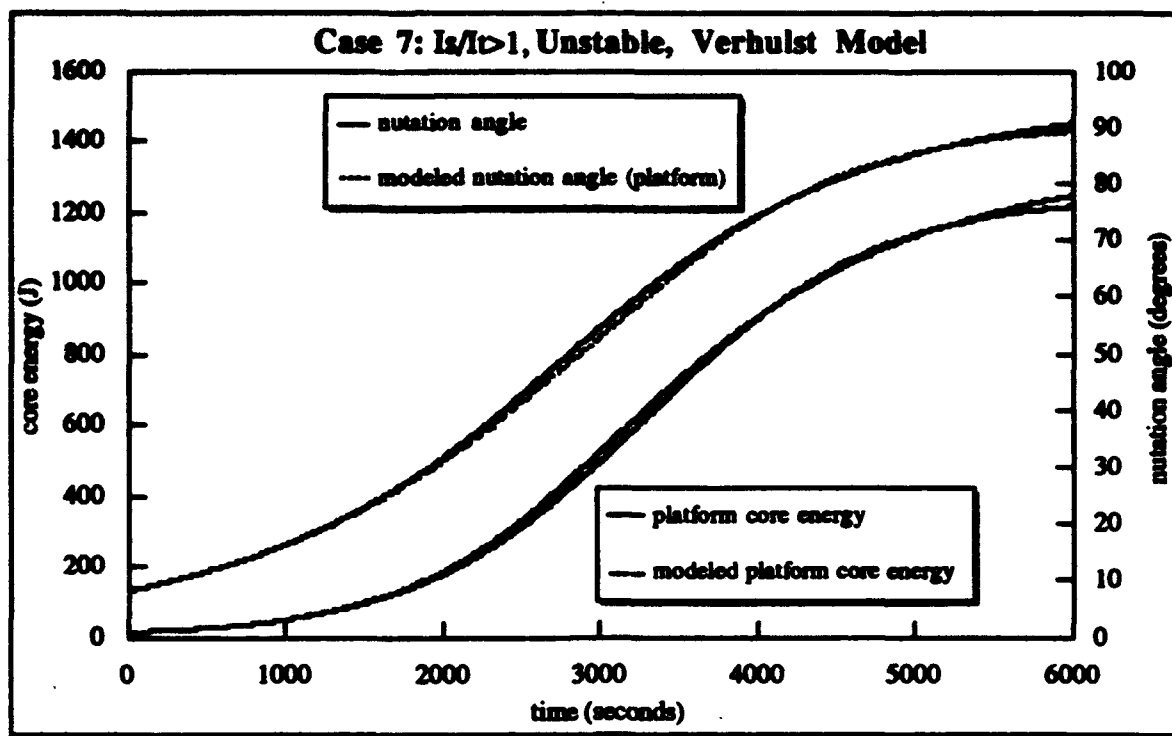


Figure (79) Modeled and Actual Platform Core Energy and Nutation Angle Versus Time

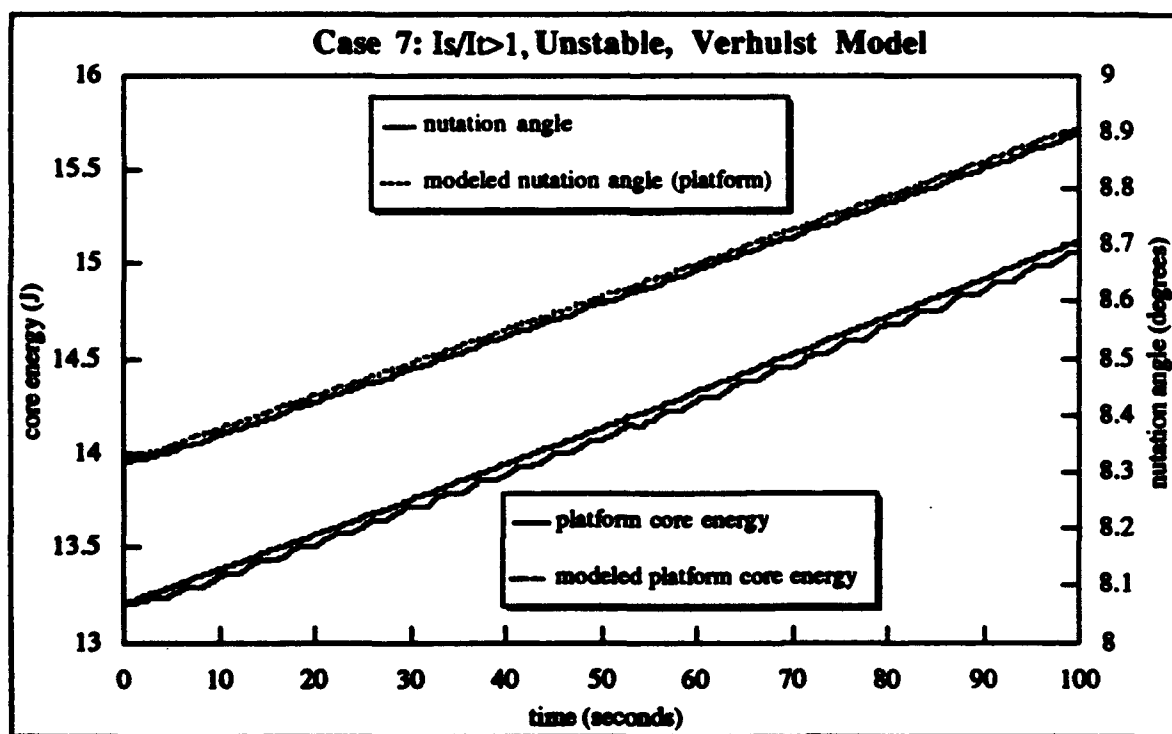


Figure (80) Modeled, Actual Platform Core Energy and Nutation Angle- First 100 Seconds

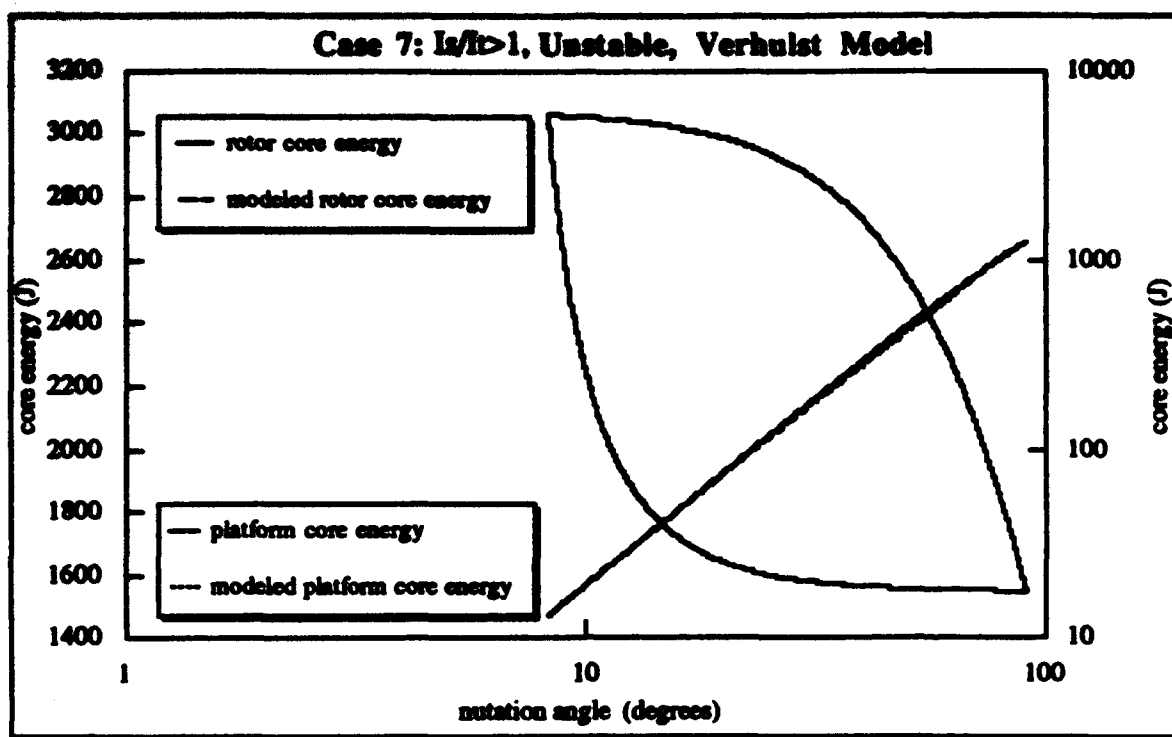


Figure (81) Core Energy Versus Nutation Angle

APPENDIX B. COMPUTER PROGRAM CODE

```

/***** declarations *****/

#include <math.h>
#include <malloc.h>
#include <stdio.h>

#define MAXSTP 150000 /* odeint */
#define TINY 1.0e-6C /* odeint */

#define PGROW -0.20 /* krqc */
#define PSNRNK -0.25 /* krqc */
#define FCOR 0.06666666666666666666666666666667 /* 1.0/15.0 krqc */
#define SAFETY 0.9 /* krqc */
#define ERRCON 6.0e-4 /* krqc */

float **y=0, *xx=0; /* defining declaration rkdummy */
int kmax=0, kount=0; /* defining declaration odeint */
float *xp=0, **yp=0, dxsav=0; /* defining declaration odeint */

/***** error function *****/
void nrerror(error_text)
char error_text[];
{
void exit();

fprintf(stderr,"Numerical Recipes run-time error...\n");
fprintf(stderr,"%s\n",error_text);
fprintf(stderr,"...now exiting to system...\n");
exit(1);
}

/***** vector function *****/
float *vectorr(nl,nh)
int nl, nh;
{
float *v;

v = (float *) malloc((unsigned) (nh-nl+1)*sizeof(float));
if (!v) nrerror("allocation failure in vector()");
return v-nl;
}

/***** matrix function *****/
float **matrix(nrl,nrh,ncl,nch)
int nrl, nrh, ncl, nch;
{
int i;
float **m;

m = (float **) malloc((unsigned) (nrh-nrl+1)*sizeof(float*));
if (!m) nrerror("allocation failure 1 in matrix()");
m -= nrl;
for (i=nrl;i<=nrh;i++)
{
m[i] = (float *) malloc((unsigned) (nch-ncl+1)*sizeof(float));
if (!m[i]) nrerror("allocation failure 2 in matrix()");
m[i] -= ncl;
}
return m;
}

/***** free vector function *****/
void free_vector(v,nl,nh)
float *v;
int nl, nh;

```



```

free((char*) (v+n1));
}

/***** free matrix function *****/
void free_matrix(m,nr1,nrh,ncl,nch)
float **m;
int nr1, nrh, ncl, nch;
{
int i;

for(i=nrh;i>=nr1;i--) free((char*) (m[i]+ncl));
free((char*) (m+nr1));
}

/***** rk4 function *****/
void rk4(y,dydx,n,x,h,yout,derivs)

float y[], dydx[], x, h, yout[];
void (*derivs)();
int n;

{
int i;
float xh, hh, h6, *dym, *dyn, *dym, *yt, *vectorr();
void free_vector();

dym = vectorr(1,n);
dyn = vectorr(1,n);
dym = vectorr(1,n);
yt = vectorr(1,n);
hh = h*0.5;
h6 = h/6.0;
xh = x+hh;
for (i=1;i<=n;i++) yt[i] = y[i]+hh*dydx[i]; /* first step */
(*derivs)(xh,yt,dym,dydx);
for (i=1;i<=n;i++) yt[i] = y[i]+hh*dym[i];
(*derivs)(xh,yt,dym,dym);
for (i=1;i<=n;i++)
{
yt[i] = y[i]+h*dym[i];
dyn[i] = dym[i]+dym[i];
}
(*derivs)(x+h,yt,dym,dym);
for (i=1;i<=n;i++) yout[i] = y[i]+h6*(dydx[i]+dym[i]+2.0*dyn[i]);
free_vector(yt,1,n);
free_vector(dym,1,n);
free_vector(dym,1,n);
free_vector(dyn,1,n);
}

/***** rk4 function *****/

void rk4(vstart,nvar,x1,x2,nstep,derivs)
int nvar,nstep;
float vstart[],x1,x2;
void (*derivs)();
{
int i, k;
float x, h;
float *v, *vout, *dv, *vectorr();
void rk4(), nrerror(), free_vector();

v = vectorr(1,nvar);
vout = vectorr(1,nvar);
dv = vectorr(1,nvar);

```

```

for (i=1;i<=nvar;i++)
{
    v[i] = vstart[i];
    y[i][1] = v[i];
}
xx[1] = x1;
x = x1;
h = (x2-x1)/nstep;
for (k=1;k<=nstep;k++)
{
    (*derivs)(x,v,dv);
    rk4(v,dv,nvar,x,h,vout,derivs);
    if (x+h == x) nrerror("Step size too small in routine RKINTIN");
    x += h;
    xx[k+1] = x;
    for (i=1;i<=nvar;i++)
    {
        v[i] = vout[i];
        y[i][k+1] = v[i];
    }
}
free_vector(dv,1,nvar);
free_vector(vout,1,nvar);
free_vector(v,1,nvar);
}

/***** rkqc function *****/
void rkqc(y,dydx,n,x,htry,eps,yscal,hdid,hnext,derivs)

float y[], dydx[], *x, htry, eps, yscal[], *hdid, *hnext;
void (*derivs)();
int n;

{
    int i;
    float xsav, hh, h, temp, errmax;
    float *dysav, *ysav, *ytemp, *vectorr();
    void rk4(), nrerror(), free_vector();

    dysav = vectorr(1,n);
    ysav = vectorr(1,n);
    ytemp = vectorr(1,n);
    xsav = (*x);

    for (i=1;i<=n;i++)
    {
        ysav[i] = y[i];
        dysav[i] = dydx[i];
    }
    h = htry;
    for ( ; ; )
    {
        hh = 0.5*h;
        rk4(ysav,dysav,n,xsav,hh,ytemp,derivs);
        *x = xsav+hh;
        (*derivs)(*x,ytemp,dydx);
        rk4(ytemp,dydx,n,*x,hh,y,derivs);
        *x = xsav+h;
        if (*x == xsav) nrerror("Step size too small in routine RKQC");
        rk4(ysav,dysav,n,xsav,h,ytemp,derivs);
        errmax = 0.0;
        for (i=1;i<=n;i++)
        {
            ytemp[i] = y[i]-ytemp[i];
            temp = fabs(ytemp[i]/yscal[i]);
            if (errmax < temp) errmax = temp;
        }
    }
}

```

```

    }
    errmax /= eps;
    if (errmax <= 1.0)
    {
        *hdid = h;
        *hnext = (errmax > ERRCON ? SAFETY*h*exp(FGROW*log(errmax)) :
        4.0*h);
        break;
    }
    h = SAFETY*h*exp(PSHRNK*log(errmax));
}
for (i=1;i<=n;i++) y[i] += ytemp[i]*FCOR;
free_vector(ytemp,1,n);
free_vector(dysav,1,n);
free_vector(ysav,1,n);
}
/***** odeint function *****/
void odeint(ystart,nvar,x1,x2,eps,h1,hmin,nok,nbad,derivs,rkqc)

float ystart[], x1, x2, eps, h1, hmin;
int nvar, *nok, *nbad;
void(*derivs)();
void(*rkqc)();

{
    int nstp, i;
    float xsav, x, hnext, hdid, h;
    float *yscal, *y, *dydx, *vectorr();
    void nrerror(), free_vector();

    yscal = vectorr(1,nvar);
    y = vectorr(1,nvar);
    dydx = vectorr(1,nvar);
    x = x1;
    h = (x2 > x1) ? fabs(h1) : -fabs(h1);
    *nok = (*nbad) = kount = 0;
    for (i=1;i<=nvar;i++) y[i] = ystart[i];
    if (kmax > 0) xsav = x-dxsav*2.0;
    for (nstp=1;nstp<=MAXSTP;nstp++)
    {
        (*derivs)(x,y,dydx);
        for (i=1;i<=nvar;i++) yscal[i] = fabs(y[i])+fabs(dydx[i]*h)*TINY;
        if (kmax > 0)
        {
            if (fabs(x-xsav) > fabs(dxsav))
            {
                if (kount < kmax-1)
                {
                    xp[++kount] = x;
                    for (i=1;i<=nvar;i++) yp[i][kount] = y[i];
                    xsav = x;
                }
            }
        }
        if ((x+h-x2)*(x+h-x1) > 0.0) h = x2-x;
        (*rkqc)(y,dydx,nvar,&x,h,eps,yscal,&hdid,&hnext,derivs);
        if (hdid == h) ++(*nok); else ++(*nbad);
        if ((x-x2)*(x2-x1) >= 0.0)
        {
            for (i=1;i<=nvar;i++)
                ystart[i] = y[i];
            if (kmax)
            {
                xp[++kount] = x;
                for (i=1;i<=nvar;i++) yp[i][kount] = y[i];
            }
        }
    }
}

```

```

        }
        free_vector(dydx,1,nvar);
        free_vector(y,1,nvar);
        free_vector(yscal,1,nvar);
        return;
    }
    if (fabs(hnext) <= hmin) nrexror("Step size too small in ODEINT");
    h = hnext;
}
nrexror("Too many steps in routine ODEINT");
}

```

```

/***** declarations *****/

#include "rkk.h"

#define N 7
#define MAXARRAY 100000
#define SQ(x) ((x)*(x))

int kount, kmax;
float **yp, *xp;
float dxsav, dxmin, dxlimit;
float I1=0.0, I2=0.0, I3=0.0, M=0.0, m=0.0, mb=0.0, a=0.0, k=0.0, c=0.0;
float I1p=0.0, I2p=0.0, I3p=0.0, Mp=0.0, mp=0.0, mbp=0.0, ap=0.0, kp=0.0, cp=0.0;
float L=0.0, sigma=0.0, MT=0.0, v=0.0, rho=0.0, rhop=0.0, L1=0.0, L2=0.0;
float A=0.0, C=0.0, J3p=0.0, w3p=0.0;

/***** EQUATIONS OF MOTION *****/
void derivs(x,y,dydx)
float x, y[], dydx[];
{
    float zeta=0.0, dydxzeta=0.0;
    float A1=0.0, A2=0.0, A3=0.0, A4=0.0, A5=0.0, A6=0.0, A7=0.0, A8=0.0;
    float A9=0.0, A10=0.0, A11=0.0, A12=0.0, A13=0.0, A14=0.0, A15=0.0, A16=0.0;
    float A17=0.0, A18=0.0, A19=0.0, A20=0.0, A21=0.0, A22=0.0, A23=0.0, A24=0.0;
    float A25=0.0, A26=0.0, A27=0.0, A28=0.0;

    float B1=0.0, B2=0.0, B3=0.0, B4=0.0, B5=0.0, B6=0.0, B7=0.0, B8=0.0;
    float B9=0.0, B10=0.0, B11=0.0, B12=0.0, B13=0.0, B14=0.0, B15=0.0, B16=0.0;
    float B17=0.0, B18=0.0, B19=0.0, B20=0.0, B21=0.0, B22=0.0, B23=0.0, B24=0.0;
    float B25=0.0, B26=0.0;

    float C1=0.0, C2=0.0, C3=0.0, C4=0.0, C5=0.0, C6=0.0, C7=0.0, C8=0.0;
    float C9=0.0, C10=0.0, C11=0.0;

    float D1=0.0, D2=0.0, D3=0.0, D4=0.0, D5=0.0, D6=0.0, D7=0.0, D8=0.0;

    float E1=0.0, E2=0.0, E3=0.0, E4=0.0, E5=0.0, E6=0.0, E7=0.0, E8=0.0;
    float E9=0.0, E10=0.0;

    float Z1=0.0, Z2=0.0, Z3=0.0, Z4=0.0, F1=0.0, F2=0.0;

    dydx[4] = y[5];
    dydx[6] = y[7];

    zeta = rho*y[4]+rhop*y[6];
    dydxzeta = rho*y[5]+rhop*y[7];

    A1 = -(A-C)*y[2]*y[3];
    A2 = J3p*sigma*y[2];
    A3 = 2*MT*zeta*dydxzeta*y[1];
    A4 = MT*SQ(zeta);
    A5 = -MT*SQ(zeta)*y[2]*y[3];
    A6 = -2*m*(zeta+L2)*y[4];
    A7 = 2*m*(zeta+L2)*y[4]*y[2]*y[3];
    A8 = -2*m*(zeta+L2)*y[5]*y[1];
    A9 = -2*m*y[4]*dydxzeta*y[1];
    A10 = 2*m*y[4]*y[5]*y[1];
    A11 = m*SQ(y[4]);
    A12 = -m*SQ(y[4])*y[2]*y[3];
    A13 = -m*y[4]*a;
    A14 = -m*y[4]*a*y[1]*y[2];
    A15 = -2*mp*(zeta-L1)*y[6];
    A16 = 2*mp*(zeta-L1)*y[6]*y[2]*y[3];
    A17 = -2*mp*(zeta-L1)*y[7]*y[1];
    A18 = -2*mp*y[6]*dydxzeta*y[1];
    A19 = 2*mp*y[6]*y[7]*y[1];
    A20 = mp*SQ(y[6]);
    A21 = -mp*SQ(y[6])*y[2]*y[3];
    A22 = -mp*y[6]*ap*cos(sigma*x);
    A23 = -mp*y[6]*ap*cos(sigma*x)*y[1]*y[2];
    A24 = mp*ap*sin(sigma*x);
    A25 = mp*ap*sin(sigma*x)*y[6]*(SQ(y[3]+sigma)-SQ(y[2]));
    A26 = A4+A6+A11+A15+A20;
    A27 = A13+A22;
    A28 = A1+A2+A3+A5+A7+A8+A9+A10+A12+A14+A16+A17+A18+A19+A21+A23+A25;

    B1 = -(C-A)*y[1]*y[3];
    B2 = -J3p*sigma*y[1];
    B3 = 2*MT*zeta*dydxzeta*y[2];
    B4 = MT*SQ(zeta);

```

```

B5 = HT*SQ(zeta)*y[1]*y[3];
B7 = -2*m*(zeta+L2)*y[4]*y[1]*y[3];
B9 = -2*m*y[4]*dydxzeta*y[2];
B11 = m*SQ(y[4]);
B13 = -m*a;
B15 = -2*mp*(zeta-L1)*y[6];
B17 = -2*mp*(zeta-L1)*y[7]*y[2];
B19 = mp*SQ(y[6]);
B21 = -mp*ap*cos(sigma*x);
B23 = -mp*ap*cos(sigma*x)*(SQ(y[3]+sigma)-SQ(y[1]))*y[6];
B25 = mp*ap*sin(sigma*x)*y[6]*y[1]*y[2];
B26 = B1+B2+B3+B5+B7+B8+B9+B10+B12+B14+B16+B17+B18+B20+B22+B24;

B6 = -2*m*(zeta+L2)*y[4];
B8 = -2*m*(zeta+L2)*y[5]*y[2];
B10 = 2*m*y[4]*y[5]*y[2];
B12 = m*SQ(y[4])*y[1]*y[2];
B14 = -m*a*y[4]*(SQ(y[3])-SQ(y[1]));
B16 = -2*mp*(zeta-L1)*y[6]*y[1]*y[3];
B18 = 2*mp*y[6]*y[2]*(y[7]-dydxzeta);
B20 = mp*SQ(y[6])*y[1]*y[2];
B23 = -mp*ap*sin(sigma*x)*y[6];
B25 = A+B4+B6+B11+B15+B19;

C1 = -2*m*a*y[5]*y[1];
C3 = m*a*y[4]*y[2]*y[3];
C5 = -mp*ap*sin(sigma*x)*y[6];
C7 = -2*mp*ap*cos(sigma*x)*y[7]*y[1];
C9 = mp*ap*cos(sigma*x)*y[6]*y[2]*y[3];
C10 = C2+C8;

C2 = -m*a*y[4];
C4 = -2*mp*ap*sin(sigma*x)*y[7]*y[2];
C6 = -mp*ap*sin(sigma*x)*y[6]*y[1]*y[1];
C8 = -mp*ap*cos(sigma*x)*y[6];
C11 = C1+C3+C4+C6+C7+C9;

D1 = m*(1-rho);
D3 = -m*a;
D5 = -m*(SQ(y[1])+SQ(y[2]))*(y[4]*(1-rho)-L2-rhop*y[6]);
D7 = k*y[4];

D2 = -mp*rho;
D4 = m*a*y[1]*y[3];
D6 = c*y[5];
D8 = D4+D5+D6+D7;

E1 = -m*rhop;
E3 = mp*ap*sin(sigma*x);
E5 = -mp*ap*cos(sigma*x);
E7 = -mp*(SQ(y[1])+SQ(y[2]))*(y[6]*(1-rhop)+L1-rho*y[4]);
E9 = kp*y[6];

E2 = mp*(1-rhop);
E4 = mp*ap*sin(sigma*x)*y[2]*(y[3]+2*sigma);
E6 = mp*ap*cos(sigma*x)*y[1]*(y[3]+2*sigma);
E8 = mp*y[7];
E10 = E4+E6+E7+E8+E9;

Z1 = ((-A27*B13)/(A26*B23)-E1/E3)/((A27*B25)/(A26*B23)+E5/E3);
Z2 = ((-A27*B21)/(A26*B23)+A24/A26-E2/E3)/((A27*B25)/(A26*B23)+E5/E3);
F1 = ((-A27*B26)/(A26*B23)+A28/A26-E10/E3)/((A27*B25)/(A26*B23)+E5/E3);
Z3 = ((C*B13)/(C10*B23)-(A27*B13)/(A26*B23))/
      ((A27*B25)/(A26*B23)-(C*B25)/(C10*B23)+C5/C10);
Z4 = ((C*B21)/(C10*B23)-(A27*B21)/(A26*B23)+A24/A26)/
      ((A27*B25)/(A26*B23)-(C*B25)/(C10*B23)+C5/C10);
F2 = ((C*B26)/(C10*B23)-C11/C10-(A27*B26)/(A26*B23)+A28/A26)/
      ((A27*B25)/(A26*B23)-(C*B25)/(C10*B23)+C5/C10);

dydx[5] = ((-F2-D8/D3)/(Z4+D2/D3)+(F1+D8/D3)/(Z2+D2/D3))/
           ((-Z1-D1/D3)/(Z2+D2/D3)+(Z3+D1/D3)/(Z4+D2/D3));

dydx[7] = ((-F2-D8/D3)/(Z3+D1/D3)+(F1+D8/D3)/(Z1+D1/D3))/
           ((-Z2-D2/D3)/(Z1+D1/D3)+(Z4+D2/D3)/(Z3+D1/D3));

dydx[3] = (dydx[5]*(C5*B13)/(C*B25)+
           dydx[7]*((C10*A24)/(C*A26)+(C5*B21)/(C*B25))+
           (C10*A28)/(C*A26)+(C5*B26)/(C*B25)-C11/C)/
           (1-(C10*A27)/(C*A26)-(C5*B23)/(C*B25));

dydx[1] = dydx[3]*(-A27/A26)+dydx[7]*(-A24/A26)+(-A28/A26);

dydx[2] = dydx[3]*(-B23/B25)+dydx[5]*(-B13/B25)+dydx[7]*(-B21/B25)-B26/B25;
}

/***** MAIN PROGRAM *****/
main()
{
  int i, j, nbad, nok;
  int l1=1000, l2=2000, l3=3000, l4=4000, l5=5000, l6=6000, l7=7000;
  int l8=8000, l9=9000, l10=10000;
  float eps, hl, hmin, dxsavg, x1, x2, xscale, *ystart;
  float H1=0.0, H2=0.0, H3=0.0, H1p=0.0, H2p=0.0, H3p=0.0, zcm=0.0, argument;

```

```

float T1=0.0, T2=0.0, T3=0.0, T4=0.0, T5=0.0, T6=0.0, T7=0.0, T8=0.0;
float T9=0.0, T10=0.0, T11=0.0, T12=0.0, T13=0.0;
float zcmrigid, It, Itp, Ittotal, Is, Isp, Istotal, wn, lambda, lamdelap;
float *ke, *kedel, *etotal, *etotaldel, *h, *hdel, *theta;
float *Ec, *Ecdel, *Ecp, *Ecpdel, *Echype, *Echypedel, *Ecphype, *Ecphypedel;
float Q, Qp, *eta, *etap, Emin, ecfactor, ecpfactor, haq, Ecfinal, Ecplinal;
float signec, signecp, signq, signqp, argp, Ecq, Ecfp;
float *Ecexp, *Ecexp, *Ecexpdel, *Ecexpdel, *etah, *etahp;

```

```

ystart = vectorr(1,N);
ke = vectorr(1,MAXARRAY);
kedel = vectorr(1,MAXARRAY);
etotal = vectorr(1,MAXARRAY);
etotaldel = vectorr(1,MAXARRAY);
h = vectorr(1,MAXARRAY);
theta = vectorr(1,MAXARRAY);
hdel = vectorr(1,MAXARRAY);
Ecexp = vectorr(1,MAXARRAY);
Ecexp = vectorr(1,MAXARRAY);

Ec = vectorr(1,MAXARRAY);
Ecpdel = vectorr(1,MAXARRAY);
Echype = vectorr(1,MAXARRAY);
Echypedel = vectorr(1,MAXARRAY);
Ecphype = vectorr(1,MAXARRAY);
Ecphypedel = vectorr(1,MAXARRAY);
eta = vectorr(1,MAXARRAY);
etap = vectorr(1,MAXARRAY);
Ecexpdel = vectorr(1,MAXARRAY);
Ecexpdel = vectorr(1,MAXARRAY);
etah = vectorr(1,MAXARRAY);
etahp = vectorr(1,MAXARRAY);

```

```

scanf("%f%f%f%f%f%f%f%f%f%f%f%f%f%f%f%f%f%f%f%f%f",
      &x2, &I1, &I3, &m, &mb, &ka, &kc, &L, &I1p, &I3p, &Mp, &mp, &ap, &kp, &cp,
      &w3p, &ystart[1], &ystart[2], &ystart[3], &ystart[4], &ystart[5],
      &ystart[6], &ystart[7], &eps, &ecfactor, &ecpfactor, &Ecq, &Ecfp);

```

```

x1=0.0001; h1=0.00001; hmin=1.0e-11; kmax=100000;
mb = m; mbp = mp; I2 = I1; I2p = I1p;
sigma = w3p-ystart[3];

```

```

/**** critical damping - input damping = 1000.0, makes it critical ****/
if (c == 1000.0) c = 1.5*sqrt(4*m*k);
if (cp == 1000.0) cp = 1.5*sqrt(4*mp*kp);

```

```

/**** establish time interval for saving data ****/
dxmin = 1.0e-4;
dxlimit = (x2-x1)/1750.0;
dxsav = (x2<20.0) ? dxmin : dxlimit;

```

```

MT = M+Mp+4.0*mb+4.0*mbp;
v = (Mp+4.0*mbp)/MT;
A = I1+I1p+2.0*mb*SQ(a)+2.0*mbp*SQ(ap)+(Mp+4.0*mbp)*(1.0-v)*SQ(L);
C = I3+I3p+4.0*mb*SQ(a)+4.0*mbp*SQ(ap);
J3p = I3p+4.0*mbp*SQ(ap);
rho = m/MT;
rho = mp/MT;
L1 = L*(M+4.0*mb)/MT;
L2 = L*(Mp+4.0*mbp)/MT;

```

```

zcmrigid = ((Mp+4.0*mbp)*L)/MT;
It = I1+M*SQ(zcmrigid)+mb*(4.0*SQ(zcmrigid)+2.0*SQ(a));
Itp = I1p+Mp*SQ(L-zcmrigid)+mbp*(4.0*SQ(L-zcmrigid)+2.0*SQ(ap));
Ittotal = It+Itp;
Is = I3+4.0*mb*SQ(a);
Isp = I3p+4.0*mbp*SQ(ap);
Istotal = Is+Isp;

```

```

odeint(ystart, N, x1, x2, eps, h1, hmin, &nok, &nbad, derivs, rkqc);

```

```

for (j=1; j<=kount; j++)
{
    zcm = ((Mp+4.0*mbp)*L+m*yp[4][j]+mp*yp[6][j])/MT;
    H1 = (I1+M*SQ(zcm)+m*(2.0*SQ(a)+4.0*SQ(zcm)+SQ(yp[4][j]))

```

```

-2.0*scm*yp[4][j]))*yp[1][j]-m*a*yp[4][j]*yp[3][j]:
H2 = (I2+H*SQ(zcm)+m*(2.0*SQ(a)+4.0*SQ(zcm)+SQ(yp[4][j])
-2.0*scm*yp[4][j]))*yp[2][j]-m*a*yp[5][j]:
H3 = -m*a*yp[4][j]*yp[1][j]+(I3+4.0*m*SQ(a))*yp[3][j]:
H1p = (I1p+Mp*SQ(L-zcm)+mp*(2.0*SQ(ap)+4.0*SQ(L-zcm)+SQ(yp[6][j])
2.0*(L-zcm)*yp[6][j]))*yp[1][j]-mp*ap*cos(sigma*xp[j])*
yp[6][j]*yp[3][j]-mp*ap*sigma*cos(sigma*xp[j])*
yp[6][j]+mp*ap*sin(sigma*xp[j])*yp[7][j]:
H2p = (I2p+Mp*SQ(L-zcm)+mp*(2.0*SQ(ap)+4.0*SQ(L-zcm)+SQ(yp[6][j])
2.0*(L-zcm)*yp[6][j]))*yp[2][j]-mp*ap*sin(sigma*xp[j])*
yp[6][j]*yp[3][j]-mp*ap*sigma*sin(sigma*xp[j])*
yp[6][j]-mp*ap*cos(sigma*xp[j])*yp[7][j]:
H3p = -mp*ap*cos(sigma*xp[j])*yp[6][j]*yp[1][j]-mp*ap*
sin(sigma*xp[j])*yp[6][j]*yp[2][j]+(I3p+4.0*mp*SQ(ap))*
(yp[3][j]+sigma):
h[j] = sqrt(SQ(H1+H1p)+SQ(H2+H2p)+SQ(H3+H3p)):
argument = (H3+H3p)/h[j]:
if(argument>0.99999999) argument = 1.0:
theta[j] = 57.2957795131*acos(argument):
hdel[j] = h[j]-h[1]:
T1 = 0.5*(I1*SQ(yp[1][j])+I2*SQ(yp[2][j])+I3*SQ(yp[3][j])):
T2 = 0.5*(I1p*SQ(yp[1][j])+I2p*SQ(yp[2][j])+I3p*
SQ(yp[3][j]+sigma)):
T3 = 0.5*m*(SQ(yp[5][j])+SQ(yp[1][j])+SQ(yp[2][j]))*SQ(yp[4][j])
-2.0*a*yp[1][j]*yp[3][j]*yp[4][j]:
T4 = 0.5*mp*(SQ(yp[7][j])+SQ(yp[6][j]))*(SQ(yp[1][j])+SQ(yp[2][j])
+2.0*ap*sin(sigma*xp[j])*yp[2][j]*yp[3][j]*yp[6][j]
-2.0*ap*cos(sigma*xp[j])*yp[1][j]*yp[3][j]*yp[6][j]):
T5 = -m*a*yp[2][j]*yp[5][j]:
T6 = -mp*(-ap*yp[7][j]*yp[2][j]*cos(sigma*xp[j])
+ap*yp[7][j]*yp[1][j]*sin(sigma*xp[j])
-ap*sigma*yp[1][j]*yp[6][j]*cos(sigma*xp[j])
-ap*sigma*yp[2][j]*yp[6][j]*sin(sigma*xp[j])):
T7 = (0.5*SQ(m*yp[5][j]+mp*yp[7][j]))/MT:
T8 = (0.5*(SQ(yp[1][j])+SQ(yp[2][j]))
*SQ(m*yp[4][j]+mp*yp[6][j]))/MT:
T9 = 0.5*(SQ(yp[1][j])+SQ(yp[2][j]))*(M+4.0*m)*SQ(L)*
SQ((Mp+4.0*mp)/MT):
T10 = 0.5*(SQ(yp[1][j])+SQ(yp[2][j]))*(Mp+4.0*mp)*SQ(L)*
SQ((M+4.0*m)/MT):
T11 = (m+mp)*(-yp[5][j])*(m*yp[5][j]+mp*yp[7][j])/MT:
T12 = -m*yp[4][j]*(SQ(yp[1][j])+SQ(yp[2][j]))*
(m*yp[4][j]+mp*yp[6][j]+(Mp+4.0*mp)*1.)/MT:

```



```

T13 = -mp*yp[6][j]*(SQ(yp[1][j])+SQ(yp[2][j]))*
      (m*yp[4][j]+mp*yp[6][j])-(H+4.0*m)*L/H;

ke[j]      = T1+T2+T3+T4+T5+T6+T7+T8+T9+T10+T11+T12+T13;
kedel[j]   = ke[j]-ke[1];
etotal[j]  = ke[j]+0.5*k*SQ(yp[4][j])+0.5*kp*SQ(yp[6][j]);
etotaldel[j] = etotal[j]-etotal[1];
Ec[j]      = 0.5*(Ittotal*(SQ(yp[1][j])+SQ(yp[2][j]))
                +Isttotal*SQ(yp[3][j]));
Ecdel[j]   = Ec[j]-Ec[1];
Ecp[j]     = 0.5*(Ittotal*(SQ(yp[1][j])+SQ(yp[2][j]))
                +Isttotal*SQ(yp[3][j]*sigma));
Ecpdel[j]  = Ecp[j]-Ecp[1];
}

vn = (Is*yp[3][1]+Isp*(yp[3][1]+sigma))/Ittotal;
lambda = vn-yp[3][1];
lambdap = vn-(yp[3][1]+sigma);
hsq = SQ(Ittotal)*(SQ(yp[1][1])+SQ(yp[2][1]))
      +SQ(Is*yp[3][1]+Isp*(yp[3][1]+sigma));

if (theta[kount]-theta[1] < 0.0)      /**** stable condition *****/
{
  if (lambda < 0.0)      { signec = 1.0; signq = 1.0; }
  else                  { signec = -1.0; signq = -1.0; }

  if (lambdap < 0.0)    { signecp = 1.0; signqp = 1.0; }
  else                  { signecp = -1.0; signqp = -1.0; }
}
else                                  /**** unstable condition *****/
{
  if (lambda < 0.0)    { signec = -1.0; signq = 1.0; }
  else                  { signec = 1.0; signq = -1.0; }

  if (lambdap < 0.0)  { signecp = -1.0; signqp = 1.0; }
  else                  { signecp = 1.0; signqp = -1.0; }
}

Ecfinal = (Ec == 0.0) ? Ec[kount] : Ec;
Ecpfinal = (Ecp == 0.0) ? Ecp[kount] : Ecp;

for(j=1;j<=kount;j++)
{
  Echype[j]      = Ec[1]*Ecfinal/(Ec[1]+(Ecfinal-Ec[1])*
                                exp(ecfactor*Ecfinal*xp[j]));

  Echypedel[j]   = Echype[j]-Echype[1];

  Ecphype[j]     = Ecp[1]*Ecpfinal/(Ecp[1]+(Ecpfinal-Ecp[1])*
                                exp(ecpfactor*Ecpfinal*xp[j]));

  Ecphypedel[j]  = Ecphype[j]-Ecphype[1];

  Q              = 2.0*Echype[j]*Isttotal*(1.0-(Isttotal/Ittotal))
                  -hsq*(Isttotal/Ittotal)*(1.0-(Isttotal/Ittotal))
                  +(Isttotal/Ittotal)*SQ(Isp)*SQ(sigma);

  Qp             = 2.0*Ecphype[j]*Isttotal*(1.0-(Isttotal/Ittotal))
                  -hsq*(Isttotal/Ittotal)*(1.0-(Isttotal/Ittotal))

```

```

        + (Istotal/Ittotal)*SQ(Is)*SQ(sigma);
    arg = ((Ittotal/(Ittotal-Istotal))
           * ((Is*sigma)+(signq*sqrt(Q))))/(sqrt(hsq));
    if (arg > 0.99999999) arg=1.0;
    etah[j] = 57.2957795131*acos(arg);

    argp = ((Ittotal/(Ittotal-Istotal))
            * ((-Is*sigma)+(signqp*sqrt(Qp))))/(sqrt(hsqp));
    if (argp > 0.99999999) argp=1.0;
    etahp[j] = 57.2957795131*acos(argp);

    Ecexp[j] = (Ec[1]-Ecfinal)*exp(ecfactor*xp[j])+Ecfinal;
    Ecexpdel[j] = Ecexp[j]-Ecexp[1];

    Ecpexp[j] = (Ecp[1]-Ecpfinal)*exp(ecpfactor*xp[j])+Ecpfinal;
    Ecpexpdel[j] = Ecpexp[j]-Ecpexp[1];

    Q = 2.0*Ecexp[j]*Istotal*(1.0-(Istotal/Ittotal))
        -hsq*(Istotal/Ittotal)*(1.0-(Istotal/Ittotal))
        + (Istotal/Ittotal)*SQ(Is)*SQ(sigma);

    Qp = 2.0*Ecpexp[j]*Istotal*(1.0-(Istotal/Ittotal))
        -hsqp*(Istotal/Ittotal)*(1.0-(Istotal/Ittotal))
        + (Istotal/Ittotal)*SQ(Is)*SQ(sigma);

    arg = ((Ittotal/(Ittotal-Istotal))
           * ((Is*sigma)+(signq*sqrt(Q))))/(sqrt(hsq));
    if (arg > 0.99999999) arg=1.0;
    eta[j] = 57.2957795131*acos(arg);

    argp = ((Ittotal/(Ittotal-Istotal))
            * ((-Is*sigma)+(signqp*sqrt(Qp))))/(sqrt(hsqp));
    if (argp > 0.99999999) argp=1.0;
    etap[j] = 57.2957795131*acos(argp);
}

/***** initialize graphics *****/
init(); color_scale="cyanblue";
grey_scale("greyscale"); window0();
bgcol(7); erase(); color(0);
move(220,-110); printf("MINGORI DUAL SPINNER MASS SPRING SYSTEM");

window(22,-85,979,872); bgcol(3);
erase(); scale(0,10000,10000,0); rect(0,0,10000,10000);
size(1,1);
move(20,110+200); date();
move(-160,110+70); printf("0");
move(10,110-90); printf("w3 - w3 initial");

vector(0,19,110,19); move(-160,19+70); printf("0");
move(10,19+200); printf("w2");

vector(0,18,110,18); move(-160,18+70); printf("0");
move(10,18+200); printf("w1");

```

```

vector(0,17,110,17): move(-160,17*70): printf("0");
                      move(10,17*200): printf("z prime dot");

vector(0,16,110,16): move(-160,16*70): printf("0");
                      move(10,16*200): printf("z prime");

vector(0,15,110,15): move(-160,15*70): printf("0");
                      move(10,15*200): printf("z dot");

vector(0,14,110,14): move(-160,14*70): printf("0");
                      move(10,14*200): printf("z");

vector(0,13,110,13): move(-160,13*70): printf("0");
                      move(10,13*200): printf("ke-ke i (r), c-c i (b)");

vector(0,12,110,12): move(-160,12*70): printf("0");
                      move(10,12*200): printf("Ec-Ec i (r), Echype-Echype i (b)");

vector(0,11,110,11): move(-160,11*70): printf("0");
                      move(10,11*200): printf("Ecp-Ecp i (r), Ecphype-Ecphype i (b)");

vector(0,0,110,0): move(-160,0*70): printf("0");
                    move(10,0*200): printf("theta, eta (b), etap (r), h - h initial");

vector(0,19+750,11,19+750): vector(19,19+750,110,19+750):
vector(0,19+500,11,19+500): vector(19,19+500,110,19+500):
vector(0,19+250,11,19+250): vector(19,19+250,110,19+250):
vector(0,19-250,11,19-250): vector(19,19-250,110,19-250):
vector(0,19-500,11,19-500): vector(19,19-500,110,19-500):
vector(0,18+250,11,18+250): vector(19,18+250,110,18+250):
vector(0,18-250,11,18-250): vector(19,18-250,110,18-250):
vector(0,18-500,11,18-500): vector(19,18-500,110,18-500):

xscale = 10000.0/xp[kount];

color(1): /**** blue - total energy, rotor hype ****/
for (j=1;j<kount;j++)
{
    vector((int)(xscale*xp[j]), (int)(13+(0.01*etotaldel[j])),
           (int)(xscale*xp[j+1]), (int)(13+(0.01*etotaldel[j+1])));
    vector((int)(xscale*xp[j]), (int)(13+(0.1*etotaldel[j])),
           (int)(xscale*xp[j+1]), (int)(13+(0.1*etotaldel[j+1])));

    vector((int)(xscale*xp[j]), (int)(12+(50.0*Echypedel[j])),
           (int)(xscale*xp[j+1]), (int)(12+(50.0*Echypedel[j+1])));

    vector((int)(xscale*xp[j]), (int)(0+(100.0*etah[j])),
           (int)(xscale*xp[j+1]), (int)(0+(100.0*etah[j+1])));
    vector((int)(xscale*xp[j]), (int)(11+(1000.0*etah[j])),
           (int)(xscale*xp[j+1]), (int)(11+(1000.0*etah[j+1])));
}

color(5): /**** purple - platform exponential****/
for (j=1;j<kount;j++)
{
    vector((int)(xscale*xp[j]), (int)(11+(50.0*Ecpexpdel[j])),
           (int)(xscale*xp[j+1]), (int)(11+(50.0*Ecpexpdel[j+1])));

    vector((int)(xscale*xp[j]), (int)(0+(100.0*etap[j])),
           (int)(xscale*xp[j+1]), (int)(0+(100.0*etap[j+1])));
    vector((int)(xscale*xp[j]), (int)(11+(1000.0*etap[j])),
           (int)(xscale*xp[j+1]), (int)(11+(1000.0*etap[j+1])));
}

```

```

    }

color(6);          /***** yellow - rotor exponential *****/
for (j=1; j<kount; j++)
{
    vector((int) (xscale*xp[j]), (int) (12+(50.0*Ecexpdel[j])),
           (int) (xscale*xp[j+1]), (int) (12+(50.0*Ecexpdel[j+1])));

    vector((int) (xscale*xp[j]), (int) (0+(100.0*eta[j])),
           (int) (xscale*xp[j+1]), (int) (0+(100.0*eta[j+1])));
    vector((int) (xscale*xp[j]), (int) (11+(1000.0*eta[j])),
           (int) (xscale*xp[j+1]), (int) (11+(1000.0*eta[j+1])));
}

color(0);          /***** black - platform hyperbolic *****/
for (j=1; j<kount; j++)
{
    vector((int) (xscale*xp[j]), (int) (11+(50.0*Ecphypedel[j])),
           (int) (xscale*xp[j+1]), (int) (11+(50.0*Ecphypedel[j+1])));

    vector((int) (xscale*xp[j]), (int) (0+(100.0*etahp[j])),
           (int) (xscale*xp[j+1]), (int) (0+(100.0*etahp[j+1])));
    vector((int) (xscale*xp[j]), (int) (11+(1000.0*etahp[j])),
           (int) (xscale*xp[j+1]), (int) (11+(1000.0*etahp[j+1])));
}

color(4);          /***** red - rotor *****/
for (j=1; j<kount; j++)
{
    vector((int) (xscale*xp[j]), (int) (110+(1432.39448783*(yp[3][j]-yp[3][1]))),
           (int) (xscale*xp[j+1]), (int) (110+(1432.39448783*(yp[3][j+1]-yp[3][1]))));

    vector((int) (xscale*xp[j]), (int) (19+(1432.39448783*yp[2][j])),
           (int) (xscale*xp[j+1]), (int) (19+(1432.39448783*yp[2][j+1])));

    vector((int) (xscale*xp[j]), (int) (18+(1432.39448783*yp[1][j])),
           (int) (xscale*xp[j+1]), (int) (18+(1432.39448783*yp[1][j+1])));

    vector((int) (xscale*xp[j]), (int) (17+(1000*yp[7][j])),
           (int) (xscale*xp[j+1]), (int) (17+(1000*yp[7][j+1])));

    vector((int) (xscale*xp[j]), (int) (16+(1000*yp[6][j])),
           (int) (xscale*xp[j+1]), (int) (16+(1000*yp[6][j+1])));

    vector((int) (xscale*xp[j]), (int) (15+(1000*yp[5][j])),
           (int) (xscale*xp[j+1]), (int) (15+(1000*yp[5][j+1])));

    vector((int) (xscale*xp[j]), (int) (14+(1000*yp[4][j])),
           (int) (xscale*xp[j+1]), (int) (14+(1000*yp[4][j+1])));

    vector((int) (xscale*xp[j]), (int) (13+(0.01*kedel[j])),
           (int) (xscale*xp[j+1]), (int) (13+(0.01*kedel[j+1])));
    vector((int) (xscale*xp[j]), (int) (13+(0.1*kedel[j])),
           (int) (xscale*xp[j+1]), (int) (13+(0.1*kedel[j+1])));

    vector((int) (xscale*xp[j]), (int) (12+(50.0*Ecdel[j])),
           (int) (xscale*xp[j+1]), (int) (12+(50.0*Ecdel[j+1])));

    vector((int) (xscale*xp[j]), (int) (11+(50.0*Ecpdel[j])),
           (int) (xscale*xp[j+1]), (int) (11+(50.0*Ecpdel[j+1])));

    vector((int) (xscale*xp[j]), (int) (0+(1000.0*hdcl[j])),
           (int) (xscale*xp[j+1]), (int) (0+(1000.0*hdcl[j+1])));
}

```

```

vector((int)(xscale*xp[j]), (int)(0+(100.0*theta[j])),
      (int)(xscale*xp[j+1]), (int)(0+(100.0*theta[j+1])));
vector((int)(xscale*xp[j]), (int)(11+(1000.0*theta[j])),
      (int)(xscale*xp[j+1]), (int)(11+(1000.0*theta[j+1])));

/*
vector((int)(xscale*xp[j]), (int)(0+(0.0001*ke[j])),
      (int)(xscale*xp[j+1]), (int)(0+(0.0001*ke[j+1])));
*/
/*
vector((int)(xscale*xp[j]), (int)(0+(0.0001*etotal[j])),
      (int)(xscale*xp[j+1]), (int)(0+(0.0001*etotal[j+1])));
*/
/*
vector((int)(xscale*xp[j]), (int)(0+(0.1*h[j])),
      (int)(xscale*xp[j+1]), (int)(0+(0.1*h[j+1])));
*/
)
window0();
color(0);

      /*** print initial, final data ***/

move(350,875); printf("          INITIAL CONDITIONS          kount = %d",kount);

/*
move(22,910);   printf("time =%3.0f seconds",xp[kount]);
move(500,910);  printf("eps = %e   %d/%d",eps,nbad,nok);

move(22,940);
printf("W1 =%4.2f W2 =%4.2f W3 =%4.2f",yp[1][1],yp[2][1],yp[3][1]);
move(500,940);  printf("w3p= %9.7f      L = %3.1f",w3p,L);

move(22,980);   printf("I1 =%4.0f I2 =%4.0f I3 =%4.0f",I1,I2,I3);
move(22,1010);  printf("M = %4.0f  m =%7.5f",M,m);
move(22,1040);  printf("a =%4.1f  k =%4.1f  c =%4.1f",a,k,c);
move(22,1070);  printf("z =%4.2f  zdot=%4.2f",yp[4][1],yp[5][1]);

move(500,980);  printf("I1p=%4.0f I2p=%4.0f I3p=%4.0f",I1p,I2p,I3p);
move(500,1010); printf("Mp =%4.0f  mp=%7.5f",Mp,mp);
move(500,1040); printf("ap=%4.1f  kp=%4.1f  cp=%4.1f",ap,kp,cp);
move(500,1070); printf("zp =%4.2f  zdotp=%4.2f",yp[6][1],yp[7][1]);

move(22,1110);  printf("h i=%9.4f  ke i=%7.1f",h[i],ke[i]);
move(22,1135);  printf("h f=%9.4f  ke f=%7.1f",h[kount],ke[kount]);
move(22,1160);  printf("hdelper=%5.2f",100.0*(h[kount]-h[1])/h[1]);
move(250,1160); printf("kedelper=%5.2f",100.0*(ke[kount]-ke[1])/ke[1]);
move(500,1160);
printf("e delper=%5.2f",100.0*(etotal[kount]-etotal[1])/etotal[1]);
move(730,1160); printf("Ecp delper=%5.2f",100.0*(Ecp[kount]-Ecp[1])/Ecp[1]);

move(500,1110); printf("Ec i=%9.4f  theta i=%7.5f",Ec[i],theta[i]);
move(500,1135); printf("Ec f=%9.4f  theta f=%7.5f",Ec[kount],theta[kount]);
*/

move(22,900);   printf("          platform          rotor");
move(22,920);   printf("I1p = %6.2f",I1p);
move(240,920);  printf("I1 = %6.2f",I1);
move(22,940);   printf("I3p = %6.2f",I3p);
move(240,940);  printf("I3 = %6.2f",I3);
move(22,960);   printf("Mp = %6.2f",Mp);
move(240,960);  printf("M = %6.2f",M);
move(22,980);   printf("mp = %6.2f",mp);
move(240,980);  printf("m = %6.2f",m);
move(22,1000);  printf("ap = %6.2f",ap);
move(240,1000); printf("a = %6.2f",a);
move(22,1020);  printf("kp = %6.2f",kp);
move(240,1020); printf("k = %6.2f",k);

```

```

move(22,1040): printf("cp      = %6.2f",cp);
move(240,1040): printf("c      = %6.2f",c);

move(22,1060): printf("L      = %6.4f",L);
move(240,1060): printf("Is/It = %6.3f",Istotal/Ittotal);

move(22,1100): printf("zp      = %6.2f",yp[6][1]);
move(240,1100): printf("z      = %6.2f",yp[4][1]);
move(22,1120): printf("dzp     = %6.2f",yp[7][1]);
move(240,1120): printf("dz      = %6.2f",yp[5][1]);
move(22,1140): printf("w3p     = %6.2f",yp[3][1]+signa);
move(240,1140): printf("w3      = %6.2f",yp[3][1]);
move(22,1160): printf("w1      = %6.2f",yp[1][1]);
move(240,1160): printf("w2      = %6.2f",yp[2][1]);

move(480,900): printf("%3.0f seconds",xp[kount]);
move(730,900): printf("h i    = %9.4f",h[1]);
move(480,920): printf("%d / %d / %d",nbad,nok,kount);
move(730,920): printf("h f    = %9.4f",h[kount]);
move(480,940): printf("eps     = %7e",eps);
move(730,940): printf("hdelp   = %5.3f",100.0*(h[kount]-h[1])/h[1]);
move(480,960): printf("ke i    = %9.4f",ke[1]);
move(730,960): printf("e i     = %9.4f",etotal[1]);
move(480,980): printf("ke f    = %9.4f",ke[kount]);
move(730,980): printf("e f     = %9.4f",etotal[kount]);
move(480,1000): printf("kedelp  = %5.3f",100.0*(ke[kount]-ke[1])/ke[1]);
move(730,1000): printf("edelp   = %5.3f",100.0*(etotal[kount]-etotal[1])/etotal[1]);

move(480,1030): printf("Ecp1    = %9.3f",Ecp[1]);
move(730,1030): printf("Ec i    = %9.3f",Ec[1]);
move(480,1050): printf("Ecpf    = %9.3f",Ecp[kount]);
move(730,1050): printf("Ec f    = %9.3f",Ec[kount]);
move(480,1070): printf("lambdap = %5.3f",lambdap);
move(730,1070): printf("lambda  = %5.3f",lambda);
move(480,1090): printf("signqp  = %5.2f",signqp);
move(730,1090): printf("signq   = %5.2f",signq);
move(480,1110): printf("dEcp/lambdap = %6.3f", (Ecp[kount]-Ecp[1])/lambdap);
move(730,1110): printf("dEc/lambda = %6.3f", (Ec[kount]-Ec[1])/lambda);

move(480,1130): printf("Ecfp    = %8.6f",Ecfp);
move(730,1130): printf("Ec f    = %8.6f",Ec f);

move(480,1155): printf("theta i = %6.2f",theta[1]);
move(620,1155): printf("etap i  = %6.2f",etap[1]);
move(760,1155): printf("eta i   = %6.2f",eta[1]);
move(480,1175): printf("theta f = %6.2f",theta[kount]);
move(620,1175): printf("etap f  = %6.2f",etap[kount]);
move(760,1175): printf("eta f   = %6.2f",eta[kount]);

    /** upper right hand corner */
move(600,-33): printf("Ec initial/final = %g / %g",Ec[1],Ec[kount]);
move(600,-13): printf("Ecp initial/final = %g / %g",Ecp[1],Ecp[kount]);
move(600,27):  printf("Ec factor / Ec f = %g / %g",ecfactor,Ecf);
move(600,47):  printf("Ecp factor / Ecp f = %g / %g",ecpfactor,Ecfp);

move(980,-33): printf("%d",nbad);
move(980,-13): printf("%d",nok);
move(980,7):   printf("%d",kount);
move(980,27):  printf("nbad");
move(980,47):  printf("nok");
move(980,67):  printf("kount");

move(980,97):  printf("%6.4f", (100.0*(ke[kount]-ke[1])/ke[1]));

```

```

move(980,117); printf("%6.4f", (100.0*(etotal[kount]-etotal[1]))/etotal[1]);
move(980,137); printf("%6.4f", (100.0*(h[kount]-h[1]))/h[1]);

move(980,157); printf("kedel");
move(980,177); printf("edelp");
move(980,197); printf("hdelp");

move(980,227); printf("%g",theta[1]);
move(980,247); printf("%g",theta[kount]);

move(980,267); printf("th 1");
move(980,287); printf("th f");

move(980,317); printf("%g",eta[1]);
move(980,337); printf("%g",eta[kount]);

move(980,357); printf("eta 1");
move(980,377); printf("eta f");

move(980,407); printf("%g",etap[1]);
move(980,427); printf("%g",etap[kount]);

move(980,447); printf("etapl");
move(980,467); printf("etapf");

move(980,497); printf("%g",Ec[kount]-Ec[1]);
move(980,517); printf("%g",lambda);
move(980,537); printf("%g",signq);

move(980,557); printf("Ecdel");
move(980,577); printf("lambda");
move(980,597); printf("signq");

move(980,627); printf("%g",Ecp[kount]-Ecp[1]);
move(980,647); printf("%g",lambdap);
move(980,667); printf("%g",signqp);

move(980,687); printf("Ecpdel");
move(980,707); printf("lambdap");
move(980,727); printf("signqp");

move(980,757); printf("%g", Istotal/Ittotal);
move(980,777); printf("Is/It");

free_matrix(y,1,N,1,MAXARRAY);
free_vector(x,1,MAXARRAY);
free_vector(y,1,N);
free_vector(ke,1,MAXARRAY);
free_vector(kedel,1,MAXARRAY);
free_vector(etotal,1,MAXARRAY);
free_vector(etotaldel,1,MAXARRAY);
free_vector(h,1,MAXARRAY);
free_vector(theta,1,MAXARRAY);
free_vector(hdel,1,MAXARRAY);
free_vector(Ecexp,1,MAXARRAY);
free_vector(Ecpexp,1,MAXARRAY);
free_vector(eta,1,MAXARRAY);
}

free_vector(Ec,1,MAXARRAY);
free_vector(Ecdel,1,MAXARRAY);
free_vector(Ecp,1,MAXARRAY);
free_vector(Ecpdel,1,MAXARRAY);
free_vector(Echype,1,MAXARRAY);
free_vector(Echypedel,1,MAXARRAY);
free_vector(Ecpype,1,MAXARRAY);
free_vector(Ecpypedel,1,MAXARRAY);
free_vector(eta,1,MAXARRAY);
free_vector(etap,1,MAXARRAY);
free_vector(Ecexpdel,1,MAXARRAY);
free_vector(Ecpexpdel,1,MAXARRAY);
free_vector(etalp,1,MAXARRAY);

```

INITIAL DISTRIBUTION LIST

- | | | |
|----|--|---|
| 1. | Defense Technical Information Center
Cameron Station
Alexandria, Virginia 22304-6145 | 2 |
| 2. | Library, Code 52
Naval Postgraduate School
Monterey, California 93943-5002 | 2 |
| 3. | LCDR V. M. Ortiz
917 Copper Stone Circle
Chesapeake, Virginia 23320 | 2 |
| 4. | Prof. I. M. Ross
Code AA/Ro
Department of Aeronautics and Astronautics
Naval Postgraduate School
Monterey, California 93943-5002 | 8 |
| 5. | Prof. H. A. Dahl
Code PH/Dh
Department of Physics
Naval Postgraduate School
Monterey, California 93943-5002 | 1 |